G Protein-Coupled Receptors in the Neuropathophysiology of Asthma

by
Irving Coy Allen, Jr.

A dissertation submitted to the faculty of the University of North Carolina at Chapel Hill in partial fulfillment of the requirements for the degree of Doctor of Philosophy in the Curriculum of Genetics and Molecular Biology

Chapel Hill
2006

Approved by:

Advisor: Beverly H. Koller, PhD
Readers: Thomas M. Coffman, MD
Raymond B. Penn, PhD
Ellen R. Weiss, PhD
Susan T. Lord, PhD
Stephen L. Tilley, MD

ABSTRACT

Irving Coy Allen, Jr.

G Protein-Coupled Receptors in the Neuropathophysiology of Asthma

(Under the direction of Dr. Beverly H. Koller, PhD)

Asthma is a complex genetic disorder with environmental influences and is characterized by airway inflammation, reversible airflow obstruction, and airway hyperresponsiveness (AHR). The arachidonic acid metabolite thromboxane A_2 (TXA_2), is a potent lipid mediator released by platelets and inflammatory cells and is capable of inducing bronchoconstriction. In the airways, it has been postulated that TXA_2 causes airway constriction by direct activation of TP receptors on airway smooth muscle (ASM) cells. Here we demonstrate that although TXA_2 can mediate a dramatic increase in ASM constriction, this response is largely dependent on vagal innervation of the airways and is highly sensitive to muscarinic acetylcholine receptor (mAChR) antagonists. Further analyses demonstrate that TP-dependent ASM constriction requires M_3 mAChR expression. To further define the mechanism underlying TXA_2 meditated airway constriction, mice carrying a Tp receptor locus that is sensitive to disruption by cre recombinase were generated. These mice were crossed with nestin-cre transgenic mice, which express cre recombinase throughout the nervous systems. Here we demonstrate that loss of the TP receptor throughout the nervous system does not significantly affect TXA_2 airway reactivity. To assess ASM TP receptor function, we crossed the floxed Tp receptor mice with SM22-cre transgenic mice, which

express cre recombinase in smooth muscle. The resultant smooth muscle TP receptor deficient animals demonstrate attenuated airway responses following aerosol challenges with TXA_2. Together, these findings suggest that TXA_2 mediates airway reactivity and AHR through collaborations between ASM Tp receptors and the M3 mAChR.

In addition to TXA_2, we also evaluated the role of NPSR1 (GPRA), a newly deorphanized G protein-coupled receptor that has been shown to be a promising candidate gene associated with asthma in human populations. We report here that the change in airway resistance in response to methacholine was identical in control and NPSR1 deficient mice and the development of allergic lung disease in NPSR1 deficient mice is unaltered. In contrast to previously published data, our analyses also failed to detect expression of NPSR1 in human lung tissue or in mice with allergic lung disease. Taken together, our studies fail to support a direct contribution of NPSR1 to asthma pathogenesis.

ACKNOWLEDGEMENTS

I would like to acknowledge the following individuals, without whom this work would not have been possible:

My advisor and mentor, Dr. Beverly Koller. Bev has always supported my research endeavors and provided me with the confidence necessary to succeed as a scientist. Most importantly, she has taught me the importance of being a careful and critical researcher. Through Bev's support, I have grown considerably both personally and professionally. It has been my honor and privilege to work with her.

The members of my dissertation committee were essential to my graduate training and success. Their scientific insight and unique perspectives strengthened my research. I would like to thank Dr. Susan Lord, Dr. Ellen Weiss, Dr. Steve Tilley, Dr. Tom Coffman, and Dr. Ray Penn for their time, guidance, and helpful suggestions.

The members of the Koller lab, past and present, who have supported me throughout this work. I would particularly like to thank: John Hartney, Dr. Steve Tilley and Alysia Lovgren for the helpful scientific discussions and technical expertise regarding airway physiology; Julie Ledford and MyTrang Nguyen for the helpful guidance related to immunology mechanisms and associated technical support; Amy Pace for sharing the GPRA project work load with me as well as assisting in various manuscript preparations; Subhashini Chandrasekharan for scientific discussions and general enlightenment; Anne Latour for assisting with genotyping and sharing her tissue culture expertise; Martina Kovarova for

sharing her mast cell culture expertise; Jay Snouwaert for help and advice with constructs and cloning schemes; Leigh Jania for her statistics consulting and substantial technical assistance; Jamie Cyphert and Matthew Wheeler for technical assistance; Soo Kim and Karen Strunk for histology assistance; and Kelly Parsons and Ken Inada for brain necropsy assistance.

I would also like to acknowledge Dr. Jurgen Wess at NIH, NIDDK for providing access to muscarinic acetylcholine receptor deficient mice; Dr. Julia Walker and Barbara Lawson at Duke University for providing surgical training in the vagotomy technique; Dr. Ray Penn and Se-Wei Wang at Wake Forest University for technical assistance and access to equipment related to tracheal ring studies; Dr. Alex Therien, Dr. Virginie Bernier, and Rino Stocco at Merck Frost Canada for sharing data related to the GPRA/NPSR project; Dr. Ellen Weiss and Rebecca Jo at UNC Chapel Hill and Dr. Fulton Wong at Duke University for guiding the GPRA/NPSR eye phenotyping project; and Dr. Sheryl Moy and Randal Nonneman of the NDRC Mouse Behavioral Phenotyping Laboratory for conducting behavioral testing on mice from the GPRA/NPSR project.

Finally, I would like to thank my friends and family. My parents have always pushed me to excel in all aspects of my life and have been my greatest supporters. Likewise, I could not have been successful in graduate school had it not been for my amazing wife Amanda. Her patience, devotion, and understanding have provided me with the strength necessary to complete this adventure. To her I owe my sanity.

TABLE OF CONTENTS

LIST OF TABLES

LIST OF FIGURES

LIST OF ABBREVIATIONS AND SYMBOLS

4-DAMP	4-diphenylacetoxy-N-methylpiperidine methiodide
5-HT	serotonin
AA	arachidonic acid
AC	adenylyl cyclase
ACh	acetylcholine
AChE	acetylcholinesterase
AD	atopic dermatitis
ADP	adenosine diphosphate
AHR	airway hyperresponsiveness
cAMP	cyclic adenosine monophosphate
ANOVA	analysis of variance
APC	antigen presenting cells
APTI	airway pressure time index
ASM	airway smooth muscle
ATP	adenosine triphosphate
β2-AR	β2-adrenergic receptor
BALF	bronchoalveolar lavage fluid
BEC	bronchial epithelial cells
BMMC	bone marrow derived mast cell culture
cDNA	complementary DNA
Ca^{2+}	intracellular calcium
CCSP	Clara cell secretory protein

C_{DYN}	dynamic compliance of the lung
CGRP	calcitonin gene-related peptide
ChAT	choline acetyltransferase
CNS	central nervous system
COPD	chronic obstructive pulmonary disease
COX	Cyclooxygenase
Cre	cyclization recombinase
CTL	cytolytic T-lymphocytes
cPGES	cytosolic Prostaglandin E synthase
DAG	1,2-diacylcerol
DNA	deoxyribonucleic acid
DNP	Anti-Dinitrophenyl
E_{DYN}	dynamic elastance of the lung
EOS	eosinophil
EP	prostanglandin E receptor
ES	embryonic stem
FEV1	forced expiratory volume in one second
FLAP	5-lipoxygenase-activating protein
FOM	forced oscillatory mechanics
FOT	forced oscillatory technique
G	tissue damping
GPCR	G-protein coupled receptor
GPRA	G-protein coupled receptor related to asthma

H	tissue elastance
H & E	hematoxylin and eosin
HETE	hydroxyeicosatetraenoic acid
HPA	hypothalamic-pituitary-adrenal axis
HPETE	hydroperoxyeicosatetraenoic acid
IgE	Immunoglobulin E
IL	interleukin
IP	prostacyclin receptors
i.p.	intraperitoneal
IP_3	inositol 1,4,5-trisphosphate
i.t.	intratracheal
i.v.	intravenous
kb	kilobase
LO	lipoxygenase
LT	leukotriene
LPS	bacterial lipopolysaccharide
LYM	lymphocytes
MAC	macrophage
mAChR	muscarinic acetylcholine receptor
MCh	methacholine
MLCK	myosin light chain kinase
mPGES1	microsomal Prostaglandin E synthase 1
mPGES2	microsomal Prostaglandin E synthase 2

NANC	nonadenergic noncholinergic
NEU	neutrophil
NOS	nitric oxide synthase
NPS	neuropeptide S
NPSR	neuropeptide S receptor
NPY	neuropeptide Y
NPYR	neuropeptide Y receptor
NSAID	non-steriodal antiinflammatory drug
OVA	ovalbumin
PAS	periodic acid-schiff reaction
PCR	polymerase chain reaction
PCLS	precision cut lung slices
PDE	phosphodiesterase
PEEP	positive end expiratory pressure
Penh	enhanced pause
PEP	peak expiatory pressure
PG	prostaglandin
PGHS	prostaglandin endoperoxide synthase
PGI_2	prostacyclin
PIP	peak inspiratory pressure
PIP2	phosphoinositol 4,5-bisphosphate
PKA	protein kinase A
PLC	phospholipase C

PNS	peripheral nervous system
RA	rheumatoid arthritis
R_{aw}	airway resistance
R_L	resistance of the lung
Rn	newtonian resistance
RP9	Retinitis pigmentosa subtype 9
SAL	saline
SEM	standard error of the mean
SNP	single nucleotide polymorphism
SP	substance P
SPC	surfactant apoprotein-C
Te	exhalation time
T_H1	helper T cell subset 1
T_H2	helper T cell subset 2
TP	thromboxane receptor
Tr	relaxation time
TXA_2	thromboxane A_2
TXS	thromboxane synthase
U46619	(15*S*)-hydroxy-9,11-epoxymethanoprosta-5*Z*,13*E*-dienoic acid
VIP	vasoactive intestinal peptide
VRR1	vasopressin receptor-related receptor 1
WBP	whole body plethysmography
wt	wild type

CHAPTER I

INTRODUCTION

The Nature and Significance Of Asthma

Asthma is a complex genetic disorder with environmental influences and is defined by the presence of chronic airway inflammation, airway hyperresponsiveness (AHR), and reversible airflow obstruction. The presence of these three cardinal features, distinguishes asthma from other obstructive airway diseases, such as chronic obstructive airway disease (COPD), cystic fibrosis (CF), and viral wheeze (159). The chronic airway inflammation associated with asthma is eosinophillic in nature and typically involves mucus hypersecretion, airway smooth muscle (ASM) hypertrophy, collagen deposition, and mast cell degranulation. In addition to airway inflammation, the presence of AHR is a common finding in asthmatic individuals and is characterized by an exaggerated response to an otherwise mildly provoking aerosol stimulus, such as methacholine (MCh). The degree of the resultant AHR has been demonstrated to correlate with asthma severity (108). While a matter of contention, it seems likely that incessant exposure of the airway smooth muscle (ASM) to inflammatory mediators is likely to modify the physiology of the smooth muscle, thus contributing to the AHR. ASM constriction also contributes to the reversible airflow obstruction that sets asthma apart from the other obstructive airway diseases. In the asthmatic airway, airflow obstruction in highly variable and can reverse either spontaneously or with treatment. Clinically, this reversible airflow obstruction is the target of most fast acting and emergency asthma therapies, such as the β-agonists that relax ASM constriction by signaling through norepenepherin receptors. Norepenepherin signaling is the primary dilatory mechanism in the airways.

For the past 20 years, a worldwide asthma epidemic has been underway, with morbidity and mortality associated with this disease increasing throughout industrialized

nations (2, 45). In the United States, asthma is now the most prevalent disease of early childhood and affects approximately 20 million people. Of these affected individuals, approximately 5 million are children under the age of 18 (1). Asthma is considered to be a potentially fatal disease that results in approximately 1.9 million emergency room visits annually and 4000 deaths per year (3). Asthma morbidity is disproportionately higher among inner-city residents and continues to increase in all age groups, sexes, and across all racial and ethnic backgrounds (127). The cost of asthma in the United States, in the year 2000, has been estimated at 13.8 billion dollars (160). This figure represents both direct costs (such as inpatient and outpatient medical care, physician services, and short-term and long-term treatment regimes) and indirect costs (such as absence from work and school, time waiting for care, and death). However, the costs associated with a diminished quality of life (such as increased anxiety, pain, and suffering) are not included in this estimate because they are difficult to accurately assess in economic terms.

The heterogeneity of the therapeutic responses to treatment and the variable underlying genetic and environmental factors that influence the risk of developing the disorder, suggests that asthma is probably not a single disease but rather a syndrome comprised of multiple diseases with a set of similar symptoms (15, 41). This syndrome has a complex heritable pattern that is influenced by a number of genes that can contribute to an individual's susceptibility to developing asthma. Previous studies have shown that children who have one parent with asthma have approximately a 25% chance for disease development, while those with both parents affected have a 50% risk of disease (109). In general, data from twin studies suggest that the concordance rate of asthma is higher among monozygotic twins compared with dizygotic twins. For example, a study involving a large

cohort of Norwegians found a concordance of asthma of 17.9% in monozygotic twins for the relative risk for development of disease versus only 2.3% for fraternal twins (59).

In general, large-scale linkage analysis projects have only recently revealed promising candidate genes for asthma and atopy. One of the earliest linkage studies for asthma susceptibility and atopy was initiated in the late 1980's and early 1990's by Cookson *et al.* and ultimately demonstrated linkage on chromosome 11, in a region later mapped to the β chain of the high affinity IgE receptor (30). However, over a decade later, the first positionally cloned gene associated with asthma susceptibility was identified as ADAM33 on chromosome 20p (152). This gene, a disintegrin and metalloproteinase homologue with functional relevance in the airways, demonstrated a powerful association in UK and US populations. However, subsequent attempts to replicate the original observations in other populations or to observe allelic association between asthma and ADAM33 polymorphisms have failed to confirm a role for this gene in asthma susceptibility (65, 74, 87, 93, 117). In the 4 years since ADAM33, no fewer than 119 other promising candidate genes have been identified through linkage analysis and/or positional cloning (Table 1.1). Over 50 of these genes have demonstrated a strong association with the asthmatic phenotype in several different human populations (reviewed in (112)). As for the asthmatic phenotype, it should also be noted that segregation analyses have demonstrated that airway hyperresponsiveness and atopy are both genetically distinct, but clinically correlated (116). While all of these genes appear to confer a moderate risk of asthma and variable effects on pathophysiology, in most cases the biological mechanisms by which these genes influence asthma and atopy remains uncharacterized.

Table 1.1. Genes associated with asthma or atopy (modified from Ober, 2006)

Gene	Chromosomal location	Gene	Chromosomal location	Gene	Chromosomal location
CLCA1	1p22	*CD14*	5q31	*AICDA*	12p13
VCAM1	1p21	*UGRP1*	5q32	*VDR*	12q13
GSTM1	1p13	*SPINK5*	5q32	*STAT6*	12q13
CHIA	1p13	*ADRB2*	5q32-34	*IFNG*	12q15
DAP3	1q22	*IL12B*	5q31-33	*NOS1*	12q24
SELP	1q24	*HAVCR1*	5q33	*FLAP*	13q12
COX2	1q31	*HAVCR2*	5q33	*CYSLTR2*	13q14
IL10	1q32	*CYFIP2*	5q33	*PHF11*	13q14
AGT	1q42	*LTC4S*	5q35	*TCRA/D*	14q11
CHRM3	1q43	*EDN1*	6p24	*CMA1*	14q11
ACP1	2p25	*HLA-G*	6p22	*PTGDR*	14q22
KCNS3	2p24	*LTA*	6p21	*PTGER2*	14q22
IL1RL1	2q11	*TNF*	6p21	*AACT*	14q32
IL1A	2q13	*HLA-DRB1*	6p21	*IL4RA*	16p12
IL1B	2q13	*HLA-DQA1*	6p21	*CARD15*	16q12
IL1RN	2q13	*HLA-DQB1*	6p21	*NOS2A*	17q11
DPP10	2q14	*TAP1*	6p21	*CCL2*	17q12
HNMT	2q22	*HLA-DPB1*	6p21	*CCL11*	17q12
STAT4	2q22	HLA	6p21	*CCL5*	17q12
CTLA4	2q33	*PAFAH*	6p12	*STAT3*	17q21
ICOS	2q33	*IFNGR1*	6q23	*CRHR1*	17q21
IL8RA	2q35	*NOD1*	7p15	*ITGB3*	17q21
IL5RA	3p26	*GPRPA*	7p14	*TBX21*	17q21
CCR3	3p21	*CCL26*	7q11	*ACE*	17q23
CCR5	3p21	*CCL24*	7q11	*TBXA2R*	19p13
TLR9	3p21	*CFTR*	7q31	*C3*	19p13
TLR10	4p14	*NOS3*	7q36	*IL12RB1*	19p13
TLR6	4p13	*DEFB1*	8p23	*TGFB1*	19q13
MUC7	4q13	*NAT2*	8p22	*SCCE*	19q13
IL8	4q13	*IKAP*	9q31	*ADAM33*	20p13
PGDS	4q22	*TLR4*	9q33	*IFNGR2*	21q22
IL15	4q31	*C5*	9q33	*MIF*	22q11
EDNRA	4q31	*GATA3*	10p14	*GSTT1*	22q11
TLR2	4q31	*CXCL12*	10q11	*TIMP1*	Xp11
IRF2	4q35	*ALOX5*	10q11	*CXCR3*	Xq13
IL3	5q23	*FCER1B*	11q12	*IL13RA1*	Xq24
CSF2	5q23	*CRTH2*	11q12		
IRF1	5q23	*CC16/CC10*	11q12		
IL5	5q23	*GSTP1*	11q13		
IL13	5q23	*IL18*	11q23		
IL4	5q23	*C3AR1*	12p13		

The History of Asthma: From Antiquity to the Modern Era

The term "Asthma" is derived from the Greek verb aazein, meaning "to exhale with open mouth or pant" and was first used in the *Iliad* of Homer to describe the breathing of a warrior who died at the end of a battle with "asthma and perspiration" (*Iliad* 0 241; reviewed in (100)). However, the history of asthma actually begins much later in Egypt in the 1870s with the discovery of the Georg Ebers Papyrus. This document, produced around 1500 BC, chronicles the lives of the Ancient Egyptians in hieroglyphics and in particular describes the use of powdered mixtures containing sesame, balsam apple, and frankincense to treat diseases of the respiratory system (which would have included asthma). This document details the placing plant extracts on heated stones and covering the extracts with a jar, which has a reed inserted through the bottom. Individuals suffering from respiratory distress would be instructed to place their mouths around the reed and swallow the aromatic fumes (43). Thus, this papyrus describes the first use of inhalational therapy as a treatment for respiratory diseases. While the Ebers Papyrus is the oldest medical document to reference therapies for respiratory diseases, historical records indicate that the Ancient Chinese were actually treating the symptoms of these diseases almost 1500 years prior to the Egyptians (Table 1.2). Around 160 BC, *The Yellow Emperor's Canon of Internal Medicine* appeared and describes the ancient use of the herb Ma Huang for respiratory ailments (129). In the 1900s, the active chemical of Ma Huang was isolated and identified as "ephedrine".

Almost a thousand years after Hippocrates first used the word asthma as a medical term to describe difficult or labored breathing, Moses Maimonides, a medieval Jewish physician and rabbi, described the first successful treatment of a patient with asthma in his *Treatise on Asthma*. In this volume, Maimonides was summoned to care for an unnamed

Table 1.2. The History Of Asthma From Antiquity To The Renaissance

3000 BC	Historical records suggest the Ancient Chinese treated asthma symptoms with Ma Huang. In the 1900's scientists identified the active chemical of Ma Huang and called it "ephedrine".
1500 BC	In Ancient Egypt, sufferers of asthma symptoms were treated with a powdered mixture of figs, grapes, beer, frankincense, and animal dung. Hieroglyphics from the period describe a treatment in which plant extracts are heated on stones and the patient would inhale the rising vapors.
718 BC	The term "Asthma" is first used as a descriptive term for shortness of breath in *The Iliad* of Homer. It is derived from the Greek verb aazein, which means to exhale with open mouth or to pant.
460-360 BC	Asthma is first used as a medical term in the writings of Hippocrates. However, the term asthma was used interchangeably with dyspnea, tachypnea, and orthopnea. The Hippocratics noted that adults were considered more prone to asthma then children, conditions worsened in warmer districts, and symptoms were more prevalent during the fall and summer months.
509 BC – 476 AD	The Ancient Romans adopted many of the medical beliefs of the Ancient Greeks and were the first to recognize the connection between dirt and disease. However, little progress was made in treating asthma, with medical texts referring to the use of vinegar, millipedes, and homogenized fox lungs
140 AD	The Greek physician Aretaeus Cappadox wrote accurate descriptions of the disease symptoms and progression. He was also the first person to characterize asthma as an autonomous clinical entity.
130 – 200 AD	Claudius Galen further characterized the symptoms of asthma and then systematically confirmed his theoretical and clinical observations with experiments on animals. In his treatise *On Anatomical Operation*, he demonstrates that surgical severing of specific muscles and nerves can induce forceful and labored breathing.
476 AD	The Middle Ages begins with the Collapse of the Roman Empire, with much of the previously learned medical knowledge lost. Asthma remedies revert back to primitive treatments such as animal bones and dung. In the Byzantine Empire, chemical burning and skin blistering was used to pull the irritating substances from the body. Arab physicians promoted arsenic based therapies as a cure for asthma.
625 – 690 AD	Bleeding was advocated as an asthma therapy in the writings of the Byzantine physician, Paulus Aegineta. This practice continued on into the 17th century.
1135 - 1204 AD	Moses Maimonides, a Jewish physician and rabbi, composes his *Treatise on Asthma*, in which he suggests that asthma may be related to environmental factors and recommended patients move to dry climates, outside of cities, with ample fresh air, clean water, and a healthy diet.
1552 AD	Gerolamo Cardano, an Italian physician was summoned to Scotland to attend to John Hamilton, Archbishop of St. Andrews who had suffered from asthma for over 10 years. Cardano determined that the Archbishop was sick because he was too hot and thus instructed the patient to go out into fresh air as often as possible and stay away from smoky fires. He also directed the Archbishop to no longer sleep on feather mattresses, as they would make him to hot. Physicians at the time did not realize the existence of allergies. In retrospect, it is likely that the Archbishop's asthma symptoms were a result of his being allergic to feathers. Thus, Cardino's approach was instantly successful, making him the most celebrated European physician of his day.

patient who suffered from severe headaches, which did not allow him to wear his turban. The patient's symptoms were similar to the common cold and always appeared during the rainy season, which forced him to gasp for air until phlegm was expelled (128). In his writings, Maimonides outlined the benefits of proper diet and the minimal use of powerful remedies. Most notably, he provides a description of the various climates of the Middle East and discusses the improvements observed in asthma suffers who relocate to the drier climates of Egypt, as well as, the benefits of fresh air, clean water, and rural living (128).

While widespread pharmacological therapy for respiratory diseases was still centuries away, by the end of the Renaissance the most common therapy for asthma focused on lifestyle changes including improved hygiene, balanced diet, fresh air, and relocation to dry climates. The Italian physician Gerolamo Cardano, who had been summonded from Italy to Scotland to attend to John Hamilton, Archbishop of St. Andrews, first described this treatment strategy in 1552 AD. The Archbishop had been severely afflicted with asthma for over a decade and because of his powerful status, his condition had attracted a lot of attention from the medical community of the period. Upon arriving Cardano assessed the Archbishop's condition and ultimately determined that his patient was sick because he was too hot. Cardano instructed the Archbishop to stay away from smoky fires and spend extended time in the fresh air. Almost serendipitously, Cardano also reasoned that the feather beds the Archbishop was sleeping on was making him too hot at night and thus, instructed his patient to avoid feather beds and only sleep upon spun silk. The Archbishop rapidly recovered and was a prominent figure throughout Scotch politics until he was hung 15 years later (39). In retrospect, the Archbishop's asthma symptoms were likely the result of his being allergic to feathers. While described throughout history, the connection between

animals and the symptoms of asthma were not fully realized until the early 1900s with S.J. Meltzer's work with antigen induced anaphylaxis in guinea pigs (Table 1.3).

Expanding upon Cardano's work, Sir John Floyer, an English physician who was also an asthma sufferer, published *A Treatise of the Asthma* in 1697. In this book, he provides a detailed account of the disease taken from 30 years of carefully documenting his own symptoms. The factors that he noted induced asthma exacerbations included exercise, air pollution, tobacco smoke, some occupations, and prior disease exposure. Floyer was the first to introduce the possibility that heredity plays some role in asthma and provides the first detailed description of the pathological changes that occur in the lungs caused by emphysema. As human autopsies were still taboo, his observations were taken from a broken-winded mare.

During the mid-nineteenth and early twentieth century, asthma was formally described as a psychoneurosis, involving both vascular and neural mechanisms. The foundation for this description was based on the early work of Henry Hyde Salter, a London physician who published his '*Treatise on Asthma; Its Pathology and Treatment*' in 1860 (Table 1.3). Although the concept of allergy had not yet been introduced, Salter discussed the relationship between animal emanations and increased episodes of asthma. Salter also alludes to the hereditary nature of the disease and also appreciated the importance of emotional disturbances in asthma (63). One of Salter's major contributions to the understanding of asthma was the production of a comprehensive classification of the stimuli associated with exacerbations. These stimuli included exercise, cold air, animal/plant emanations, and chemical and mechanical irritants. By characterizing the mechanisms by which these stimuli induced acute episodes, Salter proposed that inflammation or congestion

Table 1.3: The History Of Asthma From The Scientific Revolution To Modern Era

1656	Pierre Borel developed the first diagnostic skin test. He applied egg extracts to patient's skin to demonstrate egg sensitivities.
1697	Sir John Floyer, an English physician who was also an asthma sufferer, published *A Treatise of the Asthma*. In this book, he provides a detailed account of the disease taken from 30 years of carefully documenting his own symptoms. The factors that he noted induced asthma exacerbations included exercise, air pollution, tobacco smoke, some occupations, and prior disease exposure. He also introduced the possibility that heredity plays some role in asthma. Floyer provides the first detailed description of the pathological changes that occur in the lungs caused by emphysema. As human autopsies were still taboo, his observations were taken from a broken-winded mare.
1811	Reports from England suggest that smoking the leaves of *Datura stramonium* provides relief from asthma symptoms. Both the leaves and seeds of this plant contain atropine. Smoking atropine and ingesting anticholinergic powders remained a common therapy well into the 20th century.
1816	R.T. H. Laennec invents the stethoscope.
1819	John Bostock, a London Physician, describes a seasonal nose infection that becomes known as hay fever
1833	Atropine, an anticholinergic alkaloid, is isolated from the *Atropa belladonna* (Nightshade) plant
1844	John Hutchinson invents the Spirometer
1860	Henry Hyde Salter, a physician and asthmatic, provides a comprehensive classification of the stimuli associated with acute episodes; however, he also realized that external stimuli were not the sole cause of exacerbations. He hypothesizes that inflammation, functioning through nerves of the air tubes, could be the stimulus that induces airway muscles to contract.
1861	The methylxanthine of coffee is isolated and named "caffeine". Use of strong coffee as an asthma therapy is often attributed to Henry Hyde Salter; however, evidence suggests that Sir John Floyer actually initiated this practice.
1888	The methylxanthine of tea is isolated and named "theophylline'. In 1940, published in Cecil's *Textbook of Medicine*, the use of theophylline as a bronchodilator is encouraged and the practice continues to the present day.
1892	Sir William Osler, in his first edition of *Principles and Practice of Medicine*, connects the reduced airway function of asthma with physiological changes in the lungs that include airway hyperresponsiveness, bronchial mucosal oedema, inflammation, mucus production and the presence of octahedral crystals (Charcot-Leyden crystals) in the sputum. Osler's description of exacerbations being induced by psychogenic stimulation leads to asthma being characterized as a psychoneurosis and thus, sedatives become a common therapy.
1900	Adrenal extracts are used in the treatment of asthma.
1906	Austrian Pediatrician Clemens von Pirquet first uses the word allergy, from the Greek word 'alol' meaning change in the original state, to describe the non-disease related symptoms that developed following treatment with a horse serum antitoxin.
1910	B. Melland injects adrenaline into asthma patients and describes dramatic improvements
1910	S.J. Meltzer proposes that asthma in humans and anaphylaxis in guinea pigs are equivalent phenomena. From this point forward, asthma was no longer considered a neurosis.
1911	Henry Dale and Patrick Laidlaw found that histamine created effects similar to those described for anaphylaxis.
1914	Inhaled or injected anticholinergics become the first line asthma therapy.
1916	Isaac Chandler Walker describes positive dermal reactions of asthmatics to proteins derived from animals, foods, and bacteria.
1921	Parusnitz and Kuster identify a "reaginic antibody" that passively transfers the acute response from one individual to another. This antibody is later identified as IgE.
1922	Huber and Koessler report on the eosinophilic nature of the inflammation associated with asthma.
1920-1930	Theophylline deriviatives begin routine use as bronchodilators.
1937	Cortisone is identified as compound E from the adrenal glands
1940–1950	The anti-inflammatory actions of glucocorticosteroids were recognized.
1946	J.J. Curry characterizes the bronchial hyperresponsiveness to graded challenges of histamine.
1950	Corticosteroids become available as an inhaled asthma therapy.
1953	Riley and West propose the connection between allergens, mast cells, and histamine.
1960s	β_2-adrenergic agonists are developed for rescue bronchodilation.
1967	The Middle East herbal remedy Khellin had been used for centuries as an antispasmonic. Roger Altounyan developed the synthetic khellin analogue, disodium cromoglycate, which is safe and effective at controlling bronchospasm when inhaled.
1972	Ipatropoium bromide, a quaternary atropine derivative, is developed as an inhaled anticholinergic therapy for asthma and other obstructive airway diseases.
1975	Bengt Samuelsson describes the generation of prostaglandins and leukotrienes from arachidonic acid.
1997	The first new class of asthma drugs in 30 years appears. The 5-lipooxigenase inhibitor (zileuton) and leukotriene receptor (CysLT1) antagonists are shown to reduce asthma exacerbations and significantly improve lung function.
1997	Anti-IgE therapies are introduced in an attempt to reduce the amount of circulating IgE. Thus, this new therapy may be able to reduce the amount of corticosteroids required to control asthma exacerbations.

was capable of stimulating airway nerves to induce muscle contractions (101). The use of anticholinergic and methylxanthine-containing herbal remedies as antispasmodics dates back to antiquity; however, Salter is typically credited with characterizing the successful management of asthma with either atropine or strong coffee ((130, 131); reviewed in (26)).

Anticholinergic agents, including the modern preparations of ipratropium bromide and tiotropium bromide, have proven to be effective bronchodilators and are utilized in the management of acute asthma. However, their use as therapies in mild intermittent asthma has not been approved in the United States, despite successful clinical trials and the reported improvement of conditions in the subsets of patients who demonstrate adverse effects to adrenergic bronchodilators (70); reviewed in (22)). The recognition that the active xanthines in coffee and tea could actually be useful as bronchodilators was not realized until the 1920s; however, by the 1940s aminophylline (the ethylene diamine salt of theophylline) was widely used in the management of acute asthma (reviewed in (26)). Theophylline is currently used in asthma therapy as a third-line drug (analogous to long-acting inhaled β_2-agonist) and is utilized in difficult to treat asthma where rescue β_2-agonist and corticosteroid treatments demonstrate reduced efficiency in controlling exacerbations (26).

As the twentieth century progressed, research shifted from viewing asthma as a disease of the nervous system to a disease of smooth muscle dysfunction with substantial research efforts being shifted towards understanding the pathobiology of the disease. In 1946, J.J. Curry characterized the airway reactivity (excessive airway narrowing and bronchial hyperresponsiveness) to dose response challenges of histamine in asthmatics (reviewed in (101)). Subsequently, in 1947 the Middle Eastern herbal remedy and anti-spasmodic Khellin, was reported to have efficacy as an asthma therapeutic (5); reviewed in

(26)). However, Khellin is relatively insoluble and has a variety of undesired side effects. Its mainstream use as an asthma therapy was due to the persistence of Roger Altounyan, a physician of Middle Eastern decent, who happened to be severely asthmatic in response to guinea pig dander. Altounyan tested extracts from the active ingredients of several anti-asthmatic folk remedies on himself after inhalation of guinea pig dander and through this process identified the safe and effective synthetic khellin analogue, disodium cromoglycate (reviewed by (22, 26)). While the mode of action of this class of compounds is still incompletely understood, the cromones are useful asthma therapies that inhibit exercise-induced and allergen-induced bronchospasms (26).

During the 1970's and 1980's multiple lines of research clearly demonstrated that airway smooth muscle is the key effector of acute airway narrowing in asthma exacerbations. However, to date, investigators have not been able to conclusively identify a specific functional abnormality of smooth muscle derived from asthmatic individuals that correlates with the bronchial hyperresponsiveness observed in the diseased airway. With few exceptions, smooth muscle tissues isolated from asthmatics and assessed by isometric force generation have demonstrated normal contractile function (140). This absence of functional ASM abnormalities has lead to the development of alternative hypotheses, which attempt to explain bronchial hyperresponsiveness and airflow obstruction including: 1) excessive ASM constriction in asthma is due to decreased airway elastance; 2) increased ASM mass in the asthmatic airway is capable of generating greater total force and increased airway narrowing; and 3) airway remodeling, airway edema, and/or increased cellular infiltration amplifies luminal narrowing, regardless of ASM dysfunction (140). Despite the complete understanding of the underlying mechanisms behind airway obstruction and bronchial

hyperresponsiveness, the foundation of the current approach to asthma pharmacotherapy is based on fast acting adrenergic bronchodilators to relax ASM constriction. This class of bronchodilators was introduced to western medicine during the 1900s in the form of adrenaline injections (102) and by the 1950s, metered dose inhalers became available to deliver epinephrine and isoproterenol (22, 26). Today, the use of the relatively specific β_2-adrenergic agonists, such as albuterol, is the primary treatment of acute asthmatic airway obstruction due to the rapid onset of action, relatively minor adverse side effects, and the resultant bronchodilation lasts approximately 4 to 6 hours.

Concurrent with advances in understanding mechanisms of smooth muscle involvement in airway pathophysiology, mechanisms underlying airway inflammation were also being pursued. Airway inflammation had been observed in the lungs and sputum of asthmatic patients since the late nineteenth century. The histologic features and eosinophilic nature of this inflammation was recognized and characterized by Huber and Koessler in 1922 (67). Subsequent characterization of lung biopsies and bronchoalveolar lavage fluid (BALF) revealed that chronic inflammation was a cardinal feature of asthma pathology during all stages (reviewed in (23)). Expanding upon these studies, mast cells, eosinophils, macrophages, and specific subpopulations of T-lymphocytes were shown to have critical roles in the immunobiology of asthma (40). These leukocytes were subsequently shown to regulate allergic inflammation and establish disease chronicity through the release of inflammatory mediators, such as prostaglandins, leukotrienes, histamine and IgE, which may act either directly on airway cells or indirectly through neural mechanisms. Simultaneous to the discovery of the inflammatory aspects of asthma, the anti-inflammatory characteristics of the glucocorticoids were also being recognized. Cortisone was initially identified from

adrenal gland extracts in 1936 and was subsequently used to treat the weakness and fatigue often suffered by asthmatics (26). The anti-inflammatory aspects of glucocorticoids were not recognized until the 1940s; however, once recognized, corticosteroids were utilized as therapies for a wide variety of inflammatory conditions. Both adrenal corticotropic hormone (ACTH) and cortisone injections were used as asthma therapies during the early 1950s, ultimately leading to the development of the synthetic corticosteroid analogue beclomethasone dipropionate in 1972 (10). With the increased recognition and understanding of the underlying airway inflammatory mechanisms associated with asthma, inhaled corticosteroid therapy has become the cornerstone of chronic asthma management.

Is Asthma A Uniquely Human Disease?

Animal modeling has been vital to elucidating the pathophysiological mechanisms underlying multitudes of chronic human diseases and have been essential to the development of therapeutics to ease human suffering. The use of animal experimentation when studying the simple physiological processes associated with pulmonary disorders is well established. However, many would argue that the complexity of the human airway and the extensive structural, physiological, pharmacological, and neuronal changes that are associated AHR can not accurately be assessed in model organisms (17, 75). Indeed it appears that only humans and a limited number of other mammalian species have been shown to spontaneously develop asthma, as determined by the presence of chronic airway inflammation and eosinophilia, AHR, and reversible airflow obstruction. Of these other species, both horses and cats spontaneously develop syndromes that closely mimic the human condition. Horses develop heaves, a naturally occurring equine asthma related to

sensitization and exposure to moldy hay. Heaves is an obstructive pulmonary disease that is characterized by chronic airway inflammation, AHR, and airflow obstruction that can spontaneously reverse or be reversed following therapy. The standard of care for heaves is similar to that for human asthma, with corticosteroid therapy utilized to manage the underlying airway inflammation and β2-adrenergic agonists to relieve ASM constriction (90, 96). It has also been demonstrated that horses demonstrate high levels of IgE in response to inhaled molds and dust and also demonstrate a positive passive cutaneous anaphylaxis test. The airway obstruction associated with heaves has been observed to reverse in situations involving only brief exposures to the hay; however, continued or extended exposures can lead to an irreversible reduction in airflow (60). This suggests that, as observed in asthmatic humans, the pathogenesis of heaves may also include the remodeling of airway smooth muscle (ASM). Unlike human asthma, the airway inflammation associated with heaves is dominated by the infiltration of neutrophils, rather than eosinophils, into the lung tissue of affected horses (86, 90). Similar to heaves in the horse, feline asthma is a naturally occurring syndrome in pet cats that closely mimics the features of human asthma. Affected animals demonstrate excessive airway reflexes, mucus secretion, wheezing, and increased AHR (42). Like horses and humans, felines respond well to β2-adrenergic agonists and corticosteroid therapy. However, unlike the neutrophilic inflammation observed in horses, the airway inflammation observed in feline asthma is eosinophilic in nature and therefore provides a more accurate model of the human condition. To date, the major reluctance to use the feline asthma model is the prohibitive cost of maintaining and propagating colonies of asthmatic cats (48).

Unlike the horse and cat, no laboratory mouse strain spontaneously develops asthma. However, allergic lung disease as a surrogate model of asthma can be induced in mice by sensitization and challenge with simple protein antigens (e.g. OVA), complex microorganisms (e.g. Aspergillus), or chemical compounds (e.g. TDI). Environmentally relevant protein antigens derived from cockroaches and house dust mites have also been employed (16, 32, 168). Short-term exposure models utilizing these antigens, in particular OVA, have been evaluated extensively and reproduce many features observed in human asthma including increases in antigen-specific IgE, increases in Th2 cytokines IL-4, IL-5, and IL-13, eosinophilic lung inflammation, goblet cell metaplasia, and airway hyperresponsiveness (reviewed in(149). However, it is important to recognize that these short-term exposure models also show many important differences from human asthma including: 1) acute peribronchiolar and perivascular inflammation in the lung parenchyma (rather than inflammation within the airway wall); 2) lack of activation, degranulation, or intra-epithelial accumulation of eosinophils; 3) significantly less plasma exudation in murine vs. human airways; 4) lack of structural changes in the airway other than goblet cell metaplasia (reviewed in(81)).

The major advantage of utilizing mouse models to assess changes in airway physiology and pathology is the ease at which the mouse genome can be manipulated. It is now a relatively straightforward process to either induce or inhibit gene expression in the lungs, either constitutively or in a spatial/temporal manner (Figures 1.1 and 1.2). These methods have been used extensively to determine the function of various genes of interest in respiratory disease development and pathogenesis. Tables 1.4-1.7 list mouse lines, each carrying a null mutation in a particular gene, which have been examined in allergic asthma

models. Physiological and histopathological phenotyping of genetically altered mice is now commonly used to determine the contribution of candidate genes to asthma pathogenesis. Despite their small size, a variety of techniques have been recently introduced to allow accurate *in vivo* assessments of the physiological changes that mediate airflow obstruction and AHR in the mouse and are summarized in Table 1.8. In addition to assessing airway function, histopathological phenotypeing is also conducted in these animals and routinely includes assessments of bronchoalveolar lavage fluid (BALF) cellularity, relative cytokine and chemokine levels present in the BALF and serum, the total and specific immunoglobin levels in the serum, the extent of leukocyte infiltration into the lung tissue, and the level of mucus hypersecretion.

Allergic Airway Inflammation and Asthma

Airway obstruction and hyperresponsiveness represent cardinal features of asthma and their contribution to the disease process has been recognized for a considerable amount of time. However, the appreciation of the role of airway inflammation in asthma pathology is still relatively new. Several current models suggest that the underlying airway inflammation likely plays a critical role in airway obstruction and hyperresponsiveness; however, the relationship between inflammation and AHR is still poorly understood. The heterogeneity of the pathophysiology observed in asthmatic individuals has presented significant hurdles in understanding the underlying mechanisms affecting airway inflammation. Allergic airway inflammation is a complex process that involves a multi-step inflammatory cascade that can be grouped into seven categories: sensitization; stimulation;

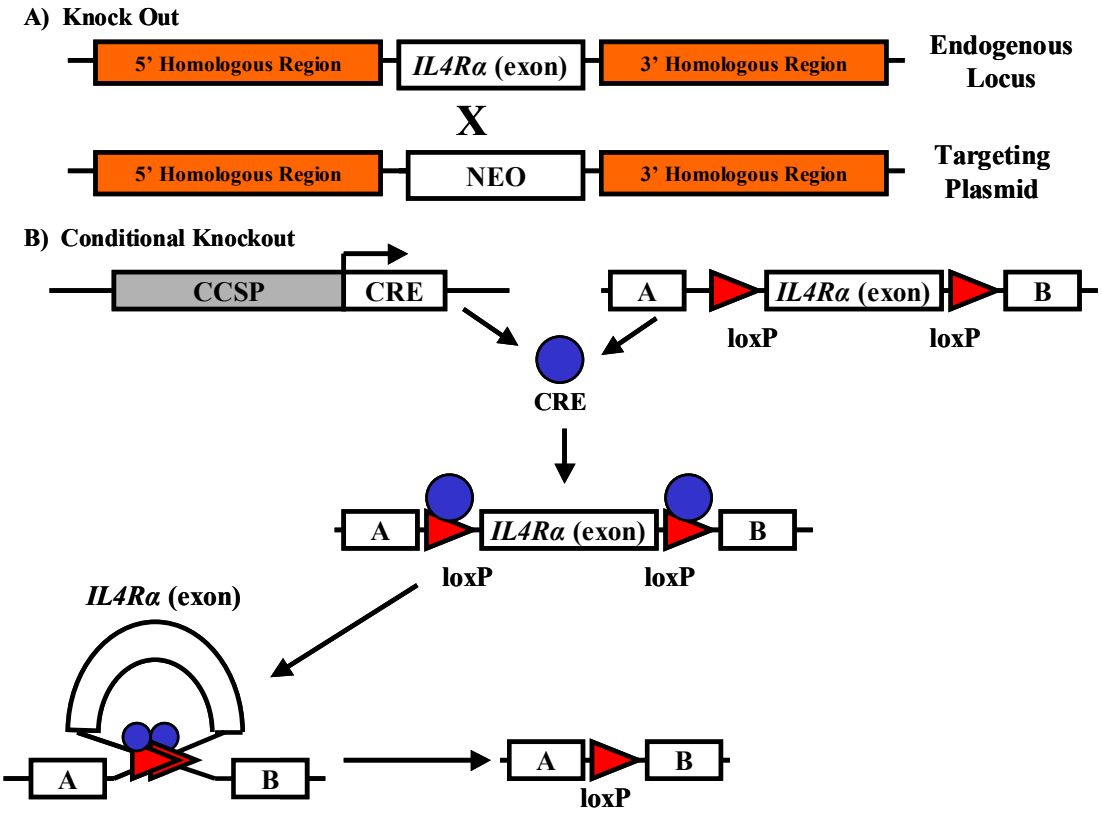

Figure 1.1. Common strategies for the creation of knockout mice. A) Schematic illustration for the development of IL-4Rα deficient mice. A targeting construct is designed containing the gene for neomycin resistance (Neo). Arms of homology are amplified from the endogenous locus from sites immediately 5' and 3' to a region critical to proper IL-4Rα functioning. These amplification products are positioned adjacent to the Neo cassette. Following homologous recombination, the targeted IL-4Rα region will be replaced with the Neo cassette. **B)** Schematic illustration of the generation of a lung specific IL-4Rα deficient mouse line. A transgene is designed containing the gene for Cre recombinase under the lung specific CCSP promoter. A second mouse is generated in which critical regions of the IL-4Rα gene are flanked by *loxP* sites. In cells carrying an integrated copy of the $loxP^2$-IL-4rα cassette, Cre mediated recombination results in excision and subsequent loss of the flanked region.

A) Transgenic

B) Lung Specific Transgenic

C) Temporal Specific Transgenic

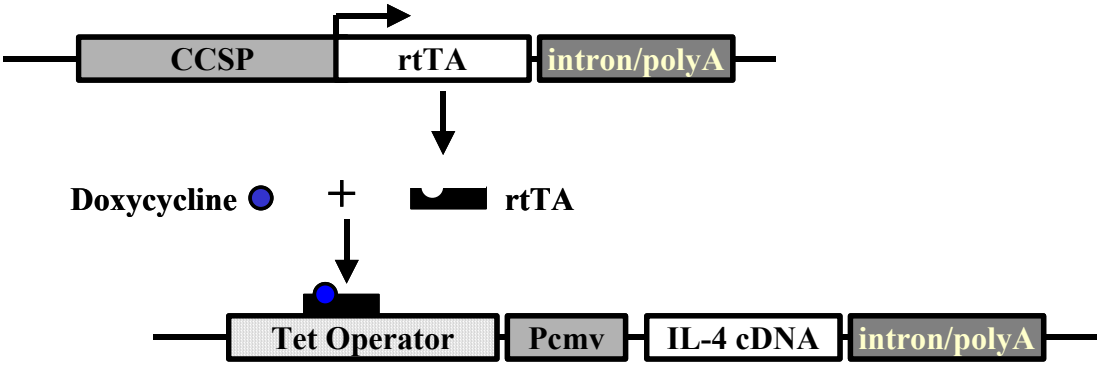

D) Temporal Specific tTS "on/off" Transgenic

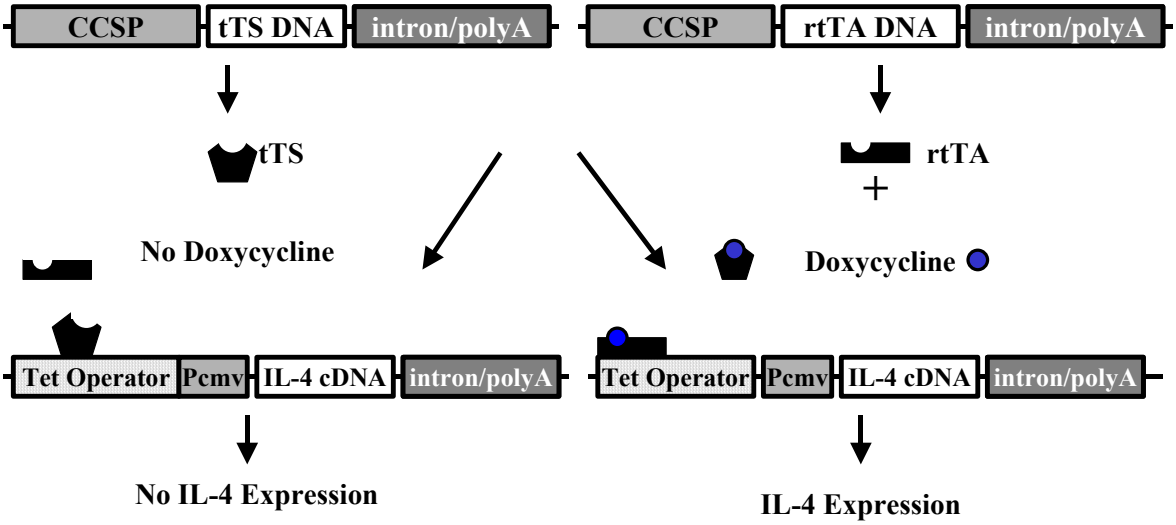

Figure 1.2. Common strategies for the creation of transgenic mice. A) Schematic illustration of an IL-4 transgene construct. A generic promoter drives expression of the IL-4 cDNA. Intronic regions and a polyadenylation sequence are included to augment transgene expression and enhance stability. **B)** Schematic illustration of a lung specific IL-4 transgene construct. The CCSP promoter facilitates lung specific constitutive expression of IL-4. **C)** Schematic illustration of a temporal specific IL-4 transgene construct. The CCSP promoter facilitates lung specific constitutive expression of the reverse tetracycline transactivator (rtTA). rtTA requires the tetracycline derivative, doxycyline, for specific DNA binding to the tetracycline operator (*tetO*). Once bound, this drives the expression of IL-4. The cytomegalovirus promoter (Pcmv) further augments expression. **D)** Schematic illustration of a temporal lung specific tTS "on/off" transgene construct. The CCSP promoter facilitates lung specific constitutive expression of both the reverse tetracycline transactivator (rtTA) and the tetracycline-controlled transcriptional silencer (tTS). In this situation, tTS binds to the tet operator in the absence of doxycycline. When doxycycline is administered, the silencer releases, allowing the rtTA to facilitate IL-4 expression. This system was designed to control for leaky transgene expression commonly encountered during the use of rtTA alone.

Table 1.4. Cytokine and Cytokine Receptor Deficient Mice

Cytokine	Mouse Strain	Inflammation Model	AHR	Eosinophilia	Airway Remodeling	References
IL-1α	BALB/c	OVA	↓	↓	na	Nakae 2003
IL-1β	BALB/c	OVA	↓	↓	na	Nakae 2003
IL-1 α/β	BALB/c	OVA	↔	↓	na	Nakae 2003
IL-1R1*	Mixed	OVA	na	↓	na	Broide 2000
IL-1R1*	BALB/c	OVA	na	↓	↓	Schmitz 2003
IL-1Ra	BALB/c	OVA	↑	↑	na	Nakae 2003
IL-1R1*	BALB/c	AF	↓	na	na	Kurup 1999
IL-4*	C57BL/6	OVA	na	↓	↑	Herrick 2000
IL-4*	BALB/c	OVA	↓	↓	↓	Leigh 2004
IL-4*	C57BL/6	OVA	↓	↓	na	Hamelmann 2000
IL-4Rα	BALB/c	OVA	na	na	↓	Whittaker 2002
IL-5	C57BL/6	OVA	↓	↓	na	Hamelmann 2000
IL-5	C57BL/6	OVA	↓	↓	↔	Foster 1996
IL-5	C57BL/6	OVA	na	↓	↓	Cho 2004
IL-5	BALB/c	IL-13	na	↓	↔	Pope 2001
IL-5Rα	BALB/c	OVA	na	↓	na	Tanaka 2004
IL-5Rα	Mixed	OVA	↓	↓	na	Tanaka 2000
IL-6	C57BL/6	OVA	↑	↑	na	Wang 2000
IL-6	BALB/c	OVA	↔	↑	↓	Qiu 2004
IL-8R	BALB/c	OVA	↓	↔	↔	De Sanctis 1999
IL-9	BALB/c	OVA	↔	↔	↔	McMillan 2002
IL-10*	C57BL/6	RW	↓	↑	na	Justice 2001
IL-10*	C57BL/6	OVA	na	↔	na	Ameredes 2001
IL-10*	Mixed	AF	↔	↑	na	Grunig 1997
IL-10*	C57BL/6	OVA	↔	↑	na	Tournoy 2000
IL-12	C57BL/6	OVA	na	↑	na	Zhao 2000
IL-12p35	C57BL/6	OVA	na	↓	na	Wang 2001
IL-12p40 (homodimer)	C57BL/6	OVA	na	↓	na	Wang 2001
IL-13*	BALB/c	OVA	↑	↔	↓	Webb 2000
IL-13*	BALB/c	OVA	↓	↑	↓	Walter 2001
IL-13*	BALB/c	OVA	na	na	↓	Whittaker 2002
IL-13*	Mixed	OVA	na	↓	na	Herrick 2003
IL-4/IL-13	BALB/c	OVA	↓	↓	↓	Walter 2001
IL-17	BALB/c	OVA	↔	↔	na	Nakae 2002

***** **Conflicting Data**
↓ **Reduced AHR or Eosinophilia compared with the wildtype animals**
↔ **No difference in AHR or Eosinophilia compared with the wildtype group**
↑ **Increased AHR or Eosinophilia compared with the wildtype animals**
na **not assessed**

Table 1.5. Chemokine and Chemokine Receptor Deficient Mice

Chemokine	Mouse Strain	Inflammation Model	AHR	Eosinophilia	Airway Remodeling	References
TNF-α	C57BL/6	OVA	↑	↑	na	Kanehiro 2001
TNFR1 (p55)	C57BL/6	OVA	↓	↓	na	Kanehiro 2002
TNFR2 (p75)	C57BL/6	OVA	↔	↓	na	Kanehiro 2002
TNFR1/ TNFR2	C57BL/6	OVA	↔	↔	↑	Rudman 2000
INF-γ	BALB/c	OVA	↔	↓	na	Hofstra 1998
FCεR1α	Mixed	OVA	↔	↓	na	Mayr 2002
CCR1	Mixed	AF	↔	↔	↓	Blease 2000
CCR2	Mixed	OVA	↔	↔	na	MacLean 2000
CCR2	Mixed	OVA	↑	↑	↑	Kim 2001
CCR2	Mixed	AF	↑	↑	↑	Blease 2000
CXCR2 (IL-8r)	not listed	AF	↑	↓	↔	Schuh 2002
CXCR2 (IL-8r)	BALB/c	OVA	↓	↔	↔	DeSanctis 1999
CXCL10	129/SV	OVA	↔	↓	na	Medoff 2002
CCR5	Mixed	AF	↓	↓	↓	Schuh 2002
CCR6	C57BL/6	CR	↓	↓	na	Lukacs 2001
eotaxin	BALB/c	IL-13	na	↔	↔	Pope 2001
eotaxin	not listed	AF	↓	↓	na	Schuh 2002
IL-5/ eotaxin	BALB/c	IL-13	na	↓	↔	Pope 2001

↓ **Reduced AHR or Eosinophilia compared with the wildtype animals**
↔ **No difference in AHR or Eosinophilia compared with the wildtype group**
↑ **Increased AHR or Eosinophilia compared with the wildtype animals**
na **not assessed**

Table 1.6. Th2 Cytokine Signaling Pathway Deficient Mice

Th2 Cytokine Signaling Pathway	Mouse Strain	Inflammation Model	AHR	Eosinophilia	Airway Remodeling	References
Fgr	C57BL/6	OVA	na	↓	na	Vicentini 2002
Hck	C57BL/6	OVA	na	↔	na	Vicentini 2002
PKCζ	129/SVJ	OVA	na	↓	na	Martin 2005
Jak3	Mixed	OVA	na	↓	na	Verbsky 2002
Stat 5α	BALB/c	OVA	na	↓	na	Kagami 2000
Stat 5β	BALB/c	OVA	na	↓	na	Kagami 2000
Stat6	C57BL/6	OVA	na	↓	na	Miyata 1999
Stat6	C57BL/6	OVA	↓	↓	na	Akimoto 1998
Stat6	Mixed	OVA	na	↓	↓	Herrick 2000
Stat4	BALB/c	CR	↓	↓	↓	Raman 2003
T-Bet (Tbx21)	not listed	OVA	↑	↑	↑	Finotto 2002
TGF-β1	C57BL/6 (HET)	OVA	↔	↑	↑	Scherf 2005

↓ Reduced AHR or Eosinophilia compared with the wildtype animals
↔ No difference in AHR or Eosinophilia compared with the wildtype group
↑ Increased AHR or Eosinophilia compared with the wildtype animals
na not assessed

Table 1.7. Prostaglandin and Leukotriene Deficient Mice

Prostaglandin/ Leukotriene	Mouse Strain	Inflammation Model	AHR	Eosinophilia	Airway Remodeling	References
PGHS-1 (Cox-1)	Mixed	OVA	↑	↑	↑	Gavett 1999
PGHS-1 (Cox-1)	Mixed	OVA	↑	↑	na	Carey 2003
PGHS-2 (Cox-2)	Mixed	OVA	↓	↑	↑	Gavett 1999
PGHS-2 (Cox-2)	Mixed	OVA	↔	↑	na	Carey 2003
PGHS-2 (Cox-2)	C57BL/6	OVA	↓	↑	↔	Nakata 2005
DP	C57BL/6	OVA	↓	↓	↓	Matsuoka 2000
IP	C57BL/6	OVA	na	↑	na	Takahashi 2002
BLT1	BALB/c	OVA	↓	↔	↓	Miyahara 2005
5-LO	Mixed	OVA	↓	↓	na	Irvin 1997

↓ Reduced AHR or Eosinophilia compared with the wildtype animals
↔ No difference in AHR or Eosinophilia compared with the wildtype group
↑ Increased AHR or Eosinophilia compared with the wildtype animals
na not assessed

Table 1.8. ***In vivo*** **physiological assessments of the mouse airway**

Method	Parameters	Advantages	Disadvantages
Whole Body Plethysmography (WBP)	Penh	1) Capacity To Measure Serial Changes Over Time 2) Evaluation of Mice During Normal Physiological Conditions 3) High Throughput and Ease of Measurement	1) Lack of Specificity of the Penh Parameter 2) Inability to Distinguish Contributions of the Upper Airway vs Lower Airway
Airway Pressure Time Index (APTI)	Airway Resistance	Only Requires Measures of Respiratory Pressures, Not Volumes or Flows	Pressure Measured Reflects Both Airway and Tissue Resistance; Thus This Is Actually An Assessment of Total Respiratory System Impedance
Equation of Motion – Single Compartment Model	Resistance (R_L) Elastance (Edyn) Compliance (Cdyn)	1) Direct Monitoring of Respiratory Mechanics 2) Can Simultaneously Assess the Level of Airway Resistance, the Ease at Which the Lungs Can Be Extended, and Lung Rigidity	The Single Compartment Model Is Based On an Oversimplified Model of the Lung; Thus, This Method Lacks the Ability to Differentiate Between Physiological Changes Occurring In Various Parts of the Respiratory Tree
Forced Oscillation Technique (FOT) – Constant Phase Model	Airway Resistance (R_{AW}) Tissue Resistance (G) Tissue Elastance (H)	Capable of Distinguishing Between Central and Peripheral Respiratory Mechanics	Similar to Other Methods Requiring Anesthesia, Airway Modulation by Neural Components May be Suppressed

cell signaling; leukocyte migration into the airways; activation of inflammatory cells; tissue stimulation/damage; and resolution. The following sections discuss the roles of key inflammatory cells and mediators involved in this inflammatory cascade.

Lymphocytes

The current paradigm to explain T-lymphocyte function in asthma has suggested that T helper type 2 (T_H2) cells mediate IgE synthesis through the activation of B-lymphocytes by IL-4, which results in the subsequent activation of mast cells (Figure 1.3). In addition to IgE synthesis, T-cells are also able to directly initiate eosinophil recruitment thorough IL-5, IL-13, and GM-CSF production (reviewed by (85)). The resultant eosinophil infiltration results in epithelial damage and ultimately results in ASM remodeling and AHR (Figure 1.3). The evidence for this is supported by the observation that asthmatic individuals present a Th2-type T-cell cytokine profile, which includes elevated levels of IL-4, IL-5, and IL-13 (125). Likewise, association studies have clearly demonstrated that increased levels of T-cell activation are associated with asthma severity, the degree of AHR, and airway eosinophil influx (123, 124, 157).

Despite the multitudes of human and animal models of allergic disease, the mechanism by which Th2 cytokines affect the cardinal features of asthma remains to be elucidated. The biological roles of IL-4 and IL-5 *in vivo* were first assessed using transgenic mice overexpressing these cytokines in lymphocytes. In 1990, Tepper et al. used an immunoglobulin promoter/enhancer to drive IL-4 transgene expression in lymphocytes (12, 151). Mice constitutively expressing increased amounts of IL-4 developed a marked increase in serum IgE and IgG1 levels, as well as, allergic inflammation in the eyes. In the same year,

Dent et al. reported their findings with transgenic mice over-expressing IL-5 (38). The expression of IL-5 was driven by its own promoter. IL-5 transgenic mice exhibited eosinophilia in the bone marrow, bloodstream, spleen, lymphoid organs, gut, and the lung. While these experiments demonstrated an *in vivo* role for these cytokines in IgE production and eosinophilia, two classic phenotypic features of asthma, it was the development of lung-specific tissue expression systems that has helped elucidate the effects of IL-4, IL-5, and other inflammatory mediators on the lung itself.

Initial studies in IL-4 deficient mice demonstrated that IL-4 was essential for the development of allergic airway inflammation, as these mice failed to demonstrate a phenotype in response to allergen challenge (11). Supporting this finding, antibody neutralization of IL-4 prior to allergen sensitization prevents the development of allergic airway inflammation; however, if the same treatment was given after sensitization but prior to allergen delivery to the lung, the antibody treatment was ineffective (31). These studies suggest that IL-4 is essential for the initial development and expansion of antigen specific Th2 polarized cells; however, it is not essential for the effector phase of the response. Prior studies of the IL-4 receptor-signaling cascade had demonstrated that this receptor and its downstream effectors were essential for the development of disease (53, 83); thus these findings suggested that another ligand could signal through the IL-4α receptor.

IL-13 has been shown to be a potent inducer of AHR, eosinophilic inflammation, and mucus hypersecretion in naïve mice when added exogenously or following targeted overexpression in the lungs (55, 165, 169). Based on the similarity of structures between IL-4 and IL-13, it was hypothesized that IL-13 may also function through the IL-4α receptor. Studies conducted with IL-13 deficient mice demonstrated that antigen sensitization and

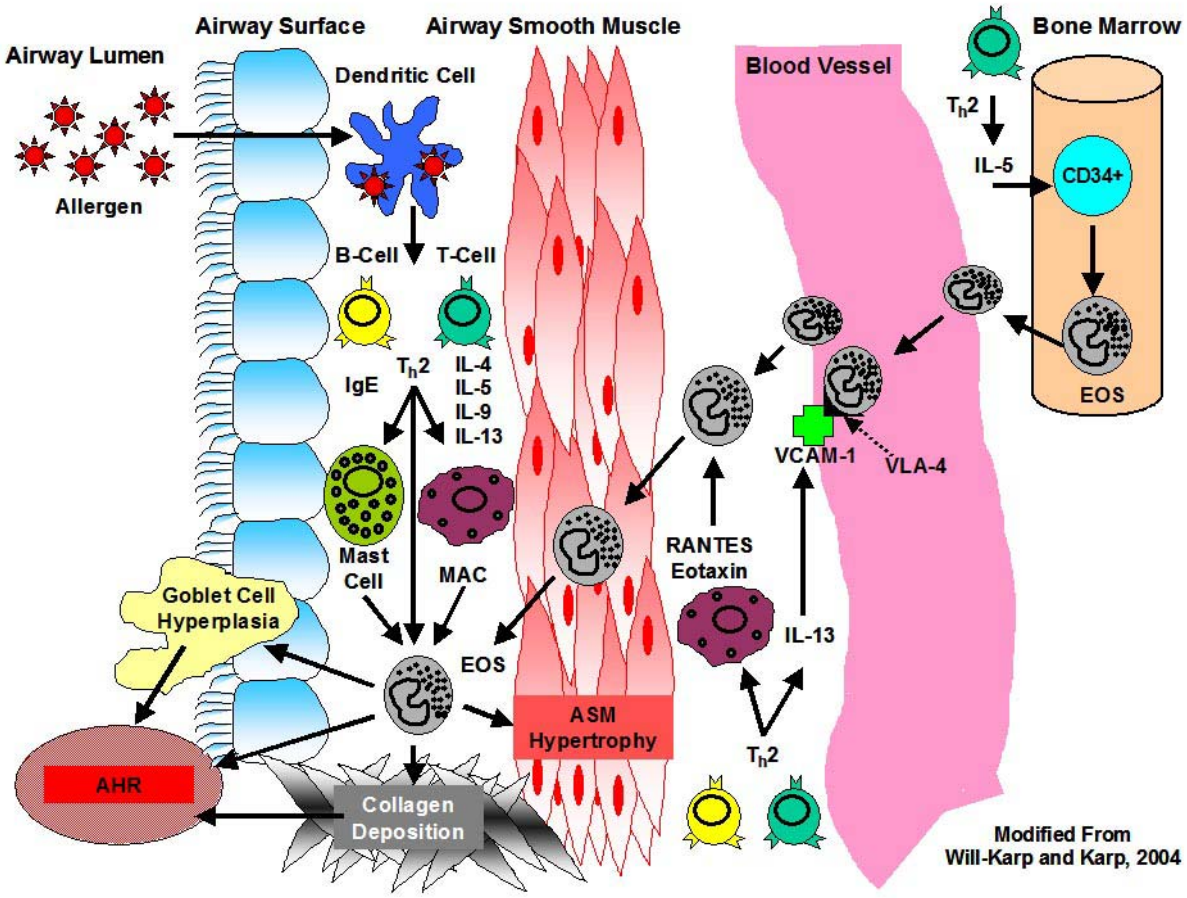
Airway Lumen
Airway Surface
Airway Smooth Muscle
Blood Vessel
Bone Marrow
Allergen
Dendritic Cell
B-Cell
T-Cell
IgE
Th2
IL-4
IL-5
IL-9
IL-13
Mast Cell
MAC
EOS
Goblet Cell Hyperplasia
AHR
Collagen Deposition
ASM Hypertrophy
RANTES
Eotaxin
VCAM-1
VLA-4
IL-13
Th2
IL-5
CD34+
EOS
Modified From
Will-Karp and Karp, 2004

Figure 1.3. Allergic Airway Inflammation. Allergic airway inflammation is initiated by allergen presentation at the airway surface by dendritic cells, which results in Th2 cell differentiation, cytokine production (IL-4, 5, 9, and 13) and allergen specific IgE production. Resident lymphocytes, macrophages, and mast cells orchestrate the ensuing inflammatory response ultimately characterized by an influx of eosinophils into the airways. CD4+ T-cell derived IL-5, IL-13, and GM-CSF facilitates the maturation of eosinophils from CD34+ progenitor cells. Once cells have committed to the eosinophil lineage, IL-5 mediates migration from the bone marrow into the vasculature. Subsequent production of IL-4 and IL-13 at sites of inflammation, induce expression of vascular cell adhesion molecule-1 (VCAM-1), which binds to the VLA-4 receptors on the eosinophil surface. This interaction facilitates the preferential extravasation of eosinophils through the vessel walls and subsequent release of eosinophil chemotactic substances, such as RANTES and eotaxin, from responding leukocytes mediate the migration of eosinophils to sites of inflammation. Though the exact role eosinophils in allergic airway disease in poorly defined, once on site, eosinophils likely contribute to the pathogenesis of allergic asthma by acting on fibroblasts, smooth muscle, and epithelial cells to ultimately cause airway hyperresponsiveness and remodeling.

challenge failed to elicit AHR or significant mucus hypersecretion, despite having increased levels of IL-4 and IL-5. These experiments were verified following the observation that increased AHR and mucus hypersecretion occurred following reconstitution of IL-13 deficient mice with recombinant IL-13 (158). Together, these data demonstrate that the biological actions of both IL-4 and IL-13 are mediated through the IL-4α receptor and IL-4 is essential for the initiation of the Th2 polarized response to allergens, while IL-13 likely mediates the primary pathophysiological immune responses.

B-lymphocytes are the primary effector cells targeted by the IL-4 and IL-13 released by T-lymphocytes. Antigen specific IgE is produced by B-cells following the isotype switching from IgM to IgE in response to either IL-4 or IL-13. IgE antibodies subsequently bind to the carboxylic fragment of the ε heavy chain of the specific high affinity FcεRI receptor, which is predominately expressed on mast cells, basophils, and dendritic cells. Following allergen exposure, cross-linking occurs between adjacent antigen binding components of IgE on mast cells, which induces degranulation and the subsequent release of mast cell derived mediators (see Mast Cells below). Since its discovery, the IgE antibody has been viewed as a potential target for asthma drug discovery. Therapeutic approaches have included attempts to desensitize atopic subjects to the triggering allergen, as well as, attempts to stimulate the anti-IgE production in the patient (reviewed in (33)).

Eosinophils

Many factors mediate eosinophil recruitment to the inflamed lungs including proinflammatory cytokine (IL-4, IL-5 and IL-13) and chemokine (Eotaxin) expression. Increasing levels of IL-4 and IL-13 induce the expression of vascular cell adhesion molecule-

1 (VCAM-1) along the pulmonary vasculature at sites of inflammation. VCAM-1 binds to the eosinophil VLA-4 receptor and leads to the extravasation of eosinophils through vessel walls into sites of inflammation (Figure 1.3) (164). Even the unique and complex structure of the pulmonary capillary bed and local hemodynamic factors can influence airway eosinophilia (98). While airway eosinophilia is a cardinal symptom of asthma, the mechanisms underlying eosinophil migration into the inflamed lung is quite complex and not completely understood. Likewise, the actual significance and function of eosinophils in the lung tissue and their effects on AHR is poorly defined. Recent eosinophil deficient mouse models have provided unique, yet divergent, insights into the role of airway eosinophilia following allergen-mediated respiratory inflammation (68, 88). Using a knockout mouse model lacking a specific high-affinity binding site for the transcription factor GATA-1, Humbles et al. demonstrated that eosinophil deficient mice have reduced features of allergic lung disease, such as airway remodeling, but are still capable of developing airway hyperreactivity and mucus hypersecretion (68). On the other hand, Lee et al. demonstrated that their eiosinophil deficient mice, which are transgenic mice that express the diphtheria toxin A chain under the control of the eosinophil peroxidase promoter (PHIL), do not develop airway hyperreactivity and demonstrate attenuated mucus hypersecretion (88). Strain variations and differences in the methods utilized to generate the eosinophil deficient mice could reconcile the apparent discrepancies observed between these two studies. However, despite the availability of eosinophil deficient mice, many questions still remain regarding the mechanism behind, and significance of, the recruitment of eosinophils into the airways of asthmatic individuals.

Mast Cells

Mast cells are the primary effector cells of acute allergic reactions and likely play a critical role in the early phase of allergic airway disease. During the sensitization period, allergen specific IgE is generated by B-lymphocytes and attach to mast cells at the high affinity FcεRI receptor. Subsequent allergen exposure induces cross-linking between adjacent antigen binding fragment components of IgE on the mast cells, which in turn induce degranulation and the secretion of mediators such as histamine, serotonin, chymase, tryptase, and various lipid mediators such as prostaglandins and leukotrienes. These mast cell mediators induce airway obstruction by inducing smooth muscle constriction, vascular leakage, and mucus hypersecretion (33). Mast cell derived cytokines and chemokines, such as IL-4, IL-5, and IL-6 can further perpetuate the inflammatory cascade through the local recruitment and activation of eosinophils and lymphocytes (33).

The exact role of mast cells in chronic airway inflammation, including the late phase responses of AHR, airway eosinophilia, and airway remodeling is controversial (148, 163). Mast cell deficient mice develop eosinophilic airway inflammation and AHR at levels similar to those observed in wild type mice (82, 111, 148, 163). However, as Williams and Galli have demonstrated, based on the OVA model employed (i.e. with or without adjuvant) conflicting data has been generated with regards to mast cell function in allergic airway disease. These data further suggest that the most likely function of mast cells in allergic airway disease is as a local amplifier of antigen-dependent inflammation through the release of proinflammatory mediators such as histamine, prostaglandin D_2, and platelet activating factor (163).

Lipid Mediators and Associated GPCRs

The Arachidonic Acid Pathway

Prostanoids, along with leukotrienes and HETES, belong to a family of mediators termed eicosanoids. Eicosanoids are formed in the organism from arachidonic acid (AA) and other polyunsaturated 20 carbon fatty acids (110). They are generally not stored free in tissue, but are synthesized as a result of membrane perturbations that cause the release of free fatty acids, generally AA, from esterified lipid sources. Release of AA from the sn-2 position of glycerol by one of several phospholipases, particularly by the action of $cPLA_2$, is the first step in the production of all eicosanoids (105). Phospholipase A_2 activity can be stimulated by complement fragments, IgE receptor activation, immune complexes, opsonized particulate matter, and microorganisms. The eicosanoid produced from the released AA depends on the expression and activity of various enzyme pathways within the cell (Figure 1.4). Prostanoids are produced when the released AA is converted into the bis-oxygenated intermediate PGH_2, a reaction catalyzed by prostaglandin endoperoxide synthase (PGHS), commonly referred to as cyclooxygenase (COX)(139). Two isoforms of this enzyme, COX-1 and COX-2, encoded by two different genes, have been characterized (138, 139). The regulation of expression of these two genes is very different. COX-1 expression can be detected at low levels in virtually all cells. However, while the expression of COX-1 differs in various cell populations, in general, the level of COX-1 changes little in response to physiological stress. In contrast, dramatic changes in the expression of COX-2 can be induced by a number of different stimuli (47, 137).

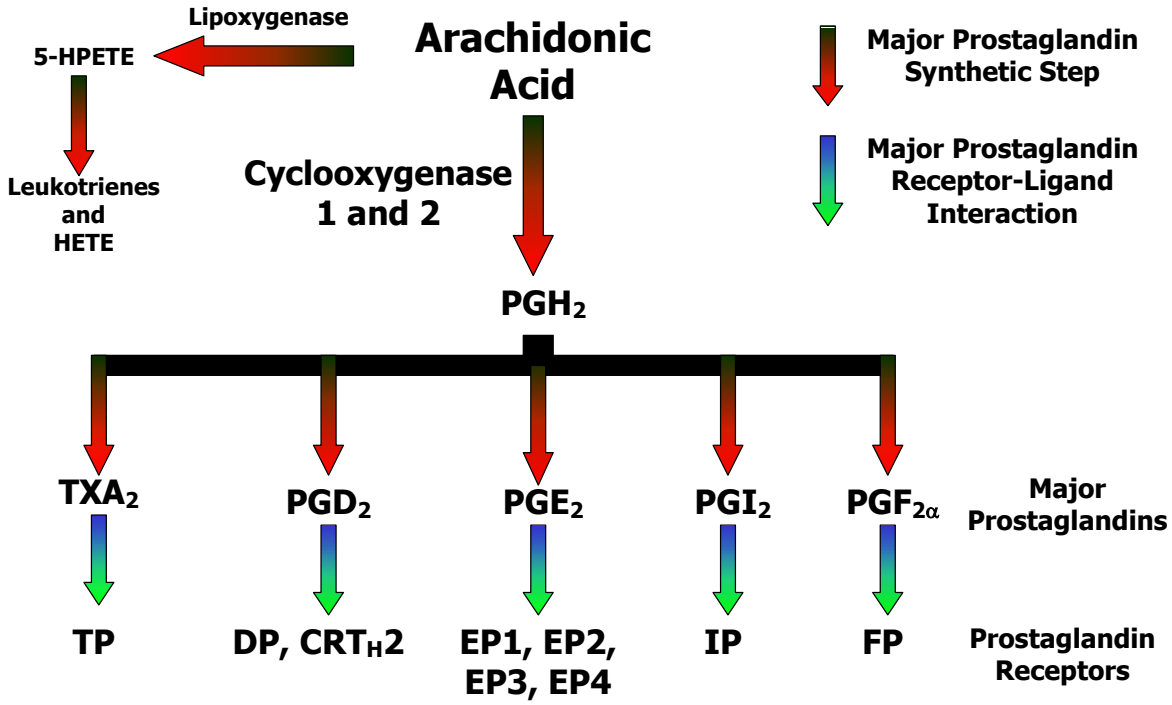

Figure 1.4. The generation and metabolism of arachidonic acid.

This simple classification of these two enzymes may be considered an over-simplification that is not applicable to all cells and organ systems. For example, expression of COX-2 has been detected in unstimulated cultured human tracheal epithelial cells, and was actually reported to be expressed at higher levels than COX-1 (156). Immunohisto-chemical examination of biopsies of airway epithelium obtained from healthy subjects also indicates that both COX-1 and COX-2 are expressed in the unchallenged airways (37). Even though expression of both COX-1 and COX-2 was detected in samples prepared from airways of stable asthmatic patients, surprisingly these studies did not demonstrate increased expression of either synthase (37). This might indicate that the increased prostanoids present in the BALF of asthmatics might be due to other factors such as increased substrate availability or production by recruited inflammatory cells.

Thromboxane

PGH_2 produced by COX is further metabolized to form PGE_2, $PGF_{2\alpha}$, PGD_2, prostacyclin (PGI_2), and thromboxane (TXA_2), all of which have diverse biological actions (Table 1.9). Thromboxane is formed by further metabolism of PGH_2 by thromboxane synthase (TXAS)(135). In aqueous solutions, TXA_2 is rapidly hydrolyzed to TXB_2, a stable and inactive metabolite. Because of its short half-life, TXA_2 functions primarily as an autocoid and its actions are limited to tissues in close proximity to the source of its synthesis. Because of the instability of TXA_2, most studies utilize the stable analogue U46619. Thromboxane synthase is present in a broad spectrum of cells and tissues, including the lung and immune cells. Elevated levels of thromboxane and other prostanoids have been measured in the BALF from asthmatic airways (94, 113, 150).

Table 1.9. Prostaglandins and Their Biological Actions

Synthase	Expression	Prostaglandin	Receptor	G-Protein	Expression	Biological Actions
TXS	Platelet	TXA_2	Tp	Gq	VSM; ASM Platelet	Constriction Aggregation
PGIS	Endothelium	PGI_2	Ip	Gs	VSM; ASM Platelet	Relaxation Declumping
PGFS	Uterus	$PGF_{2\alpha}$	Fp	Gq	USM USM	Contraction Parturition
PGDS	Mast Cells	PGD_2	Dp_1	Gs	Lung	Allergic Asthma
			Dp_2*	n/a	Lymphocytes	Chemotaxis
PGES	Various	PGE_2	Ep_1	Gq	Neurons	Pain Response
			Ep_2	Gs	Ovary	Maturation
			Ep_3	Gi	Neurons	Fever
			Ep_4	Gs	Osteoclast	Bone Resorption

* Dp_2 is a member of the chemoattractant subgroup

The actions of TXA_2, as well as other prostanoids, are mediated through binding to specific G protein coupled receptors, which are named after the native prostaglandin that is the receptors most potent agonist (Ip is the receptor for PGI_2, Tp for TXA_2) (reviewed in (28, 107)). All of the known activity of TXA_2 is mediated via a single receptor termed Tp. In humans, alternative splicing of the carboxyl-terminal tail results in two isoforms of the Tp receptor, Tpα and Tpβ (28, 57, 58, 107). The significance of the two isoforms is still unknown; however, it appears both isoforms similarly activate PLC but differently regulate adenylyl cyclase activity (61). The Tp receptor is coupled to the G_q family of proteins, and many of its physiological actions have been attributed to G_q associated activation of PLC and increases in intracellular calcium (66). Recently, it has been suggested that in airway smooth muscle cells, coupling to G_i can occur and that this coupling may be important in the growth response of smooth muscle cells to thromboxane (24). Total RNA analysis indicates that the receptor is broadly expressed throughout the mouse. A variety of cell types are known to maintain high levels of Tp receptor expression, including thymus, lung, endothelial cells, brain, and kidney (6). Tp receptor expression has also been documented on airway smooth muscle cells and expression on neurons has been implied from pharmacological studies.

Airway Smooth Muscle and Asthma

While many lung diseases have symptoms that are similar to asthma, this disease can be distinguished by variable and reversible airflow obstruction, AHR, and eosinophilic airway inflammation. However, the relationship between inflammation and asthma is complex, with no clear correlation between the severity of inflammation and the severity of airflow obstruction and AHR. While inflammation is almost always present in asthma, it is

not sufficient to explain all of the pathophysiological features of disease. In addition to the accumulation of eosinophils and lymphocytes in the airway, asthma pathophysiology also demonstrates altered smooth muscle and epithelial cell function, thickening of the sub-epithelial collagen layer, mucus cell hyperplasia/metaplasia, and smooth muscle hypertrophy and hyperplasia (77). In many cases of fatal asthma, a substantial increase in the thickness of the airway wall was observed throughout the bronchial tree, which was at least partly due to smooth muscle hypertrophy (72). Asthmatic individuals who have experienced symptoms for an extended period of time often develop a certain degree of fixed airflow obstruction, which cannot be reversed. The pathological basis for this phenomenon is largely unknown but likely involves smooth muscle hypertrophy, rather than the destructive obliterative bronchitis and emphysema that characterize the fixed airflow obstruction associated with chronic obstructive pulmonary disease (COPD).

Smooth Muscle Myogenesis

Smooth muscle cells in mature animals are highly specialized cells whose principle function is contraction. These cells typically express a unique range of contractile proteins, ion channels, and signaling molecules, which regulate the cell's contractile functions. The plasticity of smooth muscle cells allow the smooth muscle to undergo remarkable phenotypic adjustments in response to changes in the local environment and differentiates these cells from the terminally differentiated skeletal and cardiac muscle (114). In addition to profound phenotypic changes, smooth muscle cells can also undergo relatively minor changes such as alterations in calcium sensitivity and handling, which can have dramatic effects on physiology (141). During development, smooth muscle cells can exhibit a wide range of

phenotypes and exhibit very high rates of synthesis of extracellular matrix components including collagen, elastin, proteoglycans, cadherins, and integrins (115). In contrast, smooth muscle cells in mature organisms are dedicated to carrying out their contractile functions and typically demonstrate low rates of turnover/proliferation and a significantly slower rate of synthesis of extracellular matrix components (115). A variety of smooth muscle selective or specific genes and gene products have been identified that serve as useful markers of the state of smooth muscle differentiation including SM22α and the smooth muscle myosin heavy chain (SM-MHC) (50, 52, 97). In fact, the promoters for these genes have been particularly useful in directing targeted expression or deletion of various genes in smooth muscle. These promoters has been shown to produce high levels of EGFP expression in smooth muscle cells at various embryonic time points and in adult tissues (64, 119). These transgenic mice display strong vascular and airway smooth muscle specific fluorescence and there appears to be excellent overlap between fluorescence and Cre activity (64, 166).

ASM Constriction and Relaxation

Airway smooth muscle (ASM) constriction is considered to be the primary mediator of both the airway hyperresponsiveness and reversible airflow obstruction observed in the asthmatic airway (Figure 1.5). ASM is highly innervated by postganglionic parasympathetic nerves, emanating from the vagus nerve, which release endogenous acetylcholine (ACh). This endogenous ACh release activates M3 muscarinic acetylcholine receptors (mAChRs) located directly on the smooth muscle cells. Ligand binding induces a conformational change in the M3 mAChR, which results in a high affinity for the Gq protein associated with GDP. Upon binding the M3 mAChR, the Gq protein releases GDP, which exposes the binding site

to either GTP or GDP. The cytosolic concentration of GTP is significantly higher than GDP, resulting in the reaction favoring it's binding to the Gq protein. Following GTP binding to Gq, this complex dissociates from the M3 mAChR and activates Phospholipase C (PLC). Activated PLC catalyzes the hydrolysis of phosphoinositol 4,5-bisphosphate (PIP2) into 1,2-diacylglycerol (DAG) and inositol 1,4,5-trisphosphate (IP3). IP3 binds IP3 receptors on sarcoplasmic reticulum Ca^{2++} stores leading to the release of Ca^{2++} into the cytosol and subsequent binding to calmodulin. The Ca^{2++}/calmodulin complex activates myosin light chain kinase (MLCK), which subsequently phosphoryates myosin light chains. This phosphorylation promotes the ATPase activity of myosin, which is required for cross-bridge cycling and subsequent smooth muscle contraction. In addition to the M3 mAChR, other Gq protein coupled receptors are expressed on ASM and can similarly mediate contraction (Table 1.10) (reviewed in (8, 9)).

GPCRs located directly on the smooth muscle cells can also mediate ASM relaxation or suppression of constriction (Figure 1.5). The Gs-coupled β2-adrenergic receptor (β2-AR) mediated signal transduction pathway, provides an example of a well-characterized ASM relaxation mechanism. Endogenous norepinephrine or exogenously administered beta-agonists bind to and activate the β2-AR leading to a high affinity for Gs-proteins coupled with GDP. Ligand binding induces a conformational change in the β2-AR, which results in a high affinity for the Gs protein associated with GDP. Once bound to the activated receptor, as previously described for Gq-coupled receptors, the Gs protein undergoes a conformational change, which releases the GDP and allows GTP access to the binding site. Once bound, the Gs protein/GTP complex dissociates from the β2-AR and binds to membrane bound adenylyl cyclase (AC). Activated AC catalyzes the conversion of ATP into cAMP, which can then

Figure 1.5.

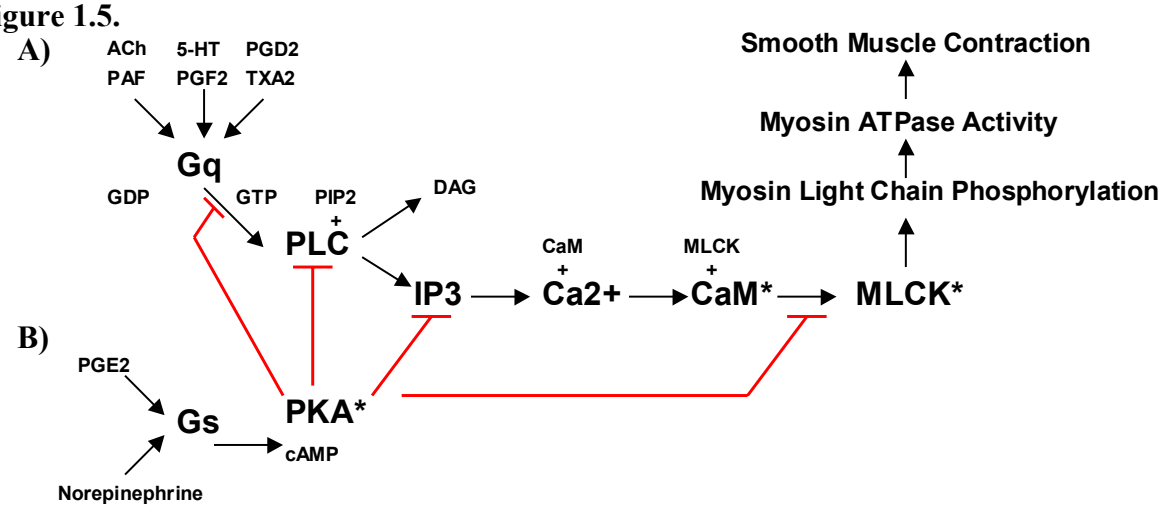

Figure 1.5. Airway Smooth Muscle Constriction and Relaxation. A) Model of Gq mediated airway smooth muscle constriction. The respective ligand activates the appropriate Gq protein coupled receptor. Once activated, the Gq+GTP complex dissociates from the GPCR and activates Phospholipase C (PLC). Activated PLC catalyses the hydrolysis of PIP2 into DAG and IP3. IP3 then binds IP3 receptors on sarcoplasmic reticular calcium stores causing the release of calcium into the cytosol. The increase in calcium promotes calcium binding to calmodulin. The resultant calcium/calmodulin complex activates Myosin Light Chain Kinase (MLCK). Activated MLCK phosphorylates myosin light chains and thereby promotes the ATPase activity of myosin, which is required for cross-bridge cycling and contraction. **B)** Model of airway smooth muscle relaxation by protein kinase activation via a Gs protein coupled receptor. Activated PKA can phosphorylate certain Gq coupled receptors, as well as PLC, both of which inhibits the Gq mediated generation of IP3. Activated PKA also phosphorylates IP3 receptors, which lowers their affinity for IP3, thereby decreasing the ability of IP3 to increase intracellular Ca levels. Activated PKA also phosphorylates MLCK, which decreases its affinity for the calcium/calmodulin complex, further reducing the contractility of airway smooth muscle.

Table 1.10. GPCRs Associated With Airway Smooth Muscle Function (modified from Billington, 2003)

Ligand	GPCR	G protein	Smooth Muscle Function
Acetylcholine	m2	Gi	Inhibition of Relaxation*
	m3	Gq	Constriction
Serotonin	5HT2a	Gq	Constriction
Adenosine	A1	Gi	Inhibition of Relaxation*
	A2b	Gs	Relaxation
Histamine	H1	Gq	Constriction Potentiation of Growth
Bradykinin	BK	Gq	Constriction
Endothelin	ET-A/B	Gq	Constriction Potentiation of Growth
Neurokinin	NK-1/2	Gq	Constriction Potentiation of Growth
Norepinephrine	β2-AR	Gs	Relaxation Growth Inhibition Cytokine/Chemokine Regulation
CysLT	CLT1R	Gq	Constriction Potentiation of Growth
PGE	EP2	Gs	Relaxation Growth Inhibition Cytokine/Chemokine Regulation
PGI	IP	Gs	Relaxation Growth Inhibition
TXA2	TP	Gq	Constriction Potentiation of Growth

* The mechanism behind Gi mediated ASM constriction is possibly mediated through inhibiting adenylyl cyclase or activating Ca^{2++} activated potassium channels

activate Protein Kinase A (PKA). Activated PKA inhibits ASM constriction through phosphorylation of Gq-coupled receptors, PLC, IP3 and MLCK. In addition to the β2-AR, other G-protein coupled receptors are expressed on ASM and can similarly mediate relaxation (Table 1.10) (reviewed in (8, 9)).

Thromboxane Mediated Constriction of Smooth Muscle and Airway Responsiveness

Ellis *et al.* reported in 1976 that when human platelets aggregate, material is released that rapidly contracts strips of coronary artery and that this response was indomethacin sensitive and was similar to that induced by thromboxane (46). Svenssen confirmed these findings by showing that thromboxane could contract guinea pig trachea (143). TXA_2 is also a potent bronchoconstricting agent in humans. Pharmacological evidence suggests that the Tp receptor not only mediates TXA_2 constriction but also that at least some of the constricting actions of PGF_{2a}, PGD_2, and 8-epi-PGF are the result of the cross-reactivity of these eicosanoids with the Tp receptor (27).

Very early studies examined the effect of a thromboxane synthesis inhibitor on bronchial responsiveness to acetylcholine in asthmatics. The provocative doses of acetylcholine produced a 20% fall in FEV1, which was increased in asthmatics receiving the thromboxane synthase inhibitor (51). Studies in dogs reported that transient exposure to U46619 caused substantial augmentation of the contractile response induced by efferent vagus nerve stimulation. These data suggested that thromboxane had a direct effect in augmenting the airway contractile response to efferent vagus nerve stimulation that was not related to generalized mechanical contraction of airway smooth muscle (106). More recent studies in the dog suggest that the interactions between the cholinergic pathways and

thromboxane might be more complex. Takata *et al.* report that the response of tracheal strips to acetylcholine was not affected by pretreatment with U46619, whereas subthreshold levels of U46619 enhanced the response of bronchial rings (147). This difference in the action of thromboxane at different levels of the airways is of clinical interest. In humans, Jones *et al.* exposed healthy and asthmatic patients to TXA_2 (73). They reported that U46619 was a potent *in vivo* bronchoconstrictor. They also report that subthreshold concentrations of U46619, but not histamine, increased methacholine airway responsiveness. More recently, a similar interaction has been described in the guinea pig. Airway hyperresponsiveness to acetylcholine was dose dependently enhanced by locally inhaled PGD_2, U46619, LTD_4, and LTE_4 (133).

Neural Mechanisms and Asthma

The nervous system is divided into the somatic nervous system and the autonomic nervous system. Organs under the control of the somatic nervous system are considered to be under voluntary control, while the autonomic nervous system regulates involuntary organ function and maintains homeostasis. The autonomic nervous system predominantly functions as an efferent system transmitting signals from the central nervous system (CNS) to the peripheral nervous system (PNS) and effects physiological functions such as heart rate and contraction, smooth muscle constriction, visual accommodation, and secretions from exocrine and endocrine glands. With few exceptions, autonomic nerves constitute all of the efferent fibres exiting the CNS; however, some afferent autonomic fibres, which mediate vasomotor and respiratory reflexes, are carried to the CNS by major autonomic nerves such

as the vagus, splanchnic, or pelvic nerves. The actual cell bodies of these afferent nerves sit just outside of the CNS in a ganglion defined as the nodose ganglion.

The autonomic nervous system is divided into the parasympathetic nervous system (PNS) and sympathetic nervous system (SNS) on the basis of anatomical and functional differences. Both systems consist of myelinated preganglionic fibres, which form synapses with unmyelinated postganglionic fibres that innervate the effector organs. These synapses typically occur in clusters and are defined as ganglia. Most organs are innervated via both sympathetic and parasympathetic nerves, which typically generate opposing actions. The SNS evokes responses such as pupil dilation, muscle vasculature dilation, and heart rate increases, which are all characteristics of the so-called "fight-or-flight" response. Opposing these actions "post-threat", the PNS has several specific functions that include stimulating the gut, constricting the pupils, and slowing the heart. The physiological state of the body at any given time represents a balance between the PNS and SNS. In fact, a long-standing hypothesis regarding asthma states that it is a disorder of the autonomic nervous system and represents an imbalance between the sympathetic and parasympathetic nervous systems (146).

Airway Afferent Innervation

Gas exchange is a dynamic and demanding process facilitated by the airways and lungs, which must adapt and respond to the demands for oxygen by tissues throughout the body. To maximize and promote efficient gas exchange, the lungs and airways rely on various afferent nerve subtypes to monitor respiration and facilitate defensive reflexes. These pulmonary afferent nerves are conducted by the vagus nerve and can be classified by

their receptor sensitivities and responses to various stimuli and individual fiber conduction velocities. The primary afferent nerves in the larynx are characterized into pressure, cold, drive, irritant, and C-fiber endings, while the afferent nerves of the trachea and bronchi are characterized into slowly adapting receptors (SARs), rapidly adapting receptors (RARs), C-fibre endings, and sensory receptors in neuroepithelial bodies (NEBs)(reviewed in (161)).

Morphologic studies have shown that approximately 75% of the afferent fibers in the bronchopulmonary vagal branches are unmyelinated C-fibers, which span the entire respiratory tract, innervating from the lung parenchyma to the large conducting airways (4). Activation of these afferents can mediate bronchospasm and facilitate the coughing reflex in humans (76). In most species, tachykinins, calcitonin gene-related peptide (CGRP), and other neuropeptides are synthesized in the cell bodies of these sensory neurons that are located in the nodose and jugular ganglia. Bronchopulmonary C-fibers are nociceptors and possess polymodial sensitivity to distinct chemical stimuli, which can be roughly divided into either exogenous chemical substances or endogenously released mediators. Capsaicin, a pungent ingredient of hot peppers, is the most extensively characterized exogenous C-fiber specific stimulant, and is often used to identify the presence of these afferent endings in tissues and organs.

Capsaicin functions through the activation of the vanilloid receptor subtype 1 (VR1), a ligand-gated, non-selective cation channel belonging to the TRP channel superfamily. In addition to capsaicin, VR1 is also responsive to acidic solutions with a pH of 5-6 and temperatures above 43^{o}C, which correspond to the acidic microenvironment produced during inflammation and ischemia, and to the threshold temperature for pain perception (84, 118). In support of these observations, naïve VR1 receptor deficient mice exhibit altered

behavioral responses to heat (>52.5^{o}C) and thermal hyperalgesia, and these mice exhibit reduced thermal hyperalgesia induced by inflammation. Likewise, isolated nerve preparations isolated from the knockout mice demonstrate significantly reduced current activity in response to acidic *in vitro* conditions (pH 5-5.3)(21, 34). Airway assessments have revealed that exposure to aerosolized capsaicin does not effect the breathing patterns of VR1$^{-/-}$ mice; however, capsaicin significantly reduces the breathing rates in wild type C57BL/6 mice (144). In addition to capsaicin, a number of other inhaled chemical irritants including ozone, sulfur dioxide, ammonia, smoke (cigarette and wood), and volatile anesthetics can have a stimulatory effect on bronchopulmonary C-fibre afferents (reviewed in (89)). Interestingly, no role was identified for the VR1 receptor in response to various airborne irritants such as acetic acid (acidic), acrolein (electrophilic), and styrene (lipophilic solvent). All of which induced similar sensory irritation responses, as evidenced by decreased breathing rates in wild type mice, VR1$^{-/-}$ mice, and wild type mice pretreated with the VR1 antagonist I-RTX (144). While no endogenous ligand for the VR1 receptor has been found, lipoxygenase and many other unsaturated fatty acids, bradykinin, ATP, PKC, and PLC all have the potential to either activate or sensitize the receptor (reviewed in (69)).

Slowly adapting pulmonary stretch receptors (SARs) are another class of afferent nerves that innervate the tracheobronchial tree and are mechanoreceptors that respond to increases in airway wall tension, while not displaying significant chemosensitive properties. During rhythmic breathing, this increase in airway wall tension leads to SAR discharge, which slowly adapts and maintains airway wall tension. In the airways, these afferent nerves innervate the smooth muscle via a complex network of nerve endings and are stimulated by vagal nerve-induced smooth muscle constriction. SARs are typically found in close

proximity to regions of dense collagen and elastic fibers, and are associated with myelinated afferent nerves ((167); reviewed in (161)). Excessive stimulation of these afferent nerves leads to shortened inspiratory time, decreased tidal volume, prolonged expiration, reflex bronchodilation, tachycardia, and systemic vasodilation. While these receptors are not considered to be chemosensory, elevated venous CO_2 results in the inhibition of SARs, which has been shown to be independent of changes in pulmonary mechanics (reviewed in (134)). This is of specific relevance to exercise induced asthma, because pulmonary arterial P_{CO2} levels increase during exercise and can easily reach levels capable of SAR inhibition (20). Thus, this could facilitate increased inspiration, reduced expiration, and enhanced bronchoconstriction. Conversely, in guinea pig models of allergic airway inflammation, SAR activity is increased following allergen challenge; thus resulting in significantly reduced inspiratory rates and tidal volumes (79). In addition to modest roles in asthma, altered SAR activity has been shown to dramatically affect other pulmonary disorders, particularly those involving altered elastance and compliance, such as emphysema and pulmonary fibrosis (reviewed in (134)).

Rapidly adapting pulmonary stretch receptors (RARs) are a third class of afferent nerves that innervate the respiratory tract from the nasopharynx/larynx to the bronchi. Unlike SARs, RARs are thinly myelinated afferent fibers (Aδ) that display an irregular discharge, and can be activated by mechanical, chemical, pathological, and inflammatory stimuli. While SAR terminals are restricted to the smooth muscle, RAR terminals are located throughout the submucosa and airway epithelium. Most importantly, RARs are stimulated by an increase in tidal volume and frequency, and a fall in compliance (162); thus RARs and SARs perform opposing motor actions in the airways of humans and guinea pigs. However,

many mammalian model organisms have SARs but lack RARs, such as mice and ferrets, and consequentially lack the ability to generate a cough reflex. Likewise, significant species differences exist in response to various RAR stimulants. For example, cigarette smoke is a potent RAR stimulate in rabbit airways, but relatively ineffective in the canine, whereas the opposite is true for other stimulants (reviewed in (132)). It is also likely that functional subpopulations of RARs exist, as suggested by the observation that no single chemical stimulant is capable of activating all RAR receptors (161).

Airway Efferent Innervation

Airway smooth muscle is innervated via both sympathetic and parasympathetic nerves which mediate bronchoconstriction and dilation. Parasympathetic nerves are the predominate contractile innervation and mediate smooth muscle function through cholinergic mechanisms. Cholinergic mediated airway smooth muscle constriction, as well as mucus hypersecretion, is mediated by muscarinic acetylcholine receptors (mAChRs) expressed by smooth muscle and submucosal glands. Muscarinic receptors on neurons are also believed to provide a feedback mechanism to modify the activity of cholinergic pathways (Figure 1.6). To date, five different muscarinic receptors have been identified (M1-5). Three of these, M1, M2 and M3, are expressed in the lung, and each of these contributes uniquely to parasympathetic regulation of airway physiology. The M3 mAChR is a G_q coupled protein receptor, expressed abundantly on airway smooth muscle, and likely to mediate the major contractile effects of acetylcholine (44). The M2 mAChR is a G_i coupled protein receptor and is also abundantly expressed by smooth muscle, where it could contribute to smooth muscle contraction by inhibiting adenylyl cyclase or activating Ca^{2++} activated potassium

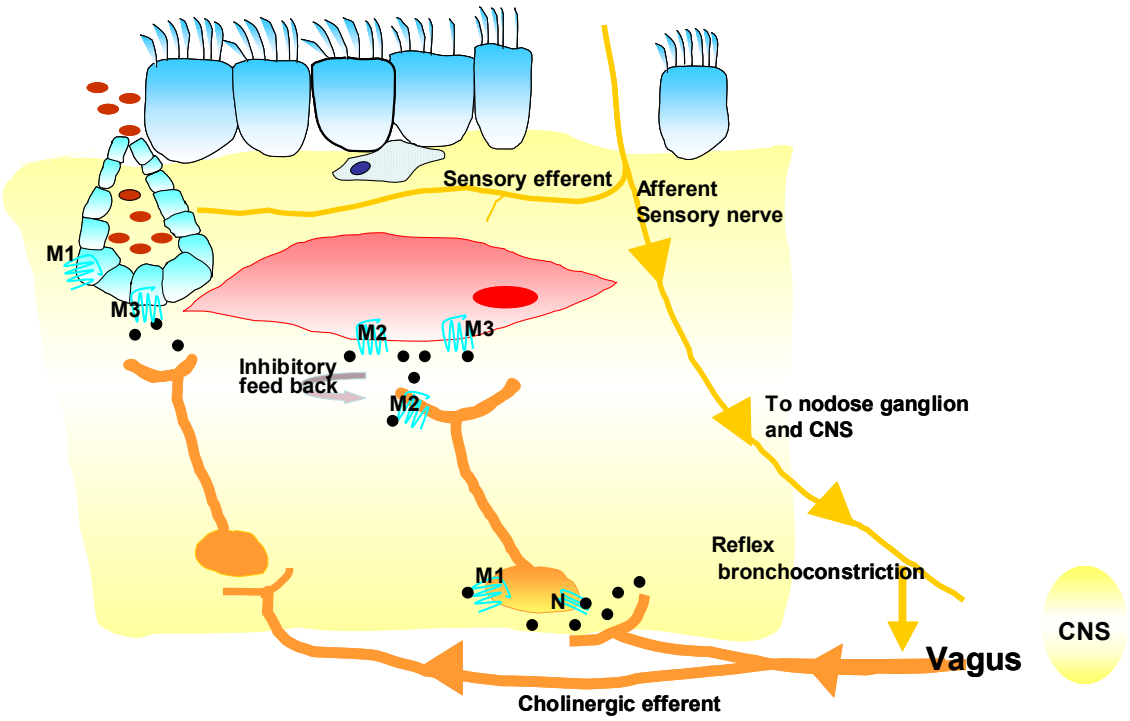

Figure 1.6. Airway Innervation and Muscarinic Receptor Expression

In the airways the vagus nerves are the primary source of acetylcholine. Acetylcholine affects most airway functions including smooth muscle constriction, mucus hypersecretion, and sensory nerve activation. Muscarinic acetylcholine receptors are the primary mediators of acetylcholine function in the airways. Both inhibitory subtypes (M2 receptors) and excitatory subtypes (M1 and M3 receptors) have been definitively localized to parasympathetic ganglia, prejunctional receptors of cholinergic nerves, and along airway and vascular smooth muscle.

channels (80). However, this receptor is also expressed prejunctionally on nerves, and pharmacological studies in humans and guinea pigs suggest that it provides a negative feedback loop limiting acetylcholine release (103). The M1 mAChR is also a G_q coupled protein receptor expressed on parasympathetic ganglia and is thought to filter the transmission of neural signals. The M1 and M3 mAChRs also localize to the submucosal gland in human bronchi, where they each contribute to mucus secretion (99, 126). In human and mouse systems, the M4 and M5 mAChRs are not thought to have a role in airway smooth muscle function.

Elucidating the physiological and pathophysiological roles of the muscarinic receptors has been complicated by the lack of subtype specific pharmacological antagonist. To circumvent this difficulty, muscarinic receptor deficient mice have been generated and their respective functional roles in airway responsiveness has been assessed. Coinciding with previous pharmacological assessments, following challenges with either increasing doses of MCh or following vagal stimulation, mAChR3$^{-/-}$ mice demonstrate a complete loss of cholinergic mediated bronchoconstriction (APTI responses). However, similar to results described by previous pharmacological studies conducted in other model organisms, the mAChR2$^{-/-}$ mice actually demonstrate significantly enhanced bronchoconstrictor responses (49). In addition to the *in vivo* analysis discussed above, *ex vivo* precision cut lung slices (PCLS) from these mice were also utilized to assess the roles of the M1, M2, and M3 mAChRs in peripheral airway constriction. As with the before mentioned *in vivo* study, PCLS from mAChR3$^{-/-}$ mice demonstrated significantly attenuated bronchoconstriction in response to muscarine administration. However, unlike the previous study, loss of the M3 mAChR did not completely inhibit muscarine mediated airway constriction, as the lung slices

from these animals only demonstrated a 60% reduction in airway constriction (142). Similar to the previous *in vivo* study, the PCLS from mAChR2$^{-/-}$ mice demonstrated rapid bronchoconstriction; however, these airways subsequently relaxed while still in the presence of muscarine. Additional assessments of PCLS from M2/M3 mAChR double knockout mice demonstrate complete inhibition of airway constriction in response to muscarine (142). This implies that in the peripheral airways, constriction is mediated by the M3 receptor and provides additional evidence supporting a role for the M2 receptor in constriction, possibly via the inhibition of relaxation. In addition to the mAChR2$^{-/-}$ and mAChR3$^{-/-}$ mice, in the peripheral airways, cumulative administration of muscarine induced significantly increased bronchoconstriction responses and significantly reduced levels of transient relaxation in the PCLS from mAChR1$^{-/-}$ mice (142). This suggests that in mice, an M1 mAChR-dependent mechanism exists, which is capable of reversing cholinergic mediated bronchoconstriction.

In addition to parasympathetic innervation, sympathetic nerves also innervate the lungs via postganglionic fibers, which release norepinerphrine. While the extent of airway sympathetic innervation is species dependent, several model organisms are known to have extensive sympathetic innervation in the lungs, including cats and guinea pigs (122). In humans, sympathetic nerves do not directly innervate the airway smooth muscle; however, sympathetic fibers extend to the submucosal mucus glands, blood vessels, and the parasympathetic ganglia, and adrenergic receptors are located extensively throughout the lung (19, 121). Adrenergic receptors are GPCRs that can be grouped into two distinct families based on their respective airway smooth muscle effects. The α_1 and the α_2 adrenergic receptors are both located on airway smooth muscle, and are associated with Gq and Gi proteins, respectively. In some species and under specific physiological conditions,

such as postjunctional β-adrenergic receptor (β_2AR) antagonism and simultaneous sympathetic nerve stimulation, α-adrenergic receptor stimulation can result in broncho-constriction. However, in humans, α-adrenergic receptor mediated bronchoconstriction is relatively nonexistent. Even in species where this bronchoconstriction has been observed, in the absence of β_2AR antagonism, noradrenaline activation of the β_2ARs is capable of overcoming any α-adrenergic receptor mediated constriction, thus evoking bronchodilation (reviewed in (18)). β_2ARs are associated with Gs proteins and stimulation by either noradrenaline or a β-agonist results in a rapid bronchodilation response. Inhaled β_2-agonists have been the cornerstone of the standard of care for asthma for over 40 years because of the rapid improvement in symptoms, as well as, preventing the onset of symptoms following exercise and exposure to allergens and/or pollutants. It is unclear whether β_2AR dysfunction directly affects the pathophysiology of asthma; however, the β_2AR gene is located in a region on chromosome 5q23-31 that has been associated with asthma, airway hyper-responsiveness, and other allergic airway phenotypes. Even though several polymorphisms have been identified in the β_2AR gene, none have been shown to directly affect the asthma phenotype. Instead, these polymorphisms may determine the extent to which the β_2AR down regulates, and therefore modifies, the overall bronchodilator response to both short acting and long acting β-agonist asthma therapy (120).

Nonadrenergic, noncholinergic (NANC) parasympathetic nerves are the primary relaxant nerves innervating the airway smooth muscle. Activation of these nerves has been shown to completely reverse preconstricted tracheal and bronchial smooth muscle preparations and completely dilate constricted guinea pig airways *in vivo* (25, 92). These nerves can be loosely divided into 2 systems, inhibitory NANC (i-NANC) and excitatory

NANC (e-NANC), based on the smooth muscle responses following nerve stimulation. The i-NANC system mediates smooth muscle relaxation, while the stimulation of the e-NANC system has multiple physiological responses, including smooth muscle constriction. However, labeling these nerves as either inhibitory or excitatory only applies to neurally mediated smooth muscle function, and may be misleading as the same transmitters can have opposite actions in other NANC mediated mechanisms affecting the mucus glands, blood vessels, and the epithelium (reviewed by (162)). While i-NANC mediated smooth muscle relaxation has been observed in all mammalian species, e-NANC mediated smooth muscle constriction has not been observed in humans.

The airway smooth muscle relaxation generated by i-NANC activation is thought to be mediated via Vasoactive Intestinal Polypeptide (VIP) and Nitric Oxide (NO). VIP is a small diffusible peptide released by NANC nerves in a Ca^{2+} dependent mechanism following stimulation, and has been demonstrated to relax airway smooth muscle when applied exogenously. *In vivo*, VIP has been shown to colocalize with acetylcholinesterase (AChE), thus the combined effects of direct VIP smooth muscle relaxation and the degradation of acetylcholine rapidly results in the relief of smooth muscle constriction. VIP is broken down by neutral endopeptidase (NEP) and various mast cell derived factors such as tryptase and chymase. While VIP is a primary i-NANC mediator in the airway of various model organisms and is abundant in human airway nerves, i-NANC facilitated relaxation in humans is not inhibited by the VIP antagonist α-chymotrypsin and VIP does not cause significant bronchodilation when applied exongenously (reviewed in (162)). However, i-NANC relaxation of bronchial smooth muscle in humans is inducible by inhibitors of NO generation. Thus, it stands to reason that NO, rather than VIP, is the primary NANC relaxant mediator in

the human lung. NO is synthesized from arginine by a family of enzymes collectively described as NOS synthases. NOS has been identified in airway nerves, and like VIP, NO diffuses readily to the smooth muscle and induces relaxation when administered exogenously. The *in vivo* mechanism of NO release is unknown; however, current literature suggests that NO exists in solution within the cytoplasm of the nerve cell and is released locally through an unknown mechanism, and is rapidly inactivated in the mucosal vasculature by hemoglobin (reviewed in (162)). Due to their roles in preventing and/or relaxing airway smooth muscle, both VIP and NO play central roles in maintaining airway caliber and likely contribute to airway pathophysiology.

In an effort to further assess VIP and NO contributions to airway responsiveness, the impact of gene loss and the effects of airway specific overexpression have been assessed in various mouse models of airway pathophysiology. In naïve mice with a targeted deletion of the VIP gene, features of airway inflammation were observed, including increased airway and BALF eosinophilia, increased levels of proinflammatory cytokines and chemokines, and increased AHR following MCh challenge (145). Following immunologic sensitization and challenge with ovalbumin, the VIP deficient mice demonstrated only marginal increases in airway and BALF eosinophilia and prolonged AHR; however, these increases were significantly higher then those observed for the wild type control animals (145). VIP exerts its influence through interactions with 2 GPCRs, $VPAC_1$ and $VPAC_2$. Mouse lines featuring disrupted $VPAC_1$ and $VPAC_2$ have been generated (54); however, the loss of these receptors on AHR has yet to be examined.

To assess the contribution of nitric oxide to airway inflammation and hyper-responsiveness, mice were generated with targeted deletions of each of the 3 nitric oxide

synthases (NOS-1, NOS-2, and NOS-3)(35, 36, 54). Targeted deletion of NOS-1, considered to be a constitutively expressed neuronal NOS, was associated with a decrease in naïve airway responsiveness to MCh administered via jugular stint and an approximately 40% drop in expired NO levels compared to wild type animals (36). This suggests that NO derived from NOS-1 is a substantial constituent of the total NO found in expired gas and may be a factor in airway constriction. Targeted deletion of NOS-2, considered to be the inducible NOS, did not appear to affect AHR, airway inflammation, and cellular recruitment to the airways following sensitization and challenge with ovalbumin (35). These findings would suggest that NOS-2 is not critical for the development of airway inflammation and alterations in lung mechanics. To further assess the role of NOS-2, externally regulatable transgenic mice that are capable of overexpressing NOS-2 in the airway (CC10-rtTA-NOS2) were generated (62). These mice are capable, in the presence of doxycycline, of producing exhaled NO, which approach equilevant values found in many asthmatic individuals. NO has been characterized as a weak bronchodilator and not surprisingly, NO induction in the mouse airway resulted in decreased baseline airway resistance and airway responsiveness to methacholine (62). However, NO has also been suggested to induce and perpetuate airway inflammation in asthmatic individuals. Thus, it was surprising that prolonged NO induction (up to 10 weeks) did not influence airway inflammation in these mice (62). Targeted deletion of NOS-3, considered to be a constitutively expressed endothelial NOS, generated mice that were significantly more hyperresponsive to MCh following OVA sensitization and challenge, when compared to the NOS-1 deficient mice. However, these animals demonstrated attenuated hyperresponsiveness when compared to the wild type animals. The

NOS-3 deficient mice did not demonstrate any alterations in airway inflammation when compared with the other NOS deficient mice or wild type animals (62).

The Stress Response and Asthma Exacerbations

Neurally mediated mechanisms directly influence normal airway tone and underlie abnormal pathophysiology. However, neural mechanisms can also indirectly modulate airway exacerbations. Asthma and other chronic inflammatory diseases, such as atopic dermatitis (AD) and rheumatoid arthritis (RA), are especially susceptible to modulation by stress and emotion (13, 14, 91, 95, 155). Indeed, many asthmatics have demonstrated a reduction in pulmonary function in response to increased anxiety levels following exposure to emotionally charged films (7), listening to stressful interactions (78), and participating in a sustained stressful life event (final academic examinations)(95). Increasing evidence suggests that the biological basis for these observations involves alterations of the stress response, which can contribute to dysfunctional interactions between the neuroendocrine and immune systems (reviewed by (155)). Many studies have demonstrated that exposure to allergens, pathogens, trauma, stress, and toxins results in the release of inflammatory mediators, which act either directly or indirectly to modify neuroendocrine function (reviewed by (56)). Central to the neuroendocrine response is the hypothalamic-pituitary-adrenal axis (HPA axis). The HPA axis is the primary mediator of neuroendocrine function and studies have demonstrated that subpopulations of asthmatic individuals have reduced HPA axis function (29).

While controversy exists regarding the significance of the stress response to immune system stimulation, the generation of mice with defective HPA axis components has allowed

significant progress to be made in defining interactions between the HPA axis and inflammatory responses. Corticotropin-releasing hormone (CRH) is the major regulator of the HPA axis. CRH is synthesized in the hypothalamus and upon release, is carried through the portal blood system to the pituitary gland. CRH interacts with the CRH type 1 receptor and stimulates the synthesis and release of ACTH from the pituitary corticotrophs (reviewed in (154)). Ultimately, ACTH stimulates the synthesis and release of glucocorticoids from the adrenals. Interestingly, basal ACTH levels are normal in CRH deficient mice; however, these animals demonstrate a significantly reduced ability to mount an adequate glucocorticoid response following physiological or behavioral stress (71, 104). Stimulation of the immune system and the release of proinflammatory cytokines have been shown to significantly induce HPA axis activity. The effect of IL-6 on the HPA axis has been the subject of extensive investigation and CRH has been shown to regulate the expression of this cytokine during inflammation (153). Using the $CRH^{-/-}$ mice in a turpentine-induced inflammation model, CRH was shown to be essential for increased ACTH levels, but not for elevated adrenal corticosterone levels (153). This study also demonstrated increased levels of plasma IL-6 associated with CRH deficiency and the complete inhibition of the HPA axis response to inflammatory stress in $CRH^{-/-}$/$IL\text{-}6^{-/-}$ mice (153). CRH deficiency has also been shown to increase airway inflammation in response to OVA sensitization and challenge (136). The $CRH^{-/-}$ mice demonstrated significantly increased airway eosinophilia (~80% - 110% increase over wild type), increased goblet cell hypertrophy (~70% increase over wild type), and increased levels of select proinflammatory cytokines (IL-4, IL-5, and IL-13). The CRH deficient mice also demonstrated significantly increased airway responsiveness, as assessed via the forced oscillation technique. While no differences were observed between

naïve wild type and mutant animals, the OVA challenged $CRH^{-/-}$ mice demonstrated significant increases in total lung resistance, elastance, and tissue damping over those increases observed in the OVA challenged wild type mice (136). Interestingly, not all indices of allergic airway inflammation were increased in the CRH deficient animals. For example, while IgE levels were increased in the serum from OVA challenged mice, no difference was observed between the wild type and $CRH^{-/-}$ mice (136). Despite these exceptions, this study suggests that CRH and the HPA axis have a significant role in mediating allergen induced airway inflammation in mouse models of asthma.

Summary

The overall aim of this dissertation was to assess the role of various GPCRs and their associated ligands in regulating ASM constriction and inflammation. The first aim of this work focuses on assessing the mechanism by which TXA_2 mediates ASM constriction in the mouse. Although it is possible that TXA_2 can mediate its effects by engaging Tp receptors directly on ASM, the mechanism by which Tp receptor activation leads to bronchoconstriction is not well defined. Here we address this question directly using both genetic and pharmacological approaches, in conjunction with both *in vivo* and *ex vivo* studies of mouse airways. The second research aim utilizes a genetic approach to further define the mechanism underlying TXA_2 meditated airway constriction. To address this aim, we generated mice carrying a Tp receptor locus that is sensitive to disruption by cre recombinase. These mice were subsequently crossed with either nestin-cre transgenic mice, which express cre recombinase throughout the nervous system, or SM22-cre transgenic mice, which express cre recombinase in smooth muscle. The *in vivo* airway mechanics of the resultant tissue specific

Tp receptor deficient mice were then characterized. The third research aim addresses the role of NPSR1 (GPRA) in airway constriction and inflammation. NPSR1 is a newly deorphanized GPCR found to be associated with asthma and atopy in human populations. Here we describe the generation of NPSR1 deficient mice and assess their airway physiology and airway inflammatory responses.

Organization of the dissertation

Chapter II of this dissertation introduces a model of thromboxane A2 mediated ASM constriction in both the naïve and inflamed lung, which is dependent upon the m3 mAChR. Chapter III further defines the mechanism behind this model utilizing a panel of conditional Tp receptor deficient mouse lines, which lack functional Tp receptors either throughout the nervous system or on smooth muscle cells. Chapter IV describes a detailed assessment of airway reactivity and inflammation development in mice deficient in the newly deorphanized GPCR, NPSR1 (GPRA). Together, the work described herein demonstrates the diverse roles of GPCRs in the neuropathophysiology of asthma.

References

1. National Health Interview Survey: National Center For Health Statistics, 2003.

2. Proceedings of the ATS workshop on refractory asthma: current understanding, recommendations, and unanswered questions. American Thoracic Society. *Am J Respir Crit Care Med* 162: 2341-2351, 2000.

3. Report on Final Mortality Statistics: National Center For Health Statistics, 2002.

4. Agostoni E, Chinnock JE, De Daly MB, and Murray JG. Functional and histological studies of the vagus nerve and its branches to the heart, lungs and abdominal viscera in the cat. *J Physiol* 135: 182-205, 1957.

5. Anrep GV BG, Kenawy MR, Misrahy G. Therapeutic uses of khellin. *Lancet*: 557-558, 1947.

6. Batshake B, Nilsson C, and Sundelin J. Structure and expression of the murine thromboxane A2 receptor gene. *Biochem Biophys Res Commun* 256: 391-397, 1999.

7. Beggs PJ and Curson PH. An integrated environmental asthma model. *Arch Environ Health* 50: 87-94, 1995.

8. Billington CK and Penn RB. m3 muscarinic acetylcholine receptor regulation in the airway. *Am J Respir Cell Mol Biol* 26: 269-272, 2002.

9. Billington CK and Penn RB. Signaling and regulation of G protein-coupled receptors in airway smooth muscle. *Respir Res* 4: 2, 2003.

10. Brown HM, Storey G, and George WH. Beclomethasone dipropionate: a new steroid aerosol for the treatment of allergic asthma. *Br Med J* 1: 585-590, 1972.

11. Brusselle G, Kips J, Joos G, Bluethmann H, and Pauwels R. Allergen-induced airway inflammation and bronchial responsiveness in wild-type and interleukin-4-deficient mice. *Am J Respir Cell Mol Biol* 12: 254-259, 1995.

12. Burstein HJ, Tepper RI, Leder P, and Abbas AK. Humoral immune functions in IL-4 transgenic mice. *J Immunol* 147: 2950-2956, 1991.

13. Buske-Kirschbaum A and Hellhammer DH. Endocrine and immune responses to stress in chronic inflammatory skin disorders. *Ann N Y Acad Sci* 992: 231-240, 2003.

14. Buske-Kirschbaum A, von Auer K, Krieger S, Weis S, Rauh W, and Hellhammer D. Blunted cortisol responses to psychosocial stress in asthmatic children: a general feature of atopic disease? *Psychosom Med* 65: 806-810, 2003.

15. Busse WW and Lemanske RF, Jr. Asthma. *N Engl J Med* 344: 350-362, 2001.

16. Campbell EM, Kunkel SL, Strieter RM, and Lukacs NW. Temporal role of chemokines in a murine model of cockroach allergen-induced airway hyperreactivity and eosinophilia. *J Immunol* 161: 7047-7053, 1998.

17. Canning BJ. Modeling asthma and COPD in animals: a pointless exercise? *Curr Opin Pharmacol* 3: 244-250, 2003.

18. Canning BJ and Fischer A. Neural regulation of airway smooth muscle tone. *Respir Physiol* 125: 113-127, 2001.

19. Carstairs JR, Nimmo AJ, and Barnes PJ. Autoradiographic localisation of beta-adrenoceptors in human lung. *Eur J Pharmacol* 103: 189-190, 1984.

20. Casaburi R, Daly J, Hansen JE, and Effros RM. Abrupt changes in mixed venous blood gas composition after the onset of exercise. *J Appl Physiol* 67: 1106-1112, 1989.

21. Caterina MJ, Leffler A, Malmberg AB, Martin WJ, Trafton J, Petersen-Zeitz KR, Koltzenburg M, Basbaum AI, and Julius D. Impaired nociception and pain sensation in mice lacking the capsaicin receptor. *Science* 288: 306-313, 2000.

22. Chu EK and Drazen JM. Asthma: one hundred years of treatment and onward. *Am J Respir Crit Care Med* 171: 1202-1208, 2005.

23. Chu HW and Martin RJ. Are eosinophils still important in asthma? *Clin Exp Allergy* 31: 525-528, 2001.

24. Citro S, Ravasi S, Rovati GE, and Capra V. Thromboxane prostanoid receptor signals through Gi protein to rapidly activate extracellular signal-regulated kinase in human airways. *Am J Respir Cell Mol Biol* 32: 326-333, 2005.

25. Clerici C, Macquin-Mavier I, and Harf A. Nonadrenergic bronchodilation in adult and young guinea pigs. *J Appl Physiol* 67: 1764-1769, 1989.

26. Cockcroft DW. Pharmacologic therapy for asthma: overview and historical perspective. *J Clin Pharmacol* 39: 216-222, 1999.

27. Coleman RA and Sheldrick RL. Prostanoid-induced contraction of human bronchial smooth muscle is mediated by TP-receptors. *Br J Pharmacol* 96: 688-692, 1989.

28. Coleman RA, Smith WL, and Narumiya S. International Union of Pharmacology classification of prostanoid receptors: properties, distribution, and structure of the receptors and their subtypes. *Pharmacol Rev* 46: 205-229, 1994.

29. Collins JV, Bellamy D, Britton MG, Townsend J, and Brown DJ. Hypothalamo-pituitary-adrenal function in intrinsic non-atopic asthma. *Thorax* 30: 578-581, 1975.

30. Cookson WO, Sharp PA, Faux JA, and Hopkin JM. Linkage between immunoglobulin E responses underlying asthma and rhinitis and chromosome 11q. *Lancet* 1: 1292-1295, 1989.

31. Coyle AJ, Le Gros G, Bertrand C, Tsuyuki S, Heusser CH, Kopf M, and Anderson GP. Interleukin-4 is required for the induction of lung Th2 mucosal immunity. *Am J Respir Cell Mol Biol* 13: 54-59, 1995.

32. Coyle AJ, Wagner K, Bertrand C, Tsuyuki S, Bews J, and Heusser C. Central role of immunoglobulin (Ig) E in the induction of lung eosinophil infiltration and T helper 2 cell cytokine production: inhibition by a non-anaphylactogenic anti-IgE antibody. *J Exp Med* 183: 1303-1310, 1996.

33. D'Amato G. Role of anti-IgE monoclonal antibody (omalizumab) in the treatment of bronchial asthma and allergic respiratory diseases. *Eur J Pharmacol* 533: 302-307, 2006.

34. Davis JB, Gray J, Gunthorpe MJ, Hatcher JP, Davey PT, Overend P, Harries MH, Latcham J, Clapham C, Atkinson K, Hughes SA, Rance K, Grau E, Harper AJ, Pugh PL, Rogers DC, Bingham S, Randall A, and Sheardown SA. Vanilloid receptor-1 is essential for inflammatory thermal hyperalgesia. *Nature* 405: 183-187, 2000.

35. De Sanctis GT, MacLean JA, Hamada K, Mehta S, Scott JA, Jiao A, Yandava CN, Kobzik L, Wolyniec WW, Fabian AJ, Venugopal CS, Grasemann H, Huang PL, and Drazen

JM. Contribution of nitric oxide synthases 1, 2, and 3 to airway hyperresponsiveness and inflammation in a murine model of asthma. *J Exp Med* 189: 1621-1630, 1999.

36. De Sanctis GT, Mehta S, Kobzik L, Yandava C, Jiao A, Huang PL, and Drazen JM. Contribution of type I NOS to expired gas NO and bronchial responsiveness in mice. *Am J Physiol* 273: L883-888, 1997.

37. Demoly P, Jaffuel D, Lequeux N, Weksler B, Creminon C, Michel FB, Godard P, and Bousquet J. Prostaglandin H synthase 1 and 2 immunoreactivities in the bronchial mucosa of asthmatics. *Am J Respir Crit Care Med* 155: 670-675, 1997.

38. Dent LA, Strath M, Mellor AL, and Sanderson CJ. Eosinophilia in transgenic mice expressing interleukin 5. *J Exp Med* 172: 1425-1431, 1990.

39. Detweiler H. An address on asthma: Its diagnosis and treatment. *The Canadian Medical Association Journal*: 661-666, 1927.

40. Djukanovic R, Wilson JW, Britten KM, Wilson SJ, Walls AF, Roche WR, Howarth PH, and Holgate ST. Quantitation of mast cells and eosinophils in the bronchial mucosa of symptomatic atopic asthmatics and healthy control subjects using immunohistochemistry. *Am Rev Respir Dis* 142: 863-871, 1990.

41. Drazen JM, Silverman EK, and Lee TH. Heterogeneity of therapeutic responses in asthma. *Br Med Bull* 56: 1054-1070, 2000.

42. Dye JA, McKiernan BC, Rozanski EA, Hoffmann WE, Losonsky JM, Homco LD, Weisiger RM, and Kakoma I. Bronchopulmonary disease in the cat: historical, physical, radiographic, clinicopathologic, and pulmonary functional evaluation of 24 affected and 15 healthy cats. *J Vet Intern Med* 10: 385-400, 1996.

43. Ebbell B. *The papyrus Ebers. The greatest Egyptian Medical document*: Copenhagen, Levin and Munksgaard, 1937.

44. Eglen RM, Hegde SS, and Watson N. Muscarinic receptor subtypes and smooth muscle function. *Pharmacol Rev* 48: 531-565, 1996.

45. Elias JA, Zhu Z, Chupp G, and Homer RJ. Airway remodeling in asthma. *J Clin Invest* 104: 1001-1006, 1999.

46. Ellis EF, Oelz O, Roberts LJ, 2nd, Payne NA, Sweetman BJ, Nies AS, and Oates JA. Coronary arterial smooth muscle contraction by a substance released from platelets: evidence that it is thromboxane A2. *Science* 193: 1135-1137, 1976.

47. Evett GE, Xie W, Chipman JG, Robertson DL, and Simmons DL. Prostaglandin G/H synthase isoenzyme 2 expression in fibroblasts: regulation by dexamethasone, mitogens, and oncogenes. *Arch Biochem Biophys* 306: 169-177, 1993.

48. Fernandes DJ, Xu KF, and Stewart AG. Anti-remodelling drugs for the treatment of asthma: requirement for animal models of airway wall remodelling. *Clin Exp Pharmacol Physiol* 28: 619-629, 2001.

49. Fisher JT, Vincent SG, Gomeza J, Yamada M, and Wess J. Loss of vagally mediated bradycardia and bronchoconstriction in mice lacking M2 or M3 muscarinic acetylcholine receptors. *Faseb J* 18: 711-713, 2004.

50. Frid MG, Moiseeva EP, and Stenmark KR. Multiple phenotypically distinct smooth muscle cell populations exist in the adult and developing bovine pulmonary arterial media in vivo. *Circ Res* 75: 669-681, 1994.

51. Fujimura M, Sasaki F, Nakatsumi Y, Takahashi Y, Hifumi S, Taga K, Mifune J, Tanaka T, and Matsuda T. Effects of a thromboxane synthetase inhibitor (OKY-046) and a lipoxygenase inhibitor (AA-861) on bronchial responsiveness to acetylcholine in asthmatic subjects. *Thorax* 41: 955-959, 1986.

52. Gabbiani G, Schmid E, Winter S, Chaponnier C, de Ckhastonay C, Vandekerckhove J, Weber K, and Franke WW. Vascular smooth muscle cells differ from other smooth muscle cells: predominance of vimentin filaments and a specific alpha-type actin. *Proc Natl Acad Sci U S A* 78: 298-302, 1981.

53. Gavett SH, O'Hearn DJ, Karp CL, Patel EA, Schofield BH, Finkelman FD, and Wills-Karp M. Interleukin-4 receptor blockade prevents airway responses induced by antigen challenge in mice. *Am J Physiol* 272: L253-261, 1997.

54. Goetzl EJ, Voice JK, Shen S, Dorsam G, Kong Y, West KM, Morrison CF, and Harmar AJ. Enhanced delayed-type hypersensitivity and diminished immediate-type hypersensitivity in mice lacking the inducible VPAC(2) receptor for vasoactive intestinal peptide. *Proc Natl Acad Sci U S A* 98: 13854-13859, 2001.

55. Grunig G, Warnock M, Wakil AE, Venkayya R, Brombacher F, Rennick DM, Sheppard D, Mohrs M, Donaldson DD, Locksley RM, and Corry DB. Requirement for IL-13 independently of IL-4 in experimental asthma. *Science* 282: 2261-2263, 1998.

56. Haddad JJ, Saade NE, and Safieh-Garabedian B. Cytokines and neuro-immune-endocrine interactions: a role for the hypothalamic-pituitary-adrenal revolving axis. *J Neuroimmunol* 133: 1-19, 2002.

57. Halushka PV. Thromboxane A(2) receptors: where have you gone? *Prostaglandins Other Lipid Mediat* 60: 175-189, 2000.

58. Halushka PV, Allan CJ, and Davis-Bruno KL. Thromboxane A2 receptors. *J Lipid Mediat Cell Signal* 12: 361-378, 1995.

59. Harris JR, Magnus P, Samuelsen SO, and Tambs K. No evidence for effects of family environment on asthma. A retrospective study of Norwegian twins. *Am J Respir Crit Care Med* 156: 43-49, 1997.

60. Herszberg B, Ramos-Barbon D, Tamaoka M, Martin JG, and Lavoie JP. Heaves, an asthma-like equine disease, involves airway smooth muscle remodeling. *J Allergy Clin Immunol* 118: 382-388, 2006.

61. Hirata T, Ushikubi F, Kakizuka A, Okuma M, and Narumiya S. Two thromboxane A2 receptor isoforms in human platelets. Opposite coupling to adenylyl cyclase with different sensitivity to Arg60 to Leu mutation. *J Clin Invest* 97: 949-956, 1996.

62. Hjoberg J, Shore S, Kobzik L, Okinaga S, Hallock A, Vallone J, Subramaniam V, De Sanctis GT, Elias JA, Drazen JM, and Silverman ES. Expression of nitric oxide synthase-2 in the lungs decreases airway resistance and responsiveness. *J Appl Physiol* 97: 249-259, 2004.

63. Holgate ST. Lessons learnt from the epidemic of asthma. *Qjm* 97: 247-257, 2004.

64. Holtwick R, Gotthardt M, Skryabin B, Steinmetz M, Potthast R, Zetsche B, Hammer RE, Herz J, and Kuhn M. Smooth muscle-selective deletion of guanylyl cyclase-A prevents the acute but not chronic effects of ANP on blood pressure. *Proc Natl Acad Sci U S A* 99: 7142-7147, 2002.

65. Howard TD, Postma DS, Jongepier H, Moore WC, Koppelman GH, Zheng SL, Xu J, Bleecker ER, and Meyers DA. Association of a disintegrin and metalloprotease 33

(ADAM33) gene with asthma in ethnically diverse populations. *J Allergy Clin Immunol* 112: 717-722, 2003.

66. Huang JS, Ramamurthy SK, Lin X, and Le Breton GC. Cell signalling through thromboxane A2 receptors. *Cell Signal* 16: 521-533, 2004.

67. Huber HL, Koessler, K.K. The pathology of bronchial asthma. *Arch Intern Med* 30: 689-760, 1992.

68. Humbles AA, Lloyd CM, McMillan SJ, Friend DS, Xanthou G, McKenna EE, Ghiran S, Gerard NP, Yu C, Orkin SH, and Gerard C. A critical role for eosinophils in allergic airways remodeling. *Science* 305: 1776-1779, 2004.

69. Hwang SW and Oh U. Hot channels in airways: pharmacology of the vanilloid receptor. *Curr Opin Pharmacol* 2: 235-242, 2002.

70. Israel E, Chinchilli VM, Ford JG, Boushey HA, Cherniack R, Craig TJ, Deykin A, Fagan JK, Fahy JV, Fish J, Kraft M, Kunselman SJ, Lazarus SC, Lemanske RF, Jr., Liggett SB, Martin RJ, Mitra N, Peters SP, Silverman E, Sorkness CA, Szefler SJ, Wechsler ME, Weiss ST, and Drazen JM. Use of regularly scheduled albuterol treatment in asthma: genotype-stratified, randomised, placebo-controlled cross-over trial. *Lancet* 364: 1505-1512, 2004.

71. Jacobson L, Muglia LJ, Weninger SC, Pac inverted question markak K, and Majzoub JA. CRH deficiency impairs but does not block pituitary-adrenal responses to diverse stressors. *Neuroendocrinology* 71: 79-87, 2000.

72. James A and Carroll N. Airway smooth muscle in health and disease; methods of measurement and relation to function. *Eur Respir J* 15: 782-789, 2000.

73. Jones GL, Saroea HG, Watson RM, and O'Byrne PM. Effect of an inhaled thromboxane mimetic (U46619) on airway function in human subjects. *Am Rev Respir Dis* 145: 1270-1274, 1992.

74. Jongepier H, Boezen HM, Dijkstra A, Howard TD, Vonk JM, Koppelman GH, Zheng SL, Meyers DA, Bleecker ER, and Postma DS. Polymorphisms of the ADAM33 gene are associated with accelerated lung function decline in asthma. *Clin Exp Allergy* 34: 757-760, 2004.

75. Joos GF. Bronchial hyperresponsiveness: too complex to be useful? *Curr Opin Pharmacol* 3: 233-238, 2003.

76. Karlsson JA, Sant'Ambrogio G, and Widdicombe J. Afferent neural pathways in cough and reflex bronchoconstriction. *J Appl Physiol* 65: 1007-1023, 1988.

77. Kay AB. Pathology of mild, severe, and fatal asthma. *Am J Respir Crit Care Med* 154: S66-69, 1996.

78. Kolbe J, Garrett J, Vamos M, and Rea HH. Influences on trends in asthma morbidity and mortality: the New Zealand experience. *Chest* 106: 211S-215S, 1994.

79. Koller EA and Ferrer P. Discharge patterns of the lung stretch receptors and activation of deflation fibres in anaphylactic bronchial asthma. *Respir Physiol* 17: 113-126, 1973.

80. Kotlikoff MI, Kume H, and Tomasic M. Muscarinic regulation of membrane ion channels in airway smooth muscle cells. *Biochem Pharmacol* 43: 5-10, 1992.

81. Kumar RK and Foster PS. Modeling allergic asthma in mice: pitfalls and opportunities. *Am J Respir Cell Mol Biol* 27: 267-272, 2002.

82. Kung TT, Stelts D, Zurcher JA, Jones H, Umland SP, Kreutner W, Egan RW, and Chapman RW. Mast cells modulate allergic pulmonary eosinophilia in mice. *Am J Respir Cell Mol Biol* 12: 404-409, 1995.

83. Kuperman D, Schofield B, Wills-Karp M, and Grusby MJ. Signal transducer and activator of transcription factor 6 (Stat6)-deficient mice are protected from antigen-induced airway hyperresponsiveness and mucus production. *J Exp Med* 187: 939-948, 1998.

84. LaMotte RH and Campbell JN. Comparison of responses of warm and nociceptive C-fiber afferents in monkey with human judgments of thermal pain. *J Neurophysiol* 41: 509-528, 1978.

85. Larche M, Robinson DS, and Kay AB. The role of T lymphocytes in the pathogenesis of asthma. *J Allergy Clin Immunol* 111: 450-463; quiz 464, 2003.

86. Lavoie JP, Maghni K, Desnoyers M, Taha R, Martin JG, and Hamid QA. Neutrophilic airway inflammation in horses with heaves is characterized by a Th2-type cytokine profile. *Am J Respir Crit Care Med* 164: 1410-1413, 2001.

87. Lee JH, Park HS, Park SW, Jang AS, Uh ST, Rhim T, Park CS, Hong SJ, Holgate ST, Holloway JW, and Shin HD. ADAM33 polymorphism: association with bronchial hyper-responsiveness in Korean asthmatics. *Clin Exp Allergy* 34: 860-865, 2004.

88. Lee JJ, Dimina D, Macias MP, Ochkur SI, McGarry MP, O'Neill KR, Protheroe C, Pero R, Nguyen T, Cormier SA, Lenkiewicz E, Colbert D, Rinaldi L, Ackerman SJ, Irvin CG, and Lee NA. Defining a link with asthma in mice congenitally deficient in eosinophils. *Science* 305: 1773-1776, 2004.

89. Lee LY and Pisarri TE. Afferent properties and reflex functions of bronchopulmonary C-fibers. *Respir Physiol* 125: 47-65, 2001.

90. Leguillette R. Recurrent airway obstruction--heaves. *Vet Clin North Am Equine Pract* 19: 63-86, vi, 2003.

91. Lehrer PM, Isenberg S, and Hochron SM. Asthma and emotion: a review. *J Asthma* 30: 5-21, 1993.

92. Li CG and Rand MJ. Prejunctional inhibition of non-adrenergic non-cholinergic transmission in the rat anococcygeus muscle. *Eur J Pharmacol* 168: 107-110, 1989.

93. Lind DL, Choudhry S, Ung N, Ziv E, Avila PC, Salari K, Ha C, Lovins EG, Coyle NE, Nazario S, Casal J, Torres A, Rodriguez-Santana JR, Matallana H, Lilly CM, Salas J, Selman M, Boushey HA, Weiss ST, Chapela R, Ford JG, Rodriguez-Cintron W, Silverman EK, Sheppard D, Kwok PY, and Gonzalez Burchard E. ADAM33 is not associated with asthma in Puerto Rican or Mexican populations. *Am J Respir Crit Care Med* 168: 1312-1316, 2003.

94. Liu KL, Hadj Aissa A, Lareal MC, Benzoni D, Sassard J, and Zech P. Basal prostaglandin synthesis by the isolated perfused rat kidney. *Prostaglandins Leukot Essent Fatty Acids* 39: 261-265, 1990.

95. Liu LY, Coe CL, Swenson CA, Kelly EA, Kita H, and Busse WW. School examinations enhance airway inflammation to antigen challenge. *Am J Respir Crit Care Med* 165: 1062-1067, 2002.

96. Lowell FC. Observations on Heaves. An Asthma-Like Syndrome in the Horse. *J Allergy Clin Immunol* 35: 322-330, 1964.

97. Mack CP and Owens GK. Regulation of smooth muscle alpha-actin expression in vivo is dependent on CArG elements within the 5' and first intron promoter regions. *Circ Res* 84: 852-861, 1999.

98. MacNee W and Selby C. New perspectives on basic mechanisms in lung disease. 2. Neutrophil traffic in the lungs: role of haemodynamics, cell adhesion, and deformability. *Thorax* 48: 79-88, 1993.

99. Malhotra AK, Pinals DA, Adler CM, Elman I, Clifton A, Pickar D, and Breier A. Ketamine-induced exacerbation of psychotic symptoms and cognitive impairment in neuroleptic-free schizophrenics. *Neuropsychopharmacology* 17: 141-150, 1997.

100. Marketos S and Ballas C. Bronchial asthma in medical literature of Greek antiquity. *Hist Sci Med* 17: 35-39, 1982.

101. McFadden ER, Jr. A century of asthma. *Am J Respir Crit Care Med* 170: 215-221, 2004.

102. Melland B. The treatment of spasmodic asthma by the hypodermic injection of adrenalin. *Lancet*: 1407-1411, 1910.

103. Minette PA and Barnes PJ. Prejunctional inhibitory muscarinic receptors on cholinergic nerves in human and guinea pig airways. *J Appl Physiol* 64: 2532-2537, 1988.

104. Muglia L, Jacobson L, Dikkes P, and Majzoub JA. Corticotropin-releasing hormone deficiency reveals major fetal but not adult glucocorticoid need. *Nature* 373: 427-432, 1995.

105. Mukherjee AB, Miele L, and Pattabiraman N. Phospholipase A2 enzymes: regulation and physiological role. *Biochem Pharmacol* 48: 1-10, 1994.

106. Munoz NM, Shioya T, Murphy TM, Primack S, Dame C, Sands MF, and Leff AR. Potentiation of vagal contractile response by thromboxane mimetic U-46619. *J Appl Physiol* 61: 1173-1179, 1986.

107. Narumiya S, Sugimoto Y, and Ushikubi F. Prostanoid receptors: structures, properties, and functions. *Physiol Rev* 79: 1193-1226, 1999.

108. National Asthma Education and Prevention Program (National Heart L, and Blood Institute), and Asthma,. Expert Panel report 2
guidelines for the diagnosis and management of asthma. NIH publication
Clinical practice guidelines (National Asthma Education and Prevention Program (National Heart, Lung, and Blood Institute)), National Institutes of Health, National Heart, Lung, and Blood Institute, Bethesda, Md., 1998.

109. Neddenriep D, Schumacher MJ, and Lemen RJ. Asthma in childhood. *Curr Probl Pediatr* 19: 325-385, 1989.

110. Needleman P, Turk J, Jakschik BA, Morrison AR, and Lefkowith JB. Arachidonic acid metabolism. *Annu Rev Biochem* 55: 69-102, 1986.

111. Nogami M, Suko M, Okudaira H, Miyamoto T, Shiga J, Ito M, and Kasuya S. Experimental pulmonary eosinophilia in mice by Ascaris suum extract. *Am Rev Respir Dis* 141: 1289-1295, 1990.

112. Ober C and Hoffjan S. Asthma genetics 2006: the long and winding road to gene discovery. *Genes Immun* 7: 95-100, 2006.

113. O'Byrne PM and Fuller RW. The role of thromboxane A2 in the pathogenesis of airway hyperresponsiveness. *Eur Respir J* 2: 782-786, 1989.

114. Owens GK. Regulation of differentiation of vascular smooth muscle cells. *Physiol Rev* 75: 487-517, 1995.

115. Owens GK, Kumar MS, and Wamhoff BR. Molecular regulation of vascular smooth muscle cell differentiation in development and disease. *Physiol Rev* 84: 767-801, 2004.

116. Palmer LJ, Burton PR, Faux JA, James AL, Musk AW, and Cookson WO. Independent inheritance of serum immunoglobulin E concentrations and airway responsiveness. *Am J Respir Crit Care Med* 161: 1836-1843, 2000.

117. Raby BA, Silverman EK, Kwiatkowski DJ, Lange C, Lazarus R, and Weiss ST. ADAM33 polymorphisms and phenotype associations in childhood asthma. *J Allergy Clin Immunol* 113: 1071-1078, 2004.

118. Reeh PW and Steen KH. Tissue acidosis in nociception and pain. *Prog Brain Res* 113: 143-151, 1996.

119. Regan CP, Manabe I, and Owens GK. Development of a smooth muscle-targeted cre recombinase mouse reveals novel insights regarding smooth muscle myosin heavy chain promoter regulation. *Circ Res* 87: 363-369, 2000.

120. Reihsaus E, Innis M, MacIntyre N, and Liggett SB. Mutations in the gene encoding for the beta 2-adrenergic receptor in normal and asthmatic subjects. *Am J Respir Cell Mol Biol* 8: 334-339, 1993.

121. Richardson J and Beland J. Nonadrenergic inhibitory nervous system in human airways. *J Appl Physiol* 41: 764-771, 1976.

122. Richardson JB. Nerve supply to the lungs. *Am Rev Respir Dis* 119: 785-802, 1979.

123. Robinson D, Hamid Q, Bentley A, Ying S, Kay AB, and Durham SR. Activation of CD4+ T cells, increased TH2-type cytokine mRNA expression, and eosinophil recruitment in bronchoalveolar lavage after allergen inhalation challenge in patients with atopic asthma. *J Allergy Clin Immunol* 92: 313-324, 1993.

124. Robinson DS, Durham SR, and Kay AB. Cytokines. 3. Cytokines in asthma. *Thorax* 48: 845-853, 1993.

125. Robinson DS, Hamid Q, Ying S, Tsicopoulos A, Barkans J, Bentley AM, Corrigan C, Durham SR, and Kay AB. Predominant TH2-like bronchoalveolar T-lymphocyte population in atopic asthma. *N Engl J Med* 326: 298-304, 1992.

126. Rogers DF. Motor control of airway goblet cells and glands. *Respir Physiol* 125: 129-144, 2001.

127. Rosenstreich DL, Eggleston P, Kattan M, Baker D, Slavin RG, Gergen P, Mitchell H, McNiff-Mortimer K, Lynn H, Ownby D, and Malveaux F. The role of cockroach allergy and exposure to cockroach allergen in causing morbidity among inner-city children with asthma. *N Engl J Med* 336: 1356-1363, 1997.

128. Rosner F. The Life of Moses Maimonides, a Prominent Medieval Physician. *Einstein Quarterly Journal of Biological Medicine* 19: 125-128, 2002.

129. Saavedra-Delgado AM and Cohen SG. Huang-Ti, the Yellow Emperor and the Nei Ching: antiquity's earliest reference to asthma. *Allergy Proc* 12: 197-198, 1991.

130. Salter HH. *On asthma: its pathology and treatment*, 1860.

131. Salter HH. On the treatment of asthma by belladonna. *Lancet*, 1869.

132. Sant'Ambrogio G and Widdicombe J. Reflexes from airway rapidly adapting receptors. *Respir Physiol* 125: 33-45, 2001.

133. Sato E, Koyama S, Okubo Y, Kubo K, and Sekiguchi M. Acetylcholine stimulates alveolar macrophages to release inflammatory cell chemotactic activity. *Am J Physiol* 274: L970-979, 1998.

134. Schelegle ES and Green JF. An overview of the anatomy and physiology of slowly adapting pulmonary stretch receptors. *Respir Physiol* 125: 17-31, 2001.

135. Shen RF and Tai HH. Thromboxanes: synthase and receptors. *J Biomed Sci* 5: 153-172, 1998.

136. Silverman ES, Breault DT, Vallone J, Subramanian S, Yilmaz AD, Mathew S, Subramaniam V, Tantisira K, Pacak K, Weiss ST, and Majzoub JA. Corticotropin-releasing hormone deficiency increases allergen-induced airway inflammation in a mouse model of asthma. *J Allergy Clin Immunol* 114: 747-754, 2004.

137. Simmons DL, Xie, W., Chipman, J.G., and Evett, G.E. Multiple cyclooxygenases: cloning of a mitogen-inducible form. In: *Prostaglandins, Leukotrienes, Lipoxins, and PAF.*, edited by Bailey JM. New York: Plenum Press, 1991, p. 67-78.

138. Smith WL, Garavito RM, and DeWitt DL. Prostaglandin endoperoxide H synthases (cyclooxygenases)-1 and -2. *J Biol Chem* 271: 33157-33160, 1996.

139. Smith WL, Meade EA, and DeWitt DL. Pharmacology of prostaglandin endoperoxide synthase isozymes-1 and -2. *Ann N Y Acad Sci* 714: 136-142, 1994.

140. Solway J and Fredberg JJ. Perhaps airway smooth muscle dysfunction contributes to asthmatic bronchial hyperresponsiveness after all. *Am J Respir Cell Mol Biol* 17: 144-146, 1997.

141. Somlyo AP and Somlyo AV. Ca2+ sensitivity of smooth muscle and nonmuscle myosin II: modulated by G proteins, kinases, and myosin phosphatase. *Physiol Rev* 83: 1325-1358, 2003.

142. Struckmann N, Schwering S, Wiegand S, Gschnell A, Yamada M, Kummer W, Wess J, and Haberberger RV. Role of muscarinic receptor subtypes in the constriction of peripheral airways: studies on receptor-deficient mice. *Mol Pharmacol* 64: 1444-1451, 2003.

143. Svenssen J, Strandberg K, Tuvemo T, and Hamberg M. Thromboxane A2: effects on airway and vascular smooth muscle. *Prostaglandins* 14: 425-436, 1977.

144. Symanowicz PT, Gianutsos G, and Morris JB. Lack of role for the vanilloid receptor in response to several inspired irritant air pollutants in the C57Bl/6J mouse. *Neurosci Lett* 362: 150-153, 2004.

145. Szema AM, Hamidi SA, Lyubsky S, Dickman KG, Mathew S, Abdel-Razek TT, Chen JJ, Waschek JA, and Said SI. Mice lacking the VIP gene show airway hyperresponsiveness and airway inflammation, partially reversible by VIP. *Am J Physiol Lung Cell Mol Physiol*, 2006.

146. Szentivanyi A. The Beta Adrenergic Theory of the Atopic Abnormality in Asthma. *The Journal of Allergy* 42: 203-232, 1968.

147. Takata S, Aizawa H, Shigyo M, Matsumoto K, Inoue H, Koto H, and Hara N. Thromboxane A2 mimetic (U-46619) induces hyperresponsiveness of smooth muscle in the canine bronchiole, but not in the trachea. *Prostaglandins Leukot Essent Fatty Acids* 54: 129-134, 1996.

148. Takeda K, Hamelmann E, Joetham A, Shultz LD, Larsen GL, Irvin CG, and Gelfand EW. Development of eosinophilic airway inflammation and airway hyperresponsiveness in mast cell-deficient mice. *J Exp Med* 186: 449-454, 1997.

149. Taube C, Dakhama A, and Gelfand EW. Insights into the pathogenesis of asthma utilizing murine models. *Int Arch Allergy Immunol* 135: 173-186, 2004.

150. Taylor IK, Ward PS, O'Shaughnessy KM, Dollery CT, Black P, Barrow SE, Taylor GW, and Fuller RW. Thromboxane A2 biosynthesis in acute asthma and after antigen challenge. *Am Rev Respir Dis* 143: 119-125, 1991.

151. Tepper RI, Levinson DA, Stanger BZ, Campos-Torres J, Abbas AK, and Leder P. IL-4 induces allergic-like inflammatory disease and alters T cell development in transgenic mice. *Cell* 62: 457-467, 1990.

152. Van Eerdewegh P, Little RD, Dupuis J, Del Mastro RG, Falls K, Simon J, Torrey D, Pandit S, McKenny J, Braunschweiger K, Walsh A, Liu Z, Hayward B, Folz C, Manning SP, Bawa A, Saracino L, Thackston M, Benchekroun Y, Capparell N, Wang M, Adair R, Feng Y, Dubois J, FitzGerald MG, Huang H, Gibson R, Allen KM, Pedan A, Danzig MR, Umland SP, Egan RW, Cuss FM, Rorke S, Clough JB, Holloway JW, Holgate ST, and Keith TP. Association of the ADAM33 gene with asthma and bronchial hyperresponsiveness. *Nature* 418: 426-430, 2002.

153. Venihaki M, Dikkes P, Carrigan A, and Karalis KP. Corticotropin-releasing hormone regulates IL-6 expression during inflammation. *J Clin Invest* 108: 1159-1166, 2001.

154. Venihaki M and Majzoub J. Lessons from CRH knockout mice. *Neuropeptides* 36: 96-102, 2002.

155. Wahle M, Krause A, Pierer M, Hantzschel H, and Baerwald CG. Immunopathogenesis of rheumatic diseases in the context of neuroendocrine interactions. *Ann N Y Acad Sci* 966: 355-364, 2002.

156. Walenga RW, Kester M, Coroneos E, Butcher S, Dwivedi R, and Statt C. Constitutive expression of prostaglandin endoperoxide G/H synthetase (PGHS)-2 but not PGHS-1 in hum an tracheal epithelial cells in vitro. *Prostaglandins* 52: 341-359, 1996.

157. Walker C, Kaegi MK, Braun P, and Blaser K. Activated T cells and eosinophilia in bronchoalveolar lavages from subjects with asthma correlated with disease severity. *J Allergy Clin Immunol* 88: 935-942, 1991.

158. Walter DM, McIntire JJ, Berry G, McKenzie AN, Donaldson DD, DeKruyff RH, and Umetsu DT. Critical role for IL-13 in the development of allergen-induced airway hyperreactivity. *J Immunol* 167: 4668-4675, 2001.

159. Wardlaw AJ, Brightling CE, Green R, Woltmann G, Bradding P, and Pavord ID. New insights into the relationship between airway inflammation and asthma. *ClinSci(Lond)* 103: 201-211, 2002.

160. Weiss KB and Sullivan SD. The health economics of asthma and rhinitis. I. Assessing the economic impact. *J Allergy Clin Immunol* 107: 3-8, 2001.

161. Widdicombe J. Airway receptors. *Respir Physiol* 125: 3-15, 2001.

162. Widdicombe JG. Autonomic regulation. i-NANC/e-NANC. *Am J Respir Crit Care Med* 158: S171-175, 1998.

163. Williams CM and Galli SJ. Mast cells can amplify airway reactivity and features of chronic inflammation in an asthma model in mice. *J Exp Med* 192: 455-462, 2000.

164. Wills-Karp M and Karp CL. Biomedicine. Eosinophils in asthma: remodeling a tangled tale. *Science* 305: 1726-1729, 2004.

165. Wills-Karp M, Luyimbazi J, Xu X, Schofield B, Neben TY, Karp CL, and Donaldson DD. Interleukin-13: central mediator of allergic asthma. *Science* 282: 2258-2261, 1998.

166. Xin HB, Deng KY, Rishniw M, Ji G, and Kotlikoff MI. Smooth muscle expression of Cre recombinase and eGFP in transgenic mice. *Physiol Genomics* 10: 211-215, 2002.

167. Yamamoto Y, Hayashi M, Atoji Y, and Suzuki Y. Vagal afferent nerve endings in the trachealis muscle of the dog. *Arch Histol Cytol* 57: 473-480, 1994.

168. Yu CK, Lee SC, Wang JY, Hsiue TR, and Lei HY. Early-type hypersensitivity-associated airway inflammation and eosinophilia induced by Dermatophagoides farinae in sensitized mice. *J Immunol* 156: 1923-1930, 1996.

169. Zhu Z, Homer RJ, Wang Z, Chen Q, Geba GP, Wang J, Zhang Y, and Elias JA. Pulmonary expression of interleukin-13 causes inflammation, mucus hypersecretion, subepithelial fibrosis, physiologic abnormalities, and eotaxin production. *J Clin Invest* 103: 779-788, 1999.

CHAPTER II

Thromboxane A_2 Induces Airway Constriction Through An M_3 Muscarinic Acetylcholine Receptor Dependent Mechanism

Thromboxane A_2 Induces Airway Constriction Through An M_3 Muscarinic Acetylcholine Receptor Dependent Mechanism

Irving C. Allen[1], John M. Hartney[1], Thomas M. Coffman[3], Raymond B. Penn[2], Jürgen Wess[4], and Beverly H. Koller[1*]

[1] Curriculum in Genetics and Molecular Biology, University of North Carolina at Chapel Hill, Chapel Hill, North Carolina, 27599

[2] Center For Human Genomics, Wake Forest University Health Science Center, Winston Salem, North Carolina, 27157

[3] Division of Nephrology, Duke University Medical Center, Durham, North Carolina, 27710

[4] Laboratory of Bioorganic Chemistry, NIDDK, Bethesda, Maryland

Nonstandard abbreviations used: Thromboxane A_2 (TXA_2); Thromboxane prostanoid receptor (TP receptor); airway smooth muscle (ASM); M_3 muscarinic acetylcholine receptor subtype (M_3 mAChR); arachidionic acid (AA); methacholine (MCh); lung resistance (R_L); bronchoaveolar lavage fluid (BALF); ovalbumin (OVA)

* Address Correspondence to: Beverly H. Koller, Curriculum in Genetics and Molecular Biology, University of North Carolina at Chapel Hill, Chapel Hill, North Carolina, 27599, USA, Phone: (919) 962-2159; Fax: (919) 843-4362; E-mail: Treawouns@aol.com

Abstract

Thromboxane A_2 (TXA_2) is a potent lipid mediator released by platelets and inflammatory cells and is capable of inducing vasoconstriction and bronchoconstriction. In the airways, it has been postulated that TXA_2 causes airway constriction by direct activation of thromboxane prostanoid (TP) receptors on airway smooth muscle cells. Here we demonstrate that although TXA_2 can mediate a dramatic increase in airway smooth muscle constriction and lung resistance, this response is largely dependent on vagal innervation of the airways and is highly sensitive to muscarinic acetylcholine receptor (mAChR) antagonists. Further analyses employing pharmacologic and genetic strategies demonstrate that TP-dependent changes in lung resistance and airway smooth muscle tension require expression of the M_3 mAChR subtype. These results raise the possibility that some of the beneficial actions of anticholinergic agents used in the treatment of asthma and COPD result from limiting physiological changes mediated through the TP receptor. Furthermore, these findings demonstrate a unique pathway for TP regulation of homeostatic mechanisms in the airway and suggest a paradigm for the role of TXA_2 in other organ systems.

Keywords

nerve

prostanoid

bronchoconstriction

asthma

vagus

Introduction

Thromboxane (TXA_2) was originally identified as the active agent in extracts of human platelets and was subsequently shown to be capable of initiating the contraction of both vascular and airway smooth muscle (ASM) (21). TXA_2 synthesis is initiated by the oxidation of arachidionic acid (AA) by either prostaglandin G/H synthase-1 (or cyclooxygenase-1) (COX-1) or prostaglandin G/H synthase-2 (COX-2) (21). The PGH_2 produced by the cyclooxygenases is metabolized to TXA_2 by thromboxane synthase, an enzyme expressed by many cell types. In the lung, for example, TXA_2 is produced by a number of cells, including the epithelia, smooth muscle and resident macrophages (39, 56). In aqueous solutions, TXA_2 is rapidly hydrolyzed to TXB_2, a stable and inactive metabolite (21). The short half life of TXA_2 suggests that it functions in an autocrine/paracrine fashion and that its actions are limited to tissues in proximity to the source of its synthesis. Because of the instability of TXA_2, most experimental studies of TXA_2 biology have utilized stable TXA_2 mimetics such as U46619 (8, 9, 32).

The actions of TXA_2, as well as those of other prostanoids, are mediated through binding to specific heterotrimeric G protein-associated prostanoid receptors. With the cloning of the TP receptor and the generation of a mouse line lacking expression of this gene, all of the *in vivo* actions of TXA_2 studied to date have been shown to be dependent on expression of this single G protein coupled receptor (30, 40, 45, 52). Most evidence supports the coupling of this receptor to the G_q family of proteins, and many of its physiological actions have been attributed to G_q -mediated activation of phospholipase C (PLC) and increases in intracellular calcium [Ca^{2+}]. In addition to ASM, many other tissues and cell types in the mouse have been reported to express TP receptors, including cells of the immune

system and epithelial cells (11, 13, 22, 37, 38, 49, 54, 56). TP receptor expression on neurons has also been implied from pharmacological studies (26, 29).

Exposure of human tracheal rings to U46619 results in cumulative, concentration-dependent contractions (3). In studies examining isolated human bronchial smooth muscle, U46619 was shown to be 300 times more potent as a constricting agent than other prostanoids. These *ex vivo* studies were consistent with studies in humans (27) and other animals (34) demonstrating that inhalation of U46619 results in rapid bronchoconstriction (12). Furthermore, some studies have even suggested that other constricting prostanoids, such as PGF_2 and PGD_2, may mediate constriction by binding the TP receptor (10, 14).

Concentrations of TXA_2 and other prostanoids in the airway are elevated in a number of lung diseases including asthma and chronic obstructive pulmonary disease (COPD) (15, 41, 42). In addition to higher concentrations, airway sensitivity to these lipid mediators is also increased in disease states (44). Although TXA_2, and possibly other lipid mediators, can mediate their effects by engaging the TP receptor on ASM, the mechanism by which TP receptor activation leads to bronchoconstriction is not well defined. Here we address this question directly using both genetic and pharmacological approaches in conjunction with both *in vivo* and *ex vivo* studies of mouse airways. Similar to observations in other species including humans, we show that inhaled TXA_2 leads to an increase in lung resistance and that TXA_2 can also mediate constriction of tracheal rings *ex vivo*. Analysis of M_3 muscarinic acetylcholine receptor subtype (M_3 mAChR) knockout mice showed that the *in vivo* airway constrictor responses to TXA_2 are primarily dependent on parasympathetic innervation of the lungs and the presence of functional M_3 mAChRs.

Methods

Experimental Animals

All studies were conducted in accordance with the National Institutes of Health Guide for the Care and Use of Laboratory Animals as well as the Institutional Animal Care and Use Committee guidelines of the University of North Carolina at Chapel Hill. Mice deficient in the TP receptor were generated and genotyped by Southern blot analysis or PCR as previously described (52). The 129 $TP^{-/-}$ mice were obtained by breeding chimeras generated from $TP^{+/-}$ 129/Olac embryonic stem (ES) cells directly with 129/SvEv females. Heterozygous animals were crossed for two consecutive generations to 129/SvEv animals to reduce the contribution of the 129/Olac substrain. The generation of mAChR3$^{-/-}$ mice has been described previously (58). The mAChR3$^{-/-}$ and corresponding mAChR$^{+/+}$ control mice are maintained on a 129SvEv (50%) X CF1 (50%) mixed genetic background. All experiments were carried out using 8-12 week old mice.

Measurement of Airway Reactivity in Intubated Mice

Mice were anesthetized with 70-90 mg/kg pentobarbital sodium (American Pharmaceutical Partners, Los Angeles, CA), tracheostomized, and mechanically ventilated at a rate of 300 breaths/min, tidal volume of 6 cc/kg, and positive end-expiratory pressure of 3-4 cm H_2O with a computer controlled small-animal ventilator (Scireq, Montreal, Canada). Once ventilated, mice were paralyzed with 0.8 mg/kg pancuronium bromide. Dynamic lung resistance (R_L) and dynamic compliance (C_{dyn}) were determined by transducing airway pressure and airflow using a precisely controlled piston during a single inspiration and

expiration with an amplitude of 150 μl and a period of one second (SnapShot). The single compartment equation of motion (Eq1) allows determination of R_L and C_{dyn} (25).

$$P(t) = R \times \dot{v}(t) + (1/C) \times V(t) + P_0 \quad \text{(Equation 1)}$$

Where P(t) = pressure at time t, R= resistance, $\dot{v}(t)$ = flow at time t, C = compliance, V(t) = volume at time t and P_0 = resting pressure (PEEP)

Five separate baseline measurements of parameters were taken before exposure to U46619. Following baseline assessments, aerosols of (15*S*)-hydroxy-9,11-epoxymethanoprosta-5*Z*,13*E*-dienoic acid (U46619)(Caymen Chemical, Ann Arbor, MI), at doses indicated (generally 10^{-6} M - 10^{-3} M), were delivered via nebulizer through a side port in the ventilator circuit for 30 seconds at a rate of 200 breaths per minute. As a response to U46619 was observed only following 10^{-4} M and 10^{-3} M doses, these concentrations were used in lieu of the full range of doses in some experiments. Following U46619 exposure, R_L was measured every 10 seconds for 3 minutes. To determine the contribution of mAChRs to the U46619 response, mice received either an intraperitoneal injection of atropine sulfate (10 μM/kg)(American Pharmaceutical Partners, Los Angeles, CA) or an i.v. injection of hexahydro-sila-difenidol p-fluorohydrocholride (4DAMP) (4ng/g)(Sigma Chemical, St. Louis, MO). Similar to other studies measuring airway resistance using these techniques (4, 23, 53), data are presented as percent baseline R_L.

A surgical vagotomy was conducted to assess the contribution of intact parasympathetic innervation. While anesthetized, the vagal nerves on each side of the

esophagus were identified under a dissecting microscope and dissected free of the fascia and carotid artery. A silk suture was passed under each vagus to allow easy identification and severing of the nerve in the ventilated animals. Mice were then tracheostomized and placed on a ventilator (Flexivent). After treatment with the paralytic agent, five snapshots were recorded. In the experimental animals, after establishment of basal lung mechanics, both vagal nerves were severed. Post-vagotomy baseline R_L and C_{dyn} was then reassessed and the mice were challenged with U46619.

Measurement of Tension Development in Tracheal Rings

Mice were euthanized by inhalation of CO_2. The tracheas were then rapidly excised in 3- to 4- mm segments, cleaned of superficial fat and connective tissue, and placed in a Krebs-Henseleit solution (53). These segments were mounted between two triangular stainless steel hooks, put into double jacketed glass organ baths containing Krebs-Henseleit solution (maintained at a pH of 7.40-7.45), and continuously gassed with carbogen (5% O_2 and 5% CO_2). The upper support for the tracheal segment was attached, via silk thread, to a FT03 isometric transducer (Astro-Med, West Warwick, RI) and force generation was recorded with a MP 100WS system (BIOPAC Systems). The rings were equilibrated in the respective buffered solutions for 30 min at a predetermined resting tension based on experimental calibration (approximately 0.5 g) (18, 47, 51). Rings were then pre-constricted with MCh (10^{-8} M), allowed to equilibrate for 10 minutes, washed 3 to 4 times, and re-equilibrated to 0.5 grams. A dose response curve was then generated with either MCh (10^{-8} M to 10^{-3} M) or U46619 (10^{-10} M to 10^{-3} M)(50).

To assess the contribution of muscarinic receptors, atropine (10^{-6} M) was added directly to the buffers of selected rings 15 min prior to experimental challenges. The response to U46619 (50 nM to 500 nM) was examined, as well as, the response to a single dose of MCh (100 μM) delivered immediately after the final dose of U46619. The response to this application of MCh is shown in the figures. The rings were then washed 3 to 4 times and a final dose of MCh (100 μM) was added to ensure tissue viability (data not shown). To assess the contribution of the M3 mAChR, rings from mAChR3$^{-/-}$ and mAChR3$^{+/+}$ mice were pre-constricted with serotonin (5-HT) (20 mM), allowed to equilibrate for 10 minutes, washed 3 to 4 times, and re-equilibrated to 0.5 grams. The response to U46619 (50 nM and 100 nM) was examined, as well as, the response to a single dose of 5-HT (20 mM) delivered immediately after the final dose of U46619. The response to this application of 5-HT is shown in the figures.

All experiments and dissections were conducted in the presence of indomethacin (10^{-6} M) (Sigma-Aldrich, St. Louis, MO) to prevent endogenous prostaglandin release. Similar to other studies using these techniques (36, 53, 57), data are presented as mg developed tension/mg tissue weight.

OVA Sensitization and Airway Challenge

Groups of mice were sensitized by i.p. injection of 20 ug of OVA (Grade V; Sigma) emulsified in 2.25 mg of aluminum hydroxide (Sigma) in a total volume of 200 ul, on days 1 and 14. Mice were challenged (45 min) via the airways with OVA (1% in saline) for 3 days (days 21 – 23) using a jet nebulizer (TSI Jet Neb). Control mouse groups received the 2

OVA immunizations but were challenged with aerosolized saline. Airway mechanics were assessed 24 hours after the final aerosol OVA or saline challenge (day 24).

Following airway assessments, mice were euthanized and approximately 1 ml of blood was collected by heart stick. Blood was allowed to coagulate and the serum was collected. Total IgE levels were determined by ELISA (ICN Biomedicals, OH). BALF was performed 5 times with 1.0 ml of sterile Hank's Buffered Saline Solution each time. Cells present in the BALF were determined using a hemacytometer. The recovered BALF fluid was centrifuged to remove cells and the IL-13 levels in the supernatant was determined using ELISA (R&D Systems, MN).

Statistical Analysis

Data are presented as the means +/- standard error of the mean (SEM). A Random Effects Model followed by Tukey's Multiple Comaprison Test was utilized to assess dose response data. Analysis Of Variance (ANOVA) followed by Tukey's Multiple Comaprison Test was performed on complex data sets. Statistical significance for single data points was assessed by the Student's two-tailed t-test. A p-value of less than 0.05 was considered statistically significant.

Results

TXA_2 increases airway constriction in a TP receptor-dependent manner.

TXA_2 has been shown to cause bronchoconstriction in a number of species. Because of the short half-life of TXA_2, experimental investigation into TXA_2/TP receptor–dependent effects typically employs the synthetic agonist U46619. Preliminary experiments verified that under our experimental conditions and with doses of U46619 generally used in *in vivo* experiments, all of the actions of this mimetic were dependent on the expression of the TP receptor. U46619 at concentrations up to 1 mM failed to elicit an increase in R_L from mice in which the gene encoding the TP receptor was disrupted by homologous recombination ($TP^{-/-}$) (Figure 2.1A). In contrast, R_L in wild type mice increased in response to 100 μM and 1 mM U46619 (Figure 2.1A). Conversely, methacholine (MCh) challenge resulted in similar increases in R_L in wild type and $TP^{-/-}$ mice (Figure 2.1B). We next examined the ability of U46619 to constrict mouse trachea. A very steep dose response was observed: U46619 elicited no significant increase in tension at doses below 10 nM while maximal responses were achieved with 100 nM of this agonist (data not shown). Consistent with our *in vivo* data, *ex vivo* tension generation in tracheal ring preparations was similar in rings from wild type and $TP^{-/-}$ mice stimulated with MCh, whereas U46619 caused significant tension generation in rings from wild type mice but not in rings isolated from $TP^{-/-}$ mice (Figure 2.1C).

Vagotomy significantly attenuates U46619-induced increases in lung resistance (R_L)

The simplest explanation for the observed changes in R_L and *ex vivo* tension generation is that binding of U46619 to TP receptors expressed by ASM directly activates G_q coupled

pathways leading to increases in $[Ca^{2+}]_i$, and that this constriction is independent of the activity of the parasympathetic innervation of the airways. To test this model, we examined the ability of U46619 to elicit an increase in R_L in animals in which the vagus nerves were surgically severed just proximal to the nodose ganglion. Sham operated animals, treated identically to the experimental animals except for the final severing of the nerve, served as controls. Baseline R_L was assessed for 5 minutes before and 5 minutes after vagotomy. Baseline R_L was higher in the mice in which the surgeries had been preformed compared to values generally observed for mice on the 129SvEv background, likely reflecting local mediator release during the surgical procedure. As expected, the lung resistance of the sham operated animals increased in response to U46619. However, the magnitude of the percent change in R_L was smaller than that previously measured in wild type 129 animals. This likely reflects the higher baseline R_L in the surgically manipulated animals. A slight but significant drop in the baseline R_L (Figure 2.2A) and an increase in airway compliance (data not shown) were observed after vagotomy. This change in baseline resistance was expected, as similar changes have been observed in other species after vagotomy (6, 7, 33). The drop in R_L reflects the loss of basal parasympathetic tone in the airways. Following establishment of post-vagotomy baseline R_L, mice were challenged with U46619 (10^{-4} M and 10^{-3} M). Although U46619 still elicited an increase in R_L in the vagotomized animals, the response was significantly attenuated compared to that observed in the sham-operated animals ($p<0.05$)(Figure 2.2B). These data suggest that *in vivo*, TXA_2 functions in part via an indirect neurally-mediated mechanism to induce ASM reactivity. This neurally-mediated mechanism functions in a concerted manner with other mechanism(s) that are not dependent on vagal innervation of the airways.

Atropine attenuates U46619 induced ASM constriction

Previous studies investigating the ability of TXA_2/U46619 to meditate direct actions on smooth muscle cells utilized *ex vivo* preparations of either tracheal rings or strips of ASM prepared from tracheae or bronchi. In our studies, tracheal rings were isolated from wild type and $TP^{-/-}$ mice and stimulated with increasing doses of U46619 (Figure 2.3A). Rings from untreated $TP^{-/-}$ mice were included in the study to control for non-receptor mediated actions of U46619 (data not shown). As expected, U46619 increased tension in the rings from wild type mice. No response was observed in the $TP^{-/-}$ animals. To determine whether the response observed with the wild type preparations was dependent on muscarinic cholinergic pathways, we next examined the ability of atropine (10^{-6} M), a nonselective mAChR antagonist, to block this response. At all stimulating concentrations of U46619, pretreatment of rings with atropine significantly attenuated tension generation. However, U46619 at doses above 100 nM provoked a significant change in tension in the atropine treated rings over baseline ($p<0.005$)(Figure 2.3A). As expected, in the presence of atropine, addition of MCh to rings contracted with 500 nM U46619 did not evoke a further increase in tension (Figure 2.3A). To ensure that the atropine-pretreated tracheal rings were still capable of MCh-induced contraction, the rings were washed multiple times to remove the atropine. MCh was subsequently added back to the ring buffer. In this case, MCh increased tension in all groups of mice, irrespective of previous treatment protocol or genotype (data not shown).

Atropine inhibits U46619 induced increases in lung resistance.

We next evaluated the ability of atropine to block U46619-mediated increases in lung resistance. $TP^{-/-}$ and wild type mice were pretreated with either atropine (10 μM/kg) or saline. Untreated $TP^{-/-}$ mice were included in the study to control for TP receptor-independent effects of U46619. Mice were intubated, baseline R_L was established, and the mice were then exposed to vehicle followed by aerosols of U46619 (10^{-4} M and 10^{-3} M). As expected, a significant increase in R_L was observed in the saline-pretreated wild type mice exposed to U46619 (Figure 2.3B). The U46619 response in the atropine-pretreated mice was significantly attenuated compared to the saline pretreated animals (Figure 2.3B). As previously observed, $TP^{-/-}$ mice failed to respond to U46619 (Figure 2.3B).

The M_3 mAChR receptor-preferring antagonist 4DAMP significantly attenuates U46619-induced increases in lung resistance.

ASM expresses the $G_{q/11}$ coupled M_3 mAChR and both pharmacological studies and studies with mice lacking this receptor indicate that airway constriction in response to cholinergic agents is mediated primarily through this receptor (19, 43, 46, 48). The muscarinic antagonist 4DAMP preferentially binds to the M_3 mAChR receptor (5); however, it also displays high affinity for M_1, M_4, and M_5 mAChRs (5). Therefore, we determined the lowest dose of 4DAMP that completely blocks MCh-induced changes in airway resistance in the mouse. This dose of 4DAMP (4 ng/g; data not shown), when delivered by i.v. injection prior to challenge with U46619, significantly inhibited U46619-induced increases in R_L, with values never significantly exceeding those recorded for the $TP^{-/-}$ mice (Figure 2.4).

Mice lacking the M_3 mAChR demonstrate a significant decrease in U46619-induced airway smooth muscle constriction and lung resistance.

To further demonstrate the role of muscarinic cholinergic pathways in TXA_2-mediated changes in airway constriction, we examined the response to U46619 in mice lacking the M_3 mAChR ($mAChR3^{-/-}$). Tracheal rings from $mAChR3^{-/-}$ and age/strain-matched control mice were exposed to constricting doses of U46619. A significant increase in tension was observed in the wild type control animals following exposure to 50 nM and 100 nM of agonist. Consistent with the ability of atropine to modulate contraction of the tracheal rings, response of the $mAChR3^{-/-}$ tracheas was dramatically attenuated at both concentrations of U46619 examined. However, a small but significant increase in constriction was still observed in $mAChR3^{-/-}$ tracheal rings in response to U46619 (Figure 2.5A). To verify that the altered response of the $mAChR3^{-/-}$ rings did not reflect a fundamental defect in smooth muscle function as a consequence of loss of this receptor and to verify that the preparations used in this study were viable, we examined the response of these same tracheas to serotonin. A robust increase in tension was observed following treatment of both wild type and $mAChR3^{-/-}$ trachea with this constricting agent.

We next examined the ability of thromboxane to increase lung resistance in mice lacking the M_3 mAChR. As seen in Figure 2.5B, loss of the M3 mAChR significantly attenuates the U46619-induced increases in R_L. Greater than 80% of the response to U46619 (10^{-3} M) was lost in the $mAChR3^{-/-}$ mice. However, consistent with our findings in experiments examining the effects of atropine, $mAChR3^{-/-}$ mice showed a small but significant increase in R_L in response to U46619 (Figure 2.5B). These data suggest a predominant role for the M_3 mAChR in TXA_2-mediated airway constriction.

TP receptor-mediated changes in R_L are enhanced in the allergic inflamed airway, but remain sensitive to atropine.

Allergic airway inflammation was induced in wild type and $TP^{-/-}$ mice. All mice were immunized via i.p. injection with ovalbumin (OVA)/alum. To induce allergic lung disease, mice were challenged with aerosols of OVA. Control animals were exposed to aerosols of saline. Twenty-four hours after the final exposure to antigen or saline, mice were intubated and exposed to increasing doses of U46619. As depicted in Figure 2.6, the response to both 10^{-4} M and 10^{-3} M U46619 was substantially increased in OVA-challenged wild type mice compared to saline exposed control animals. Thus, as observed in humans, the bronchoconstricting actions of TXA_2 are dramatically enhanced in the inflamed airway (1). No significant change in R_L in response to U46619 was observed in $TP^{-/-}$ mice, confirming that even in the inflamed airway the response to U46619 remains dependent on TP receptor expression (Figure 2.6). We next determined whether, similar to the response in naïve mice, the response of mice with allergic lung disease to U46619 was sensitive to atropine. Alternatively, we considered the possibility that the M_3 receptor-independent TP response is amplified in the inflamed lung. To distinguish between these two possibilities, a group of OVA challenged mice and their corresponding saline challenged controls received a single i.p. treatment of atropine just prior to intubation and measurement of airway mechanics. As seen in Figure 2.6, the response of the mice with allergic lung disease to U46619 was dramatically reduced. The response remaining in these animals was not significantly greater than the response to U46619 measured in atropine treated naïve animals. Thus, the

mechanism by which U46619 mediates the increased responsiveness in the diseased animal is similarly dependent on an intact muscarinic cholinergic pathway(s).

At the end of the measurements of lung mechanics, as described above, the induction of allergic airway disease was verified by determining serum IgE levels, cellularity of bronchoalveolar lavage (BALF), and histopathology of the lungs. Increases of similar magnitude were observed in total BALF cell counts (3.3×10^6 total cells in OVA treated animals vs 1×10^5 in saline treated animals) and airway eosinophilia (approximately 80% of cells present were eosinophils) between the OVA-challenged $TP^{-/-}$ and wild type mice (data not shown). Likewise, a similar increase in IgE levels (2500 ng/ml in OVA vs 225 ng/ml in saline) and IL-13 levels (550 pg/lung after OVA challenge vs undetectable in saline treated) were observed between the OVA-challenged $TP^{-/-}$ and wild type mice (data not shown).

Figure 2.1

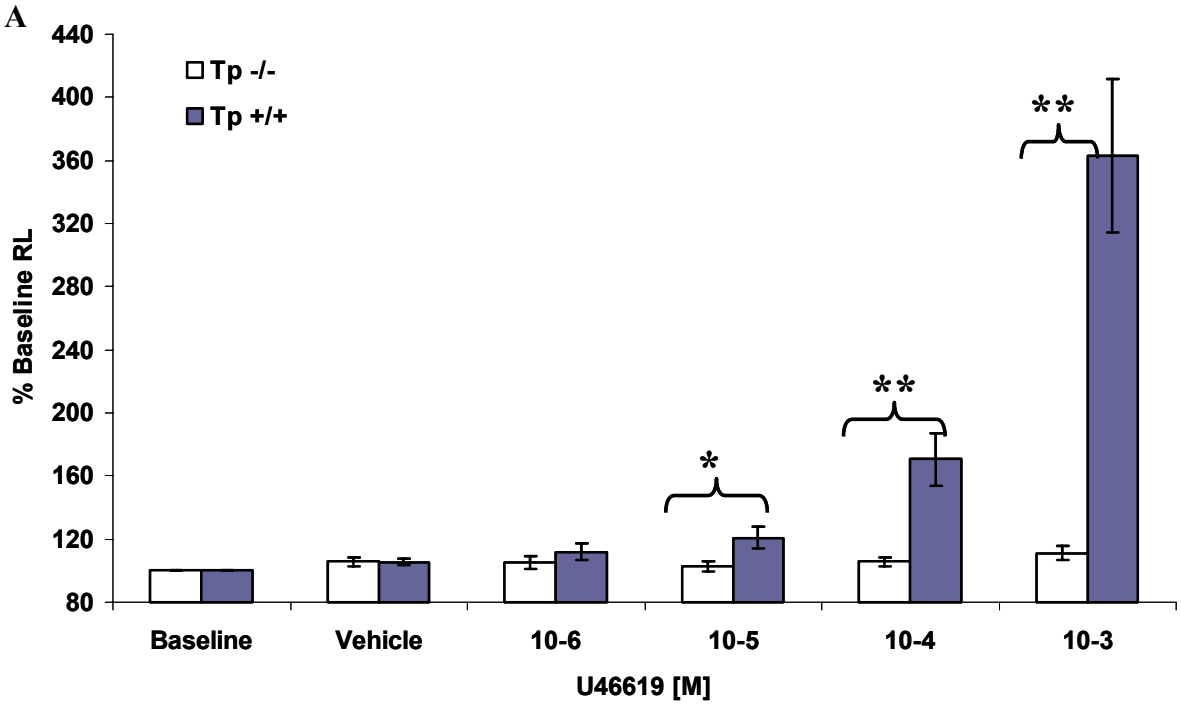
A
Tp -/-
Tp +/+
% Baseline RL
440
400
360
320
280
240
200
160
120
80
*
**
**
Baseline
Vehicle
10-6
10-5
10-4
10-3
U46619 [M]

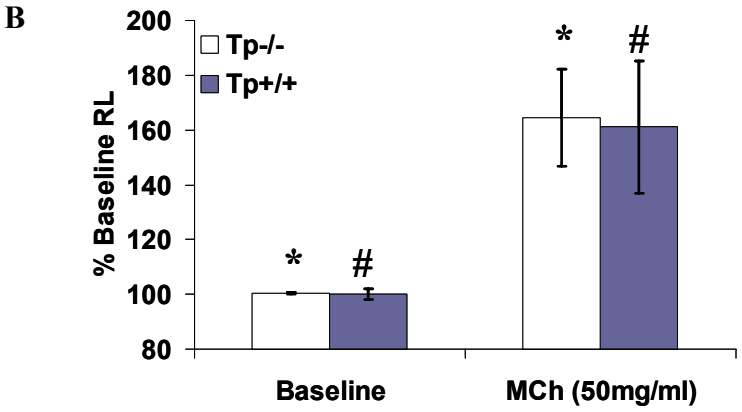
B
Tp-/-
Tp+/+
% Baseline RL
200
180
160
140
120
100
80
*
#
*
#
Baseline
MCh (50mg/ml)

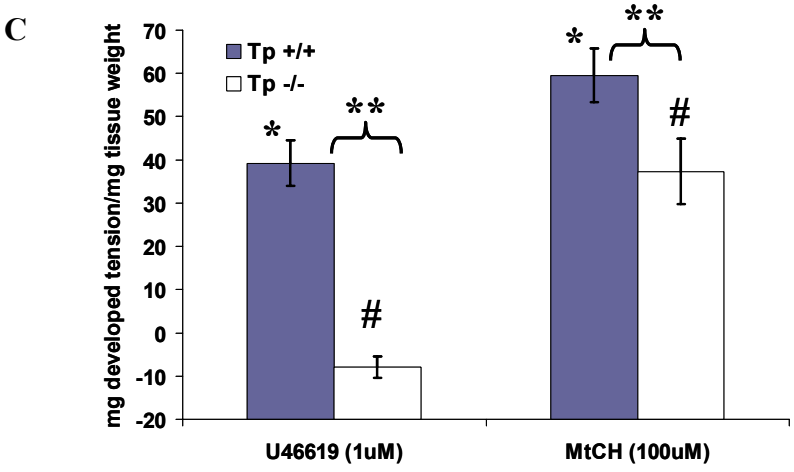
C
Tp +/+
Tp -/-
mg developed tension/mg tissue weight
70
60
50
40
30
20
10
0
-10
-20
*
**
#
*
**
#
U46619 (1uM)
MtCH (100uM)

Figure 2.1. Changes in airway physiology of wild type and $TP^{-/-}$ mice in response to the TXA_2 analog U46619 and MCh. A) Change in lung resistance (R_L) of $TP^{+/+}$ and $TP^{-/-}$ mice in response to U46619. Following baseline measurements, the airways were exposed to aerosolized vehicle followed by increasing doses of aerosolized U46619 (10^{-6} M to 10^{-3} M). The percent change in R_L from baseline increased significantly in the wild type mice exposed to 10^{-4} M and 10^{-3} M U46619 as compared with no increase in R_L in $TP^{-/-}$ mice. $TP^{+/+}$ mice, n=34; $TP^{-/-}$ mice, n=13 (**p<0.005). **B)** $TP^{-/-}$ and $TP^{+/+}$ mice demonstrate similar increases in R_L following exposure to methacholine (MCh). $TP^{+/+}$ and $TP^{-/-}$ mice were subjected to aerosolized vehicle and 1 bolus dose of aerosolized MCh (50 mg/ml = 255.1 mM). The percent increase from baseline was similar for both $TP^{+/+}$ and $TP^{-/-}$ mice. $TP^{+/+}$ mice, n=5; $TP^{-/-}$ mice, n=5 (*, # p<0.05). **C)** Contraction of $TP^{-/-}$ and $TP^{+/+}$ tracheal rings. Excised tracheal rings from both $TP^{+/+}$ and $TP^{-/-}$ mice were challenged with a single dose of U46619 (1 μM) and the change in tension recorded. This was followed by treatment with MCh (100 μM). Ring tension was significantly increased following addition of U46619 in rings from $TP^{+/+}$ mice while no increase was observed in rings from $TP^{-/-}$ mice. Ring tension was significantly increased in response to MCh in both groups. $TP^{+/+}$ mice, n=3; $TP^{-/-}$ mice, n=3 (**p<0.007; #, *p<0.05).

Figure 2.2

A)

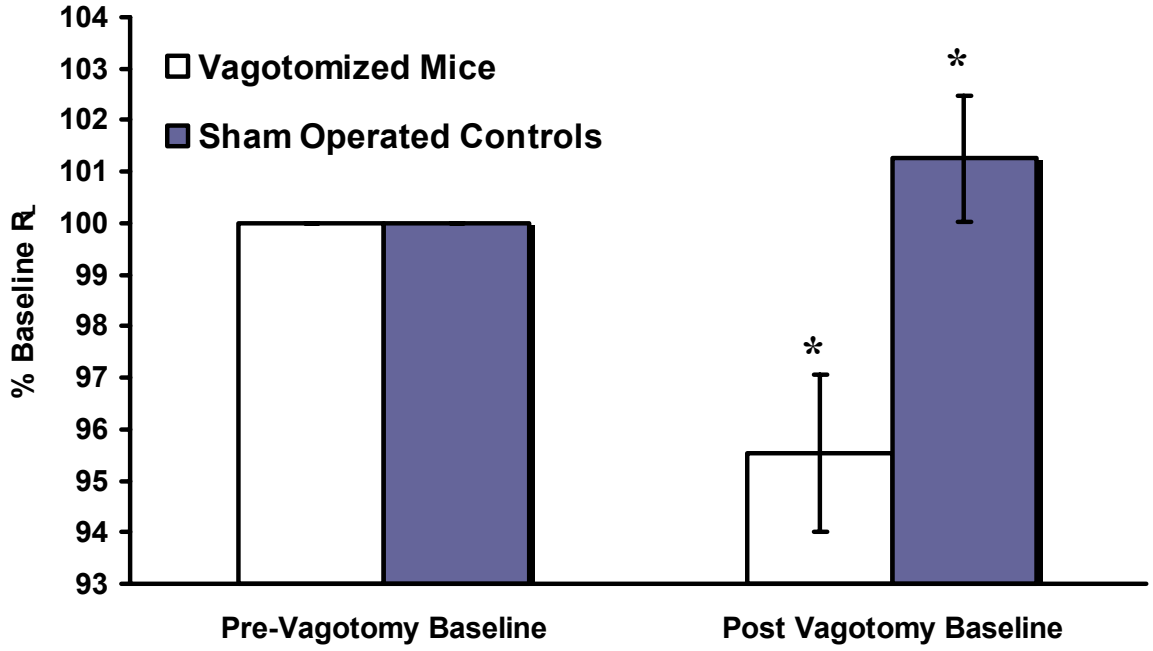
Vagotomized Mice
Sham Operated Controls
% Baseline R_L
104
103
102
101
100
99
98
97
96
95
94
93
*
*
Pre-Vagotomy Baseline
Post Vagotomy Baseline

B)

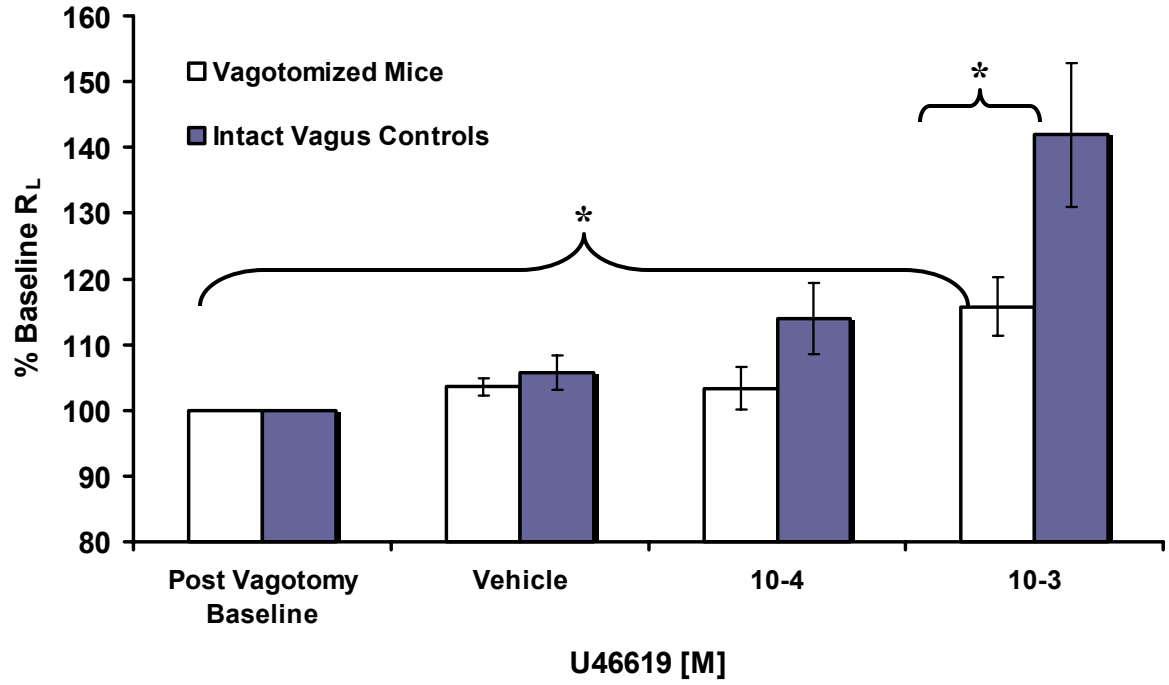
Vagotomized Mice
Intact Vagus Controls
% Baseline R_L
160
150
140
130
120
110
100
90
80
*
*
Post Vagotomy Baseline
Vehicle
10-4
10-3
U46619 [M]

Figure 2.2. Vagotomy significantly attenuates change in airway resistance induced by U46619 challenge. A) Parasympathetic tone in mouse lung. Mice were anesthetized and the vagal nerve dissected free of the fascia and carotid artery. Mice were tracheostomized and placed on a ventilator (Flexivent). After treatment with a paralytic agent, five snapshots were recorded. In one group of animals, after establishment of basal lung mechanics, the vagus nerves were severed. The percent change in R_L from the pre-cut baseline decreased significantly in vagotomized mice as compared to the surgical controls. $TP^{+/+}$ mice, n=10; vagotomized $TP^{+/+}$ mice, n=9 (* $p<0.05$). **B)** The response to U46619 is attenuated in vagotomized mice. Following the baseline assessment described above, vagotomized mice and the surgical controls were exposed to vehicle for 20 seconds and airway reactivity was assessed every 10 seconds for the next three minutes. Mice were then exposed to increasing doses of the TXA_2 analog U46619 and the change in lung mechanics after each dose was recorded. The response of the vagotomized mice was significantly attenuated at the highest dose of U46619 (* $p<0.05$). Importantly, a significant response to U46619 could still be measured in the vagotomized animals.

Figure 2.3

A)

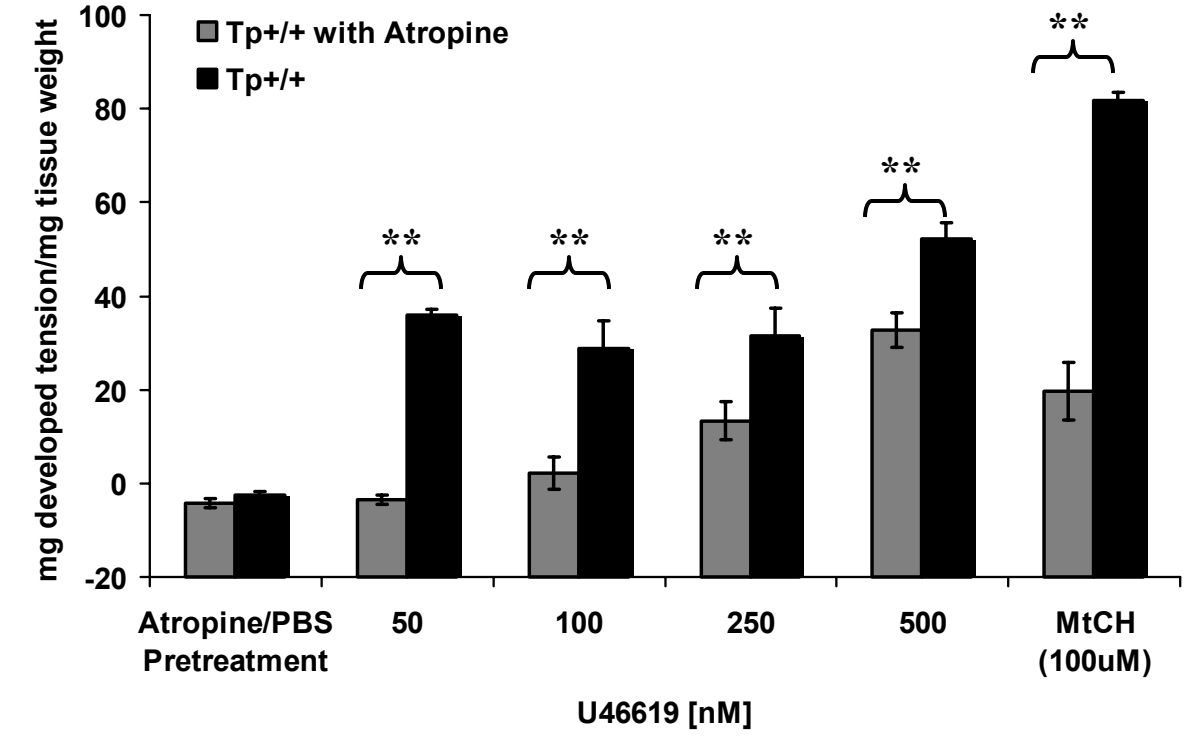
Tp+/+ with Atropine
Tp+/+
mg developed tension/mg tissue weight
100
80
60
40
20
0
-20
**
**
**
**
**
Atropine/PBS Pretreatment
50
100
250
500
MtCH (100uM)
U46619 [nM]

B)

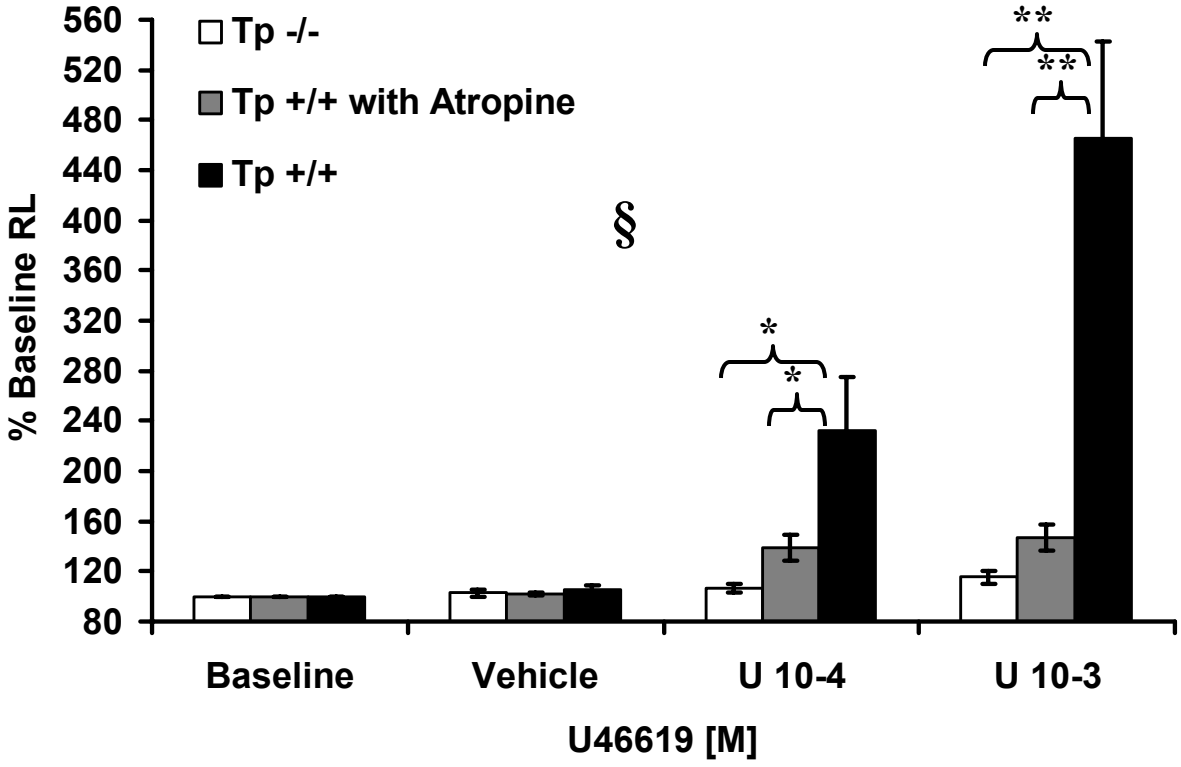
Tp -/-
Tp +/+ with Atropine
Tp +/+
§
% Baseline RL
560
520
480
440
400
360
320
280
240
200
160
120
80
**
**
*
*
Baseline
Vehicle
U 10-4
U 10-3
U46619 [M]

Figure 2.3. Atropine attenuates U46619 mediated changes in ASM constriction and lung resistance. **A)** Atropine partially blocks the contractile response to U46619. Excised tracheal rings from $TP^{+/+}$ mice were incubated in either the presence or absence of atropine (10^{-6} M), challenged with increasing doses of U46619 (50 – 500 nM), and challenged with a bolus dose of MCh (100 μM). Atropine significantly reduced the average tension during all doses tested. $TP^{+/+}$ mice with atropine, n=17; $TP^{+/+}$ mice, n=11 (**p<0.005). **B)** Atropine attenuates U46619 mediated changes in lung resistance (R_L). The change in R_L in response to U46619 in intubated $TP^{+/+}$ mice pretreated with atropine (10μM/kg i.p.), $TP^{+/+}$ mice pretreated with saline, and $TP^{-/-}$ mice was determined. Mice were subjected to aerosolized vehicle followed by increasing doses of aerosolized U46619 (from 10^{-6} to 10^{-3} M; 10^{-6} and 10^{-5} M data not shown). Following the U46619 challenge, the response to aerosolized MCh (50 mg/ml = 255.1 mM) was measured (data not shown). A dose-dependent increase in R_L was observed in the $TP^{+/+}$ mice in response to U46619 and this response was absent in the $TP^{-/-}$ animals. Pretreatment with atropine dramatically attenuated the response of $TP^{+/+}$ mice to U46619. As expected, atropine pretreatment inhibited the MCh response (data not shown). Atropine pretreated $TP^{+/+}$ mice, n=10; saline pretreated $TP^{+/+}$ mice, n=10; $TP^{-/-}$ mice, n=11 (§p<0.05; *p<0.05; **p<0.005).

Figure 2.4

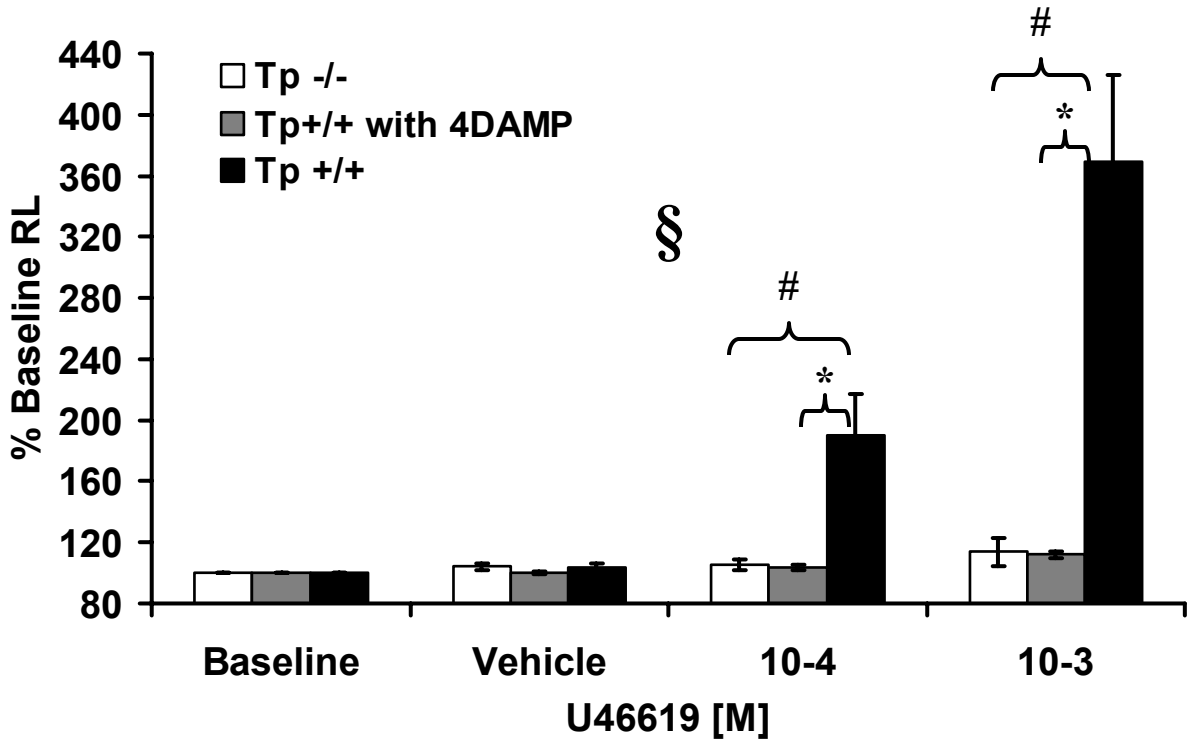
Tp -/-
Tp+/+ with 4DAMP
Tp +/+
% Baseline RL
440
400
360
320
280
240
200
160
120
80
§
#
*
#
*
Baseline
Vehicle
10-4
10-3
U46619 [M]

Figure 2.4. The M_3 mAChR-preferring antagonist 4DAMP attenuates U46619 mediated lung resistance. The change in R_L in response to U46619 in intubated $TP^{+/+}$ mice pretreated with 4DAMP (4 ng/g; i.v. injection), $TP^{+/+}$ mice treated with vehicle, and $TP^{-/-}$ mice was determined. A dose-dependent increase in R_L was observed in the $TP^{+/+}$ mice in response to U46619 and this response was absent in the $TP^{-/-}$ animals. Pretreatment with 4DAMP inhibited the response of wild type mice to U46619 and no significant increase in R_L was observed in this group over that measured in $TP^{-/-}$ animals. 4DAMP pretreated $TP^{+/+}$ mice, n=10; Vehicle pretreated $TP^{+/+}$ mice, n=21; $TP^{-/-}$ mice, n=3 (§$p<0.05$; #$p<0.05$; *$p<0.005$).

Figure 2.5

A

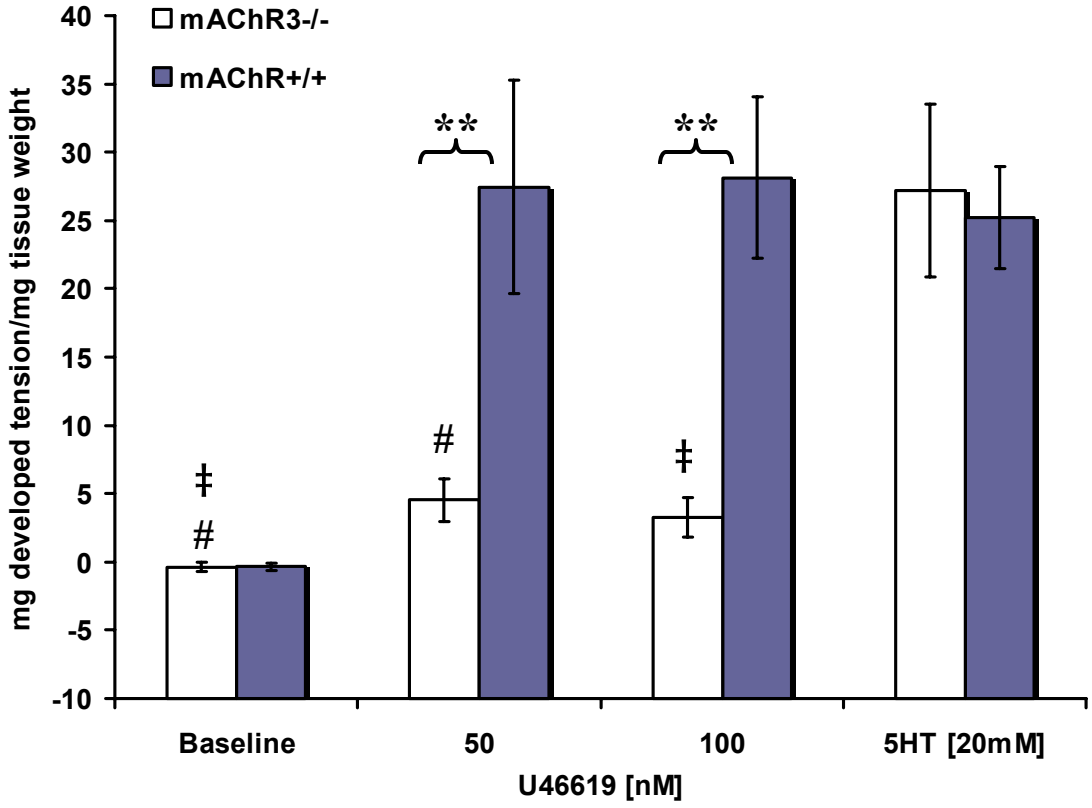
mAChR3-/-
mAChR+/+
mg developed tension/mg tissue weight
40
35
30
25
20
15
10
5
0
-5
-10
**
**
‡
#
#
‡
Baseline
50
100
5HT [20mM]
U46619 [nM]

B

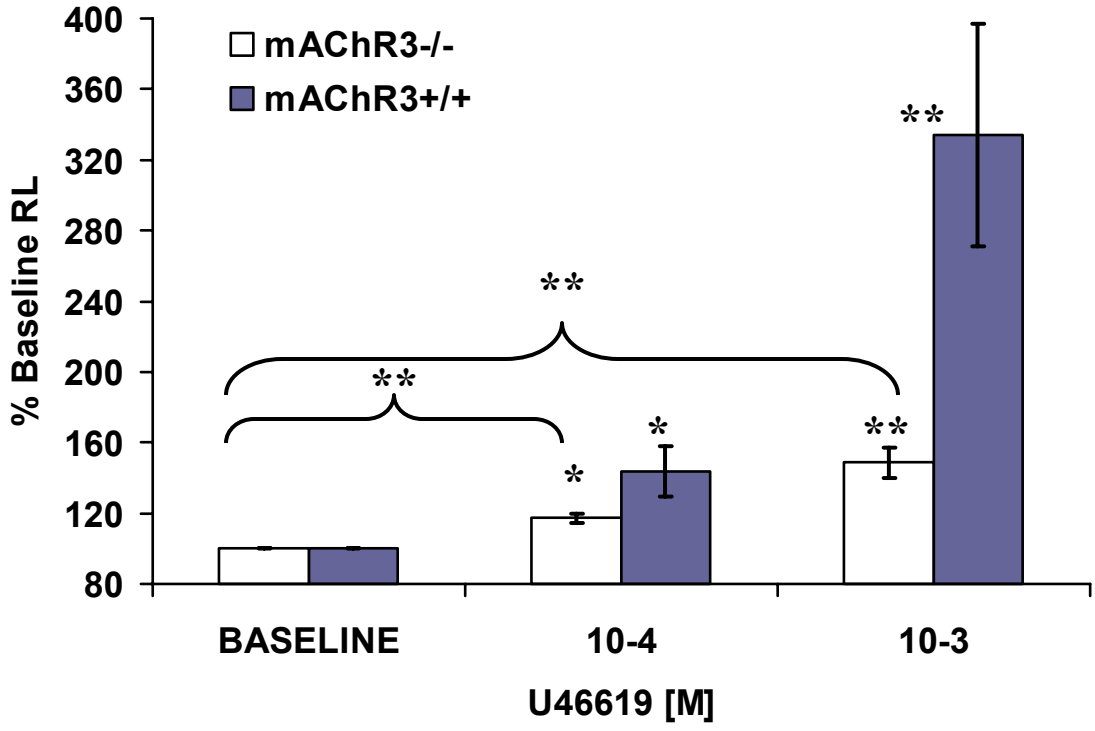
mAChR3-/-
mAChR3+/+
% Baseline RL
400
360
320
280
240
200
160
120
80
**
**
*
*
**
**
BASELINE
10-4
10-3
U46619 [M]

Figure 2.5. ASM constriction and lung resistance following U46619 treatment is attenuated in mice lacking the M_3 mAChR (mAChR3$^{-/-}$). A) Tracheal rings from mAChR3$^{-/-}$ mice demonstrated attenuated contractile responses to U46619. Excised tracheal rings from mAChR3$^{+/+}$ and mAChR3$^{-/-}$ mice were exposed to U46619 (50 nM and 100 nM) and changes in tension were recorded. Ring tension was significantly increased following addition of U46619 in rings from mAChR3$^{+/+}$ mice. A small, but significant, increase in average tension was observed in mAChR3$^{-/-}$ mice at both U46619 doses. To verify the viability of the rings, these manipulations were followed by treatment with a constricting dose of serotonin (5-HT) (20 mM). No difference in 5-HT mediated constriction was observed between the mAChR3$^{+/+}$ and mAChR3$^{-/-}$ tracheal rings. mAChR3$^{+/+}$ mice, n=7; mAChR3$^{-/-}$ mice, n=8 (**p<0.005; #p<0.05; ‡p<0.05). **B)** The change in R_L in response to U46619 in intubated mAChR3$^{+/+}$ mice was significantly attenuated. Mice were subjected to a 20-second aerosolization of increasing doses of U46619 (10^{-4} to 10^{-3} M). A dose-dependent increase in R_L was observed in the mAChR3$^{+/+}$ mice in response to U46619 and this response was significantly attenuated in the mAChR3$^{-/-}$ animals. mAChR3$^{+/+}$ mice, n=5; mAChR3$^{-/-}$ mice, n=7 (*p<0.05; **p<0.005).

Figure 2.6

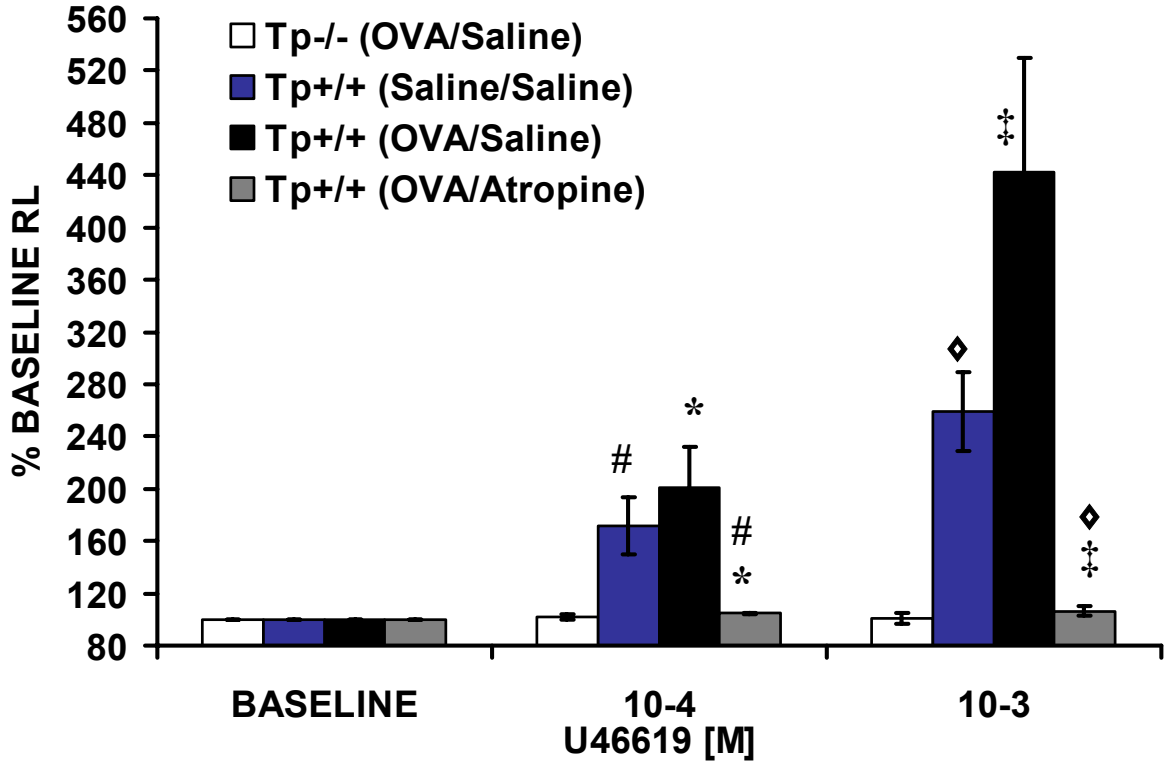
Tp-/- (OVA/Saline)
Tp+/+ (Saline/Saline)
Tp+/+ (OVA/Saline)
Tp+/+ (OVA/Atropine)
% BASELINE RL
560
520
480
440
400
360
320
280
240
200
160
120
80
#
*
#
*
◊
‡
◊
‡
BASELINE
10-4
10-3
U46619 [M]

Figure 2.6. Atropine inhibits U46619 mediated changes in resistance in the inflamed lung. Atropine inhibits U46619 mediated changes in lung resistance (R_L) following challenges with 1% Ovalbumin (OVA). The change in R_L in response to U46619 in intubated $TP^{+/+}$ mice, $TP^{+/+}$ mice pretreated with atropine (10μM/kg i.p.), $TP^{+/+}$ mice treated with saline, and $TP^{-/-}$ mice was determined. Mice were subjected to a 30 second aerosolization of increasing doses of U46619 (10^{-4} and 10^{-3} M), followed by 3 minutes of response measurements. A dose-dependent increase in R_L was observed in the $TP^{+/+}$ mice and in the OVA challenged $TP^{+/+}$ mice in response to U46619 and this response was absent in the $TP^{-/-}$ animals. Pretreatment with atropine inhibited the response of the wild type mice to U46619. Furthermore, no significant increase in R_L was observed in the atropine pretreated group over that measured in $TP^{-/-}$ animals. $TP^{+/+}$ mice, n = 11; atropine pretreated $TP^{+/+}$ mice, n=6; saline pretreated $TP^{+/+}$ mice, n=24; $TP^{-/-}$ mice, n=6 (*$p<0.05$; #$p<0.05$; ♦$p<0.05$; ‡$p<0.05$).

Figure 2.7

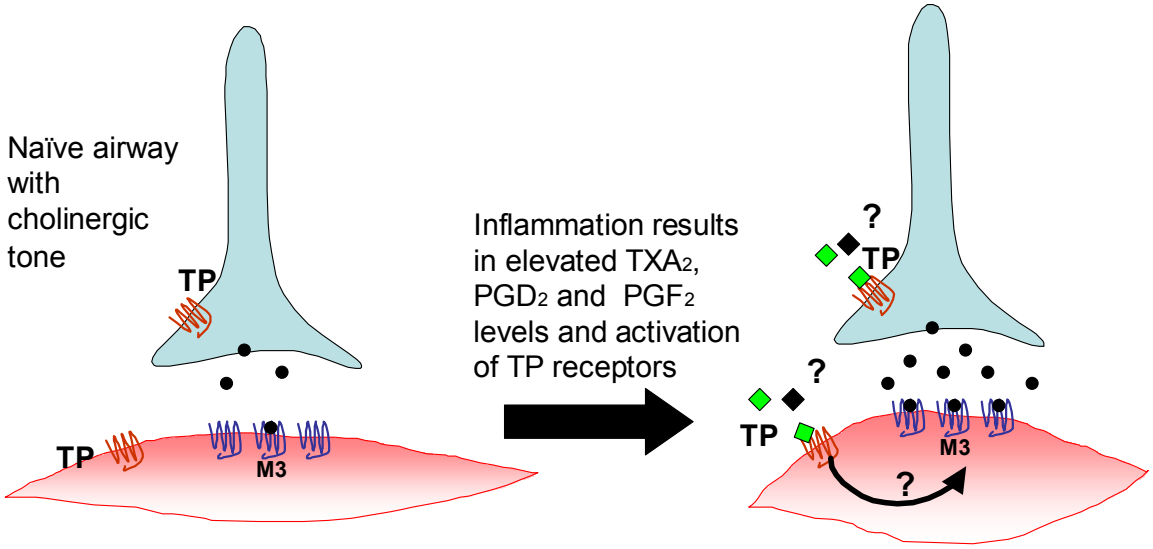
Naïve airway with cholinergic tone
TP
TP
M3
Inflammation results in elevated TXA2, PGD2 and PGF2 levels and activation of TP receptors
?
TP
?
TP
M3
?

Figure 2.7. Possible mechanism for TP dependent alteration in airway resistance. In the naïve healthy airway, basal release of acetylcholine by pre-synaptic cholinergic neurons are responsible for the resting tone of the airways. Increased production of TXA_2, the primary ligand of the TP receptor, or increased production of PGD_2 or PGF_2, results in increased TP receptor activation. TP receptors expressed by pre-synaptic cholinergic neurons increase the release of acetylcholine, which in turn results in increased activation of M_3 mAChRs present on smooth muscle cells and contraction of the smooth muscle. Alternately, or in addition, the prostanoids might engage post-junctional TP receptors present on the airway smooth muscle. Cooperativity between the activated TP receptor and the M_3 mAChR, stimulated by the low levels of basal acetylcholine, results in contraction of the airway smooth muscle. The interactions between these two receptors may simply reflect an additive effect of stimulation of two G_q associated receptors, or a unique relationship between TP receptors and M_3 mAChRs in airway smooth muscle cells.

Discussion

TXA_2 is a potent mediator of human airway constriction. The expression of the TP receptor on ASM, combined with the early demonstration of the ability of TXA_2 to mediate constriction of vascular smooth muscle, suggested that TXA_2-induced increases in airway resistance are mediated through direct actions of TXA_2 on ASM. However, results from the present study demonstrate that in both the naïve and inflamed airway, the constrictor effect of TXA_2 is dependent on the activity of muscarinic cholinergic pathways.

We utilized both pharmacological and genetic approaches to establish the role of the cholinergic pathways in TP receptor-mediated changes in airway and lung resistance. U46619-mediated increases in R_L were largely attenuated when animals were treated with the nonselective muscarinic receptor antagonist atropine or the M_3 receptor-preferring antagonist 4DAMP. Consistent with these findings, U46619 caused only minimal increases in R_L in both mAChR3$^{-/-}$ mice (suggesting a primary role for the M_3 mAChR subtype) and vagotomized mice (suggesting a dependence on parasympathetic innervation).

A number of mechanisms that are consistent with our findings can be proposed (Figure 2.7). For example, stimulation of ASM TP receptors may result in an increase in intracellular Ca^{2+}. This increase in Ca^{2+} is insufficient to mediate significant ASM contraction. However, binding of TXA_2 to the TP receptor potentiates the activity of the M_3 mAChR, thereby increasing the sensitivity of the M_3 mAChR to its cognate physiologic ligand, acetylcholine. With the loss of vagal tone, the release of acetylcholine diminishes, as does the ability of the muscle to respond to TP receptor activation. A number of possible mechanisms by which TXA_2 binding to the TP receptor can alter the activity of a co-expressed G_q coupled receptor can be envisioned, including the formation of heterodimers or

simple additive effects of receptor-specific induced changes in intracellular Ca^{2+} or other second messengers. In support of this mechanism, both TP receptors (16, 24) and muscarinic receptors (31, 55, 59, 60) have been shown to form heterodimers with other GPCRs. Implicit in this model is the existence of a basal tone of the ASM and constitutive release of acetylcholine in the unprovoked airway. We report here, consistent with findings in other species (6, 7, 20, 33), that a basal ASM tone can be measured in mice, as indicated by a decrease in lung resistance following vagotomy.

Our data are also consistent with alternate pathways, which also involve constitutive release of acetylcholine from parasympathetic nerves (Figure 2.7). In this example, the release of acetylcholine from the postsynaptic neurons is enhanced by TXA_2 binding to presynaptic TP receptors on the vagus nerve. Activation of these TP receptors on the nerve or nerve terminals results in a substantial increase in ACh release. After vagotomy, this constitutive release is diminished and thus is no longer potentiated by activation of TP receptors on nerve termini. Consistent with this model, TP receptors are expressed throughout the CNS and spinal cord. However, there is little information concerning the expression of TP receptors by either sensory or afferent nerves of the airways. This model, in which TP receptor activation mediates constriction by modulating neural activity, is consistent with early studies in dogs (2). These studies showed that TXA_2 potentiated vagal nerve neuro-effector transmission in ASM tissue. Contractions of canine tracheal smooth muscle (*ex vivo* preparations) were induced by electrical field stimulation (EFS) or by acetylcholine in the presence or absence of U46619. Although U46619 had no effect on the contractile response of acetylcholine when applied exogenously to smooth muscle, it significantly increased the amplitude of the EFS evoked contractions in an atropine sensitive

manner (2). These results suggest that, in canines, U46619 has a prejunctional action stimulating increased acetylcholine release from vagal nerve terminals through TP receptors (2). There is some limited evidence that TXA_2 can directly stimulate nerves. Nerve fibers isolated from felines, including unmyelinated vagal afferent nerves from the lung and nerves originating from skeletal muscle of the hindlimb, were reported to respond to U46619 (28, 29).

Both mechanisms described above are consistent with the observation that atropine decreased the response of tracheal rings to TXA_2 and that rings from mice lacking the M3 mAChR have a diminished response to TXA_2. Previous tracheal ring studies have demonstrated that after removal of vagal signaling, the concentration of acetylcholine at the neuroeffector junction is directly proportional to its rate of release, rate of diffusion, and rate of enzymatic hydrolysis (20). Acetylcholine levels are preserved at neuroeffector junctions and these stores are capable of maintaining muscarinic tone and effective cholinergic signaling for an extended amount of time after eliminating efferent vagal activity (20).

TXA_2 is a potent vaso- and broncho- constricting agent. We demonstrate here that the full action of TXA_2 is dependent on intact parasympathetic innervation and the presence of M_3 mAChRs in both the healthy and inflammed airway. These findings also raise the possibility that the TP receptor interacts with muscarinic cholinergic pathways in other biological systems. Anti-cholinergic agents continue to be used in the treatment of severe asthma and COPD. Our work suggests that these drugs, by blocking M_3 receptors, may act downstream of a number of important bronchoconstricting agents, such as TXA_2, that mediate their actions through prostanoid receptors.

References

1. Aizawa H, Inoue H, Nakano H, Matsumoto K, Yoshida M, Fukuyama S, Koto H, and Hara N. Effects of thromboxane A2 antagonist on airway hyperresponsiveness, exhaled nitric oxide, and induced sputum eosinophils in asthmatics. *Prostaglandins Leukot Essent Fatty Acids* 59: 185-190, 1998.

2. Aizawa H, Takata S, Shigyo M, Matsumoto K, Koto H, Inoue H, and Hara N. Effect of BAY u3405, a thromboxane A2 receptor antagonist, on neuro- effector transmission in canine tracheal tissue. *Prostaglandins Leukot Essent Fatty Acids* 53: 213-217, 1995.

3. Armour CL, Johnson PRA, Alfredson ML, and Black JL. Characterization of Contractile Prostanoid Receptors on Human Airway Smooth-Muscle. *Eur J Pharmacol* 165: 215-222, 1989.

4. Blanchet MR, Israel-Assayag E, and Cormier Y. Modulation of airway inflammation and resistance in mice by a nicotinic receptor agonist. *Eur Respir J* 26: 21-27, 2005.

5. Caulfield MP and Birdsall NJM. International Union of Pharmacology. XVII. Classification of muscarinic acetylcholine receptors. *Pharmacol Rev* 50: 279-290, 1998.

6. Clement MG, Mortola JP, Albertini M, and Aguggini G. Effects of vagotomy on respiratory mechanics in newborn and adult-pigs. *J Appl Physiol* 60: 1992-1999, 1986.

7. Colebatch HJH, and D.F.J. Halmagyi. Effect of vagotomy and vagal stimulation on lung mechanics and circulation. *J Appl Physiol* 18: 881-887, 1963.

8. Coleman RA, Humphrey PP, Kennedy I, Levy GP, and Lumley P. Comparison of the actions of U-46619, a prostaglandin H2-analogue, with those of prostaglandin H2 and thromboxane A2 on some isolated smooth muscle preparations. *Br J Pharmacol* 73: 773-778, 1981.

9. Coleman RA and Kennedy I. Characterization of the prostanoid receptors mediating contraction of guinea-pig isolated trachea. *Prostaglandins* 29: 363-375, 1985.

10. Coleman RA and Sheldrick RL. Prostanoid-induced contraction of human bronchial smooth muscle is mediated by TP-receptors. *Br J Pharmacol* 96: 688-692, 1989.

11. Craven PA, Studer RK, and DeRubertis FR. Thromboxane/prostaglandin endoperoxide-induced hypertrophy of rat vascular smooth muscle cells is signaled by protein kinase C-dependent increases in transforming growth factor-beta. *Hypertension* 28: 169-176, 1996.

12. Crystal RG, Barnes PJ, West JB, Weibel ER. The Lung Scientific Foundations (2 ed.). Philadelphia-New York: Lippincott-Raven, 1997, p. 2811.

13. D'Angelo DD, Terasawa T, Carlisle SJ, Dorn GW, 2nd, and Lynch KR. Characterization of a rat kidney thromboxane A2 receptor: high affinity for the agonist ligand I-BOP. *Prostaglandins* 52: 303-316, 1996.

14. Daray FM, Minvielle AI, Puppo S, and Rothlin RP. Vasoconstrictor effects of 8-iso-prostaglandin E2 and 8-iso-prostaglandin F(2alpha) on human umbilical vein. *Eur J Pharmacol* 499: 189-195, 2004.

15. Davi G, Basili S, Vieri M, Cipollone F, Santarone S, Alessandri C, Gazzaniga P, Cordova C, and Violi F. Enhanced thromboxane biosynthesis in patients with chronic obstructive pulmonary disease. The Chronic Obstructive Bronchitis and Haemostasis Study Group. *Am J Respir Crit Care Med* 156: 1794-1799, 1997.

16. Djellas Y, Antonakis K, and Le Breton GC. A molecular mechanism for signaling between seven-transmembrane receptors: evidence for a redistribution of G proteins. *Proc Natl Acad Sci USA* 95: 10944-10948, 1998.

17. Drazen JM, Finn PW, and De Sanctis GT. Mouse models of airway responsiveness: Physiological basis of observed outcomes and analysis of selected examples using these outcome indicators. *Annu Rev Physiol* 61: 593-625, 1999.

18. Duguet A, Biyah K, Minshall E, Gomes R, Wang CG, Taoudi-Benchekroun M, Bates JHT, and Eidelman DH. Bronchial responsiveness among inbred mouse strains - Role of airway smooth-muscle shortening velocity. *Am J Respir Crit Care Med* 161: 839-848, 2000.

19. Fisher JT, Vincent SG, Gomeza J, Yamada M, and Wess J. Loss of vagally mediated bradycardia and bronchoconstriction in mice lacking M-2 or M-3 muscarinic acetylcholine receptors. *FASEB J* 18: -, 2004.

20. Gertner A, Brombergerbarnea B, Traystman R, and Menkes H. Maintenance of muscarinic tone after vagotomy in the lung periphery. *J Appl Physiol* 57: 278-283, 1984.

21. Hamberg M, Svensson J, and Samuelsson B. Thromboxanes: a new group of biologically active compounds derived from prostaglandin endoperoxides. *Proc Natl Acad Sci USA* 72: 2994-2998, 1975.

22. Hirata M, Hayashi Y, Ushikubi F, Yokota Y, Kageyama R, Nakanishi S, and Narumiya S. Cloning and expression of cDNA for a human thromboxane A2 receptor. *Nature* 349: 617-620, 1991.

23. Homma T, Bates JH, and Irvin CG. Airways hyperresponsiveness induced by cationic proteins in vivo: site of action. *Am J Physiol Lung Cell Mol Physiol*, 2005.

24. Huang J, Ramamurthy, S.K., Lin, X., Le Breton, G.C. Cell signaling through thromboxane A2 receptors. *Cellular Signalling* 16: 521-533, 2004.

25. Irvin CG and Bates JH. Measuring the lung function in the mouse: the challenge of size. *Respir Res* 4: 4, 2003.

26. Janssen LJ and Daniel EE. Prejunctional and postjunctional effects of a thromboxane mimetic in canine bronchi. *Am J Physiol* 261: L271-L276, 1991.

27. Jones GL, Saroea HG, Watson RM, and O'Byrne PM. Effect of an inhaled thromboxane mimetic (U46619) on airway function in human subjects. *Am Rev Respir Dis* 145: 1270-1274, 1992.

28. Karla W, Shams H, Orr JA, and Scheid P. Effects of the thromboxane-A2 mimetic, U46,619, on pulmonary vagal afferents in the cat. *Respir Physiol* 87: 383-396, 1992.

29. Kenagy J, VanCleave J, Pazdernik L, and Orr JA. Stimulation of group III and IV afferent nerves from the hindlimb by thromboxane A(2). *Brain Res* 744: 175-178, 1997.

30. Kinsella BT, OMahony DJ, and Fitzgerald GA. The human thromboxane A2 receptor alpha isoform (TP alpha) functionally couples to the G proteins G(q) and G(11) in vivo and is activated by the isoprostane 8-epi prostaglandin F-2 alpha. *J Pharmacol Exp Ther* 281: 957-964, 1997.

31. Lee NH and Fraser CM. Cross-talk between m1 muscarinic acetylcholine and beta 2-adrenergic receptors. cAMP and the third intracellular loop of m1 muscarinic receptors confer heterologous regulation. *J Biol Chem* 268: 7949-7957, 1993.

32. Liel N, Mais DE, and Halushka PV. Binding of a thromboxane A2/prostaglandin H2 agonist [3H]U46619 to washed human platelets. *Prostaglandins* 33: 789-797, 1987.

33. Lim TPK, U.C. Luft, and F.F. Grodins. Effects of cervical vagotomy on pulmonary ventilation and mechanics. *J Appl Physiol* 13: 317-324, 1958.

34. Lotvall J, Elwood W, Tokuyama K, Sakamoto T, Barnes PJ, and Chung KF. A thromboxane mimetic, U-46619, produces plasma exudation in airways of the guinea pig. *J Appl Physiol* 72: 2415-2419, 1992.

35. Martin TR, Gerard NP, Galli SJ, and Drazen JM. Pulmonary responses to bronchoconstrictor agonists in the mouse. *J Appl Physiol* 64: 2318-2323, 1988.

36. McGraw DW, Almoosa KF, Paul RJ, Kobilka BK, and Liggett SB. Antithetic regulation by beta-adrenergic receptors of G(q) receptor signaling via phospholipase C underlies the airway beta-agonist paradox. *J Clin Invest* 112: 619-626, 2003.

37. Morinelli TA, Zhang LM, Newman WH, and Meier KE. Thromboxane A2/prostaglandin H2-stimulated mitogenesis of coronary artery smooth muscle cells involves activation of mitogen-activated protein kinase and S6 kinase. *J Biol Chem* 269: 5693-5698, 1994.

38. Namba T, Sugimoto Y, Hirata M, Hayashi Y, Honda A, Watabe A, Negishi M, Ichikawa A, and Narumiya S. Mouse thromboxane-A2 receptor - cdna cloning, expression and northern blot analysis. *Biochem Biophys Res Commun* 184: 1197-1203, 1992.

39. Nusing R, Lesch R, and Ullrich V. Immunohistochemical localization of thromboxane synthase in human tissues. *Eicosanoids* 3: 53-58, 1990.

40. Offermanns S and Simon MI. G-alpha(15) and G-alpha(16) couple a wide variety of receptors to phospholipase-C. *J Biol Chem* 270: 15175-15180, 1995.

41. Pratico D, Basili S, Vieri M, Cordova C, Violi F, and Fitzgerald GA. Chronic obstructive pulmonary disease is associated with an increase in urinary levels of isoprostane F2alpha-III, an index of oxidant stress. *Am J Respir Crit Care Med* 158: 1709-1714, 1998.

42. Robinson C, Hardy CC, and Holgate ST. Pulmonary synthesis, release, and metabolism of prostaglandins. *J Allergy Clin Immunol* 76: 265-271, 1985.

43. Roffel AF, Meurs H, Elzinga CRS, and Zaagsma J. Characterization of the muscarinic receptor subtype involved in phosphoinositide metabolism in bovine tracheal smooth-muscle. *Br J Pharmacol* 99: 293-296, 1990.

44. Sato T, Iwama T, Shikada K, and Tanaka S. Airway hyperresponsiveness to acetylcholine induced by aerosolized arachidonic acid metabolites in guinea-pigs. *Clin Exp Allergy* 26: 957-963, 1996.

45. Shenker A, Goldsmith P, Unson CG, and Spiegel AM. The G protein coupled to the thromboxane A2 receptor in human platelets is a member of the novel Gq family. *J Biol Chem* 266: 9309-9313, 1991.

46. Stengel PW, Gomeza J, Wess J, and Cohen ML. M-2 and M-4 receptor knockout mice: Muscarinic receptor function in cardiac and smooth muscle in vitro. *J Pharmacol Exp Ther* 292: 877-885, 2000.

47. Streefkerk JO, de Groot AA, Pfaffendorf M, and van Zwieten PA. Influence of the nature of pre-contraction on the responses to commonly employed vasodilator agents in rat-isolated aortic rings. *Fundam Clin Pharmacol* 16: 485-494, 2002.

48. Struckmann N, Schwering S, Wiegand S, Gschnell A, Yamada M, Kummer W, Wess U, and Haberberger RV. Role of muscarinic receptor subtypes in the constriction of peripheral airways: Studies on receptor-deficient mice. *Mol Pharmacol* 64: 1444-1451, 2003.

49. Swanson ML, Lei ZM, Swanson PH, Rao CV, Narumiya S, and Hirata M. The expression of thromboxane A2 synthase and thromboxane A2 receptor gene in human uterus. *Biol Reprod* 47: 105-117, 1992.

50. Takata S, Aizawa H, Shigyo M, Matsumoto K, Inoue H, Koto H, and Hara N. Thromboxane A2 mimetic (U-46619) induces hyperresponsiveness of smooth muscle in the canine bronchiole, but not in the trachea. *Prostaglandins Leukot Essent Fatty Acids* 54: 129-134, 1996.

51. Tazzeo T, Miller J, and Janssen LJ. Vasoconstrictor responses, and underlying mechanisms, to isoprostanes in human and porcine bronchial arterial smooth muscle. *Br J Pharmacol* 140: 759-763, 2003.

52. Thomas DW, Mannon RB, Mannon PJ, Latour A, Oliver JA, Hoffman M, Smithies O, Koller BH, and Coffman TM. Coagulation defects and altered hemodynamic responses in mice lacking receptors for thromboxane A2. *J Clin Invest* 102: 1994-2001, 1998.

53. Tilley SL, Hartney JM, Erikson CJ, Jania C, Nguyen M, Stock J, McNeisch J, Valancius C, Panettieri RA, Jr., Penn RB, and Koller BH. Receptors and pathways mediating the effects of prostaglandin E2 on airway tone. *Am J Physiol Lung Cell Mol Physiol* 284: L599-L606, 2003.

54. Tosun M, Paul RJ, and Rapoport RM. Role of extracellular Ca++ influx via L-type and non-L-type Ca++ channels in thromboxane A2 receptor-mediated contraction in rat aorta. *J Pharmacol Exp Ther* 284: 921-928, 1998.

55. Tsai W, Morielli AD, and Peralta EG. The m1 muscarinic acetylcholine receptor transactivates the EGF receptor to modulate ion channel activity. *EMBO J* 16: 4597-4605, 1997.

56. Ushikubi F, Aiba Y, Nakamura K, Namba T, Hirata M, Mazda O, Katsura Y, and Narumiya S. Thromboxane A2 receptor is highly expressed in mouse immature thymocytes and mediates DNA fragmentation and apoptosis. *J Exp Med* 178: 1825-1830, 1993.

57. Wang YX, Zheng YM, Mei QB, Wang QS, Collier ML, Fleischer S, Xin HB, and Kotlikoff MI. FKBP12.6 and cADPR regulation of Ca2+ release in smooth muscle cells. *Am J Physiol Lung Cell Mol Physiol* 286: C538-546, 2004.

58. Yamada M, Miyakawa T, Duttaroy A, Yamanaka A, Moriguchi T, Makita R, Ogawa M, Chou CJ, Xia B, Crawley JN, Felder CC, Deng CX, and Wess J. Mice lacking the M3 muscarinic acetylcholine receptor are hypophagic and lean. *Nature* 410: 207-212, 2001.

59. Zeng F and Wess J. Molecular aspects of muscarinic receptor dimerization. *Neuropsychopharmacology* 23: S19-31, 2000.

60. Zeng FY and Wess J. Identification and molecular characterization of m3 muscarinic receptor dimers. *J Biol Chem* 274: 19487-19497, 1999.

CHAPTER III

Thromboxane Mediates Airway Reactivity and Hyperresponsiveness Through Collaborations Between Smooth Muscle TP Receptors and The M3 Muscarinic Acetylcholine Receptor

Abstract

Thromboxane A_2 (TXA_2) is a potent lipid mediator released by platelets and inflammatory cells and is capable of inducing vasoconstriction and bronchoconstriction. In the airways, recent studies have demonstrated that TXA_2 mediated increases in airway smooth muscle (ASM) constriction is dependent on vagal innervation and that thromboxane prostanoid (TP) receptor mediated changes in airway constriction requires the expression of the M_3 muscarinic acetylcholine receptor (mAChR). To further define the mechanism underlying TXA_2 meditated airway constriction, we generated mice carrying a TP receptor locus that is sensitive to disruption by Cre recombinase. These mice were crossed with *Nestin-Cre*^{tg} transgenic mice, which express Cre recombinase throughout both the central and peripheral nervous systems. Here we demonstrate that loss of the TP receptor throughout the nervous system does not significantly affect naïve airway reactivity induced by the stable TXA_2 analog, U46619. Because we did not observe a robust phenotype in the neurally TP receptor deficient animals, the floxed *Tp* receptor mice were subsequently crossed with *SM22-Cre*^{tg} transgenic mice, which express Cre recombinase in smooth muscle cells. The resultant smooth muscle TP receptor deficient animals demonstrate attenuated airway responses following aerosol challenges with U46619 and also exhibit attenuated TXA_2 mediated airway hyperreactivity (AHR) to cholinergic stimuli. Together, these findings suggest that TXA_2 mediates airway reactivity and AHR through collaborations between ASM TP receptors and the M3 mAChR or associated signaling pathways.

Keywords

asthma; Cre recombinase; *SM22*; *Nestin*; thromboxane; bronchoconstriction

Introduction

Since its discovery and description as the active extract from human platelets (21), thromboxane A_2 (TXA_2) has been the focus of intense research describing the interactions of this prostanoid with components of the cardiovascular system. Production of TXA_2 results in the promotion of platelet aggregation, increased cholesterol loading, and vascular smooth muscle proliferation (39). However, TXA_2 is also capable of inducing potent smooth muscle constriction, which can influence diverse physiological processes including vasoconstriction, bronchoconstriction, uterine contractions, and intestinal contractions. Similar to other prostanoids, TXA_2 synthesis is initiated by the oxidation of arachidonic acid (AA) by either cyclooxygenase-1 (COX-1) or cyclooxygenase-2 (COX-2) into prostaglandin H_2 (PGH_2). The thromboxane synthase enzyme (TXAS) catalyzes the isomerization of PGH_2 to generate TXA_2, which has a very short half-life in aqueous solution and is rapidly hydrolyzed to the stable inactive metabolite thromboxane B_2 (TXB_2). Because of this instability, most experimental studies of TXA_2 biology have utilized stable TXA_2 mimetics such as U46619 (10, 11, 36). TXA_2 exerts its biological functions through interactions with the heterotrimeric G-protein coupled thromboxane prostanoid (TP) receptor (33, 44, 53, 57). All of the known physiologic functions of TXA_2 are dependent upon the expression of this receptor, which associates with the Gq family of proteins and asserts most of its physiological actions through the activation of phospholipase C (PLC) and increases in intracellular calcium concentrations ($[Ca^{2+}]_i$).

Pharmacological assessments with selective TXA_2 antagonists and conventional TP receptor deficient mouse lines have been crucial in implicating TXA_2 in a number of pathophysiological conditions including cardiovascular disease (45), intrauterine growth

retardation (48), various kidney diseases (12, 14, 18), and angiogenesis (5). In addition to these disorders, pharmacological and genetic approaches have been essential in establishing TXA_2 as a potent mediator of human and mouse airway constriction, where it has been shown to be capable of influencing a variety of mechanisms associated with lung diseases such as asthma and chronic obstructive pulmonary disease (COPD)(2, 3, 15, 54). However, the intrinsic limitations of pharmacological assessments (potency, specificity, and dosage) have hampered efforts to explore many of the underlying mechanisms affecting these pathophysiological processes. Likewise, conventional TP receptor deficient mice, which lack functional TP receptors in all cell types, lack the resolution to discern which TP receptors are responsible for specific physiological outcomes. This is especially troublesome in tissues where multiple cell types express TP receptors.

Considerable evidence has suggested that TXA_2 mediates airway smooth muscle (ASM) constriction through neural mechanisms affecting acetylcholine release (30, 51, 55). Indeed, the TP receptor has been found expressed on neurons and in discrete regions of the brain, where TXA_2 has been implicated in the proliferation and survival of oligodendrocytes (6, 37). Though no direct evidence has demonstrated that these receptors are present on peripheral or sensory nerves, peripheral neuron expression of TP receptors has been implied from pharmacological studies (29). Nerve fibers isolated from felines, including unmyelinated vagal afferent nerves from the lung, have been reported to respond to U46619 stimulation (31, 32). Likewise, U46619 has also been reported to potentiate vagal nerve neuro-effector transmission in ASM tissue (2). Contractions of canine smooth muscle preparations were induced by either electrical field stimulation (EFS) or by ACh in the presence or absence of U46619. The TXA_2 analog did not affect the contractile response of

ACh when applied exogenously to smooth muscle; however, it significantly increased the amplitude of the EFS-evoked contractions in an atropine sensitive manner (2). These results suggest that, at least in canines, TXA_2 has a pre-junctional role in stimulating ACh release from vagal nerve terminals in a TP receptor dependent mechanism.

Supporting these data, recent studies have demonstrated in both the naïve and inflamed airway, that the constrictor effect of TXA_2 is dependent on the activity of muscarinic receptor mediated cholinergic pathways (3). U46619-mediated increases in lung resistance were largely attenuated when animals were treated with the nonselective muscarinic receptor antagonist atropine or the M_3 muscarinic acetylcholine receptor (mAChR)-preferring antagonist 4DAMP. Consistent with these findings, U46619 was shown to induce only minimal increases in lung resistance in both $mAChR3^{-/-}$ mice (suggesting a primary role for the M_3 mAChR subtype) and vagotomized mice (suggesting a dependence on parasympathetic innervation) (3). A possible model suggested by these findings describes a situation whereby the release of acetylcholine from the postsynaptic neurons is enhanced by TXA_2 binding to presynaptic TP receptors on the vagus nerve. Activation of these TP receptors on the nerve or nerve terminals results in a substantial increase in ACh release and the subsequent increase in M3 mAChR mediated ASM constriction.

Bronchoconstriction is a dynamic process that involves ASM and parasympathetic innervation, and can also be influenced by bronchial epithelial cells and leukocytes. Each of these cell types has been suggested to express TP receptors (8, 9, 29, 32, 38, 59), thus the classical pharmacological and genetic techniques are inadequate to further define the *in vivo* mechanism underlying TXA_2 induced ASM constriction. Here we directly assess the contribution of neurally expressed TP receptors in mediating airway reactivity, by generating

mice carrying a *Tp* locus that is sensitive to disruption by Cre recombinase. The floxed *Tp* mice were crossed with a mouse line in which *Cre* expression is under the control of the nerve cell specific *Nestin* promoter. We show that loss of neurally expressed TP receptors does not appear to dramatically affect increases in airway reactivity in response to U46619 in these animals. In addition to neural expression, TP receptors are also abundantly expressed on ASM cells. To evaluate the role of these receptors, mice carrying the floxed *Tp* locus were crossed with a mouse line in which *Cre* expression is under the control of the smooth muscle specific *SM22* promoter. Here we demonstrate that the *in vivo* increases in airway reactivity in response to U46619 challenge are attenuated in the smooth muscle specific TP receptor deficient mice. We also demonstrate that the *in vivo* generation of U46619 mediated AHR to cholinergic stimuli is also attenuated in mice lacking smooth muscle TP receptors. Together, these findings suggest that TXA_2 induced ASM constriction and AHR are predominately mediated by TP receptors expressed by the smooth muscle.

Methods

Generation of mice carrying a Tp locus sensitive to Cre mediated disruption

Segments of the *Tp* receptor gene were amplified by PCR. The resultant PCR products were utilized to create a plasmid capable of undergoing homologous recombination with the endogenous locus and in doing so, introduce loxP sites flanking the major coding exon of the TP receptor (Figure 3.1). Three fragments of the *Tp* receptor gene were amplified using the following primer sets: 5'-ATAAGCTTGCGGCCGCAGTTTCCCTGGT GGTACGTG-3' and 5'-ATATCGATTAGCCCTAGCTGTCCTGGAA-3' (to amplify a 3073 bp region of homology in intron 1), 5'-GCTGCCTCAAAGAAAGGGTA-3' and 5'-GTGCGG CCGCTCCTAAAGCCCCAAAGACCT-3' (to amplify a 1032 bp region containing exon 2), and 5'-GTGGATCCCTGCAGGATGTAACAGGAAAGA-3' and 5'-GTGGTACCAGAACCCATCCCAGTTCTGA-3' (to amplify a 4424 bp region of homology in intron 2). These fragments were sub-cloned into the pCR 2.1 vector (Invitrogen) and sequenced to verify that the PCR amplification did not introduce mutations into essential sequences. The fragment corresponding to intron 2 was directly cloned into the pXenaLF^2 vector, 3' to the neomycin cassette and 5' to the pgk-tk cassette (Figure 3.1). The pXenaLF^2 vector contains the selectable marker gene for neomycin resistance (pgk-neo) flanked on both 5' and 3' sides by a loxP and frt site. The fragments corresponding to intron 1 and exon 2 of the *Tp* receptor were subcloned 5' and 3' of the loxP cassette, respectively, in the pNebLox vector. This generated a fragment of *Tp* receptor DNA with a loxP site placed in intron 1. This newly generated 5'arm-loxP-exon 2 cassette was subsequently removed from pNebLox and cloned into the pXenaLF^2 vector, 5' to its loxP cassette (Figure 3.1).

The targeting plasmid was linearized with PvuI and introduced into embryonic stem (ES) cells derived from 129/SvEv mice and transformants were isolated using standard methodologies (40). A DNA probe corresponding to the region immediately downstream of the targeted region (3' probe) was generated as previously described (57) and a probe corresponding to exon 2 of the *Tp* receptor (internal probe) was generated using the following primer sets: 5'-GCTGCCTCAAAGAAAGGGTA-3' and 5'-GTGCGGCCGCTCC TAAAGCCCCAAAGACCT-3'. These probes were used to identify targeted ES cells by Southern blot and were used to confirm the incorporation of loxP sites in successfully targeted ES cells. These probes were also used to genotype the resultant mice. ES cells in which the plasmid integrated by homologous recombination and contained the loxP-exon2-loxP-flp-neo-flp cassette were used to generate chimeric animals, which in turn were bred to generate animals heterozygous for the floxed allele. The neomycin gene was then removed by breeding the heterozygous mice with C57BL/6J mice that express of flp recombinase in the germline (B6;SJL-Tg(ACTFLPe)9205Dym/J, Jackson Laboratories). Following digestion with BamHI, the exon 2 probe discussed above was utilized to confirm the removal of the neomycin cassette.

Mice expressing Cre recombinase under the control of the SM22 promoter are commercially available (STOCK Tg(Tagln-cre)1Her/J, Jackson Laboratory) and maintained on a mixed genetic background of 129S5/SvEvBrd, C57BL/6, and SJL. These animals have been shown to express Cre recombinase throughout the smooth muscle from all tissues examined, including the lungs (7, 26, 35). C57BL/6J mice expressing Cre recombinase under the control of the *Nestin* promoter are also commercially available (B6.Cg-Tg(Nes-cre)1Kln/J**,** Jackson Laboratory). These mice express *Cre* early in embryonic development in

cell lineages that give rise to all neurons including sensory neurons, neurons of the CNS, and parasympathetic and sympathetic pathways (34). The introduction of these transgenes onto the 129/SvEv *Tp*$^{-/-}$ background was initiated. A DNA probe corresponding to the region immediately 5' of the targeted region was generated by PCR (5'-AACCTGAGTCTGTGG GGTTG-3' and 5'-ACAAGCATCAAGGAGGGATG-3') and was used, in conjunction with a BamHI digest, to assess *Tp* exon 2 removal by Cre/lox in selected tissues. All animal studies were conducted in accordance with the National Institutes of Health Guide for the Care and Use of Laboratory Animals as well as the Institutional Animal Care and Use Committee (IACUC) guidelines of the University of North Carolina at Chapel Hill.

Measurement of Airway Reactivity in Intubated Mice

Mice were anesthetized with 70-90 mg/kg pentobarbital sodium (American Pharmaceutical Partners, Los Angeles, CA), tracheostomized, and mechanically ventilated at a rate of 300 breaths/min, tidal volume of 6 cc/kg, and positive end-expiratory pressure of 3-4 cm H_2O with a computer controlled small-animal ventilator (Scireq, Montreal, Canada). Once ventilated, mice were paralyzed with 0.8 mg/kg pancuronium bromide. Following baseline assessments, mice were exposed to aerosol challenges by directing the inspiratory line through the aerosolization chamber of an ultrasonic nebulizer connected through a sideport in the ventilator circuit. Animals were ventilated at a rate of 200 breaths/min for 30 seconds with a tidal volume of 0.15 mls. Immediately following the aerosol challenge, the nebulizer was isolated from the inspiratory circuit and the original mechanical ventilation was resumed. Forced Oscillatory Mechanics (FOM) were determined every 10 seconds for the following 3 minutes, as previously described (62). Briefly, following passive expiration,

a broadband (1-19.625 Hz) volume perturbation was applied to the lungs while the pressure required to generate the perturbations was assessed (20, 58, 62). The resultant pressure and flow data were fit into a constant phase model as previously described (22, 62). Similar to other studies assessing forced oscillatory mechanics, we confined our analysis to R_{aw} (Rn; Newtonian resistance), which assesses the flow resistance of the conducting airways and G (tissue damping), which reflects tissue resistance (58, 62). To assess thromboxane mediated airway reactivity, mice were exposed to aerosol challenges of the stable thromboxane analog U46619 (Caymen Chemical, Ann Arbor, MI) as previously described (3). Briefly, mice were exposed to a 30-second aerosol dose response challenge of 10^{-5} M, 10^{-4} M, and 10^{-3} M. Following each aerosol challenge, airway responses were assessed for 3 minutes as previously described (3).

TXA_2 mediated airway hyperresponsiveness to cholinergic stimuli

Because thromboxane has also been suggested to induce airway hyperresponsiveness, we also assessed the increases in airway mechanics to methacholine, an acetylcholine analog, following pretreatment with a mildly provoking dose of U46619. Airways were exposed to a 30-second aerosol dose of U46619 (10^{-4} M), MCh (6 mg/ml)(Sigma Chemical, St. Louis, MO), or saline and changes in airway mechanics were assessed for 3 minutes. Following this exposure, mice were challenged with a 30-second aerosol dose of U46619 (10^{-4} M), MCh (6 mg/ml), Serotonin (5 mg/ml)(Sigma Chemical, St. Louis, MO), Adenosine (6 mg/ml)(Sigma Chemical, St. Louis, MO), $PGF_{2\alpha}$ (10^{-4} M) (Caymen Chemical, Ann Arbor, MI), or PGD_2 (10^{-4} M) (Caymen Chemical, Ann Arbor, MI).

Statistical Analysis

Data are presented as the means +/- standard error of the mean (SEM). A Random Effects Model followed by the Tukey-Kramer Honestly Significant Difference (HSD) was utilized to assess dose response data. Analysis Of Variance (ANOVA) followed by Tukey-Kramer HSD for multiple comparisons was performed on complex data sets. Statistical significance for single data points was assessed by the Student's two-tailed t-test. A p-value of less than 0.05 was considered statistically significant.

Results

Generation of mice with tissue specific loss of the TP receptor

The development of mouse lines in which loss of gene expression is restricted to specific populations of cells requires the placement of loxP sites around a critical exon of the gene under study. To obtain a Cre recombinase-mediated deletion of the TP receptor, a targeting vector was designed which would introduce a Neo cassette flanked by loxP-frt sites downstream from exon 2. A third loxP site was introduced into the first intron of the murine *Tp* receptor gene, thereby flanking exon 2, with loxP sites (Figure 3.1A). Exon 2 contains the ATG start codon and encodes 6 of the 7 transmembrane domains of the TP receptor. Following electroporation of the targeting plasmid, Southern blot analysis of the ES cell clones was used to identify those carrying a floxed *Tp* allele. For the initial screen, ES clones were digested with BamHI and probed with a 3' probe that lies outside of the targeting plasmid. Digestion of the DNA from eight neomycin resistant clones produced the 7.4 kb fragment that is indicative of successful integration of the targeting plasmid via homologous recombination (Figure 3.1B). These clones were then probed with an internal, exon 2 specific probe to identify those producing a 6.5 kb fragment, which suggests that the floxed *Tp* exon 2 and loxP-frt-neo-loxP-frt cassette were successfully integrated (Figure 3.1C). The targeted ES cell clones were further analyzed to identify those in which the crossover event during homologous recombination resulted in the introduction of the 5' loxP site in addition to the neomycin gene at the *Tp* locus. DNA was digested with BamHI and EcoRI and analyzed by Southern blot using the exon 2 probe, which recognizes a 7.4 kb wild type allele and a 5.5 kb fragment in those clones in which the crossover event failed to introduce the 5' loxP site. The probe is expected to hybridize to a 3.3 kb fragment both in ES cells in which

the targeting plasmid integrated randomly and in those clones which underwent homologous recombination with the desired crossover event. Clone number 7, was the only ES cell clone identified as clearly carrying a floxed *Tp* receptor exon 2 allele (Figure 3.1D). Subsequently, mouse lines were generated from this ES cell line.

The *Nestin*^{tg} transgene was obtained on a C57BL/6 genetic background, while the SM22 transgene was on a mixed genetic background (129S5/SvEvBrd, C57BL/6, and SJL). Additionally, removal of the neo gene from the *Tp* locus of the 129 ES cell derived mice required crossing the mice with the germline-flp transgenic line, which is on a C57BL/6 genetic background. Thus, as the various lines required for this study were not on a uniform background, it was essential that littermates (which on average are expected to have an equal composition of B6, 129, and SJL alleles) be generated for these studies.

Because of the difficulty of obtaining sufficient numbers of experimental animals by simply intercrossing the $Tp^{loxTp/+}$ and the *Cre*^{tg}-transgene positive $Tp^{loxTp/+}$ mice (only 1 in 8 mice would be expected to be useful), we first crossed the transgenic mice with $Tp^{-/-}$ animals on a 129/SvEv genetic background. The *Cre*^{tg}-transgene positive female $Tp^{+/-}$ mice were then crossed to mice homozygous for the Tp^{loxTp} allele. Four different genotypes of mice were generated from this cross at approximately equal frequencies. The $Tp^{loxTp/+}$ mice should behave essentially the same as wild type mice, since the presence of the loxP sites in the introns of the TP receptor is not expected to affect gene expression. The $Tp^{loxTp/-}$ mice generated would be expected to have a slight attenuation of response based on our previous studies showing a decrease in the response of heterozygous animals (Supplemental Figure E3.1). The response of these mice should be indistinguishable from that of the *Cre*^{tg}-transgene positive $Tp^{loxTp/+}$ animals, if TP receptor expression is critical in the Cre

recombinase expressing tissues, as either the smooth muscle ($Tp^{loxTp/+\ Tgln+\ ve}$) or neural ($Tp^{loxTp/+\ nestin+}$) tissues will essentially be +/- for the *Tp*. If this is not the critical tissue type, then these mice should behave similar to a wild type mouse. The Cre^{tg}-transgene positive $Tp^{loxTp/-}$ mice are expected to have no expression of *Tp* in the smooth muscle ($Tp^{loxTp/-\ Tgln+\ ve}$) or neural ($Tp^{loxTp/-\ nestin+}$) tissues and are heterozygous for *Tp* in all other tissues. Thus the ideal comparisons should be made between the Cre^{tg}-transgene positive $Tp^{loxTp/-}$ mice and their $Tp^{loxTp/-}$ littermates. However, we would expect if a particular tissue is critical for a response, the following rank order of responses is predicted (from lowest to highest): Cre^{tg}-transgene positive $Tp^{loxTp/-} < Tp^{loxTp/-} = Cre^{tg}$-transgene positive $Tp^{loxTp/+} < Tp^{loxTp/+}$. Wild type 129/SvEv and $Tp^{-/-}$ co-isogenic mice were included as controls in all experiments.

Southern blot analysis was utilized on select tissues to demonstrate successful, tissue specific, disruption of the TP receptor. Tissues were harvested from $Tp^{loxTp/+}$ mice, which either carried the Cre^{tg} under the control of the *SM22* (transgelin; Tgln) promoter (Tgln+) or were negative for the Cre^{tg} transgene (Tgln-)(Figure 3.2A). Tissues were harvested that demonstrate high concentrations of smooth muscle (trachea, intestine, and uterus). Control tissues were also harvested including cardiac muscle (heart), skeletal muscle, and kidney (high TP receptor expression). DNA was extracted from each of these tissues and digested with BamHI for Southern blot analysis with probes specific for *Cre* (data not shown), exon 2 (data not shown), and for a region 5' of exon 2. All tissues demonstrate the endogenous 11.2 kb fragment indicative of the wild type allele and a 4.5 kb fragment indicative of the floxed *Tp* allele. However, an additional 3.3 kb fragment is present in smooth muscle containing tissues, which suggests successful disruption of the TP receptor, at least in some cells (Figure 3.2A). To further examine TP receptor loss in the ASM, 3 denuded tracheas were pooled

together from either $Tp^{loxTp/+}$ or $Tp^{loxTp/-}$ mice, which either carried the SM22- Cre^{tg} transgene or were transgene negative (Figure 3.2B).

Tissues were also harvested from $Tp^{loxTp/+}$ and $Tp^{loxTp/-}$, which carried the Cre^{tg} transgene under the control of the *Nestin* promoter. The brain, intestine, and kidney were harvested and Southern blot analysis was performed as described above. Animals that are wild type for the TP receptor ($Tp^{+/+}$ and the $Tp^{loxTp/+}$ mice) demonstrate an 11.2 kb fragment, while mice that carry the TP receptor disrupted by insertion of a neomycin cassette ($Tp^{loxTp/-nestin+}$ and $Tp^{loxTp/-}$ mice) demonstrate a 4.1 kb fragment (Figure 3.2C). In non-neuronal tissues (kidney and intestine) a 4.5 kb fragment is present that represents the intact floxed *Tp* receptor. However, in the brain, a 3.3 kb fragment is generated in the *Nestin*+ mice that is indicative of successful neural disruption of the TP receptor by Cre recombinase (Figure 3.2C).

Neurally deficient TP receptor mice demonstrate increased airway resistance (R_{aw}) and tissue damping (G) following stimulation with TXA_2

Previous reports suggest that TXA_2 contributes to ASM constriction through the potentiation of vagal nerve neuro-effector transmission (2). Inflammatory mediators such as TXA_2 could affect neural activity at a variety of levels, including the primary afferent sensory nerve, autonomic ganglia, and autonomic neuroeffector junction. If this hypothesis were true, we would expect that U46619 induced increases in R_{aw} and G would be severely attenuated in mice with reduced neural expression of TP receptors. U46619 induced a significant, dose dependent increase in both R_{aw} and G in wild type mice ($Tp^{+/+}$), while TP receptor deficient animals ($Tp^{-/-}$) were unresponsive (Supplemental Figure E3.1A and B).

No significant differences in R_{aw} or G were observed between any of the experimental mice, regardless of genotype or Cre expression (Figure 3.3A and B). While no significant differences in baseline measurements were observed between any of the mouse groups (data not shown), all animals carrying the floxed *Tp* allele demonstrated significant increases in both R_{aw} and G in response to U46619 compared with the 129/SvEv coisogenic $Tp^{-/-}$ mice. However, the N1 generation floxed *Tp* mice demonstrated reduced increases in R_{aw} and significantly attenuated increases in G compared with the 129/SvEv $Tp^{+/+}$ animals (Figure 3A and B; Supplemental Figure E3.1A and B).

Airway resistance (R_{aw}) and tissue damping (G) are attenuated in naïve smooth muscle TP receptor deficient mice after exposure to TXA_2

Neural disruption of the TP receptor failed to significantly attenuate airway reactivity to U46619, suggesting that TXA_2 mediated airway constriction may be mediated by other cell types known to express the TP receptor. TXA_2 receptor expression by smooth muscle cells is well documented, as is the ability of TP receptor activation to mediate increases in $[Ca^{++}]_i$ in cultured human primary ASM cells (50). Here, we sought to examine the possibility that TXA_2 mediated increases in airway reactivity could be mediated by TP receptors located directly on ASM cells. If this hypothesis were true, we would expect that U46619 induced increases in R_{aw} and G would be severely attenuated in mice with reduced expression of TP receptors on smooth muscle. As mentioned above, U46619 induced a significant, dose dependent increase in both R_{aw} and G in wild type mice ($Tp^{+/+}$), while TP receptor deficient animals ($Tp^{-/-}$) were unresponsive (Supplemental Figure E3.1A and B). Like the $Tp^{-/-}$ animals, the $Tp^{loxTp/-\ Tgln+\ ve}$ smooth muscle receptor deficient mice also demonstrated significantly attenuated R_{aw} and G responses compared to the $Tp^{loxTp/+}$ wild

type mice. The heterozygous $Tp^{loxTp/-}$ animals demonstrated an intermediate phenotype. These mice demonstrated significantly enhanced R_{aw} and increased G compared with the $Tp^{loxTp/-\ Tgln+\ ve}$ smooth muscle receptor deficient mice and significantly attenuated R_{aw} and reduced G compared with the $Tp^{loxTp/+}$ wild type animals (Figure 3.4A and B). The $Tp^{loxTp/+\ Tgln+\ ve}$ smooth muscle heterozygous animals demonstrated significantly increased R_{aw} that was reduced, but not significantly, compared to levels observed for the $Tp^{loxTp/+}$ wild type mice. (Figure 3.4A). These animals demonstrated an intermediate G phenotype, which was neither significantly increased compared to the $Tp^{loxTp/-\ Tgln+\ ve}$ smooth muscle receptor deficient mice nor significantly decreased compared to the $Tp^{loxTp/+}$ wild type animals (Figures 3.4B).

Exposure to TXA_2 increases airway sensitivity to cholinergic stimuli

The ability of U46619 to induce AHR to muscarinic receptor agonists has been characterized in a variety of model organisms (23, 52, 56). However, while this phenomenon has been identified in canine, guinea pig, and human studies, the mechanism behind this increased sensitivity is not well defined. Therefore, we sought to assess and characterize this TXA_2 mediated AHR in mice. Both $Tp^{+/+}$ and $Tp^{-/-}$ mice were exposed to a mildly provoking dose of U46619 (10^{-4} M), which induces a moderate but significant increase in R_{aw} in the $Tp^{+/+}$ animals, while being relatively non-provoking by assessments with both the G parameter and in the single compartment model (R_L)(Supplemental Figure E3.2A; Supplemental Figure E3.3A and B). The initial treatment with U46619 (Challenge 1) was followed, 3 minutes later, by exposure to a weakly provoking dose of methacholine (6 mg/ml). This dose of MCh typically induces an increase of approximately 15% to 25% of baseline R_{aw} and G (Supplemental Figure E3.3A and B). Following the initial challenge

(Challenge 1) with U46619 or PBS, all of the mice demonstrated increases in R_{aw} following subsequent exposures to MCh (Figure 3.5A). However, no additional increase in MCh responsiveness was observed in mice pretreated with MCh (Figure 3.5A). In contrast to the R_{aw} results, the G results demonstrated that pretreatment with the 10^{-4} M dose of U46619 induces a robust MCh response. This response is significantly greater than that observed in the PBS pretreated $Tp^{+/+}$ mice, the U46619 pretreated $Tp^{-/-}$ mice, and the MCh pretreated $Tp^{+/+}$ mice. This increase is highly noticeable when utilizing the equation of motion to describe the single compartment model of the lung and assessing lung resistance (R_L)(Supplemental Figure E3.1A). While the most dramatic effects were observed for MCh responses following U46619 pretreatment, exposure to 10^{-4} M U46619 also increased both R_{aw} and G in response to subsequent challenges with U46619 (Supplemental Figure E3.3C and D). No significant increases were observed in R_{aw} or G following pretreatment with U46619 for serotonin (5-HT), adenosine, prostaglandin D_2 (PGD2), or prostaglandin $F_2\alpha$ (PGF2) (Figure 3.5C and D).

Synergy between the TXA_2 and cholinergic pathways are mediated, at least in part, by smooth muscle TP receptors

As discussed above, we have demonstrated, *in vivo*, that mild or nonprovoking doses of TXA_2 can augment the response of airways to methacholine in mice. This potentiation appears to be due to a unique interaction between TP receptors and muscarinic receptors, as none of the other agonists were capable of inducing the robust increases observed in response to MCh when administered following U46619 pretreatment. Because we identified a primary role for smooth muscle TP receptors in mediating U46619 induced airway reactivity

in the naïve model described above, we next wanted to assess whether induction of AHR is dependent on smooth muscle expression of TP receptors. As discussed above, we assessed the ability of U46619 to enhance the response to low doses of MCh in the smooth muscle TP receptor deficient mice (Figure 3.6). MCh provoked an increase in R_{aw} in the wildtype $Tp^{loxTp/+}$ mice, while only a minimal increase was detected in the smooth muscle TP receptor deficient $Tp^{loxTp/-\ Tgln+\ ve}$ animals (Figure 3.6A). The $Tp^{loxTp/+\ Tgln+\ ve}$ smooth muscle heterozygous animals demonstrated an increase in R_{aw} following MCh challenge that was indistinguishable from the $Tp^{loxTp/+}$ wild type mice, while only trivial increases in R_{aw} were observed for the $Tp^{loxTp/-}$ heterozygous animals (Figure 3.6A). As observed previously, 10^{-4} M U46619 did not induce a significant increase in G (data not shown). Following subsequent challenge with MCh, significant increases were observed in the $Tp^{loxTp/+}$ wild type mice and $Tp^{loxTp/+\ Tgln+\ ve}$ smooth muscle heterozygous animals, while the $Tp^{loxTp/-}$ heterozygous mice produced an intermediate response that was neither significantly increased over the $Tp^{loxTp/-\ Tgln+\ ve}$ smooth muscle receptor deficient mice nor reduced versus the $Tp^{loxTp/+}$ wild type and $Tp^{loxTp/+\ Tgln+\ ve}$ smooth muscle heterozygous animals (Figure 3.6B). Only a moderate increase in G was observed in the $Tp^{loxTp/-\ Tgln+\ ve}$ smooth muscle deficient mouse line, which was significantly reduced compared with the $Tp^{loxTp/+}$ wild type and $Tp^{loxTp/+\ Tgln+\ ve}$ smooth muscle heterozygous animals (Figure 3.6B).

Figure 3.1

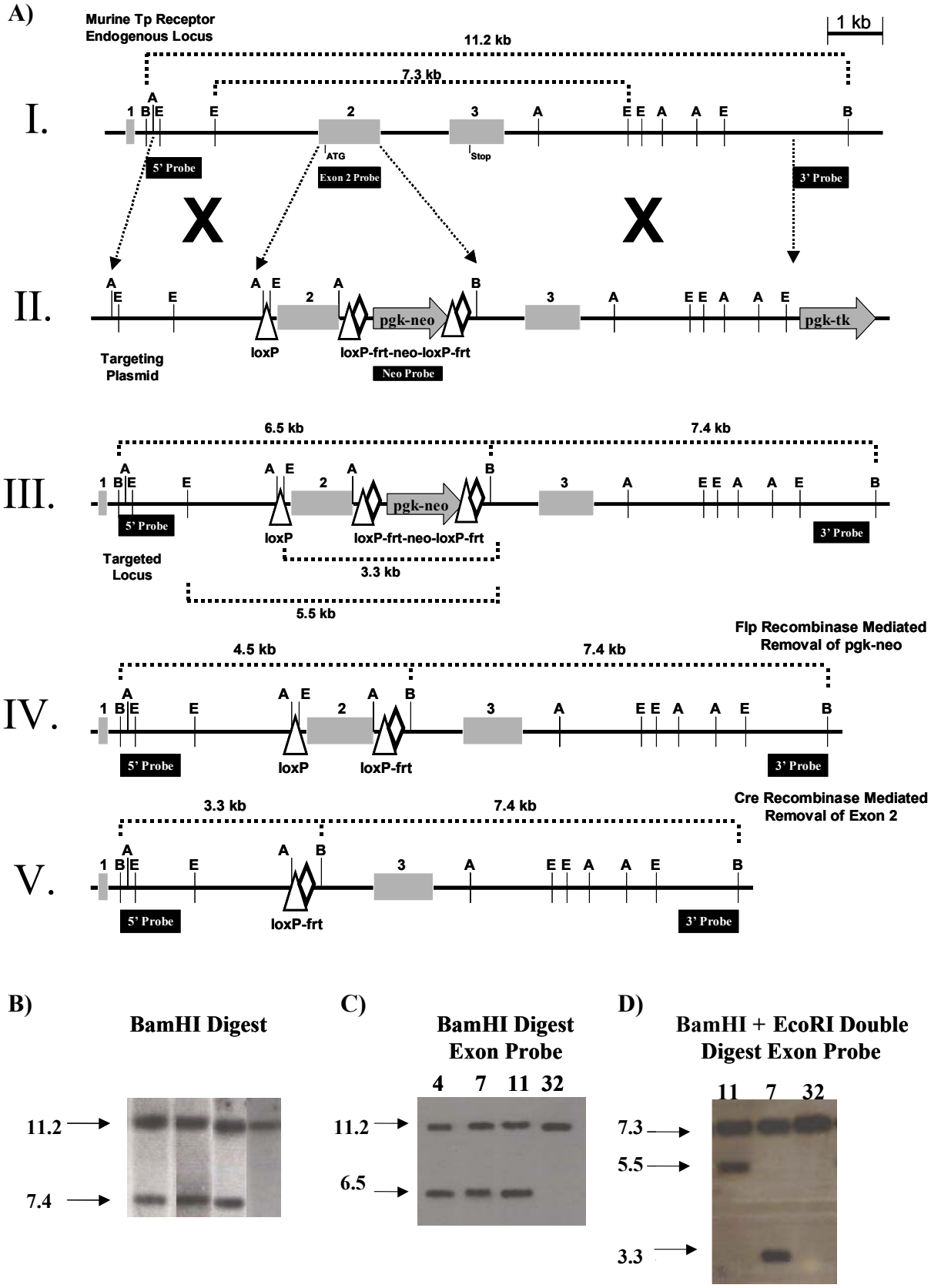
A)
Murine Tp Receptor
Endogenous Locus
1 kb
11.2 kb
7.3 kb
I.
5' Probe
Exon 2 Probe
3' Probe
ATG
Stop
II.
Targeting
Plasmid
loxP
loxP-frt-neo-loxP-frt
pgk-neo
pgk-tk
Neo Probe
III.
6.5 kb
7.4 kb
Targeted
Locus
3.3 kb
5.5 kb
IV.
Flp Recombinase Mediated
Removal of pgk-neo
4.5 kb
7.4 kb
loxP-frt
V.
Cre Recombinase Mediated
Removal of Exon 2
3.3 kb
7.4 kb
B)
BamHI Digest
11.2
7.4
C)
BamHI Digest
Exon Probe
4 7 11 32
11.2
6.5
D)
BamHI + EcoRI Double
Digest Exon Probe
11 7 32
7.3
5.5
3.3

Figure 3.1. Schematic depicting the generation of a floxed *Tp* allele in ES cells. A) The organization of the endogenous locus, the targeting plasmid, and the *Tp* allele generated after homologous recombination of the plasmid with the wild type *Tp* allele are shown. The fragments of DNA required for assembly of the targeting plasmid are prepared from genomic DNA isolated from 129 derived ES cells and primers designed using the sequence for the *Tp* gene available in the Celera mouse genome. The fragments are cloned into the vector pXenaLF2, which was constructed specifically for the rapid assembly of plasmids capable of generating floxed alleles. The loxP sites are denoted with triangles, the frt sites by diamonds, and the neo gene is represented by the shaded arrow. Relevant restriction sites are abbreviated as follows: B, BamHI; A, ApaI; E, EcoRI. Greyed boxes represent coding Tp receptor exons. **B-D)** Southern blot analysis of the ES cell clones to identify those carrying a floxed *Tp* allele. DNA was prepared from neomycin resistant clones obtained after electroporation of the targeting plasmid into ES cells. A 3' probe not included in the targeting plasmid was used as a first screen to identify those ES cell clones in which the plasmid was integrated by homologous recombination. Eight such clones were identified and further analyzed using a *Tp* exon 2 specific probe. Some of the targeted ES cell clones were further analyzed to identify those in which the crossover event during homologous recombination resulted in introduction of the 5' lox site in addition to the neomycin gene at the *Tp* locus. To do this, DNA was digested with BamHI and EcoRI and analyzed by Southern blot using the exon 2 probe. This probe recognizes a 7.4 kb wild type allele and a 5.5 kb fragment in those clones in which the crossover event failed to introduce the 5'loxP site. The probe is expected to hybridize to a 3.3 kb fragment both in ES cells in which the targeting plasmid integrated randomly and in those clones which underwent homologous

recombination with the desired crossover event. Clone number seven clearly represents such an ES cell clone.

Figure 3.2

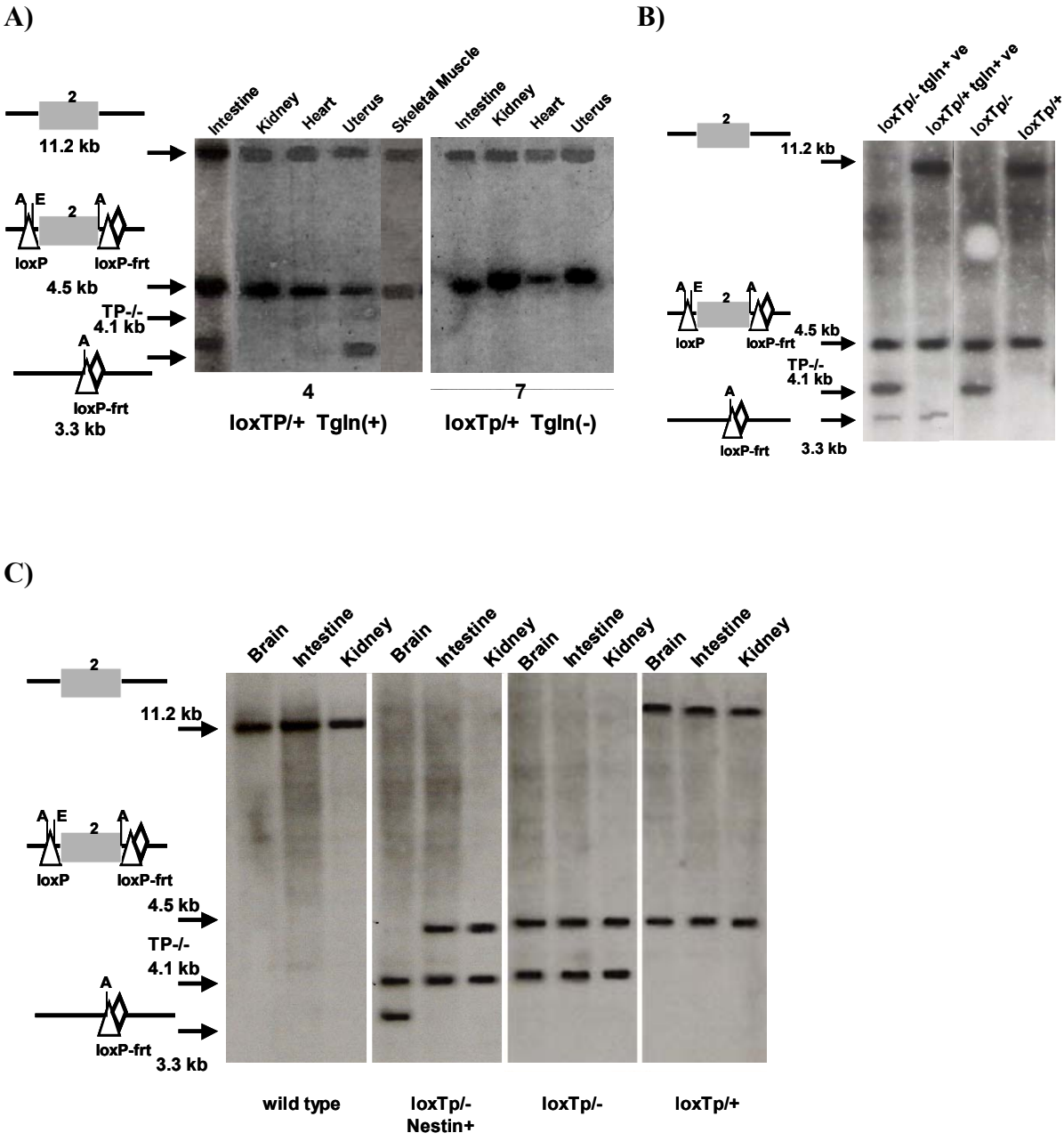
A)
B)
C)
2
11.2 kb
A E 2 A
loxP
loxP-frt
4.5 kb
TP-/-
4.1 kb
A
loxP-frt
3.3 kb
Intestine
Kidney
Heart
Uterus
Skeletal Muscle
4
loxTP/+ Tgln(+)
7
loxTp/+ Tgln(-)
loxTp/- tgln+ ve
loxTp/+ tgln+ ve
loxTp/-
loxTp/+
Brain
wild type
loxTp/-
Nestin+

Figure 3.2. Southern Blot characterization of floxed *Tp* mice. A) Southern blot analysis of organs and tissues from TP receptor wild type mice carrying the floxed *Tp* allele (loxTp/+) either with (Tgln+) or without (Tgln-) the Cre^{tg} transgene under the control of the *SM22* (transgelin; Tgln) promoter. Smooth muscle containing tissues (Intestine and Uterus) demonstrate smooth muscle specific disruption of the TP receptor. **B)** Southern blot analysis of tracheas harvested and pooled from TP receptor wild type (loxTp/+) or TP receptor deficient (loxTp/-) mice carrying the floxed *Tp* allele either with (Tgln/+) or without (Tgln/-) the Cre^{tg} transgene under the control of the *SM22* promoter. Airway smooth muscle specific disruption of the TP receptor was observed in the tgln/+ preparations. **C)** Southern blot analysis of organs and tissues from TP receptor wild type (loxTp/+) or TP receptor deficient (loxTp/-) mice carrying the floxed *Tp* allele either with (*Nestin*+) or without (*Nestin*-) the Cre^{tg} transgene under the control of the *Nestin* promoter. Neural specific disruption of the TP receptor was observed in brain preparations.

Figure 3.3

A)

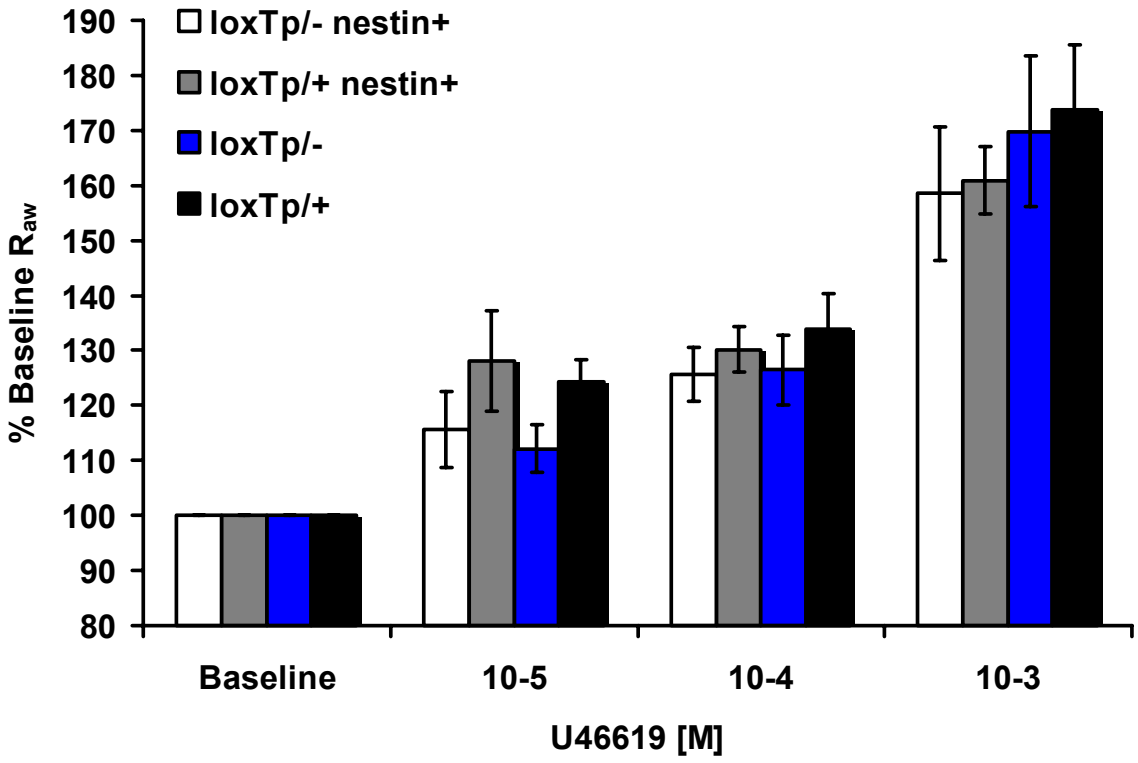
loxTp/- nestin+
loxTp/+ nestin+
loxTp/-
loxTp/+
% Baseline R_{aw}
190
180
170
160
150
140
130
120
110
100
90
80
Baseline
10-5
10-4
10-3
U46619 [M]

B)

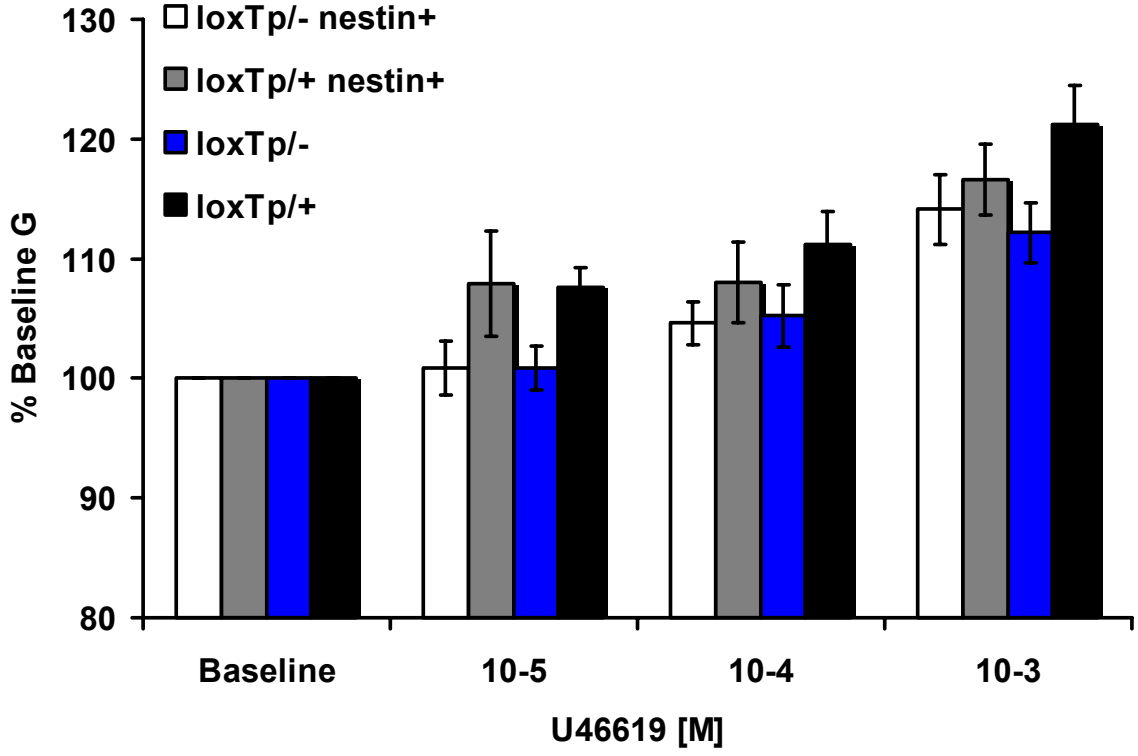
loxTp/- nestin+
loxTp/+ nestin+
loxTp/-
loxTp/+
% Baseline G
130
120
110
100
90
80
Baseline
10-5
10-4
10-3
U46619 [M]

Figure 3.3. Neural specific deletion of TP receptors does not significantly affect airway resistance and tissue damping induced by U46619 aerosol challenge. No significant differences in **A)** airway resistance (R_{aw}) or **B)** tissue damping (G) were detected for any of the mice carrying the floxed *Tp* allele. All mice demonstrated significantly increased R_{aw} and G, compared to 129/SvEv co-isogenic $Tp^{-/-}$ animals (Supplemental Figure 1). $Tp^{loxTP/-}$, n = 9; $Tp^{loxTp/+}$, n = 15; $Tp^{loxTp/-\ nestin+}$, n = 6; $Tp^{loxTp/+\ nestin+}$, n = 9.

Figure 3.4

A)

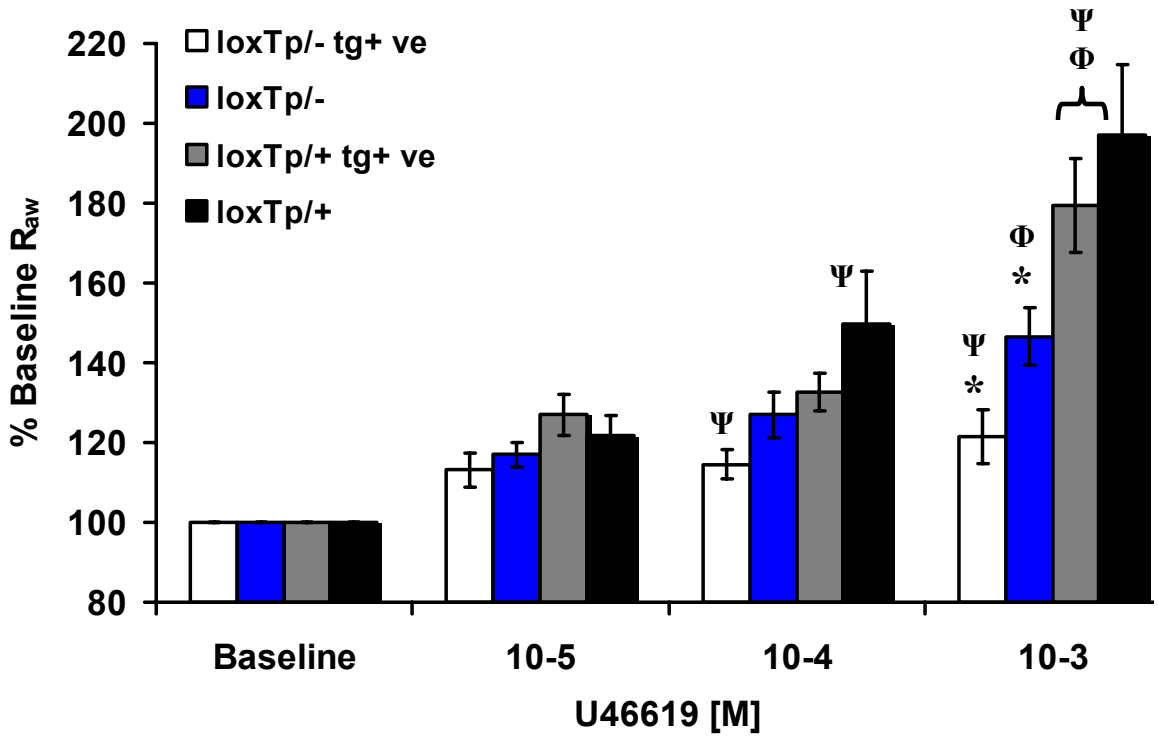
loxTp/- tg+ ve
loxTp/-
loxTp/+ tg+ ve
loxTp/+
% Baseline R_{aw}
220
200
180
160
140
120
100
80
Baseline
10-5
10-4
10-3
U46619 [M]
Ψ
Φ
*

B)

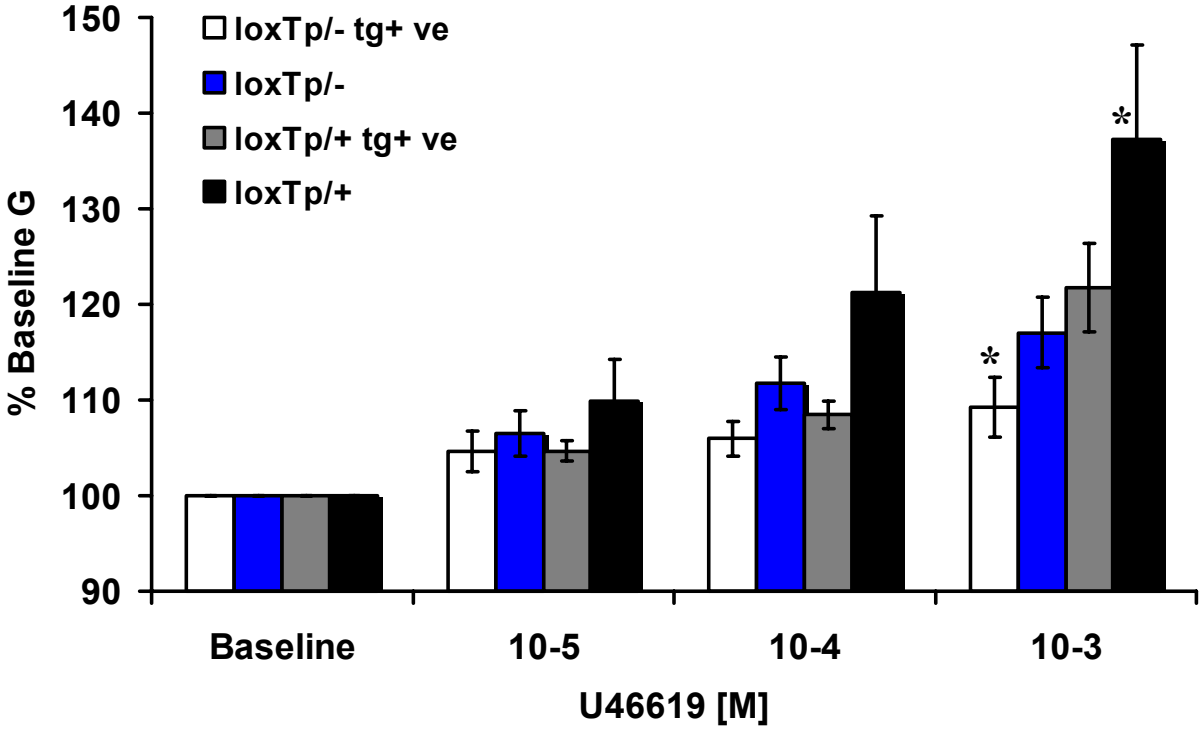
loxTp/- tg+ ve
loxTp/-
loxTp/+ tg+ ve
loxTp/+
% Baseline G
150
140
130
120
110
100
90
Baseline
10-5
10-4
10-3
U46619 [M]
*

Figure 3.4. Smooth muscle specific deletion of TP receptors significantly attenuates airway resistance and tissue damping induced by U46619 aerosol challenge. A) Airway resistance (R_{aw}) and **B)** tissue damping (G) are significantly reduced in TP receptor deficient mice carrying the floxed *Tp* allele and the Cre^{tg} transgene under the control of the SM22 promoter (loxTp/- Tgln+ ve). The wild type mice carrying the floxed *Tp* allele (loxTp/+) demonstrated a significant increase in the U46619 response. The heterozygous wild type mice carrying the floxed *Tp* allele and the Cre^{tg} transgene (loxTp/+ Tgln+ ve) (thus heterozygous for the TP receptor on the smooth muscle) and TP receptor deficient mice carrying the floxed *Tp* allele but no Cre^{tg} transgene (loxTp/-)(thus heterozygous in all tissues) demonstrated intermediate phenotypes in response to U46619 challenge. However, the loxTp/+ Tgln+ ve animals demonstrated a significant increase in R_{aw} compared to the loxTp/- mice, but was slightly reduced versus the loxTp/+ animals. $Tp^{loxTp/-}$, n = 12; $Tp^{loxTp/+}$, n = 12; $Tp^{loxTp/-\ Tgln+\ ve}$, n = 10; $Tp^{loxTp/+\ Tgln+\ ve}$, n = 17 (*$p < 0.05$; $\Psi p < 0.05$; $\Phi p < 0.05$).

Figure 3.5

A)

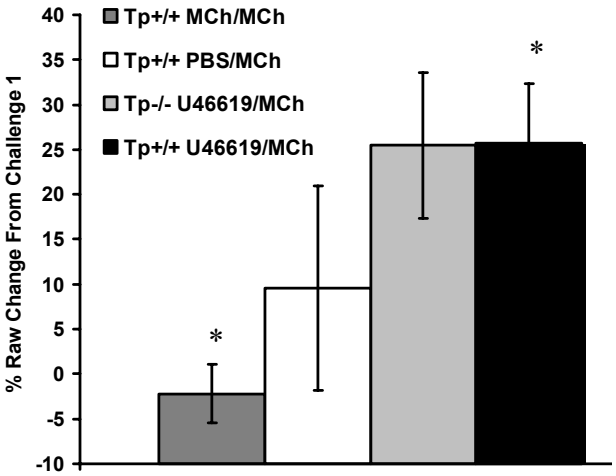

B)

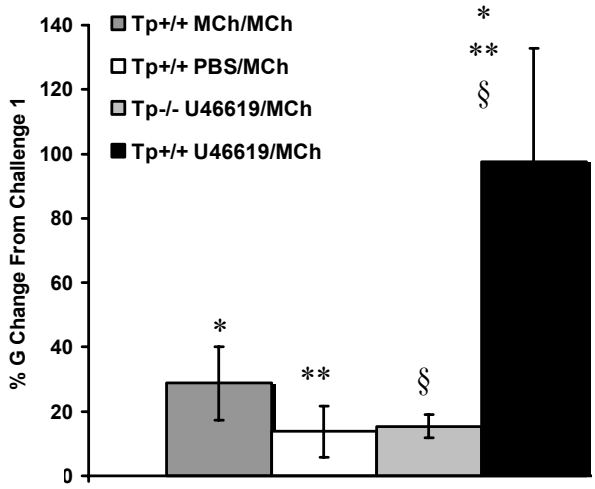

C)

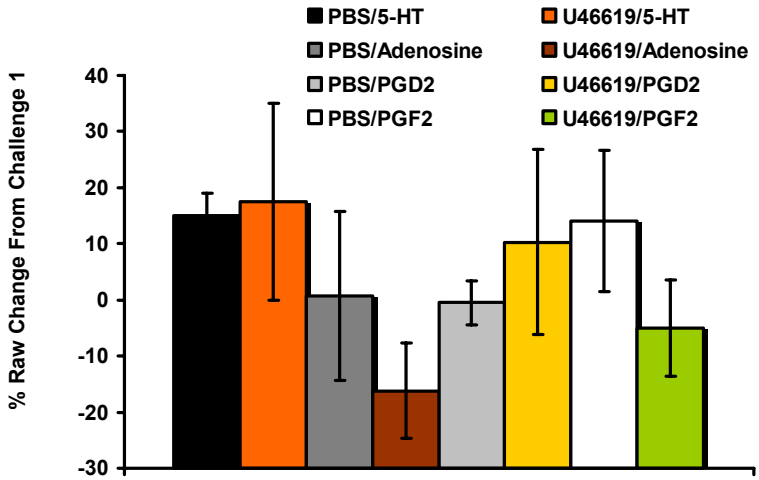

D)

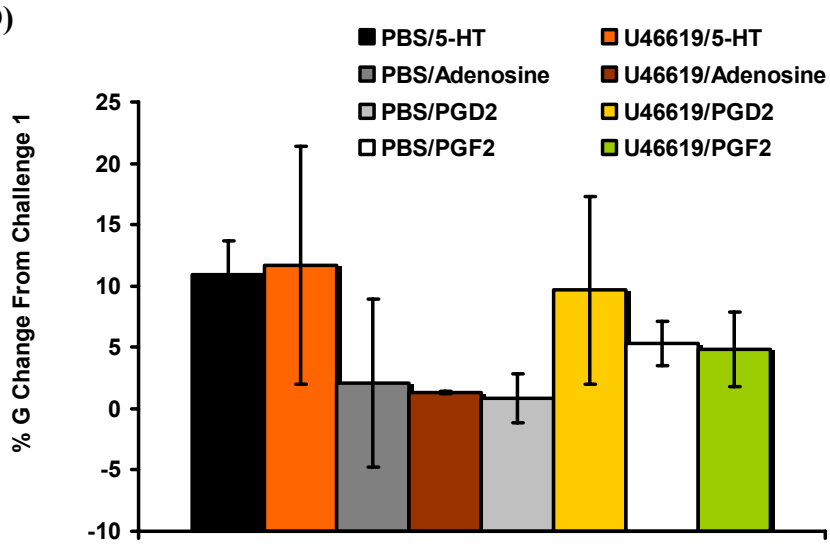

Figure 3.5. Increased sensitivity of airways to cholinergic stimuli after exposure to nonprovoking doses of TXA_2. Airways were exposed to low levels of U46619 (10^{-4} M) followed by subsequent cholinergic stimulation with low levels of MCh (6 mg/ml). Two groups of 129/SvEv wild type mice and a group of 129/SvEv co-isogenic *Tp*$^{-/-}$ mice were intubated and baseline lung mechanics established. A cohort of wild type and *Tp*$^{-/-}$ mice were then exposed to an aerosol produced from a $1x10^{-4}$ M solution of U46619. The second group of wild type mice was only treated with vehicle, and a third group of wild type animals were treated with an aerosol produced from a 6 mg/ml solution of methacholine (MCh). Within 3 minutes of vehicle, U46619, or MCh treatment, all groups of mice were exposed to an aerosol produced from a 6 mg/ml solution of MCh, which has been demonstrated to be only mildly provoking. Data are shown as the % change in R_{aw} or G observed between challenge 1 and challenge 2. **A)** The initial challenge (Challenge 1) of U46619 and MCh provoked slight increases in R_{aw} in the *Tp*$^{+/+}$ mice (Supplemental Figure 3). The second challenge of MCh did not induce further increases in airway resistance in mice pretreated with MCh. However, all of the other groups demonstrated small increases in R_{aw} following subsequent aerosol exposure to 6 mg/ml of methacholine. *Tp*$^{+/+}$ (PBS to MCh), n = 7; *Tp*$^{+/+}$ (MCh to MCh), n = 4; *Tp*$^{+/+}$ (U46619 to MCh), n = 12; *Tp*$^{-/-}$ (U46619 to MCh), n = 4 (*$p < 0.05$). **B)** The initial challenge (Challenge 1) of both U46619 and MCh were nonprovoking, as determined by the G parameter (data not shown). The subsequent challenge with the 6 mg/ml dose of MCh produces only a modest increase in the vehicle challenged mice and MCh pretreated animals. In contrast, a robust response to this dose of MCh was observed in wild type mice pretreated with the nonprovoking dose of U46619. The dependence of this response on the specific interaction of U46619 with the TP receptor was further

demonstrated by the fact that only a modest response to this dose of methacholine could be measured in the $Tp^{-/-}$ mice. $Tp^{+/+}$ (PBS to MCh), n = 7; $Tp^{+/+}$, n = 12; $Tp^{-/-}$, n = 4 (*p < 0.05; **p < 0.01; §p < 0.01). **C - D)** In addition to assessing the response to MCh, the effects of exposing mice to a mildly provoking dose of U46619 (10^{-4} M) followed by exposure to serotonin (5-HT) (5 mg/ml), adenosine (6 mg/ml), prostaglandin D_2 (PGD2)(10^{-4} M), and prostaglandin $PGF_{2\alpha}$ (PGF2)(10^{-4} M) were also assessed. No increases in AHR were observed for any of these mediators. PBS/5-HT, n = 4; U46619/5-HT, n = 4; PBS/adenosine, n = 3; U46619/adenosine, n = 3; PBS/PGD2, n = 7; U46619/PGD2, n = 3; PBS/PGF2, n = 12; U46619/PGF2, n = 3.

Figure 3.6

A)

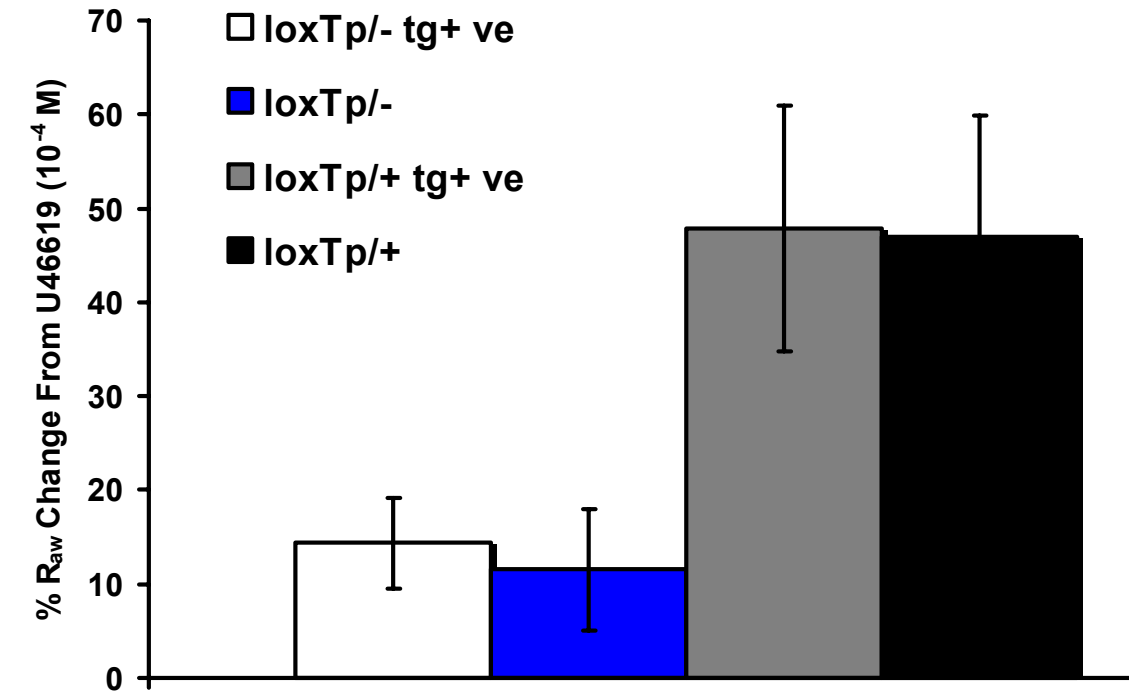
loxTp/- tg+ ve
loxTp/-
loxTp/+ tg+ ve
loxTp/+
% Raw Change From U46619 (10-4 M)
70
60
50
40
30
20
10
0

B)

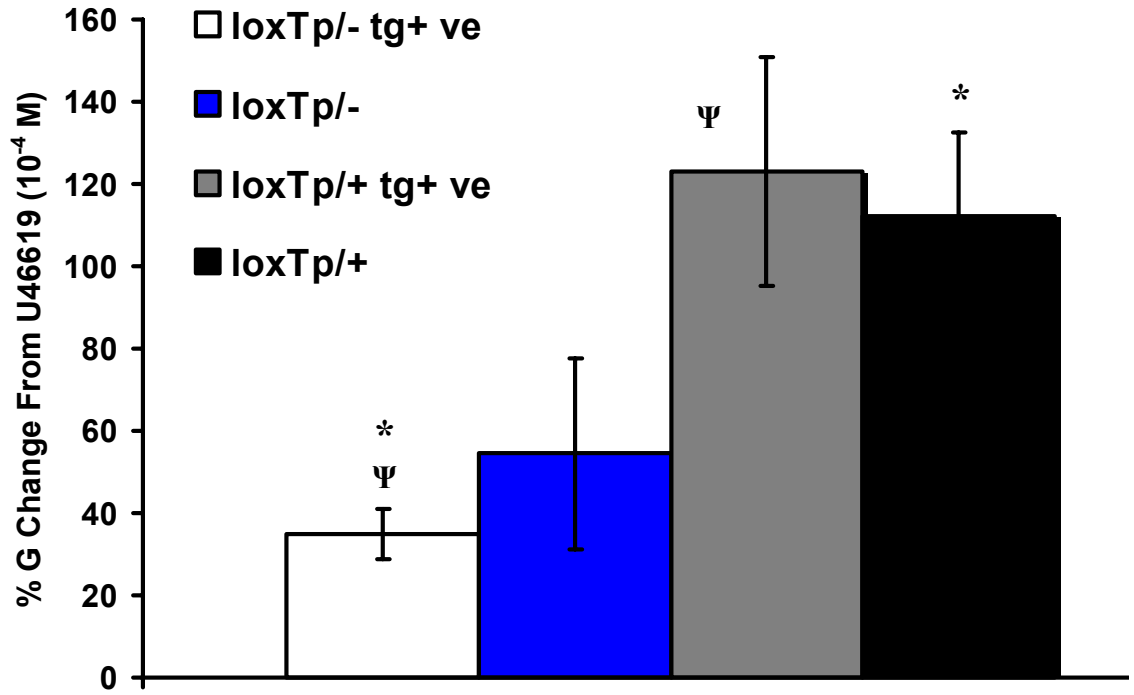
loxTp/- tg+ ve
loxTp/-
loxTp/+ tg+ ve
loxTp/+
% G Change From U46619 (10-4 M)
160
140
120
100
80
60
40
20
0
*
Ψ
Ψ
*

Figure 3.6. Synergy between the thromboxane and cholinergic pathways are mediated, at least in part, by smooth muscle TP receptors. Smooth muscle TP receptor deficient mice were exposed to low levels of U46619 (10^{-4} M) followed by subsequent cholinergic stimulation with low levels of MCh (6 mg/ml). **A)** U46619 induced a modest increase the MCh R_{aw} response in $Tp^{loxTp/+}$ (wild type) and $Tp^{loxTp/+\ Tgln+\ ve}$ (smooth muscle heterozygous) mice. Only small increases were observed in the $Tp^{loxTp/-}$ (heterozygous) or the $Tp^{loxTp/-\ Tgln+\ ve}$ (smooth muscle Tp receptor deficient mice). **B)** U46619 induced a significant increase the MCh G response in $Tp^{loxTp/+}$ and $Tp^{loxTp/+\ Tgln+\ ve}$ mice. The $Tp^{loxTp/-}$ mice demonstrated an intermediate phenotype, which was not significantly different from any of the other groups of animals. No significant increase was observed in the $Tp^{loxTp/-\ Tgln+\ ve}$. Data are shown as the % change in R_{aw} or G observed between the initial challenge of U46619 (10^{-4}M) and the subsequent challenge with MCh (6 mg/ml)(*$p < 0.05$; Ψ$p < 0.05$).

Figure 3.7

A) Interactive Pathway Model

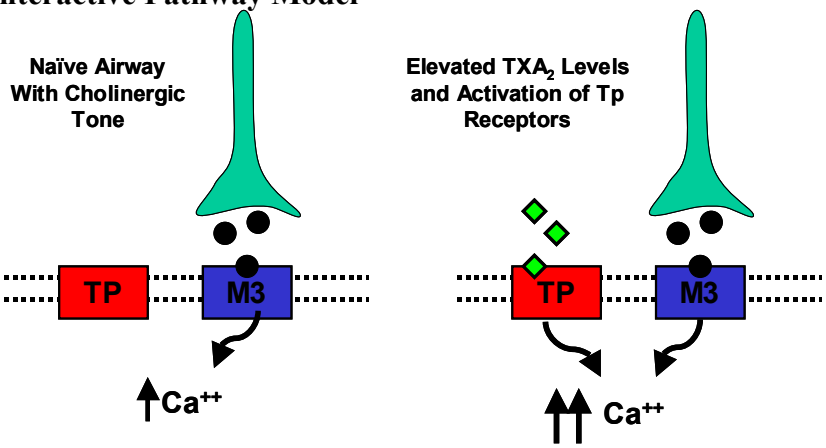

B) Dimer Formation Model

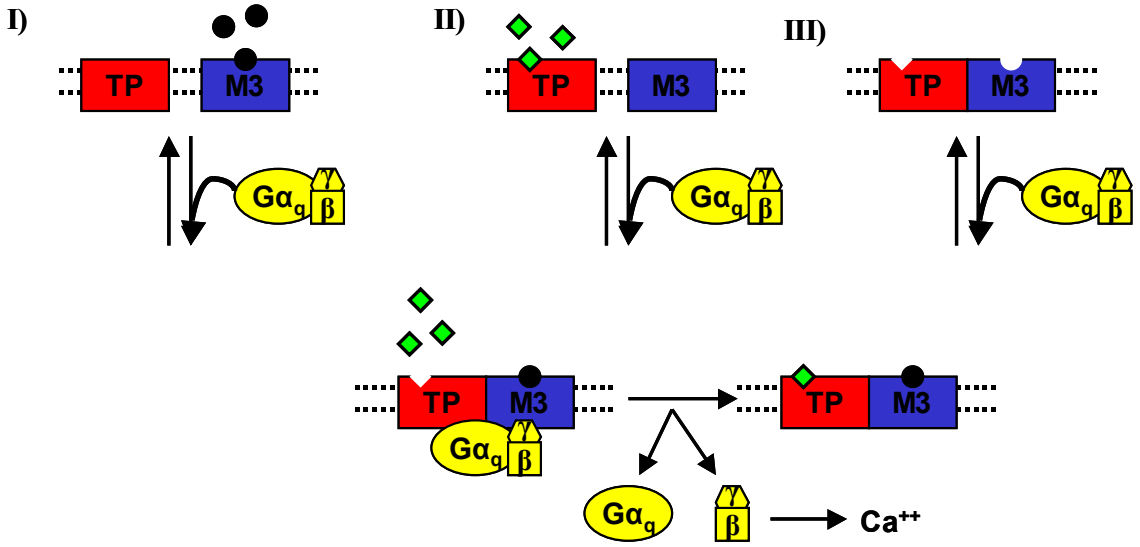

C) G Protein Redistribution Model

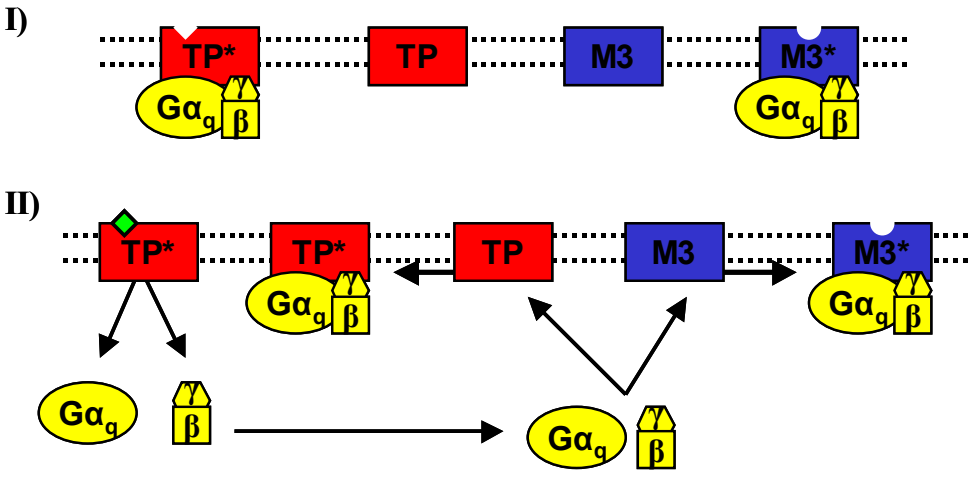

Figure 3.7. Schematic depicting possible models of TP receptor and M3 mAChR mediated airway smooth muscle constriction. A) Interactive Pathways Model: TP receptor stimulation fails to increase intracellular Ca^{++} to levels sufficient to mediate smooth muscle constriction. Acetylcholine acts on M3 mAChRs to maintain cholinergic tone. However, binding of TXA_2 to its receptor potentates the activity of the M3 mAChR, thereby increasing the sensitivity of this receptor to basal release of acetylcholine and leading to increased intracellular Ca^{++} and smooth muscle constriction. **B) Dimer Formation Model:** I) and II) Agonist binding to a GPCR monomer drives heterodimer formation or III) the agonist could bind to a preexisting dimer. Loading the GPCR with agonist induces a conformational shift that allows the accommodation of the heterotrimeric G protein binding. GPCR activation results in the dissociation of the G protein subunits ultimately resulting in increased intracellular Ca^{++} and increased smooth muscle constriction. **C) G Protein Redistribution Model:** A Gα or βγ driven competition may exist between the TP receptor and the M3 mAChR. Upon TP receptor activation, the disassociation of these subunits and the subsequent reassociation to the mAChR, or even other TP receptors, is capable of shifting the M3 mAChR to a higher affinity state and thereby enhancing M3 mAChR mediated signaling events.

Thromboxane Mediates Airway Reactivity and Hyperresponsiveness Through Collaborations Between Smooth Muscle Tp Receptors and The M3 Muscarinic Acetylcholine Receptor

Online Data Supplement

Supplemental Figure E3.1

A)

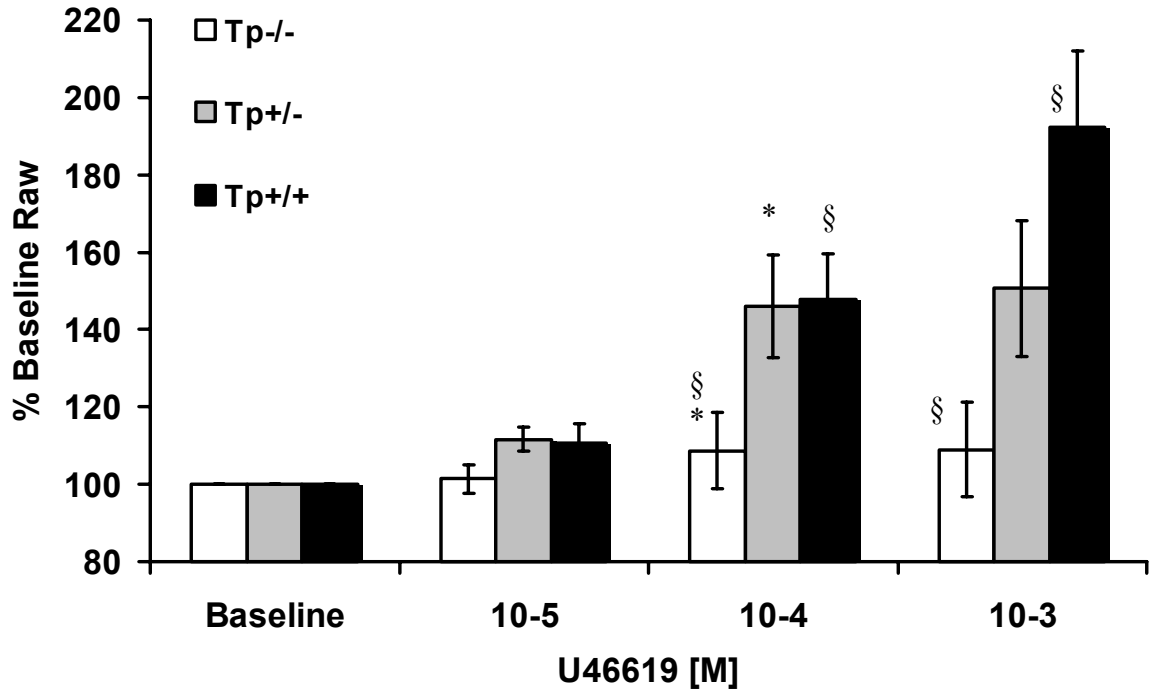

B)

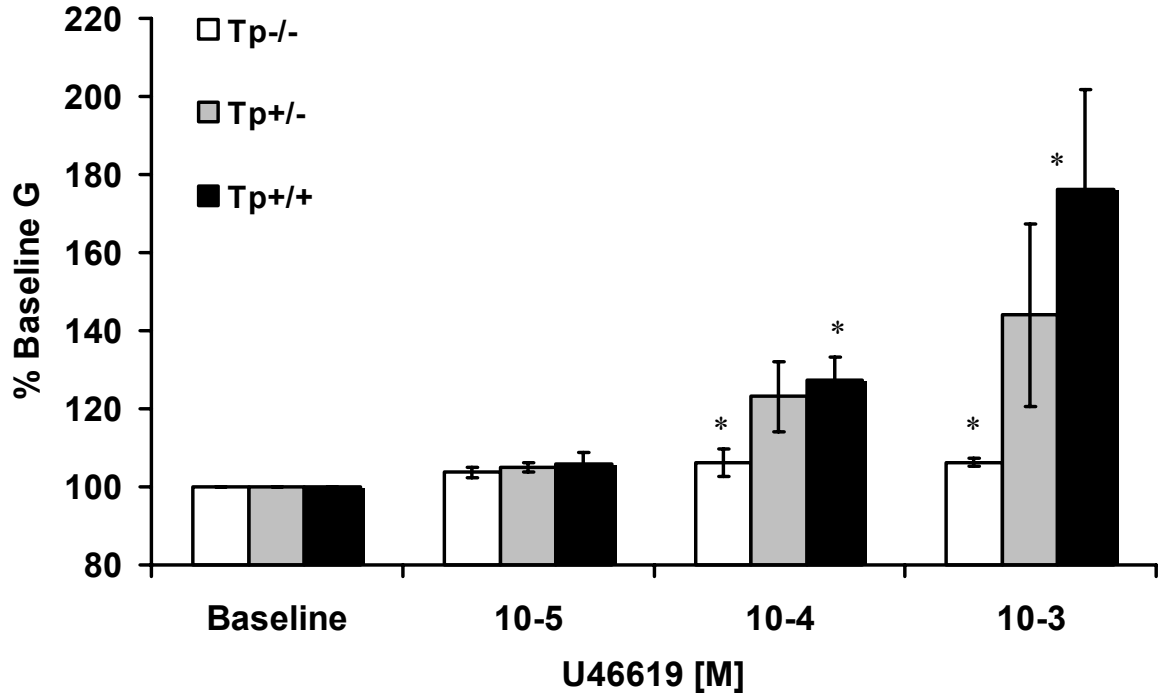

Supplemental Figure E3.1. Mice heterozygous for the TP receptor ($Tp^{+/-}$) demonstrate an intermediate response to a U46619 dose response challenge. Increases in both **A)** airway reactivity (R_{aw}) and **B**) tissue damping (G) were observed in the TP receptor wildtype mice ($Tp^{+/+}$), while no increases were observed for the TP receptor deficient mice ($Tp^{-/-}$). Mice that were heterozygous for the TP receptor ($Tp^{+/-}$) demonstrated intermediate phenotypes, which were neither significantly increased compared to the $Tp^{-/-}$ mice (with the exception of the 10^{-4} M U46619 dose under the Raw parameter) nor significantly reduced versus the $Tp^{+/+}$ animals. $Tp^{-/-}$, n = 12; $Tp^{+/-}$, n = 6; $Tp^{+/+}$, n = 18 (*p < 0.05; §p < 0.01).

Supplemental Figure E3.2

A)

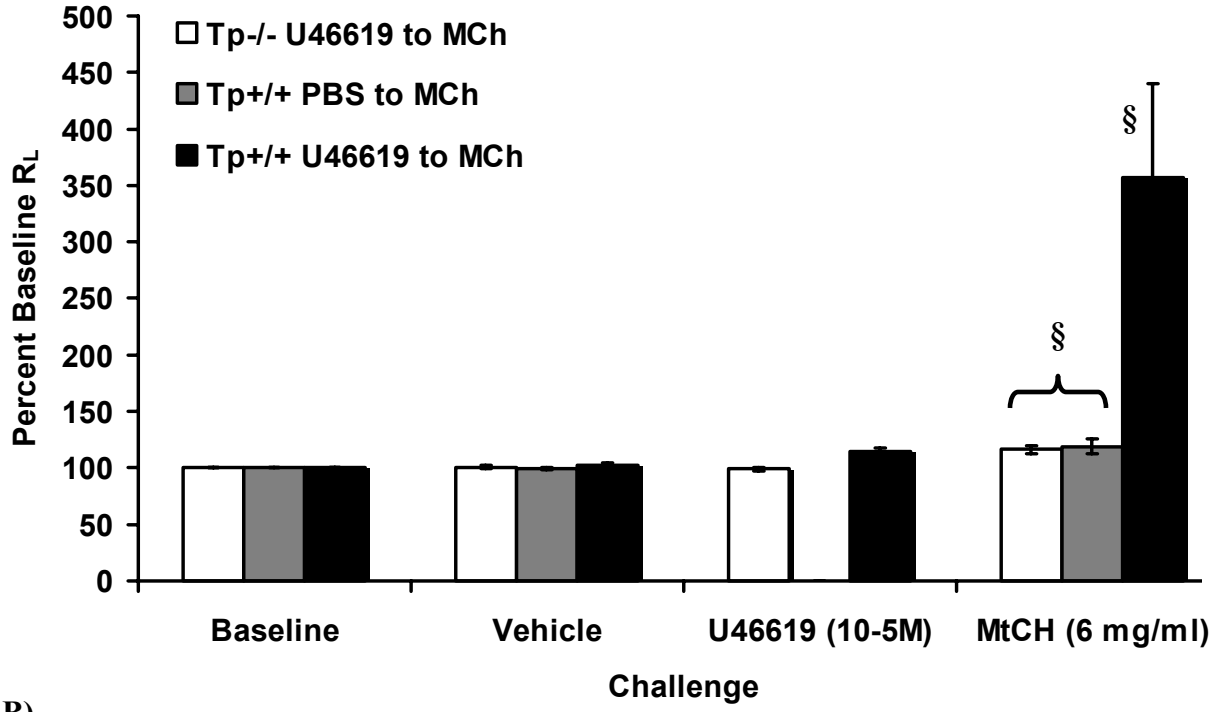

B)

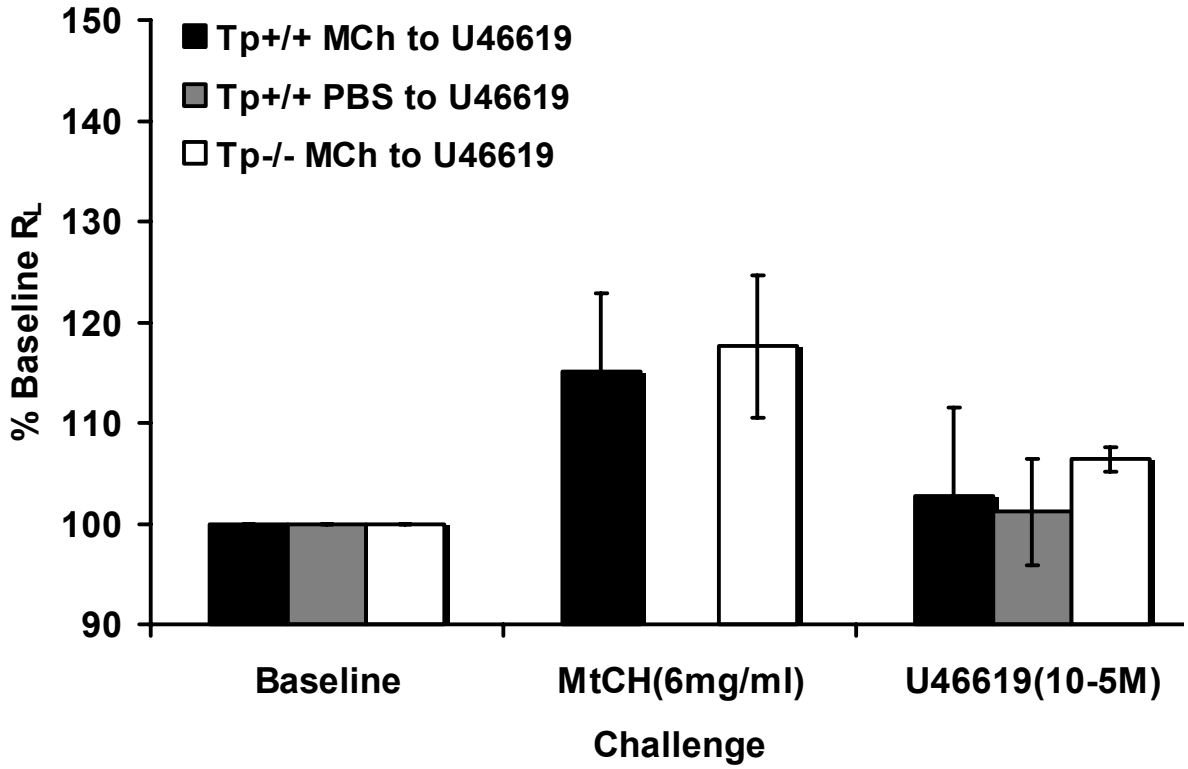

Supplemental Figure E3.2. Increased sensitivity of airways to cholinergic stimuli after exposure to nonprovoking doses of TXA_2. A) We examined the impact of exposure of airways to low levels of the TXA_2 mimetic U46619 to subsequent cholinergic stimulation using the single compartment model of the lung. Two groups of wild type mice and a group of 129/SvEv co-isogenic *Tp*$^{-/-}$ mice were intubated and baseline lung mechanics established and designed as 100% R_L. A cohort of wild type and *Tp*$^{-/-}$ mice were then exposed to vehicle followed by an aerosol produced from a $1x10^{-5}$ M solution of U46619. The second group of wild type mice was only exposed to vehicle. As previously shown, this low level of U46619 does not result in a measurable increase in R_L in wild type mice. Within 3 minutes of either vehicle or U46619 treatment, all groups of mice were exposed to a nonprovoking dose of MCh. As expected, the vehicle treated wild type mice showed no increase in R_L in response to aerosols of 6mg/ml of MCh. In contrast, a robust response to this dose of MCh was observed in wild type mice pretreated with U46619. The dependence of this response on the specific interaction of U46619 with the TP receptor was further demonstrated by the fact that no response to this dose of MCh could be measured in the *Tp*$^{-/-}$ mice. *Tp*$^{-/-}$ with U46619, n = 7; *Tp*$^{+/+}$ no U46619, n = 5; *Tp*$^{+/+}$ with U46619, n = 5 (§$p < 0.01$). **B)** We also examined the impact of exposure of airways to low levels of cholinergic stimulation with subsequent Tp receptor stimulation. A cohort of wild type and *Tp*$^{-/-}$ mice were exposed to vehicle followed by an aerosol produced from 6mg/ml MCh. The second group of wild type mice was only treated with vehicle. This low level of MCh produces a small increase in R_L in wild type mice; however this increase is not significant ($p = 0.09$). Within 3 minutes of vehicle or MCh treatment, all groups of mice were exposed to a nonprovoking dose of U46619. None of the animals demonstrated increases in R_L in response to aerosols of 10^{-5}M U46619.

Supplemental Figure E3.3

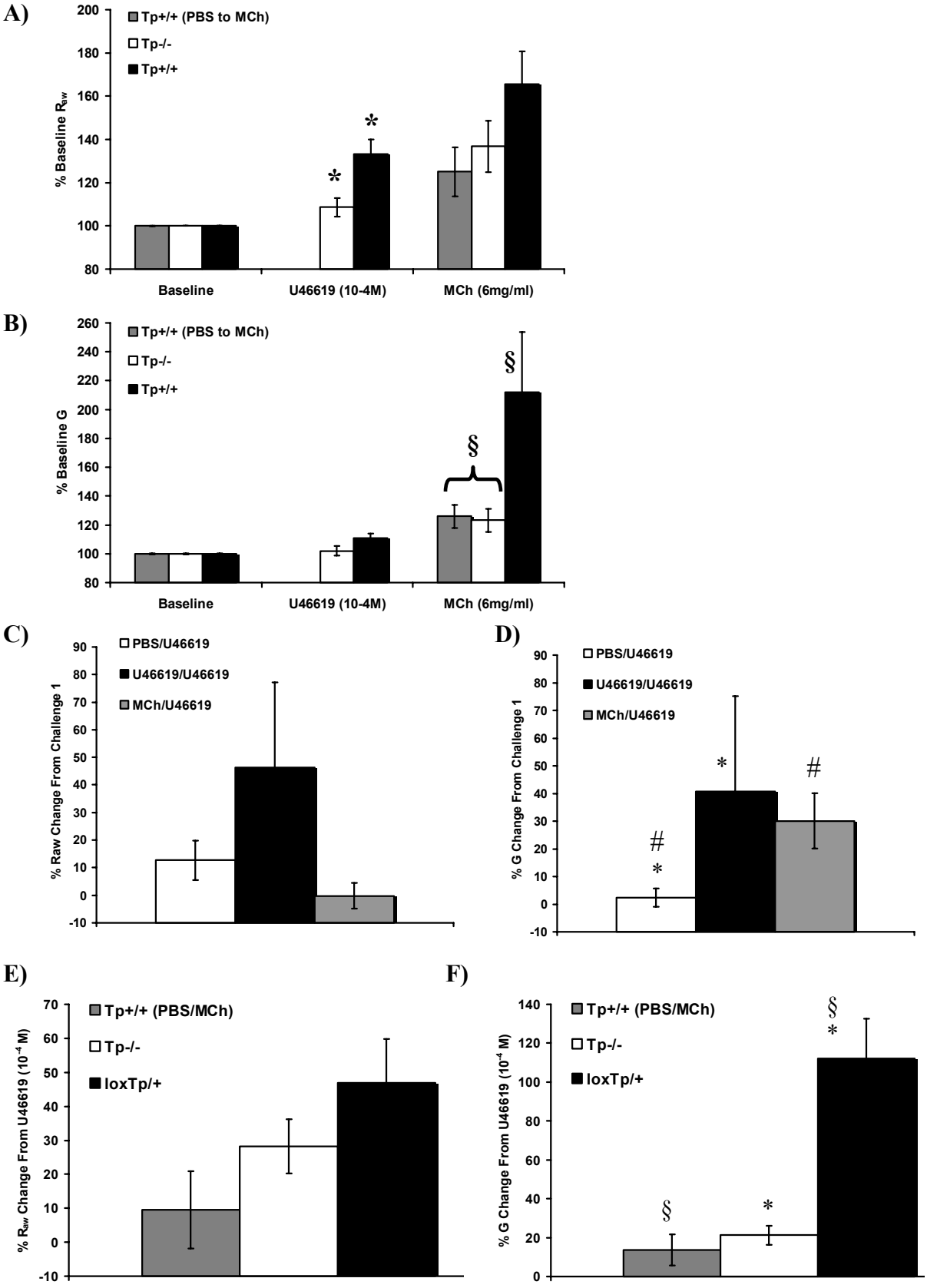

Supplemental Figure E3.3. Increased sensitivity of airways to cholinergic stimuli after exposure to nonprovoking doses of TXA_2. Airways were exposed to low levels of U46619 (10^{-4} M) followed by subsequent cholinergic stimulation with low levels of MCh (6 mg/ml). Two groups of 129/SvEv wild type mice and a group of 129/SvEv co-isogenic *Tp*$^{-/-}$ mice were intubated and baseline lung mechanics established. A cohort of wild type and *Tp*$^{-/-}$ mice were then exposed to vehicle followed by an aerosol produced from a $1x10^{-4}$ M solution of U46619. The second group of wild type mice was only treated with vehicle, and a third group of wild type animals were treated with an aerosol produced from a 6 mg/ml solution of methacholine (MCh). Within 3 minutes of vehicle, U46619, or MCh treatment, all groups of mice were exposed to an aerosol produced from a 6 mg/ml solution of MCh, which has been demonstrated to be only mildly provoking. **A)** All three groups of mice demonstrated increases in airway R_{aw} in response to subsequent aerosol exposure to 6 mg/ml of methacholine. However, mice pretreated with U46619 demonstrated the greatest increase. *Tp*$^{+/+}$ (PBS to MCh), n = 7; *Tp*$^{+/+}$, n = 12; *Tp*$^{-/-}$, n = 4 (*$p < 0.05$). **B)** U46619 did not provoke an increase in tissue damping (G) in the wild type animals. The 6 mg/ml dose of MCh produces only a modest increase in the vehicle challenged animals. In contrast, a robust response to this dose of methacholine was observed in wild type mice pretreated with U46619. The dependence of this response on the specific interaction of U46619 with the TP receptor was further demonstrated by the fact that only a modest response to this dose of methacholine could be measured in the *Tp*$^{-/-}$ mice. *Tp*$^{+/+}$ (PBS to MCh), n = 7; *Tp*$^{+/+}$, n = 12; *Tp*$^{-/-}$, n = 4 (§$p < 0.01$). **C – D)** The impact of low level TP receptor stimulation was assessed following airway exposure to low levels of cholinergic stimulation or TP receptor stimulation. Mice were exposed to mildly provoking doses of either MCh (6 mg/ml),

U46619 (10^{-4} M), or PBS for 30 seconds, followed by assessments of airway resistance (Raw) and tissue damping (G). Immediately following these initial challenges (Challenge 1), mice were exposed to a second mildly provoking dose of either MCh (6 mg/ml) or U46619 (10^{-4} M)(Challenge 2). Data are shown as the % change in R_{aw} or G observed between challenge 1 and challenge 2. PBS/MCh, n = 7; U46619/MCh, n = 12; MCh/MCh, n = 4; PBS/U46619, n = 15; U46619/U46619, n = 3; MCh/U46619, n = 3 (*$p < 0.05$; #$p < 0.05$; **$p < 0.01$). **E and F)** Smooth muscle TP receptor deficient mice were exposed to low levels of U46619 (10^{-4} M) followed by subsequent cholinergic stimulation with low levels of MCh (6 mg/ml). Data are shown as the % change in R_{aw} or G observed between the U46619 challenge and the MCh challenge. **E)** U46619 induced a small, but insignificant increase the MCh R_{aw} response in $Tp^{loxTp/+}$ (wild type) mice compared with the $Tp^{-/-}$ animals and the animals exposed to PBS prior to the second challenge with MCh. **F)** U46619 induced a significant increase the MCh G response in $Tp^{loxTp/+}$ mice. No significant increase was observed in the $Tp^{-/-}$ mice pretreated with U46619 or from $Tp^{+/+}$ mice receiving PBS prior to the MCh challenge (*$p < 0.05$; Ψ$p < 0.01$; §$p < 0.01$).

Discussion

Extensive characterization of TXA_2 mediated airway reactivity has suggested that this potent lipid mediator indirectly induces ASM constriction by potentiating the neuro-effector transmission of cholinergic stimuli. The basis for this hypothesis stems from microelectrode and tension recording assessments of smooth muscle cells and nerve preparations isolated from the canine trachea. Under these *ex vivo* conditions, sub-threshold levels of TXA_2 (10^{-10}-10^{-7} M, depending on study) do not affect the membrane potential, input membrane resistance, or the sensitivity to acetylcholine of canine trachea smooth muscle cells; however, this concentration is sufficient to significantly increase the amplitude of contractions evoked by electrical field stimulation (EFS)(2, 28). This amplification has been shown to be sensitive to atropine, tetrodotoxin, and selective TXA_2 antagonists. Expanding upon these findings, the ability of TXA_2 to augment the *in situ* central airway contraction of the canine trachea following efferent nerve stimulation was also assessed (41). These studies monitored airway responses to intravenous drug administration and vagal stimulation by *in situ* isometric measurements of tracheal smooth muscle tension. These data demonstrate that U46619 substantially augments the tracheal contraction induced by vagal stimulation. However, when acetylcholine was given instead of vagal stimulation, U46619 did not enhance the tracheal contractions (41). It was therefore reasoned that U46619 potentiation is caused by a pre-junctional action rather than by nonspecific pre-contraction of ASM with another agonist. Based on previous work demonstrating that U46619 did not enhance afferent vagal stimulation of canine ASM (47) and the observation that canine airways lack non-adrenergic innervation (24), the authors presumed that TXA_2 augmentation depended on efferent pre-junctional vagal mechanisms (41).

In addition to data generated with canine tracheal preparations, data that supports the enhancement of neural signaling via TXA_2 has also been generated by assessments of canine bronchial preparations. As with tracheal preparations, U46619 has also been demonstrated to constrict bronchial smooth muscle. To further characterize this constriction, microelectrode studies demonstrated that sub-threshold doses of U46619 (10^{-9} M) greatly potentiated the amplitude (252%) and the duration (over 2-fold) of the EFS excitatory junction potential (EJP) without significantly altering the membrane potential or tonic contractions of the ASM (1, 29). This pre-junctional effect was shown to be sensitive to TXA_2 receptor antagonists and therefore suggests that U46619 is capable of pre-junctionally stimulating nerves, via the Tp receptor, to enhance the release of ACh (29).

While the Tp receptor has not been definitively localized on nerves of the PNS, it's presence has been inferred by pharmacological assessments and Tp receptor mRNA has been localized to nodose ganglion neurons from rabbits (32, 61). Early functional *in vivo* studies in cats demonstrated that afferent nerves could be stimulated following the local infusion of arachidonic acid (AA) into the hindlimb circulation (49). This stimulation was abolished following pretreatment with cyclooxygenase inhibitors, thus suggesting that a metabolite of AA was the culprit behind this stimulation. These early studies suggested that TXA_2 might contribute to these responses. Indeed, TXA_2 has been shown to be capable of mediating changes in bradycardia through a neurally mediated mechanism. In these studies, U46619 was directly applied to the epicardial surface of the heart with no effect on cardiac function in either cats or rabbits (46, 60). However, in both species, intravenous injections of U46619 was shown to evoke a viscerosomatic reflex that was capable of inhibiting somatomotor activity, which resulted in a decreased heart rate in rabbits and inhibition of the knee-jerk

response in cats (46, 60). In both studies, these responses were eliminated after bilateral cervical vagotomy. In the airway, additional *in vivo* studies have demonstrated that U46619 is capable of stimulating vagal afferent C-fibres, slowly adapting pulmonary receptors (SARs), and rapidly adapting pulmonary receptors (RARs)(31) and thus implies that in the lung, TXA_2 may be able to modify airway responses through vagally derived afferent nerves.

Based on the extensive data suggesting that TXA_2 mediated ASM constriction is neurally mediated, it was surprising that we did not observe a more dramatic phenotype in mice lacking neural expression of Tp receptors. One possible explanation for this observation is that Tp receptors may still be intact on peripheral neurons. While we demonstrate the successful disruption of the Tp receptor in the brain (CNS), we do not specifically assess nerves of the peripheral nervous system (PNS). Nestin is an intermediate filament protein that is ubiquitously expressed in neuroepithelial precursor cells, which will ultimately differentiate into all types of neurons and glia, including nerves of the PNS (63). Thus, we made the assumption that *Nestin* driven Cre recombinase would be an appropriate system to disrupt neurally expressed TP receptors in both the CNS and PNS. However, to further resolve this issue, it may be necessary to cross the $Tp^{nestin+}$ animals generated in this study with a reporter mouse, such as the C57BL/6J-*Gtrosa*26^{tm2Sor} (Rosa26) mice, that carry a loxP-disrupted β-galactosidase gene to verify Cre recombinase activity in the PNS. Following this strategy, peripheral tissues including the lungs and trachea could be harvested and processed for LacZ histochemistry (X-gal staining) and then counterstained immunohistochemically for a nerve specific marker, such as PGP9.5. While inefficient *Nestin* mediated Cre recombinase disruption is one possible scenario to explain the lack of phenotype, genetic background issues may also be obscuring the actual impact from neural

disruption of the TP receptor in the *Tp*$^{nestin+}$ animals and their *Tp*$^{nestin-}$ littermates. These mice are all N1 generation animals and have a significant C57BL/6 genetic contribution. In general, C57BL/6 mice typically demonstrate significantly reduced airway reactivity. The strong C57BL/6 contribution is evidenced in our data by the reduced R_{aw} responses and significantly attenuated G responses in the *Nestin*^{tg} animals compared to the 129/SvEv mice (Figure 3.3A and B; Supplemental Figure E3.1A and B). It may be necessary to continue backcrossing these animals onto the 129/SvEv background to further verify the impact of neural Tp receptor disruption.

Because we failed to observe a dramatic decrease in airway reactivity in the neural TP receptor deficient animals, we next assessed the ability of smooth muscle TP receptors to influence airway mechanics in response to U46619. Extensive data clearly demonstrates that TP receptors are expressed on smooth muscle (13, 25, 42) and as discussed above, several studies have suggested that these receptors may functionally contribute to ASM constriction. To disrupt the smooth muscle TP receptors, we chose to cross the floxed *Tp* mice with transgenic animals expressing Cre-recombinase under the control of the SM22 promoter. The *SM22*-Cre animals have demonstrated highly efficient Cre-mediated recombination in smooth muscle cells (19). Here, we demonstrate that Cre-mediated disruption of the smooth muscle TP receptors was successful in uterine, intestinal, and tracheal smooth muscle. In addition to these tissues, the lungs were also harvested and assessed by Southern blot; however, we failed to observe the 3.3 kb fragment indicative of successful Cre mediated recombination (data not shown). This was most likely due to the low abundance of ASM present in the lungs compared to other cell types. Previous studies assessing the expression pattern of the *SM22- Cre*^{tg} transgene have demonstrated, following breeding of the *SM22-*

Cre^{tg} mice with the ROSA-26 β-gal reporter animals, that efficient recombination does occur in the ASM of the lung (26). It is also important to note that Cre-mediated recombination is not 100% efficient, thus some smooth muscle cells will inevitably fail to undergo recombination.

Previously, we predicted that if a particular tissue is critical for the TXA_2 response, we should observe the following rank order: *Cre*^{tg} -transgene positive *Tp*$^{loxTp/-}$ < *Tp*$^{loxTp/-}$ = *Cre*^{tg}-transgene positive *Tp*$^{loxTp/+}$< *Tp*$^{loxTp/+}$. This prediction is similar to what we observed for the smooth muscle TP receptor deficient mice. The *Tp*$^{loxTp/-\ Tgln+\ ve}$ mice demonstrate both attenuated TXA_2 mediated airway reactivity and reduced AHR to cholinergic stimuli. Likewise, both *Tp*$^{loxTp/-}$ heterozygous and *Tp*$^{loxTp/+\ Tgln+\ ve}$ smooth muscle heterozygous animals demonstrated intermediate responses for both R_{aw} and G, while *Tp*$^{loxTp/+}$ wild type mice demonstrated significantly increased airway responses to TXA_2. However, the *Tp*$^{loxTp/+\ Tgln+\ ve}$ smooth muscle *Tp* heterozygous mice demonstrated significantly increased R_{aw} in response to TXA_2 and significantly increased R_{aw} and G in response to MCh in the TXA_2 mediated AHR model, when compared with the *Tp*$^{loxTp/-}$ heterozygous animals. The simplest explanation for these data is that TP receptors on other tissues may contribute to TXA_2 mediated AHR. In addition to smooth muscle and neural TP receptors, high levels of TP receptors are also expressed on bronchial epithelial cells and resident leukocytes in the lung (43, 59). Activation of TP receptors on other tissue types may contribute to the increase in airway reactivity observed in these animals. However, if this hypothesis were true, we would also expect to see an intermediate increase in AHR in the *Tp*$^{loxTp/-\ Tgln+\ ve}$ smooth muscle TP receptor deficient animals, whose responses were similar to those observed for the *Tp*$^{-/-}$ mice. While we cannot fully discount the possibility that TP receptors expressed on other tissues

may contribute to the TXA_2 response, the data presented here strongly suggests that TXA_2 mediates increases in airway reactivity and AHR through direct interactions with smooth muscle TP receptors.

A number of models could be proposed to describe possible mechanisms involved in the modulation of smooth muscle TP receptor signaling that are consistent with our previous work showing a dependence on both intact vagal innervation and the M3 mAChR for TXA_2 mediated ASM constriction (3)(Figure 3.7). Because TP receptors and M3 mAChRs are both present on smooth muscle, one potential model suggests that stimulation of the TP receptor fails to increase intracellular Ca^{++} to levels sufficient to mediate constriction. However, binding of TXA_2 to its receptor potentates the activity of the M3 mAChR, thereby increasing the sensitivity of this receptor to basal release of acetylcholine (Figure 3.7A). While this is the simplest model, other possible models can be envisioned, which reflect a possible modulation of M3 mAChR signaling by the TP receptor. It is well established that G-protein coupled receptors (GPCR) function via distinct signal transduction pathways; however, it is also accepted that "cross-talk" or synergy can also occur. This synergism can occur through mechanisms such as heterodimerization, cross-reactions among GPCR downstream effectors, and G-protein redistribution (27). While neither heterodimerization nor downstream effector cross-signalling have been defined for TP receptors, some evidence does suggest the TP receptor is capable of cross-talk with other GPCRs via redistribution of G-proteins. Evidence for this stems from data suggesting synergism between platelet PAR1 receptors and TP receptors, as well as, anecdotal evidence suggesting a similar synergism between platelet-activating factor (PAF) and Tp receptors (16). The PAR1/TP synergism model describes a dynamic equilibrium between the TP

receptor and other GPCRs that couple to the same Gα-subunits as TP (27). Following this model, a Gα driven competition may exist between TP and other GPCRs. Upon activation, the disassociation of the Gα-subunit from these GPCRs, and the subsequent Gα reassociation to TP is capable of shifting TP to a higher affinity state and thereby enhancing TP receptor mediated signaling events (16, 17). It is temping to speculate a similar synergism may exist between the TP receptor and the M3 mAChR (Figure 3.7C).

Our data extends the findings that TXA_2 contributes to the development of allergic airway disease and in particular to changes in airway reactivity through its ability to amplify the actions of ACh. Based on the data generated here for the smooth muscle TP receptor deficient mice, it is likely that the primary mechanism by which TXA_2 induces airway reactivity and enhances subsequent responses to ACh is via the direct activation of ASM Tp receptors. Following activation, the TP receptors collaborate through a currently undefined mechanism with M3 mAChRs to initiate ASM constriction. The extent to which TXA_2 contributes to the asthmatic condition in humans is still undetermined. However, the improvement in subpopulations of asthma patients following TXA_2/TP or muscarinic receptor antagonist therapies suggests that the mechanisms outlined above may play an important, yet limited, role in asthma pathophysiology.

References

1. Abela AP and Daniel EE. Neural and myogenic effects of cyclooxygenase products on canine bronchial smooth muscle. *Am J Physiol* 268: L47-55, 1995.

2. Aizawa H, Takata S, Shigyo M, Matsumoto K, Koto H, Inoue H, and Hara N. Effect of BAY u3405, a thromboxane A2 receptor antagonist, on neuro- effector transmission in canine tracheal tissue. *Prostaglandins LeukotEssentFatty Acids* 53: 213-217, 1995.

3. Allen IC, Hartney JM, Coffman TM, Penn RB, Wess J, and Koller BH. Thromboxane A2 induces airway constriction through an M3 muscarinic acetylcholine receptor-dependent mechanism. *Am J Physiol Lung Cell Mol Physiol* 290: L526-533, 2006.

4. Arimura A, Asanuma F, Yagi H, Kurosawa A, and Harada M. Involvement of thromboxane A2 in bronchial hyperresponsiveness but not lung inflammation induced by bacterial lipopolysaccharide in guinea pigs. *Eur J Pharmacol* 231: 13-21, 1993.

5. Ashton AW and Ware JA. Thromboxane A2 receptor signaling inhibits vascular endothelial growth factor-induced endothelial cell differentiation and migration. *Circ Res* 95: 372-379, 2004.

6. Blackman SC, Dawson G, Antonakis K, and Le Breton GC. The identification and characterization of oligodendrocyte thromboxane A2 receptors. *J Biol Chem* 273: 475-483, 1998.

7. Boucher P, Gotthardt M, Li WP, Anderson RG, and Herz J. LRP: role in vascular wall integrity and protection from atherosclerosis. *Science* 300: 329-332, 2003.

8. Bresnahan BA, Le Breton GC, and Lianos EA. Localization of authentic thromboxane A2/prostaglandin H2 receptor in the rat kidney. *Kidney Int* 49: 1207-1213, 1996.

9. Chen Z, Prasad S, and Cynader M. Localisation of thromboxane A2 receptors and the corresponding mRNAs in human eye tissue. *Br J Ophthalmol* 78: 921-926, 1994.

10. Coleman RA, Humphrey PP, Kennedy I, Levy GP, and Lumley P. Comparison of the actions of U-46619, a prostaglandin H2-analogue, with those of prostaglandin H2 and thromboxane A2 on some isolated smooth muscle preparations. *Br J Pharmacol* 73: 773-778, 1981.

11. Coleman RA and Kennedy I. Characterisation of the prostanoid receptors mediating contraction of guinea-pig isolated trachea. *Prostaglandins* 29: 363-375, 1985.

12. Craven PA, Melhem MF, and DeRubertis FR. Thromboxane in the pathogenesis of glomerular injury in diabetes. *Kidney Int* 42: 937-946, 1992.

13. Craven PA, Studer RK, and DeRubertis FR. Thromboxane/prostaglandin endoperoxide-induced hypertrophy of rat vascular smooth muscle cells is signaled by protein kinase C-dependent increases in transforming growth factor-beta. *Hypertension* 28: 169-176, 1996.

14. DeRubertis FR and Craven PA. Eicosanoids in the pathogenesis of the functional and structural alterations of the kidney in diabetes. *Am J Kidney Dis* 22: 727-735, 1993.

15. Devillier P and Bessard G. Thromboxane A2 and related prostaglandins in airways. *Fundam Clin Pharmacol* 11: 2-18, 1997.

16. Djellas Y, Antonakis K, and Le Breton GC. A molecular mechanism for signaling between seven-transmembrane receptors: evidence for a redistribution of G proteins. *Proc Natl Acad Sci U S A* 95: 10944-10948, 1998.

17. Djellas Y, Antonakis K, and Le Breton GC. Shifts in the affinity distribution of one class of seven-transmembrane receptors by activation of a separate class of seven-transmembrane receptors. *Biochem Pharmacol* 59: 1521-1529, 2000.

18. Endoh M, Kashem A, Yamauchi F, Yano N, Nomoto Y, Sakai H, and Kurokawa K. Expression of thromboxane synthase in kidney tissues from patients with IgA nephropathy. *Clin Nephrol* 47: 168-175, 1997.

19. Frutkin AD, Shi H, Otsuka G, Leveen P, Karlsson S, and Dichek DA. A critical developmental role for tgfbr2 in myogenic cell lineages is revealed in mice expressing SM22-Cre, not SMMHC-Cre. *J Mol Cell Cardiol* 41: 724-731, 2006.

20. Gomes RF, Shen X, Ramchandani R, Tepper RS, and Bates JH. Comparative respiratory system mechanics in rodents. *J Appl Physiol* 89: 908-916, 2000.

21. Hamberg M, Svensson J, and Samuelsson B. Thromboxanes: a new group of biologically active compounds derived from prostaglandin endoperoxides. *Proc Natl Acad Sci U S A* 72: 2994-2998, 1975.

22. Hantos Z, Adamicza A, Govaerts E, and Daroczy B. Mechanical impedances of lungs and chest wall in the cat. *J Appl Physiol* 73: 427-433, 1992.

23. Held HD, Martin C, and Uhlig S. Characterization of airway and vascular responses in murine lungs. *Br J Pharmacol* 126: 1191-1199, 1999.

24. Hendrix SG, Munoz NM, and Leff AR. Physiological and pharmacological response of canine bronchial smooth muscle in situ. *J Appl Physiol* 54: 215-224, 1983.

25. Hirata M, Hayashi Y, Ushikubi F, Yokota Y, Kageyama R, Nakanishi S, and Narumiya S. Cloning and expression of cDNA for a human thromboxane A2 receptor. *Nature* 349: 617-620, 1991.

26. Holtwick R, Gotthardt M, Skryabin B, Steinmetz M, Potthast R, Zetsche B, Hammer RE, Herz J, and Kuhn M. Smooth muscle-selective deletion of guanylyl cyclase-A prevents the acute but not chronic effects of ANP on blood pressure. *Proc Natl Acad Sci U S A* 99: 7142-7147, 2002.

27. Huang JS, Ramamurthy SK, Lin X, and Le Breton GC. Cell signalling through thromboxane A2 receptors. *Cell Signal* 16: 521-533, 2004.

28. Inoue T and Ito Y. Pre- and post-junctional actions of prostaglandin I2, carbocyclic thromboxane A2 and leukotriene C4 in dog tracheal tissue. *Br J Pharmacol* 84: 289-298, 1985.

29. Janssen LJ and Daniel EE. Prejunctional and Postjunctional Effects of a Thromboxane Mimetic in Canine Bronchi. *Am J Physiol* 261: L271-L276, 1991.

30. Jones GL, Lane C, and O'Byrne PM. Effect of an inhaled thromboxane mimetic (U46619) on in vivo pulmonary resistance and airway hyperresponsiveness in dogs. *J Physiol* 453: 59-67, 1992.

31. Karla W, Shams H, Orr JA, and Scheid P. Effects of the Thromboxane-A2 Mimetic, U46,619, on Pulmonary Vagal Afferents in the Cat. *Resp Physiol* 87: 383-396, 1992.

32. Kenagy J, VanCleave J, Pazdernik L, and Orr JA. Stimulation of group III and IV afferent nerves from the hindlimb by thromboxane A(2). *Brain Res* 744: 175-178, 1997.

33. Kinsella BT, OMahony DJ, and Fitzgerald GA. The human thromboxane A2 receptor alpha isoform (TP alpha) functionally couples to the G proteins G(q) and G(11) in vivo and is activated by the isoprostane 8-epi prostaglandin F-2 alpha. *J Pharmacol Exp Ther* 281: 957-964, 1997.

34. Knoepfler PS, Cheng PF, and Eisenman RN. N-myc is essential during neurogenesis for the rapid expansion of progenitor cell populations and the inhibition of neuronal differentiation. *Genes Dev* 16: 2699-2712, 2002.

35. Li M, Tian Y, Fritzsch B, Gao J, Wu X, and Zuo J. Inner hair cell Cre-expressing transgenic mouse. *Genesis* 39: 173-177, 2004.

36. Liel N, Mais DE, and Halushka PV. Binding of a thromboxane A2/prostaglandin H2 agonist [3H]U46619 to washed human platelets. *Prostaglandins* 33: 789-797, 1987.

37. Lin X, Ramamurthy SK, and Le Breton GC. Thromboxane A receptor-mediated cell proliferation, survival and gene expression in oligodendrocytes. *J Neurochem* 93: 257-268, 2005.

38. Miggin SM and Kinsella BT. Expression and tissue distribution of the mRNAs encoding the human thromboxane A2 receptor (TP) alpha and beta isoforms. *BiochimBiophysActa* 1425: 543-559, 1998.

39. Mitchell JA and Warner TD. COX isoforms in the cardiovascular system: understanding the activities of non-steroidal anti-inflammatory drugs. *Nat Rev Drug Discov* 5: 75-86, 2006.

40. Mohn A and Koller BH. In: *DNA Cloning 4*, edited by Glover DM and Hames BD. New York: Oxford University Press, 1995, p. 143-184.

41. Munoz NM, Shioya T, Murphy TM, Primack S, Dame C, Sands MF, and Leff AR. Potentiation of vagal contractile response by thromboxane mimetic U-46619. *J Appl Physiol* 61: 1173-1179, 1986.

42. Namba T, Sugimoto Y, Hirata M, Hayashi Y, Honda A, Watabe A, Negishi M, Ichikawa A, and Narumiya S. Mouse thromboxane A2 receptor: cDNA cloning, expression and northern blot analysis. *Biochem Biophys Res Commun* 184: 1197-1203, 1992.

43. Nusing R, Lesch R, and Ullrich V. Immunohistochemical localization of thromboxane synthase in human tissues. *Eicosanoids* 3: 53-58, 1990.

44. Offermanns S and Simon MI. G-Alpha(15) and G-Alpha(16) Couple a Wide Variety of Receptors to Phospholipase-C. *J Biol Chem* 270: 15175-15180, 1995.

45. Patrono C, Patrignani P, and Davi G. Thromboxane biosynthesis and metabolism in cardiovascular and renal disease. *J Lipid Mediat* 6: 411-415, 1993.

46. Pickar JG. The thromboxane A2 mimetic U-46619 inhibits somatomotor activity via a vagal reflex from the lung. *Am J Physiol* 275: R706-712, 1998.

47. Quan SF, Moon MA, and Lemen RJ. Effects of arachidonic acid, PGF2 alpha, and a PGH2 analogue on airway diameters in dogs. *J Appl Physiol* 53: 1005-1014, 1982.

48. Rocca B, Loeb AL, Strauss JF, 3rd, Vezza R, Habib A, Li H, and FitzGerald GA. Directed vascular expression of the thromboxane A2 receptor results in intrauterine growth retardation. *Nat Med* 6: 219-221, 2000.

49. Rotto DM and Kaufman MP. Effect of metabolic products of muscular contraction on discharge of group III and IV afferents. *J Appl Physiol* 64: 2306-2313, 1988.

50. Sachinidis A, Flesch M, Ko Y, Schror K, Bohm M, Dusing R, and Vetter H. Thromboxane A2 and vascular smooth muscle cell proliferation. *Hypertension* 26: 771-780, 1995.

51. Saroea HG, Inman MD, and O'Byrne PM. U46619-induced bronchoconstriction in asthmatic subjects is mediated by acetylcholine release. *Am J Respir Crit Care Med* 151: 321-324, 1995.

52. Sato T, Iwama T, Shikada K, and Tanaka S. Airway hyperresponsiveness to acetylcholine induced by aerosolized arachidonic acid metabolites in guinea-pigs. *Clin Exp Allergy* 26: 957-963, 1996.

53. Shenker A, Goldsmith P, Unson CG, and Spiegel AM. The G protein coupled to the thromboxane A2 receptor in human platelets is a member of the novel Gq family. *J Biol Chem* 266: 9309-9313, 1991.

54. Shirai M, Ninomiya I, and Sada K. Thromboxane A2/endoperoxide receptors mediate cholinergic constriction of rabbit lung microvessels. *J Appl Physiol* 72: 1179-1185, 1992.

55. Shirai M, Ninomiya I, and Sada K. Thromboxane-a(2) Endoperoxide Receptors Mediate Cholinergic Constriction of Rabbit Lung Microvessels. *Journal of Applied Physiology* 72: 1179-1185, 1992.

56. Takata S, Aizawa H, Shigyo M, Matsumoto K, Inoue H, Koto H, and Hara N. Thromboxane A2 mimetic (U-46619) induces hyperresponsiveness of smooth muscle in the canine bronchiole, but not in the trachea. *Prostaglandins LeukotEssentFatty Acids* 54: 129-134, 1996.

57. Thomas DW, Mannon RB, Mannon PJ, Latour A, Oliver JA, Hoffman M, Smithies O, Koller BH, and Coffman TM. Coagulation defects and altered hemodynamic responses in mice lacking receptors for thromboxane A2. *JClinInvest* 102: 1994-2001, 1998.

58. Tomioka S, Bates JH, and Irvin CG. Airway and tissue mechanics in a murine model of asthma: alveolar capsule vs. forced oscillations. *J Appl Physiol* 93: 263-270, 2002.

59. Ushikubi F, Aiba Y, Nakamura K, Namba T, Hirata M, Mazda O, Katsura Y, and Narumiya S. Thromboxane A2 receptor is highly expressed in mouse immature thymocytes and mediates DNA fragmentation and apoptosis. *J Exp Med* 178: 1825-1830, 1993.

60. Wacker MJ, Tehrani RN, Smoot RL, and Orr JA. Thromboxane A(2) mimetic evokes a bradycardia mediated by stimulation of cardiac vagal afferent nerves. *Am J Physiol Heart Circ Physiol* 282: H482-490, 2002.

61. Wacker MJ, Tyburski JB, Ammar CP, Adams MC, and Orr JA. Detection of thromboxane A(2) receptor mRNA in rabbit nodose ganglion neurons. *Neurosci Lett* 386: 121-126, 2005.

62. Wagers SS, Norton RJ, Rinaldi LM, Bates JH, Sobel BE, and Irvin CG. Extravascular fibrin, plasminogen activator, plasminogen activator inhibitors, and airway hyperresponsiveness. *J Clin Invest* 114: 104-111, 2004.

63. Zimmerman L, Parr B, Lendahl U, Cunningham M, McKay R, Gavin B, Mann J, Vassileva G, and McMahon A. Independent regulatory elements in the nestin gene direct transgene expression to neural stem cells or muscle precursors. *Neuron* 12: 11-24, 1994.

CHAPTER IV

Expression and function of NPSR1/GPRA in the lung before and after induction of asthma-like disease

Expression and function of NPSR1/GPRA in the lung before and after induction of asthma-like disease

Irving C. Allen[1], Amy J. Pace[2], Leigh A. Jania[2], Julie G. Ledford[1], Anne M. Latour[2,3], John N. Snouwaert[2,3], Virginie Bernier[4], Rino Stocco[4], Alex G. Therien[4], and Beverly H. Koller[1,2,3]

[1] Curriculum in Genetics and Molecular Biology, [2]Department of Genetics, [3] Department of Medicine, University of North Carolina at Chapel Hill, Chapel Hill, North Carolina, 27599; [4] Department of Biochemistry and Molecular Biology, Merck Frosst Canada Ltd., Kirkland, QC, Canada, H9H 3L1

Running Title: Expression and function of NPSR1/GPRA in the lung

Address Correspondence To: Beverly H. Koller, Department of Genetics, CB# 7264, University of North Carolina at Chapel Hill, North Carolina, 27599-7264, Phone: 919-962-2159, Fax: 919-843-4682, E-mail: Treawouns@aol.com

† This article has an online data supplement

Abstract

A genetic contribution to asthma susceptibility is well recognized, and linkage studies have identified a large number of genes associated with asthma pathogenesis. Recently, a locus encoding a seven transmembrane protein was shown to be associated with asthma in founder populations. The expression of the protein GPRA (G protein-coupled receptor for asthma susceptibility) in human airway epithelia and smooth muscle, and its increased expression in a mouse model of asthma, suggested that a gain-of-function mutation in this gene increased the disease risk. However, we report here that the development of allergic lung disease in GPRA deficient mice is unaltered. A possible explanation for this finding became apparent upon reexamination of the expression of this gene. In contrast to initial studies, our analyses failed to detect expression of GPRA in human lung tissue or in mice with allergic lung disease. We identify a single parameter that distinguishes GPRA deficient and wild type mice. While the change in airway resistance in response to methacholine was identical in control and GPRA deficient mice, the mutant animals showed an attenuated response to thromboxane, a cholinergic receptor dependent bronchoconstricting agent. Taken together, our studies fail to support a direct contribution of GPRA to asthma pathogenesis. However, our data suggests that GPRA may contribute to the asthmatic phenotype by altering the activity of other pathways, such as neurally mediated mechanisms, that contribute to disease. This interpretation is supported by high levels of GPRA expression in the brain and its recent identification as the neuropeptide S receptor.

Keywords:

Neuropeptide S; G protein coupled receptor; allergic lung disease; anaphylaxis

Introduction

Asthma is a complex genetic disorder with heterogeneous phenotypes and is strongly influenced by environmental factors. A strong genetic predisposition to asthma is well recognized. Over the past decade, linkage analyses for asthma susceptibility loci have identified several candidate regions. A recent addition to the pool of candidate genes associated with asthma susceptibility and atopy has been identified using genome-wide linkage scans and positional cloning on chromosome 7p15-p14 (19, 20). Using founder populations from Finnish and French-Canadian cohorts, this study identified 2 candidate genes within this region. One, a putative gene with a large open reading frame, was designated asthma-associated alternatively spliced gene 1 (AAA1). Expression analyses showed some weak hybridization to lung RNA, however the open reading frame for this gene is not preserved in mouse. The second gene identified on the other strand of an overlapping region of DNA encodes a 7 transmembrane domain (7TM) protein. Termed G protein-coupled receptor for asthma susceptibility (GPRA), an asthma-associated single nucleotide polymorphism (SNP) identified in this study alters the primary structure of this gene: the polymorphism results in the substitution of an isoleucine for the asparagine located at position 107 of the protein in affected individuals. Excitement regarding this newly identified asthma candidate gene was fueled by the demonstration that the GPRA protein was expressed at high levels in the lung, particularly in tissues obtained from asthmatic patients.

Since this initial genetic study, GPRA polymorphisms have been found to be associated with asthma and atopy in other populations. Studies of multiple western European populations revealed an association of GPRA haplotypes with asthma and atopy (18, 23). Likewise, assessments of a Chinese population revealed an association between a previously

uncharacterized GPRA haplotype and methacholine induced airway hyperresponsiveness, thus extending the association findings to a non-Caucasian population (7). In contrast to these original analyses and association studies, a high-resolution fine mapping study screening SNPs on chromosome 7p in German and Swedish populations, as well as a phylogenetic analysis of GPRA associated SNP haplotypes within a Korean population, failed to show GPRA linkage or association with asthma (14, 28). Additional association studies in individuals of northern European descent also failed to show association with the GPRA risk haplotypes and atopic dermatitis, a chronic recurring inflammatory skin disease that is characterized by high serum IgE levels and the recruitment of Th_2 lymphocytes (31, 34).

The 7TM receptor encoded in the asthma associated locus and termed GPRA was independently identified and characterized as the vasopressin receptor-related receptor 1 (VRR1) (9). VRR1 is expressed in the retina and has been mapped between markers associated with retinitis pigmentosa subtype 9 (9, 16). Likewise, GPRA has also been described as the receptor for neuropeptide S (NPSR1), a novel neuropeptide that potently modulates arousal and could also regulate anxiolytic-like effects. Both the ligand and the receptor were shown to be expressed at extremely high levels in the brain (37). Biochemical studies using cell lines have shown that GPRA/NPSR indeed couples to G proteins. Interestingly, these transfection studies in HEK293 cells show that GPRA/NPSR couples to both Gq and Gs pathways, induces calcium mobilization, and increases adenylate cyclase activity (9). Which of these pathways dominates in nontransformed cells is not yet clear. However, similar studies have also demonstrated that the N107I polymorphism, while not

altering ligand binding affinity, results in a gain-of-function mutation defined by an increase in agonist potency (4, 26).

The GPRA gene encodes a unique and recently deorphanized G-protein coupled receptor (GPCR), which was originally identified as GPR154. Alternative splicing of the gene results in variants that differ from one another in the primary amino acid structure of the cytoplasmic domain. Antibodies generated against C terminal peptides of two of the GPRA isoforms demonstrated expression of the A isoform in the airways of both asthmatic and healthy individuals. In contrast, expression of the B isoform was detected in airway epithelial cells in healthy individuals and predominately in the airway smooth muscle cells in asthmatics (20, 35). Laitinen *et al*. also reported that GPRA expression could be detected in the mouse lung and that the expression increased in a mouse model of asthma. These data suggest that the mouse might provide a useful model for study of the role of GPRA in human disease. Towards this end, we report here the generation of a mouse line deficient in GPRA expression as well as the characterization of this mouse in the ovalbumin induced mouse model of allergic lung disease.

Methods

Generation of GPRA-deficient mice

Segments of the NPSR1/GPRA encoding gene were amplified by PCR and used to create a plasmid capable of undergoing homologous recombination with the endogenous locus. Two 5 kb fragments of the *Npsr1/Gpra* gene were amplified using the following primer sets: 5'-GCGGC CGCAAGATGCCCACCCAGTAAGAAATC-3'and 5'-GTCGA CCTAGGTAGAGGCATACAGCAGGACAA-3' and 5'-GGTACCCGGGCCATGGGG AACAGAACGGAGAT-3' and 5'-GCAATTGAGCCCCACCAAGCAAACTGT-3'. The fragments were then cloned 5' and 3' of the neomycin gene in the pXena vector. This targeting plasmid is designed to replace a 744 bp region containing the majority of exon 4 with the neomycin cassette. Exon 4 includes regions of the gene encoding the 3rd transmembrane spanning domain and regions of the i2 intracellular loop. The plasmid was linearized and introduced into embryonic stem cells derived from 129/SvEv mice, and transformants were isolated using standard methodologies (24). A DNA probe corresponding to the region immediately 5' of the targeted region generated by PCR (5'-GCTCATGTGTTTTCTTTCCTTATCT-3' and 5'-ACCTCCCATGCCCACTCGT-3') was used to identify targeted ES cells by Southern blot. A second probe, corresponding to DNA encoding exon 4, was generated by PCR (5'-CCATCG TTTACCCCATGAAG-3' and 5'-CCTGGTACCCCAACAGTAGC-3') and was used to verify the loss of the region of the gene during the homologous recombination event. ES cells carrying the correctly modified locus were used to generate chimeric animals, which in turn were bred to 129/SvEv, C57BL/6, or BALB/c mice. Those carrying the mutant allele were identified by either Southern blot analysis using the probes described above or by PCR analysis (common: 5'-

GTGGGTACATGAGAAGGTTAGGAG-3'; endogenous: CCTTATCCTCAAACCACGA AGTAT-3'; targeted: AAATGCCTGCTCTTTACTGAAGG) of DNA prepared from tail biopsies. We designate this mutation GPRA$^{\Delta 94\text{-}159}$; however, in the interest of brevity, we will refer to mice homozygous for the mutation as GPRA$^{-/-}$. All studies were conducted in accordance with the National Institutes of Health Guide for the Care and Use of Laboratory Animals as well as the Institutional Animal Care and Use Committee guidelines of the University of North Carolina at Chapel Hill.

Northern and RT-PCR Analysis of Gpra RNA present in GPRA$^{\Delta 94\text{-}159}$ homozygous animals.

Total RNA was isolated from the brains of GPRA$^{-/-}$ and GPRA$^{+/+}$ mice by phenol/chloroform extraction using RNABee (Tel-test) as instructed by the manufacturer. For northern blot analysis, 20 μg of total RNA was electrophoresed on a 1.1% formaldehyde, 1.2% agarose gel and transferred to an Immobilon-NC nitrocellulose membrane (Millipore Corp.). After transfer, the filters were hybridized with a full-length α[^{32}P]-dCTP random-labeled *Npsr1/Gpra* cDNA probe in Quick-Hyb (Stratagene) for 1 hour at 68°C. The mRNA from the GPRA$^{-/-}$ animals was also used to generate cDNA by reverse transcriptase PCR, using the primers TGGGAAACTCTGTTGTGCTG (forward) and GAGATGAGCCCTC GGTTGTA (reverse). The resultant cDNA product was cloned into the TA Cloning Vector pCR®2.1 (Invitrogen, Carlsbad, CA). Subsequent sequencing verified the formation of a splice variant lacking exons 3 and 4.

Measurement of Airway Reactivity in Conscious Mice

Airway reactivity was assessed by evaluating enhanced pause (Penh) at baseline and after increasing doses of methacholine (MCh). The Penh calculation is based on inspiratory pressure, expiratory pressure, and expiratory time, and its use as a measure of airway reactivity has been previously validated (11). Spontaneously breathing, unrestrained, conscious, mice were placed in a Biosystem XA whole body plethysmograph (Buxco Electronics, Troy, NY). Animals were placed in individual 80 ml chambers, and each chamber was ventilated by bias airflow at 0.2 liters/min. Baseline Penh was assessed for 5 minutes followed by a 2 minute aerosolization of vehicle (PBS) and increasing doses of MCh (12, 25 and 50 mg/ml) (Sigma-Aldrich, St. Louis, MO). The response for each aerosol challenge was assessed for 2 minutes.

Measurement of Airway Reactivity in Intubated Mice

Mice were anesthetized with 70-90 mg/kg pentobarbital sodium (American Pharmaceutical Partners, Los Angeles, CA), tracheostomized, and mechanically ventilated at a rate of 300 breaths/min, tidal volume of 6 cc/kg, and positive end-expiratory pressure of 3-4 cm H_2O with a computer controlled small-animal ventilator (Scireq, Montreal, Canada). Once ventilated, mice were paralyzed with 0.8 mg/kg pancuronium bromide. Following baseline assessments, mice were exposed to aerosol challenges by directing the inspiratory line through the aerosolization chamber of an ultrasonic nebulizer connected through a sideport in the ventilator circuit. Animals were ventilated at a rate of 200 breaths/min for 30 seconds with a tidal volume of 0.15 mls. Immediately following the aerosol challenge, the nebulizer was isolated from the inspiratory circuit and the original mechanical ventilation

was resumed. Forced Oscillatory Mechanics (FOM) were determined every 10 seconds for the following 3 minutes. Briefly, following passive expiration, a broadband (1-19.625 Hz) volume perturbation was applied to the lungs while the pressure required to generate the perturbations was assessed. The resultant pressure and flow data were fit into a constant phase model as previously described (12). Similar to other studies assessing forced oscillatory mechanics, we confined our analysis to: R_{aw} (Rn; Newtonian resistance), which assesses the flow resistance of the conducting airways; G (tissue damping), which reflects tissue resistance; and H (tissue elastance), which reflects the tissue rigidity (33).

Induction and Assessment of Allergic Airway Inflammation

To assess ovalbumin (OVA) induced airway inflammation, groups of mice were sensitized by i.p. injection of 20 μg of OVA (Grade V; Sigma) emulsified in 2.25 mg of aluminum hydroxide (Sigma) in a total volume of 200 μl, on days 1 and 14. Mice were challenged (45 min) via the airways with OVA (1% in saline) for 5 days (days 21 – 25) using an ultrasonic nebulizer (DeVillbiss Health Care, Somerset, PA). Control mouse groups received the two OVA immunizations but were challenged with aerosolized saline. Airway reactivity was assessed 24 hours after the final aerosol OVA or saline challenge (day 26).

Following airway assessments, mice were euthanized, and approximately 1 ml of blood was collected by cardiac puncture. Blood was allowed to coagulate, and the serum was collected. Total IgE levels were determined by ELISA (ICN Biomedicals, OH). Bronchoalveolar lavage (BAL) was performed 5 times with 1.0 ml of sterile Hank's Buffered Saline Solution (HBSS) each time. The number of cells present in the BALF was determined using a hemacytometer. A differential cell count was conducted on a cytospin prepared from

150 µl of BAL fluid and stained with either fast green and neutral red or Diff-Quik solution (Sigma). The remaining BAL fluid was centrifuged to remove cells, and the IL-13 level in the supernatant was determined using ELISA (R&D Systems, MN).

For histopathologic examination, lungs were fixed by inflation (20 cm pressure) and immersion in 10% formalin. To evaluate airway eosinophilia, fixed lung slices were subjected to hematoxylin and eosin (H & E) staining. To assess goblet cell hyperplasia, serial sections of the left lobes of the lungs that yield maximum longitudinal visualization of the intrapulmonary main axial airway were analyzed following Alcian-blue/periodic acid-schiff reaction (PAS) staining. To avoid bias for a certain region, and to consistently view the identical region in all slides, a 2-mm length of airway, located midway along the length of the main axial airway, was digitally imaged. Using ImageJ software (NIH, National Technical Information Service, Springfield, VA), the area and length of the PAS/AB-stained region in the sections were measured and the data expressed as the mean volume density (V_s = nl/mm^2 basal lamina $\pm$ SEM of PAS/AB-stained material within the epithelium) as previously described (18).

Induction and Assessment of LPS Induced Acute Airway Inflammation

To assess lipopolysaccharide (LPS) induced airway inflammation, groups of mice were anesthetized by isoflurane inhalation, and lipopolysaccharide (LPS)(Sigma) isolated from *Escherichia coli* (sterile serotype 0111:B4) was instilled intratracheally (i.t.) as previously described (32). Control mouse groups received an i.t. dose of saline. Rectal temperatures and baseline Penh were assessed every 4 hours following LPS administration and were utilized as surrogate markers of inflammation. Cohorts of mice were euthanized 18 to 24

hours post LPS exposure, and BALF was collected as described above. Total cell counts were determined and differential staining was conducted as described above. The leukocyte composition of the BALF was determined based on morphological criteria.

Passive Airway Anaphylaxis

Mice were sensitized by intravenous (i.v.) injection with 20 μg of human monoclonal anti-dinitrophenyl (DNP) IgE (Sigma) in 200 μl of sterile PBS. Twenty-four hours after anti-DNP IgE injection, mice were anesthetized, tracheostomized, and mechanically ventilated as previously described. Baseline airway mechanics were assessed for 2 minutes, and passive systemic anaphylaxis was induced via i.v. injection of human DNP-albumin (Sigma) in 250 μl of sterile PBS. Immediately following anaphylaxis induction, airway resistance (R_{aw}) was assessed for 3 minutes. Control mice received either an IgE injection and no DNP-albumin or DNP-albumin and no IgE. Age and sex matched mast cell deficient mice ($Kit^{W\text{-}sh}/Kit^{W\text{-}sh}$, The Jackson Laboratory) were used to confirm mast cell participation in this assay.

NPSR1/GPRA Expression Analysis

Total RNA was isolated from various tissues and cells, including the lungs from naïve and ovalbumin challenged mice (see OVA protocol above), various human cell lines, and primary cells derived from the airways. Samples of epithelial/fibroblast cells from asthmatic and control airways were generated from lung biopsies as previously described (25) and generously provided by F. Goulet, Laval University, Quebec, Canada. *Npsr1/Gpra* expression was analyzed by northern blot, as described above, or by quantitative RT-PCR

(TaqMan) using commercially available primer sets. Total RNA was purified via a Qiaprep RNeasy Kit (Qiagen) and the quality of the RNA was evaluated with an Agilent 2100 Bioanalyzer. 5-10 μg of RNA was reverse transcribed using the High-Capacity cDNA Archive Kit (Applied Biosystems) according to the manufacturer's instructions. cDNA was amplified with Taqman PCR Universal Master Mix (Applied Biosystems) using the Applied Biosystems 7900 HT Fast Real-Time PCR System. All samples were run in quadruplicate and relative expression was determined by normalizing samples to *β-actin*, *18S rRNA, GAPDH, β2M*, and *HPRT* housekeeping genes. *Muc5AC* expression was also assessed as described above in selected tissues. Data was analyzed using the comparative C_T method ($\Delta\Delta C_T$). All primer/probe sets were commercially available and obtained from Applied Biosystems. For human cells, RNA was isolated and *NPSR1/GPRA* expression quantified as described above, with the following exceptions. Cells or biopsy-derived samples were first lysed by addition of Trizol reagent (Gibco), and RNA was extracted according to manufacturer's instructions prior to purification using the Qiaprep Rneasy mini kit (Qiagen). Samples were run in duplicate and normalized to *GAPDH* expression.

Statistical Analysis

Data are presented as the means +/- standard error of the mean (SEM). A Random Effects Model followed by the Tukey-Kramer Honestly Significant Difference (HSD) was utilized to assess dose response data. Analysis Of Variance (ANOVA) followed by Tukey-Kramer HSD for multiple comparisons was performed on complex data sets. Statistical significance for single data points was assessed by the Student's two-tailed t-test. A p-value of less than 0.05 was considered statistically significant.

Results

Targeted disruption of the Gpra gene

NPSR1/GPRA is highly conserved: both the structure of the gene and the primary structure of the protein are highly similar between mice and humans. Previous data has demonstrated that an Asn107Ile polymorphism is found at higher frequency in the affected human population (20). However, in all the mouse genomes examined, including inbred and wild derived strains, the amino acid encoded at position 107 corresponds to Ile. Interestingly, this Ile is also present in the rat, dog, cow, and chimp *Npsr1/Gpra* genes. Thus, the gain-of-function mutation associated with asthma in humans is the common, if not the only allele present in other species. Therefore, mice express the form of NPSR1/GPRA associated with disease in humans. However, we reasoned that if a modest increase in activity of this receptor leads to enhanced disease in humans, complete loss of expression might attenuate disease in a mouse model of asthma.

A targeting vector was designed which would disrupt the normal expression of this gene (Figure 4.1A). Homologous recombination of the targeting plasmid with the endogenous gene removes the majority of exon 4 while leaving the splice acceptor site intact. Exon 4 encodes the majority of the 3rd transmembrane spanning domain and a portion of the i2 intracellular loop. Therefore, this deletion removes regions of the GPRA protein that are critical for ligand binding. A variety of studies have demonstrated that loss of the 3rd transmembrane domain of G-protein coupled receptors prevents ligand coupling and induces major conformational changes. Examination of the litters resulting from the intercross of heterozygous animals revealed the presence of animals homozygous for the mutant allele at expected frequencies (Figure 4.1B). Southern analysis of DNA prepared from tail biopsies

from these animals verified that the recombination event had resulted in the deletion of the majority of exon 4, as no hybridization was detected with a probe specific for this region of the *Npsr1/Gpra* gene. No gross anatomical or morphological differences were observed in GPRA deficient mice. GPRA deficient mice demonstrated normal blood cell composition and blood chemistry (Table E4.1). Analysis of leukocyte populations from the thymus, spleen, and lymph nodes with T cell, B cell, and macrophage markers revealed no aberrations in development of the immune system in the GPRA deficient animals (Figure E4.1).

To verify that the recombination event had indeed resulted in the alteration of the *Npsr1*/*Gpra* transcript, RNA was prepared from the brains of GPRA$^{-/-}$ and wild type animals and analyzed by northern blot (Figure 4.1C). The *Npsr1/Gpra* mRNA present in preparations from GPRA$^{-/-}$ animals is of lower molecular weight, but similar in abundance, to the native mRNA present in wild type mice (Figure 4.1C). To verify that the RNA transcript from the GPRA deficient mice lacks the coding information included in the region of the gene lost during the homologous recombination event, cDNA was prepared from the control animals and mice homozygous for the mutation. The region of the transcript extending from exon 2 to exon 5 was then amplified, cloned, and sequenced. This analysis indicated that the transcript present in the mutant animals consisted of a splice variant lacking exons 3 and 4. Because the mouse codon orthologous to isoleucine 107 is located in exon 3 of the mouse gene, an additional consequence of this splice variant formation is the loss of this codon in the mutant mice. This splice variant has recently been identified in a human lung epithelial carcinoma cell line (NCI-H358) and was termed GPRA-F (AY310332)(33). Transfection of this transcript into COS1 cells yielded a protein; however, analysis of these transfected cells showed that GPRA-F failed to properly integrate into the cell membrane and is not a

functional GPCR (35). We therefore refer to the mice homozygous for the mutant allele as GPRA$^{-/-}$ mice.

Airway mechanics in naïve GPRA$^{-/-}$ mice after exposure to bronchoconstricting agents

Previous studies reported that GPRA was expressed by airway smooth muscle cells (20). These studies also suggested that the expression of the Asn107Ile variant by these cells contributes to the pathogenesis of asthma (20). To begin to test this hypothesis, we determined the impact of complete loss of functional GPRA on basal airflow and basal airway mechanics. In addition, we determined if loss of GPRA modulates the changes in breathing patterns or airway mechanics observed upon exposure to bronchoconstricting agents such as methacholine (MCh). We also determined whether bronchoconstriction observed after passive anaphylaxis is altered in mice lacking functional NPSR1/GPRA.

Breathing patterns of wild type and NPSR1/GPRA deficient mice were analyzed by whole body plethysmography (WBP). Studies were carried out using wild type and GPRA$^{-/-}$ mice on three different genetic backgrounds. The first group of animals analyzed consisted of 129/SvEv mice and co-isogenic GPRA$^{-/-}$ animals. In addition, GPRA$^{-/-}$ mice and wild type littermates were generated after the backcross of the mutation onto the C57BL/6 and BALB/c genetic backgrounds for three generations. No difference in baseline Penh was observed in any of the GPRA deficient populations, and methacholine elicited a similar increase in Penh in the GPRA deficient mice compared to their genetically matched controls (Figure E4.2 A, B, and C; respectively).

We next determined if changes in airway mechanics could be observed in naïve GPRA$^{-/-}$ mice. For this analysis, we utilized a computer-controlled small animal ventilator,

highly sensitive pressure transducers, and software (Flexivent) to record airway opening pressures, volume, and airflow. Changes in lung mechanics were determined using the constant phase model. Three different parameters were compared: airway resistance (R_{aw}), tissue resistance (G), and tissue elastance (H). No difference in these parameters was observed between 129/SvEv and co-isogenic $GPRA^{-/-}$ naïve unchallenged mice (Figure 4.2). Exposure of the mice to MCh resulted in an increase in all three parameters, in particular, airway and tissue resistance. The magnitude of these changes did not differ significantly between the wild type and mutant mouse lines. Similar studies comparing $GPRA^{-/-}$ BALB/c and C57BL/6 mice to their respective genetically matched controls also failed to identify a role for NPSR1/GPRA in changes in lung mechanics in response to methacholine (data not shown). Exposure of the mice to serotonin (5-HT) also resulted in an increase in R_{aw}, G, and H. However, similar to the MCh responses, the magnitude of these changes did not differ significantly between the wild type and mutant mouse lines (data not shown).

Activation of mast cells by IgE and antigen results in release of potent bronchoconstricting agents including leukotrienes, prostaglandins, serotonin, and histamine. As these mediators contribute to the reversible airway obstruction characteristic of asthma, it was of interest to determine whether loss of GPRA altered the changes in lung mechanics measured after mast cell degranulation (Figure 4.3). Passive anaphylaxis was induced in $GPRA^{-/-}$ 129/SvEv mice and in co-isogenic controls by injection of animals with monoclonal antibody to DNP. Twenty-four hours later, mice were anesthetized, tracheostomized, and mechanically ventilated. After establishment of baseline airway mechanics, mice received antigen (DNP) i.v., and the change in airway mechanics was measured. Passive anaphylaxis resulted in a large increase in airway resistance (R_{aw}) (Figure 4.3A). A robust increase in R_{aw}

was also observed in the GPRA deficient mice, but the magnitude of this change did not differ from the co-isogenic control animals. A smaller change in tissue resistance (G) and elastance (H) is observed after induction of passive anaphylaxis (data not shown). Again, no difference was observed in these parameters between $GPRA^{-/-}$ and control animals. As expected, the airway mechanics of mice that received either antibody or antigen alone did not change significantly from baseline (Figure 4.3A), nor was there a significant change in lung mechanics observed upon treatment of mast cell deficient $Kit^{W\text{-}sh}/Kit^{W\text{-}sh}$ mice with antigen and antibody (Figure 4.3B).

GPRA deficient mice demonstrate normal allergic airway inflammation responses

Sensitization of mice with ovalbumin followed by exposure of the animals to aerosols of antigen results in development of lung inflammation, which models some aspects of asthma. GPRA expression in the lung was reported to increase 7 fold after induction of a similar model of allergic lung disease (20). It was therefore reasonable to assume that functions of GPRA in the lung might be highlighted in animals with this disease. Allergic lung disease was induced in 129/SvEv and co-isogenic $GPRA^{-/-}$ mice, and the development of inflammation and changes in airway mechanics were assessed in the two groups twenty-four hours after the final exposure to antigen (Figure 4.4).

The total number of cells present in the BALF was significantly increased in both the wild type and $GPRA^{-/-}$ mice following OVA challenge. However, no significant difference was noted between the wild type and $GPRA^{-/-}$ mice (Figure 4.4A). Furthermore, no difference could be identified in the total leukocyte composition of the BALF assessed by morphological criteria (data not shown). IL-13 levels are increased in the BALF after

induction of allergic airway disease and are critical to the development of AHR and goblet cell metaplasia/hyperplasia. IL-13 levels were assessed via ELISA in BALF collected from OVA immunized and either OVA or saline challenged animals (Figure 4.4B). A significant increase in IL-13 was observed in OVA immunized/OVA challenged mice, irrespective of the genotype of the mice (Figure 4.4B).

Histological and morphometric assessment of the lungs of mice that were sensitized and exposed to antigen revealed similar increases in the number of goblet cells in GPRA deficient and wild type mice (Figure 4.4D). As expected, few PAS+ cells were observed in the OVA immunized/saline challenged mice (data not shown). In mouse models of asthma, the induction of pulmonary *Muc5ac* gene expression correlates with goblet cell hyperplasia/metaplasia and the increased production of airway mucus. To further evaluate mucus production in GPRA deficient mice, *Muc5ac* expression was assessed by quantitative rt-PCR (TaqMan) on RNA prepared from the lungs of OVA and saline challenged animals (Figure 4.4E). A significant increase in *Muc5ac* expression was observed in OVA immunized/OVA challenged mice, irrespective of genotype (Figure 4.4E). However, again no difference was observed between the wild type and GPRA deficient mice. As expected, no increase in *Muc5ac* expression was observed in OVA immunized/saline challenged mice (Figure 4.4E).

In addition to finding an association between GPRA and the asthmatic phenotype, recent studies have also suggested an association between polymorphisms in GPRA and elevated serum IgE levels (18, 20, 23). Increased serum IgE is observed in the OVA model of allergic lung disease and, not surprisingly, the IgE is specific for ovalbumin. Total IgE levels were assessed via ELISA in serum collected from OVA immunized and either OVA or

saline challenged animals (Figure 4.4C). As expected, a significant increase in total IgE was observed in OVA immunized/OVA challenged mice; however, the magnitude of this increase was not significantly different in the GPRA$^{-/-}$ animals (Figure 4.4C).

NPSR1/GPRA deficiency has no effect on the induction of airway hyperresponsiveness (AHR) in the OVA model of allergic airway disease

As discussed above, no difference was observed in the airway mechanics of the naïve NPSR1/GPRA mice in response to constricting agents such as methacholine (Figure 4.2) and serotonin (data not shown). In addition, the increase in airway resistance during passive anaphylaxis was not affected by the absence of functional NPSR1/GPRA (Figure 4.3). However, it is possible that contribution of this protein to airway physiology becomes apparent only in the inflamed lung. We therefore examined baseline airway mechanics and the change in airway mechanics in response to methacholine in 129/SvEv mice and co-isogenic GPRA$^{-/-}$ animals after induction of allergic airway disease (Figure 4.4, F-H). None of the three described parameters, airway resistance (R_{aw}), tissue or distal lung resistance (G), or elastance (H) differed between the GPRA$^{-/-}$ animals and similarly treated controls.

GPRA deficient mice demonstrate normal inflammatory responses in an LPS mediated acute model of airway inflammation

Endotoxin, a constituent of gram-negative bacteria, and its functional derivative lipopolysaccharide (LPS), are ubiquitous in the environment and particularly concentrated in several occupational, industrial, and domestic settings. Several lines of evidence suggest that inhalation of LPS causes an inflammatory response and increases airway reactivity in

asthmatics. This raises the possibility that GPRA could contribute indirectly to the development of asthma by altering the sensitivity of individuals to other immunological stimuli in the lung such as LPS. $GPRA^{-/-}$ mice and co-isogenic 129 controls were treated with 50 μg of LPS i.t., and the resultant changes in body temperature, breathing patterns (Penh), and inflammation were monitored. Control animals of both genotypes were treated with vehicle. Previous studies indicated that maximum changes in these three parameters are observed in 129 mice sixteen to twenty hours after exposure to LPS. As seen in Figure 4.5A and B, administration of LPS induced a dramatic drop in body temperature and a significant increase in baseline Penh, irrespective of genotype. LPS exposure results in recruitment of neutrophils to the lung. No significant difference was observed in either the number or composition of cells present in the BALF as assessed by morphological criteria (Figure 4.5C).

GPRA is highly expressed in the CNS with only minimal airway expression

The inability to discern changes in airway mechanics and in the development of allergic lung disease in GPRA deficient mice was surprising given the high levels of GPRA expression reported in the lung and the elevation in GPRA expression in this model of asthma. It was therefore of interest to reexamine this finding and verify that this was indeed the case in co-isogenic mice on the 129 genetic background, which were utilized in the majority of our experiments. The $2^{-\Delta\Delta Ct}$ method was used for analysis of expression of NPSR1 after induction of allergic lung disease. ΔCt is defined as the difference between the threshold cycle (Ct) of the gene of interest and the internal reference (housekeeping) gene of choice. Internal reference genes are genes whose expression is not expected to change as a

result of the experimental manipulation, such as the induction of allergic lung disease. Because their expression remains constant, internal references can be used to normalize expression of the gene of interest, NPSR1. This normalization corrects for differences in NPSR1 expression in the allergic lung that might be due to slight variations in quality or quantity of RNA between preparations. Before initiating these studies, we first tested a number of commonly used internal reference (housekeeping) genes to determine their suitability for examination of changes of gene expression in the lung after induction of allergic lung disease. To do this, we examined the number of cycles required to detect expression (fluorescence above background) of the gene in the healthy and inflamed lung (threshold cycle; Ct). We found that after approximately 20 cycles, *β-actin* expression was detected in the healthy lung. However, when RNA was prepared from the inflamed tissue, *β-actin* mRNA was less abundant and over 30 cycles were required to detect expression (Ct = 30) (Figure 4.6A). The lower abundance of the *β-actin* mRNA could reflect changes in cells of the lung or the fact that much of the RNA present in the inflamed lung is derived from infiltrating leukocytes. Regardless, this change in Ct made *β-actin* an inappropriate internal reference gene when comparing healthy and inflamed lungs. Likewise, increased threshold cycles (Ct) for *gapdh*, *hprt*, and *β2M* were also observed in the inflamed lung, and use of these housekeeping genes would, therefore, overestimate increases of the test gene expression. We found that 18S ribosomal RNA was the only RNA whose expression itself did not significantly change after induction of allergic airway disease (Figure 4.6A). To our surprise, the levels of *Gpra* expressed in the naïve lungs were extremely low and these levels did not increase in the inflamed lung when 18s was used to normalize expression (Figure 4.6B). To reconcile this with previous reports, we next determined whether use of other

internal reference genes could lead to the supposition that expression of GPRA is increased in the inflamed mouse lung. When other housekeeping genes were utilized in the analysis, such as *β-actin*, there was no difficulty in reporting an increase in *Npsr1/Gpra* expression in the lungs of mice with allergic airway disease (Figure 4.6C). To verify that our primer sets were appropriate for the analysis, we examined other tissues, including various regions of the brain and the retina. The relative levels of expression of *GPRA* in these tissues mimicked those reported by Xu *et al.* during an extensive evaluation of the expression of NPSR1 in the mouse (37). Thus, the primers and conditions used in the studies detect differences in *GPRA* expression between various tissues. While the results shown in Figure 6 were obtained using mice on the 129 genetic background subjected to the OVA-challenge model described herein, we also failed to observe an upregulation of the *GPRA* gene and ligand (NPS) in BALB/c mice subjected to OVA- and IL-13-challenge models of asthma in which robust inflammation, mucus, and airway hyperreactivity endpoints were observed (data not shown).

GPRA is expressed in retina and hypothalamus, but not in human lung cells

Our expression analysis fails to support the expression of substantial levels of *GPRA* in the mouse lung or the previously reported increase in this expression after induction of allergic lung disease. It was therefore of interest to reexamine the expression of NPSR1/GPRA in humans, since expression in humans but not in the mouse would simply suggest that the mouse is not the appropriate model for studying the contribution of this gene to asthma. Initial reports indicated that this GPCR is expressed in both epithelial cells and airway smooth muscle cells in the lung (20, 35). Analysis of human airway-derived cell lines and primary cells by quantitative PCR failed to detect significant levels of GPRA mRNA in various epithelial (A549, H292,

NHBE), smooth muscle (BSMC) and fibroblast (MRC5, HFL1, NHLF) cell lines and primary cells, with the exception of one out of three samples of NHBE cells which showed low but significant expression. In contrast, significant GPRA expression was observed in commercial brain, retina, and hypothalamus cDNA libraries (Figure 4.6D). As additional controls, we observed high levels of GPRA mRNA in GPRA-A and GPRA-B-transfected CHO cells (not shown), ruling out the possibility that the probe and primers used for quantitative PCR in this study are specific to only one of the two GPRA isoforms. Since the possibility exists that expression of this GPCR is upregulated only in lungs of asthmatics, we also examined mRNA levels in cells derived from lung biopsies (graciously provided by F. Goulet, Laval University, Quebec, Canada) from both normal controls (n=4) and asthmatics (n=8). These samples, containing epithelial cells and fibroblasts, were prepared as previously described (25). Again, there was no significant expression of GPRA in either normal or asthmatic lung, with the exception of two of the normal samples that contained significant but very low mRNA levels (Figure 4.6D). These data are in contradiction with previous findings (35) showing not only that GPRA expression is increased in asthmatics but also that the GPRA-B isoform is ubiquitously expressed in a variety of tissues and cell lines.

GPRA may participate in an indirect, neurally mediated mechanism of smooth muscle constriction

High levels of NPSR1/GPRA are expressed in the brain and by neuronal cell lines. This raises the interesting possibility that the linkage of the polymorphism in the NPSR1/GPRA receptor to asthma reflects a contribution of the nervous system, perhaps through cholinergic pathways, to the development of asthma. To begin to address this

possibility, we examined the change in airway responsiveness of the 129/SvEv GPRA$^{-/-}$ mice and their genetic controls to thromboxane. Previous studies have demonstrated that the increase in airway and tissue resistance in the mouse in response to this agent is dependent on an intact cholinergic pathway (2). As seen in Figure 7, we assessed changes in airway reactivity utilizing forced oscillatory mechanics (FOM) in the co-isogenic 129Sv/Ev mice. As described previously, mice were subjected to aerosolized vehicle (data not shown), followed by dose response challenges of U46619 (10^{-5} – 10^{-3} M). U46619 challenge induced a robust increase in airway reactivity, regardless of genotype (Figure 4.7). Increasing doses of U46619 generated equivalent increases in G and H (Figures 4.7B and C); however, GPRA deficient mice demonstrated a modest but significant attenuation in R_{aw} at the highest concentration of U46619 tested (10^{-3} M)(Figure 4.7A). This decrease in the R_{aw} response and lack of differences in either G or H following U46619 challenge is interesting because it suggests a role for GPRA in mediating vagal nerve responses in the conducting airways. In the mouse, airway innervation is higher in the conducting airways and significantly decreases towards the peripheral airways. Thus, these combined data suggest a potential role for GPRA in indirect mechanisms affecting airway smooth muscle constriction.

Figure 4.1
A

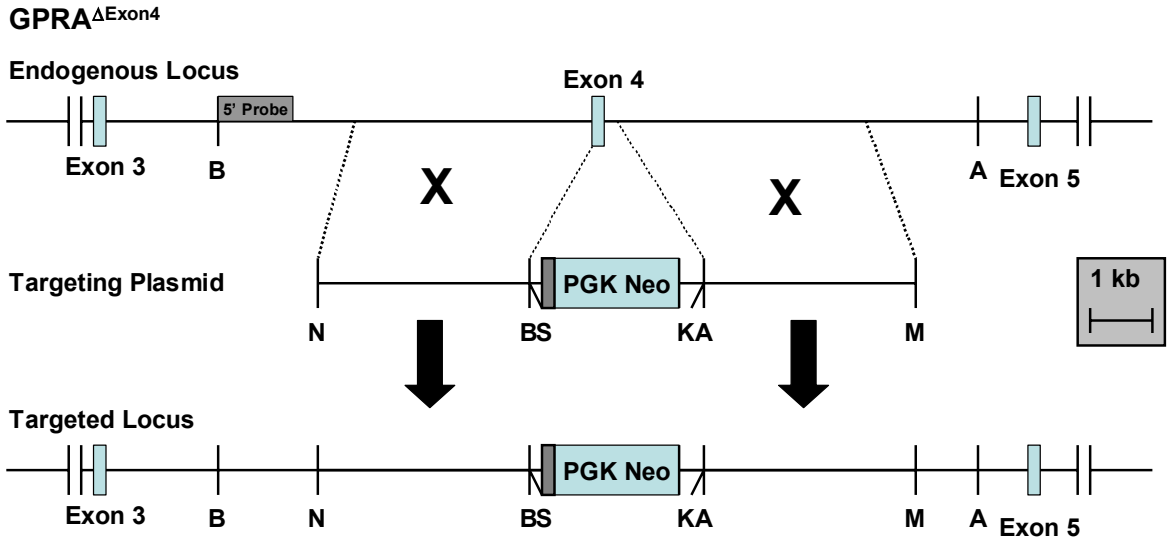

B

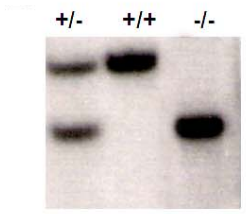

C

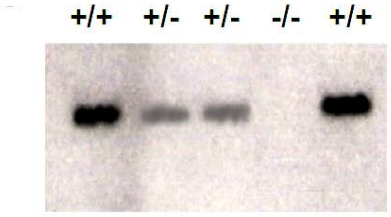

D

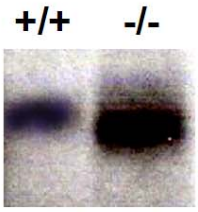

E

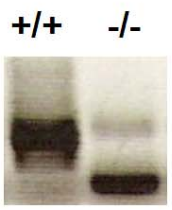

Figure 4.1. Generation of a mouse line with a deletion in the *Gpra* gene. (A) Restriction maps of the endogenous *Gpra* locus, the *Gpra* targeting construct, and the targeted locus after homologous recombination with the targeting plasmid. Upon homologous recombination, the *GPRA*$^{\Delta 94\text{-}159}$ construct replaces a 744 bp region of the *Gpra* gene, which includes the majority of exon 4, with the selectable marker gene neomycin (neo). This deletion is predicted to remove the 3rd transmembrane domain and second exoloop of the G-protein coupled receptor. Relevant restriction sites are abbreviated as follows: B, BamHI; N, NotI; S, SalI; K, KpnI; A, ApaI; M, MfeI. **(B)** Southern blot analyses of offspring generated by the intercross of mice heterozygous for the *Gpra* mutant allele. A 521 bp genomic fragment that hybridizes upstream of the targeted region was used as a probe to detect the change in BamHI restriction fragment length that occurs with proper integration of the targeting construct. **(C)** Southern blot analysis of the *GPRA*$^{\Delta 94\text{-}159}$ mice to confirm the deletion of the desired region. A 631 bp genomic fragment that includes exon 4 was used as a probe to confirm the loss of this region in the *GPRA*$^{\Delta 94\text{-}159}$ homozygous animals. **(D)** Northern analysis of *Gpra* expression in the brains of wild type and *GPRA*$^{\Delta 94\text{-}159}$ homozygous animals. Abundant *Gpra* RNA is observed in wild type mice, whereas a smaller *Gpra* transcript resulting from the deletion of exon 4 is seen in RNA prepared from *GPRA*$^{\Delta 94\text{-}159}$ mice. Analysis with a Cyclooxygenase 2 specific probe indicates equal RNA sample loading (not shown). **(E)** Analysis of the truncated *Gpra* mRNA expressed by the *GPRA*$^{\Delta 94\text{-}159}$ animals by rt-PCR. rt-PCR of RNA from wild type animals yields a fragment of 604 bp, whereas a fragment of approximately 406 bp was amplified from the homozygous mutant cDNAs. Subsequent cloning and sequencing of the resultant cDNA from the

GPRA$^{\Delta 94\text{-}159}$ animals confirmed that an alternative splicing event joining exon 2 to exon 5 has occurred. If transcribed, this would encode a protein lacking exons 3 and 4.

Figure 4.2

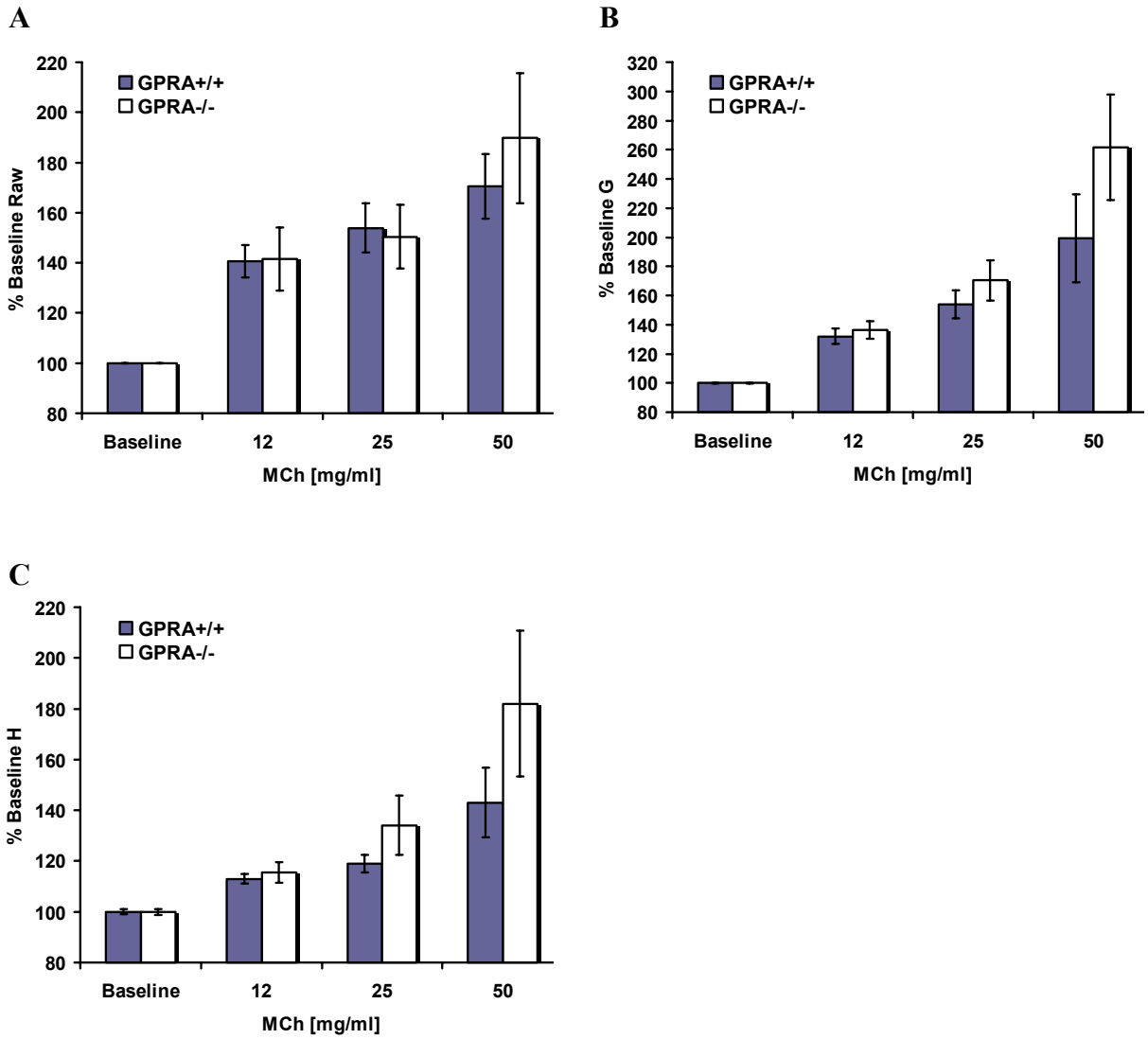
A
GPRA+/+
GPRA-/-
% Baseline Raw
220
200
180
160
140
120
100
80
Baseline
12
25
50
MCh [mg/ml]
B
GPRA+/+
GPRA-/-
% Baseline G
320
300
280
260
240
220
200
180
160
140
120
100
80
Baseline
12
25
50
MCh [mg/ml]
C
GPRA+/+
GPRA-/-
% Baseline H
220
200
180
160
140
120
100
80
Baseline
12
25
50
MCh [mg/ml]

Figure 4.2. Changes in airway physiology of wild type and GPRA$^{-/-}$ mice in response to methacholine. **(A)** Airway resistance (R_{aw}), **(B)** tissue damping (G), and **(C)** tissue elastance (H) were assessed in 129/SvEv co-isogenic wild type and GPRA$^{-/-}$ mice in response to MCh. The percent change in R_{aw}, G, and H from baseline increased significantly in all animals, regardless of genotype. GPRA$^{+/+}$ mice, n=15; GPRA$^{-/-}$ mice, n=9.

Figure 4.3

A

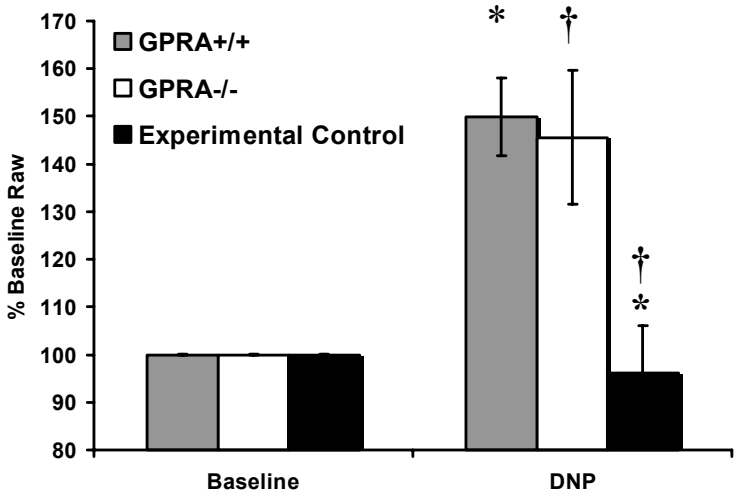
GPRA+/+
GPRA-/-
Experimental Control
% Baseline Raw
170
160
150
140
130
120
110
100
90
80
Baseline
DNP

B

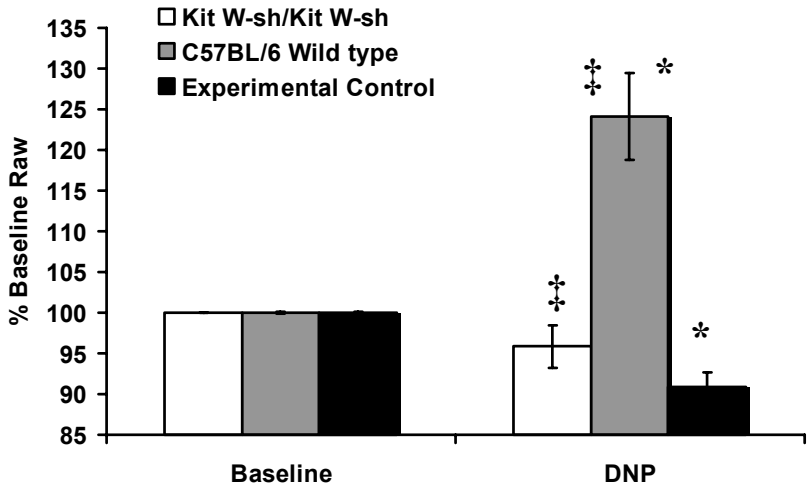
Kit W-sh/Kit W-sh
C57BL/6 Wild type
Experimental Control
% Baseline Raw
135
130
125
120
115
110
105
100
95
90
85
Baseline
DNP

Figure 4.3. Mast cell mediated airway anaphylaxis in wild type and GPRA$^{-/-}$ mice. Mast cell function and changes in R_{aw} in response to mast cell degranulation were assessed in a model of passive systemic anaphylaxis. **(A)** DNP administration caused a significant increase in R_{aw} in all mice regardless of genotype. No significant increases in either G or H were observed (data not shown). GPRA$^{+/+}$, n = 4; GPRA$^{-/-}$, n = 4; Experimental controls, n = 4 (*$p < 0.05$; †$p < 0.05$). **(B)** To confirm that this airway anaphylaxis is indeed an assay of mast cell function, mast cell deficient mice (Kit$^{W\text{-}sh}$/Kit$^{W\text{-}sh}$) were also assessed. The mast cell deficient mice failed to demonstrate an increase in R_{aw} in response to DNP administration. Mast Cell Deficient, n = 10; C57BL/6 Wild Type, n = 7; Experimental Controls, n = 2 (‡$p < 0.001$; *$p < 0.05$).

Figure 4.4

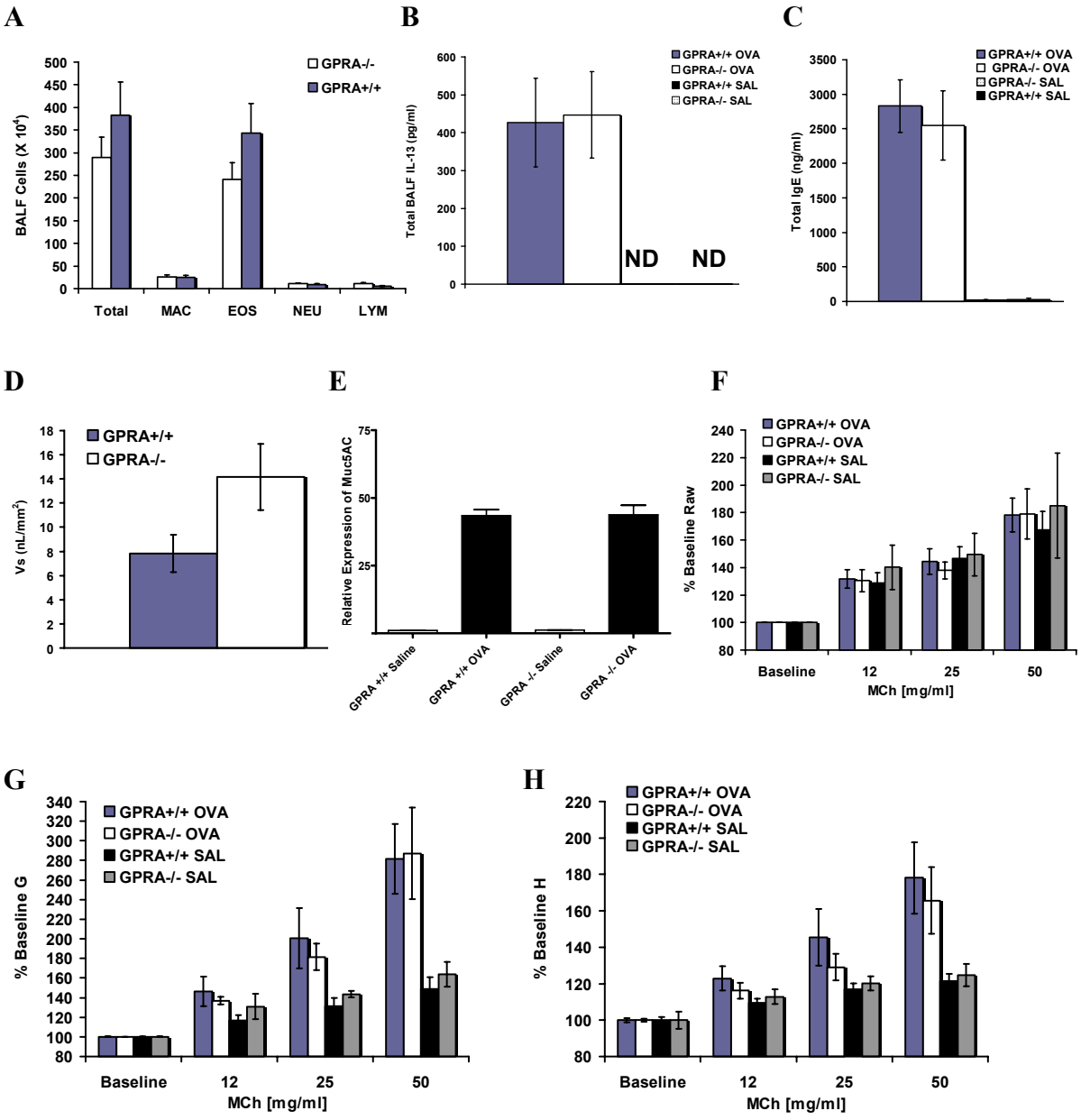
A
B
C
BALF Cells (X 10⁴)
GPRA-/-
GPRA+/+
Total
MAC
EOS
NEU
LYM
Total BALF IL-13 (pg/ml)
GPRA+/+ OVA
GPRA-/- OVA
GPRA+/+ SAL
GPRA-/- SAL
ND
ND
Total IgE (ng/ml)
D
E
F
Vs (nL/mm²)
Relative Expression of Muc5AC
GPRA +/+ Saline
GPRA +/+ OVA
GPRA -/- Saline
GPRA -/- OVA
% Baseline Raw
Baseline
12
25
50
MCh [mg/ml]
G
H
% Baseline G
% Baseline H

Figure 4.4. Allergic airway inflammation in wild type and GPRA$^{-/-}$ mice. Allergic lung disease was induced in 129/SvEv co-isogenic wild type and GPRA$^{-/-}$ mice. **(A)** Increases of similar magnitude were observed in the cellularity and composition of bronchoalveolar lavage fluid (BALF) between the OVA-challenged GPRA$^{-/-}$ and wild type mice. OVA GPRA$^{+/+}$, n = 16; OVA GPRA$^{-/-}$, n = 14; SAL GPRA$^{+/+}$, n = 9; SAL GPRA$^{-/-}$, n = 9. Histological scoring of H & E stained lung slices demonstrated a significant increase in inflammatory cells present in the lungs of OVA sensitized and challenged mice, regardless of genotype (data not shown). **(B)** A significant increase in total BALF IL-13 levels was detected following OVA sensitization and challenge, regardless of genotype. IL-13 levels from the OVA immunized/saline challenged mice were below the detection limits of this assay. OVA GPRA$^{+/+}$, n = 16; OVA GPRA$^{-/-}$, n = 14; SAL GPRA$^{+/+}$, n = 9; SAL GPRA$^{-/-}$, n = 9. **(C)** A significant increase in total serum IgE levels was detected following OVA sensitization and challenge, regardless of genotype. Total serum IgE levels failed to increase above baseline levels in the OVA sensitized/saline challenged mice, and no significant difference was detected between genotypes. No significant differences were observed between baseline total IgE levels in the serum of naïve GPRA$^{+/+}$ and GPRA$^{-/-}$ mice (data not shown). OVA GPRA$^{+/+}$, n = 16; OVA GPRA$^{-/-}$, n = 14; SAL GPRA$^{+/+}$, n = 9; SAL GPRA$^{-/-}$, n = 9. **(D)** Sections through the main bronchiole of the left lobe of the lung were stained with PAS/AB, and the volume of PAS/AB-stained mucosubstance per square millimeter of basal lamina (Vs) was determined. A significant increase in airway mucus production was observed in mice of both genotypes. No significant differences in mucus production were observed between GPRA$^{+/+}$ and GPRA$^{-/-}$ mice; however, a slightly larger increase was observed in the GPRA$^{-/-}$ mice ($p = 0.11$). OVA GPRA$^{+/+}$, n = 16; OVA GPRA$^{-/-}$, n = 14;

(saline data not shown). **(E)** A significant increase in *Muc5AC* expression was detected with no significant differences observed between GPRA$^{+/+}$ and GPRA$^{-/-}$ mice. Relative expression was determined by standardizing samples to the 18S housekeeping gene. OVA sensitized/saline challenged mice, n = 3/genotype; OVA sensitized/OVA challenged mice, n = 3/genotype. **(F-H)** The change in respiratory mechanics, assessed as R_{aw} **(F)**, G **(G)** and H **(H),** in intubated mice was determined in response to MCh for OVA immunized/OVA challenged and OVA immunized/saline challenged wild type and GPRA$^{-/-}$ mice. Dose dependent increases in R_{aw}, G, and H were observed in all mice, regardless of genotype. Wild type and GPRA$^{-/-}$ OVA immunized and challenged mice demonstrated an increase in airway hyperresponsiveness as determined by increased G and H. OVA GPRA$^{+/+}$, n = 16; OVA GPRA$^{-/-}$, n = 14; SAL GPRA$^{+/+}$, n = 5; SAL GPRA$^{-/-}$, n = 3.

Figure 4.5

A)

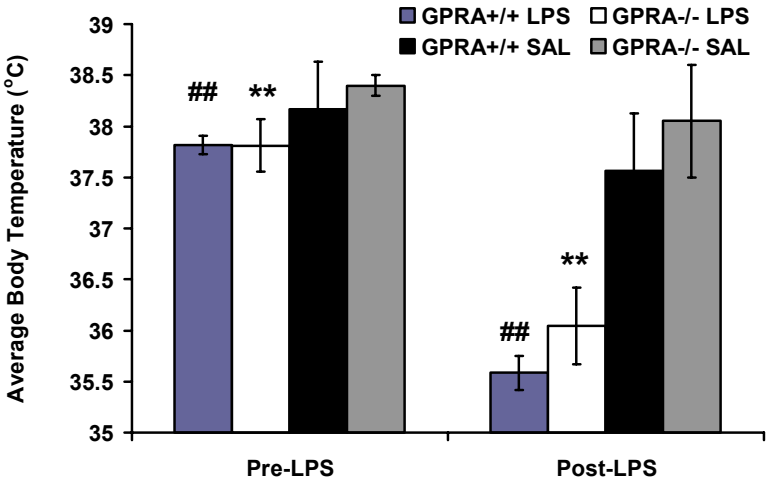

B)

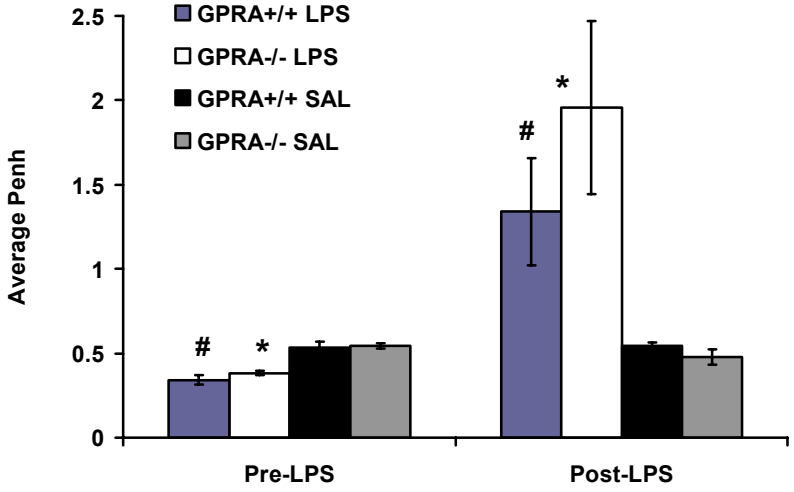

C)

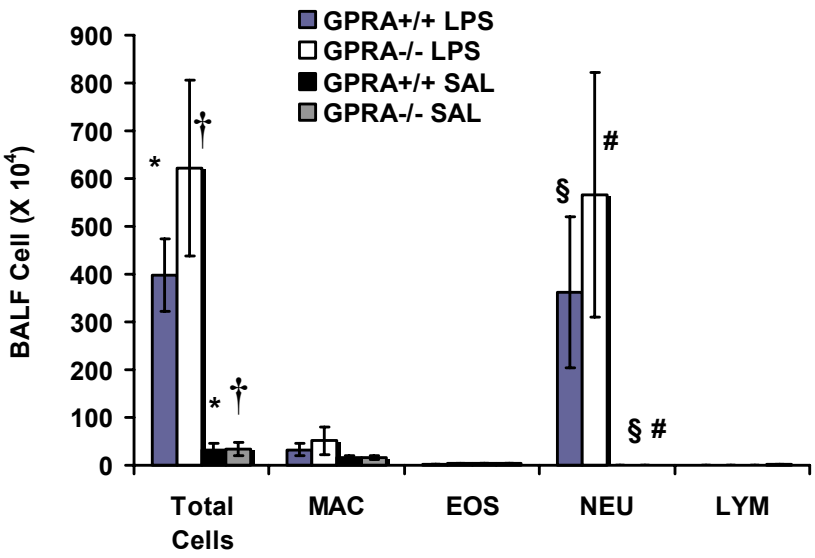

Figure 4.5. LPS mediated acute lung inflammation in wild type and GPRA$^{-/-}$ mice. Acute lung inflammation was induced in C57BL/6 wild type and GPRA$^{-/-}$ mice. Mice were challenged via intratracheal (i.t.) instillation with either LPS (1 mg/ml) or sterile saline. **(A)** LPS induced a significant drop in body temperature in both wild type and GPRA$^{-/-}$ mice. LPS GPRA$^{+/+}$, n = 14; LPS GPRA$^{-/-}$, n = 13; SAL GPRA$^{+/+}$, n = 3; SAL GPRA$^{-/-}$, n = 3 (**p < 0.005; ##p<0.005). **(B)** LPS induced a significant increase in baseline Penh in both wild type and GPRA$^{-/-}$ mice. LPS GPRA$^{+/+}$, n = 14; LPS GPRA$^{-/-}$, n = 13; SAL GPRA$^{+/+}$, n = 3; SAL GPRA$^{-/-}$, n = 3 (*p < 0.01; #p<0.01). **(C)** Increases of similar magnitude were observed in the cellularity and composition of bronchoalveolar lavage fluid (BALF) in LPS-challenged wild type and GPRA$^{-/-}$ mice. LPS GPRA$^{+/+}$, n = 11; LPS GPRA$^{-/-}$, n = 10; SAL GPRA$^{+/+}$, n = 3; SAL GPRA$^{-/-}$, n = 3 (*p < 0.05; §p < 0.05; †p <0.05; #p < 0.05).

Figure 4.6

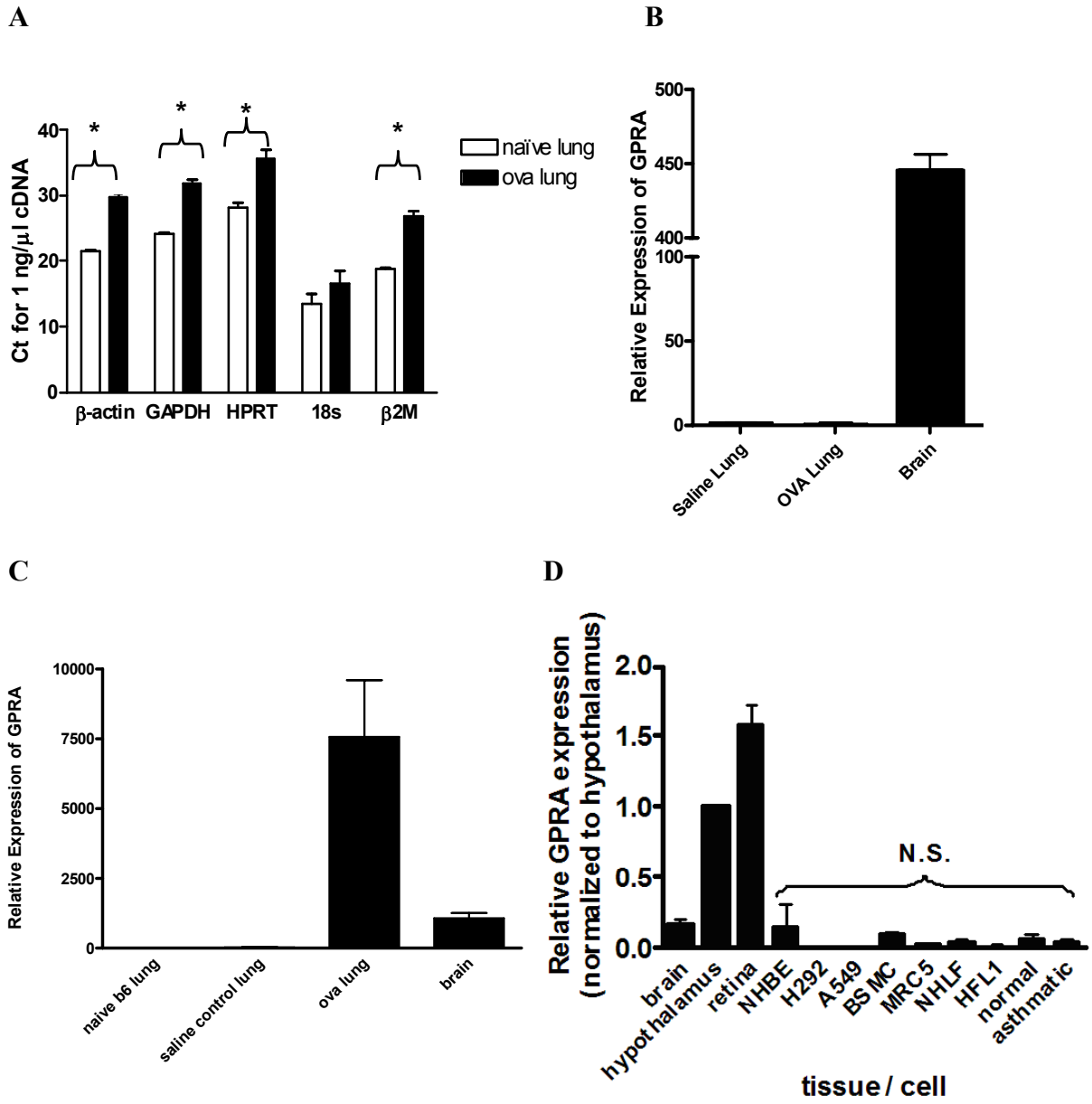
A
B
C
D
Ct for 1 ng/µl cDNA
naïve lung
ova lung
β-actin
GAPDH
HPRT
18s
β2M
Relative Expression of GPRA
Saline Lung
OVA Lung
Brain
naive b6 lung
saline control lung
ova lung
brain
Relative GPRA expression (normalized to hypothalamus)
N.S.
brain
hypothalamus
retina
NHBE
H292
A549
BS MC
MRC5
NHLF
HFL1
normal
asthmatic
tissue / cell

Figure 4.6. GPRA expression in human and mouse tissues. (A) A comparison of threshold cycles for common housekeeping genes used to normalize rt-PCR data. OVA inflammation significantly alters housekeeping gene expression. The 18S gene appeared to be the only appropriate housekeeping gene assessed for use in normalizing RT-PCR data from the inflamed lung (*$p<0.05$ compared to naïve lung). **(B)** No increase in *Gpra* transcript levels was detected following challenges with 1% Ovalbumin (OVA). Mice were sensitized to OVA and subjected to aerosol challenges with either OVA or saline. The lung and trachea were removed immediately following the final aerosol challenge and total RNA was extracted. *Gpra* expression was assessed by quantitative RT-PCR (TaqMan) using commercially available primer sets. Whole brains were removed from naïve animals to serve as positive controls for real time assessments. Relative expression was determined by standardizing samples to the 18S housekeeping gene. OVA sensitized/saline challenged mice, n = 3; OVA sensitized/OVA challenged mice, n = 3; naïve mice, n=3. **(C)** Analysis of *Gpra* expression assessed by quantitative RT-PCR and normalized with *β-actin*. **(D)** *GPRA* expression in human tissues and cells. Levels of *GPRA* cDNA were measured in cDNA libraries of brain, hypothalamus, or retina, or in various airway derived cells and cell lines following conversion of mRNA to cDNA using reverse transcriptase. *GPRA* levels were assessed by quantitative PCR (TaqMan) using commercially available primer sets. Relative expression was determined by standardizing samples to *GAPDH* levels and normalizing to a hypothalamus cDNA library. "Normal" and "asthmatic" refer to cells obtained from biopsies of non-asthmatic (n=4) and asthmatic (n=8) individuals, respectively. For the indicated cells and cell lines (labeled as "N.S."), the measured cycle thresholds were indistinguishable from those obtained in identical samples that had not been treated with reverse transcriptase, with

the exception of 1 of 3 NHBE samples and 2 out of 4 “normal” samples, for which very low but significant levels were detected. Each bar represents the mean ± S.D. of 2 to 8 independent samples. A representative experiment is shown.

Figure 4.7

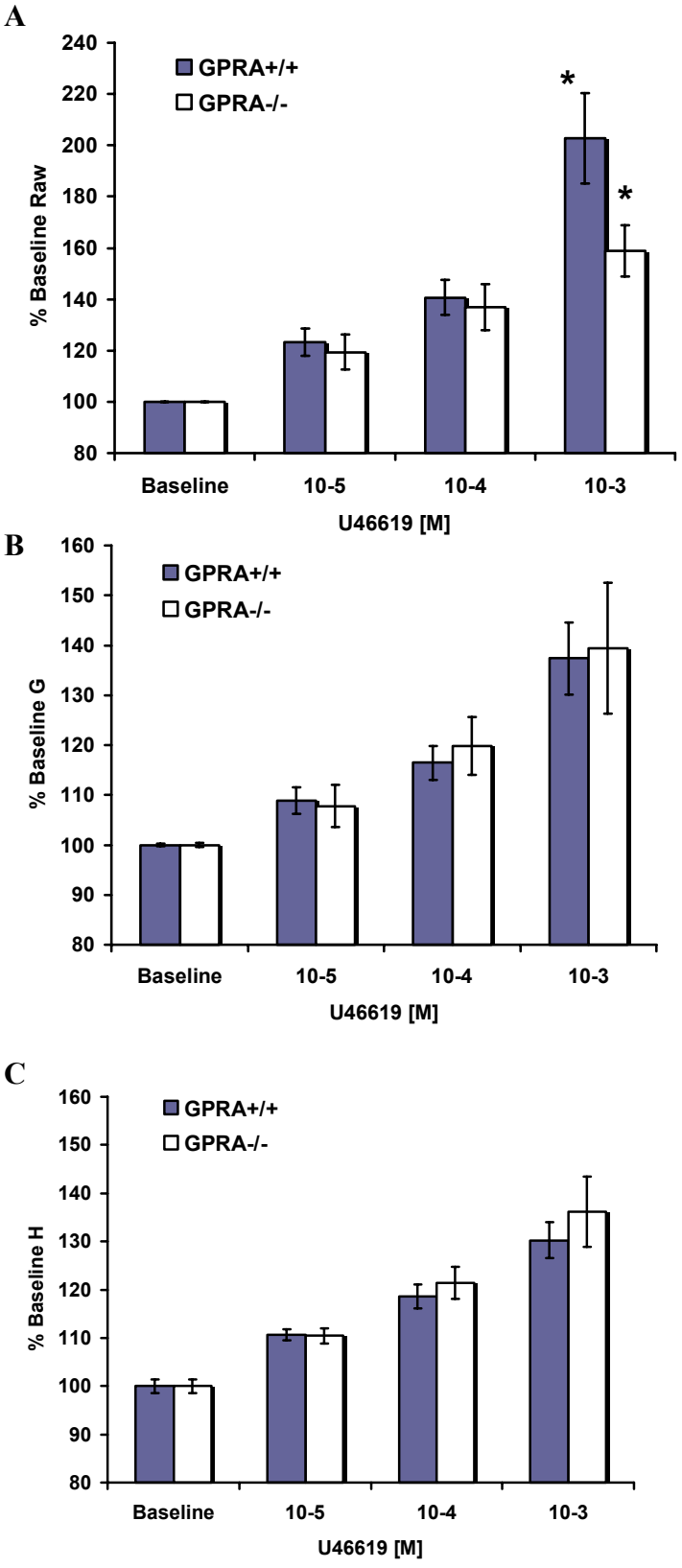
A
GPRA+/+
GPRA-/-
% Baseline Raw
240
220
200
180
160
140
120
100
80
*
*
Baseline
10-5
10-4
10-3
U46619 [M]
B
GPRA+/+
GPRA-/-
% Baseline G
160
150
140
130
120
110
100
90
80
Baseline
10-5
10-4
10-3
U46619 [M]
C
GPRA+/+
GPRA-/-
% Baseline H
160
150
140
130
120
110
100
90
80
Baseline
10-5
10-4
10-3
U46619 [M]

Figure 4.7. Changes in airway physiology of wild type and GPRA$^{-/-}$ mice in response to a thromboxane A2 analog (U46619). R_{aw} **(A)**, G **(B)**, and H **(C)** were assessed in wild type and GPRA$^{-/-}$ mice in response to U46619, which induces airway smooth muscle constriction through an indirect, neurally mediated mechanism. The percent change in R_{aw}, G, and H from baseline increased significantly in all animals, regardless of genotype. However, GPRA deficient mice demonstrated a significantly attenuated R_{aw} response following U46619 challenge. GPRA$^{+/+}$ mice, n=17; GPRA$^{-/-}$ mice, n=16 (*p = 0.038).

Expression and function of NPSR1/GPRA in the lung before and after induction of asthma-like disease

Irving C. Allen[1,5], Amy J. Pace[2,5], Leigh A. Jania[2], Julie G. Ledford[1], Anne M. Latour[2,3], John N. Snouwaert[2,3], Virginie Bernier[4], Rino Stocco[4], Alex G. Therien[4], and Beverly H. Koller[1,2,3]

[1] Curriculum in Genetics and Molecular Biology, [2]Department of Genetics, [3] Department of Medicine, University of North Carolina at Chapel Hill, Chapel Hill, North Carolina, 27599; [4] Department of Biochemistry and Molecular Biology, Merck Frosst Canada Ltd., Kirkland, QC, Canada, H9H 3L1; [5] These authors contributed equally to the generation of this manuscript

Online Data Supplement

Table E4.1

	WBC ($L\ 10^3/min^3$)	RBC ($10^6/min^3$)	PLT ($H\ 10^3/min^3$)	HGB (g/dl)	HCT (%)
$GPRA^{+/+}$	2.13 ± 0.33	7.86 ± 2.10	979.67 ± 130.56	12.33 ± 2.92	41.07 ± 11.39
$GPRA^{-/-}$	1.67 ± 0.12	8.53 ± 0.14	990.67 ± 40.92	13.13 ± 0.26	43.37 ± 0.29

	MCV (fl)	MCH (pg)	MCHC (g/dl)	RDW (L %)	MPV (fl)
$GPRA^{+/+}$	51.67 ± 0.88	16.17 ± 0.87	31.27 ± 2.22	14.1 ± 0.25	5.53 ± 0.12
$GPRA^{-/-}$	51 ± 0.58	15.4 ± 0.21	30.33 ± 0.43	12.9 ± 0.15	5.3 ± 0.06

	LYM ($L\ 10^3/min^3$)	MON ($L\ 10^3/min^3$)	GRA ($L\ 10^3/min^3$)
$GPRA^{+/+}$	1.37 ± 0.15	0.13 ± 0.07	0.63 ± 0.12
$GPRA^{-/-}$	1.27 ± 0.12	0.1 ± 0	$0.3 \pm 3.14 \times 10^{-9}$

	MON (%)	GRA (%)	EOS (%)	LYM (%)
$GPRA^{+/+}$	8.23 ± 1.32	22.2 ± 2.80	5.03 ± 0.77	69.57 ± 4.12
$GPRA^{-/-}$	7.1 ± 0.49	13.87 ± 2.80	3.57 ± 0.35	79.03 ± 1.41

Table E4.1. Complete Blood Counts. The red blood cell, white blood cell and platelet composition of both $GPRA^{+/+}$ and $GPRA^{-/-}$ mice fall within normal reference ranges. RBC, Red blood cells; HGB, Hemoglobin; HCT, Hematocrit; MCV, Mean Corpuscular Volume; MCH, Mean Corpuscular Hemoglobin; MCHC, Mean Corpuscular Hemoglobin Concentration; RDW, Red Cell Distribution Width; PLT, Platelets Count; MPV, Mean Platelet Volume; WBC, White Blood Cells; LYM, Lymphocytes; MON, Monocytes; EOS, Eosinophils; GRA, Granulocytes. All mice are on the 129SvEv coisogenic background. $GPRA^{+/+}$ (n = 4); $GPRA^{-/-}$ (n = 4)

Figure E4.1

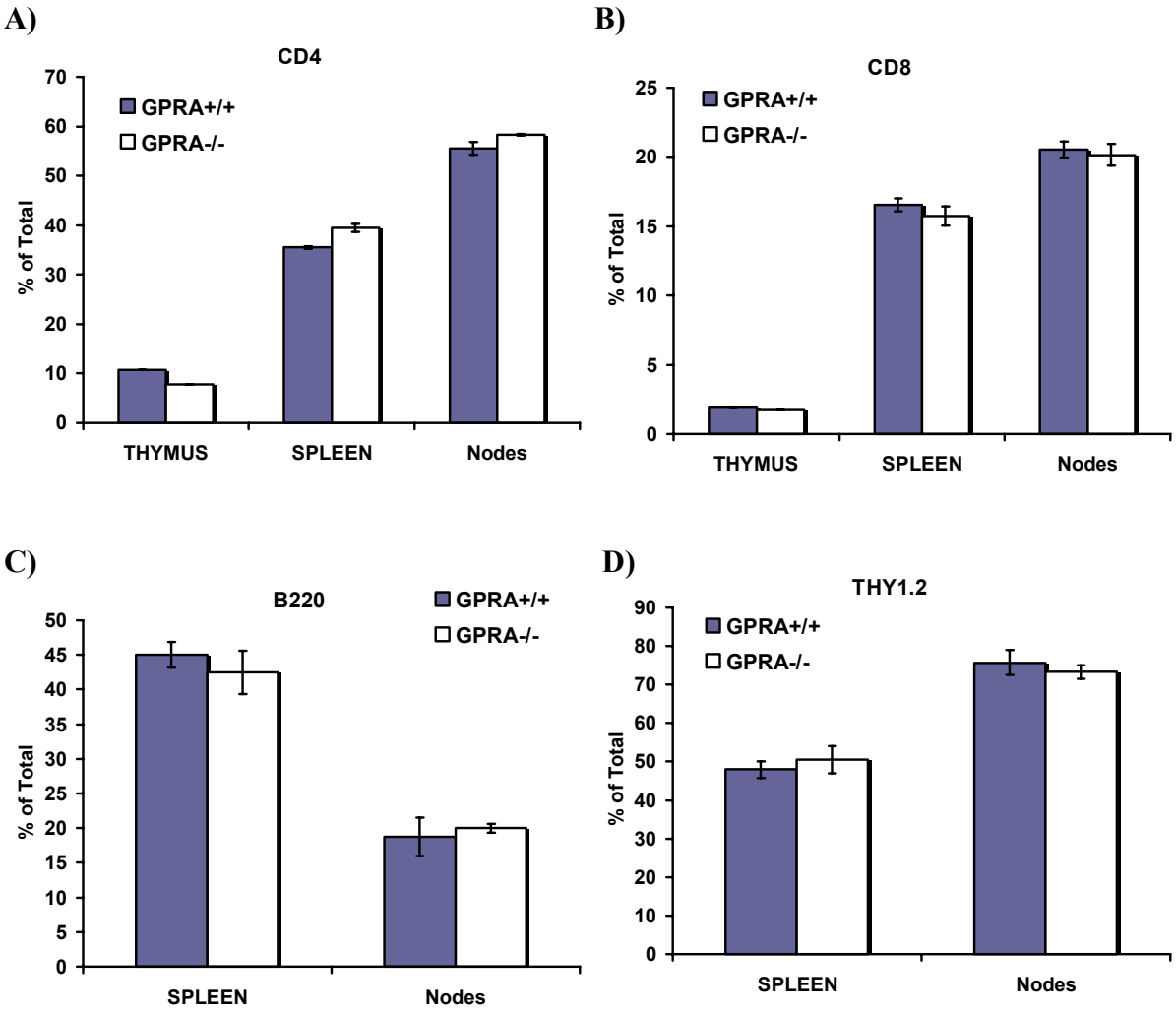
A)
CD4
GPRA+/+
GPRA-/-
% of Total
70
60
50
40
30
20
10
0
THYMUS
SPLEEN
Nodes
B)
CD8
GPRA+/+
GPRA-/-
% of Total
25
20
15
10
5
0
THYMUS
SPLEEN
Nodes
C)
B220
GPRA+/+
GPRA-/-
% of Total
50
45
40
35
30
25
20
15
10
5
0
SPLEEN
Nodes
D)
THY1.2
GPRA+/+
GPRA-/-
% of Total
90
80
70
60
50
40
30
20
10
0
SPLEEN
Nodes

Figure E4.1. FACS Scan Analysis. No significant differences were detected in the immune cell composition between $GPRA^{-/-}$ and $GPRA^{+/+}$ mice on the 129/SvEv coisogenic background. Thymus: GPRA+/+ (n = 1), GPRA-/- (n = 1); Spleen: GPRA+/+ (n = 4), GPRA-/- (n = 4); Lymph Nodes: GPRA+/+ (n = 3), GPRA-/- (n = 3).

Figure E4.2

A)

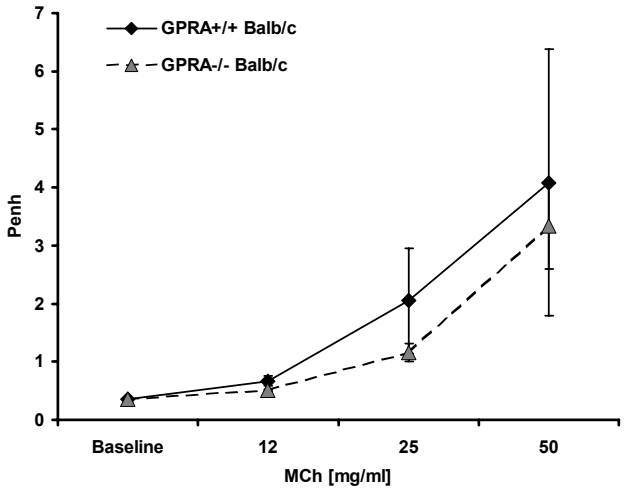

B)

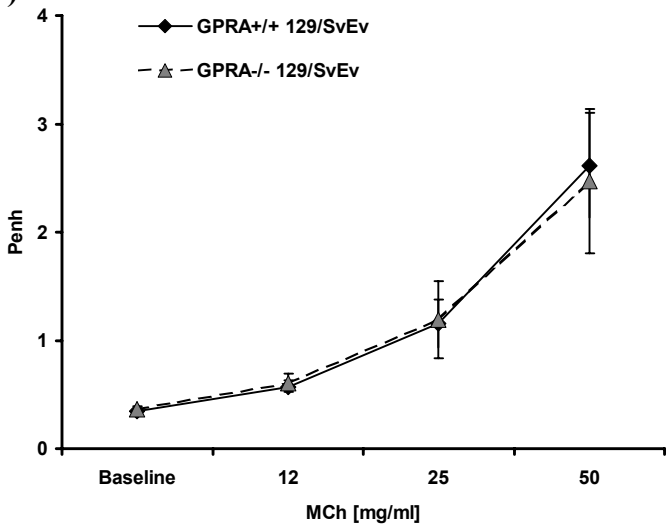

C)

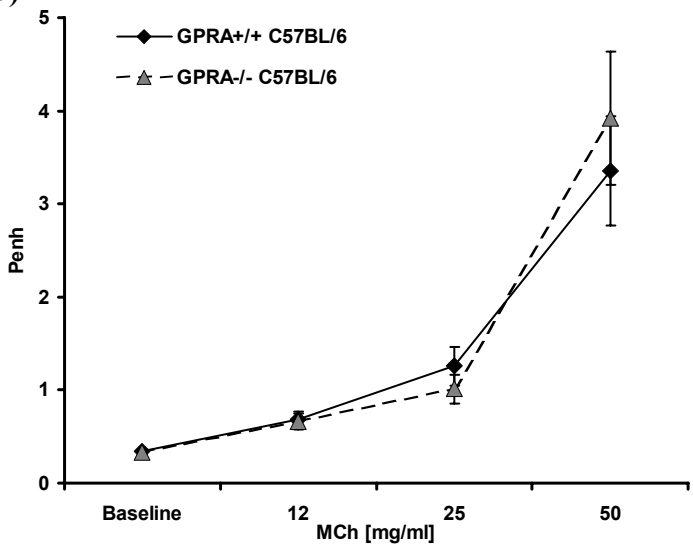

Figure E4.2. Methacholine response in conscious, unrestrained wild type and GPRA$^{-/-}$ mice. Changes in enhanced pause (Penh) of GPRA$^{+/+}$ and GPRA$^{-/-}$ mice in response to MCh was assessed in mice backcrossed onto BALB/c **(A)**, 129/SvEv **(B)** and C57BL/6 **(C)** backgrounds. Following baseline measurements, the airways were exposed to aerosolized vehicle (not shown) followed by increasing doses of aerosolized MCh (12 mg/ml to 50 mg/ml). The average Penh increased significantly in all groups of mice regardless of genotype or strain. GPRA$^{+/+}$ mice: BALB/c, n = 3; 129/SvEv, n = 15; C57BL/6, n = 9; GPRA$^{-/-}$ mice: BALB/c, n = 4; 129/SvEv, n = 7; C57BL/6, n = 7.

Discussion

Previous studies reported a dramatic increase in the expression of NPSR1/GPRA in the mouse lung after induction of allergic lung disease, suggesting that the mouse was likely to provide a model for the study of the role of this gene in the pathogenesis of asthma. As a first step to examine the functional significance of GPRA in the development of disease in the mouse lung, we generated a mouse lacking the functional receptor. A deletion mutation introduced into the exon encoding a portion of the 3rd transmembrane domain not only results in the loss of codons encoding a.a. residues 94 to 159 from the mouse genome, but also results in an alteration in the splicing pattern of the gene, such that the major transcript remaining in the mutant mouse line is predicted to produce an isoform incapable of integration into the cell membrane (previously characterized (35)). Despite the loss of functional NPSR1/GPRA, we detected no difference in the development of allergic lung disease in these mice. Neither qualitative nor quantitative differences in the cellular infiltrate, or the development of AHR in response to methacholine, distinguished the mutant mice from littermate controls.

A number of explanations are possible for the failure to observe differences in the development of disease between the GPRA$^{-/-}$ and littermate control mice. First, it is possible that, while loss of the receptor has little impact on the development of disease because of compensatory pathways, the expression of an allele encoding a gain-of-function mutation in GPRA would result in increased signaling and might result in more severe disease. Unfortunately, this hypothesis is not easily tested in the mouse. As discussed above, all mouse strains examined to date express the disease associated *Gpra* allele. Given our difficulty in observing a measurable consequence as a result of the complete loss of GPRA, it

is unlikely that introducing the codon for asparagine at position 107 will alter the development of disease in the mouse asthma model.

We cannot rule out the possibility that the inflammation models we have chosen for testing the role of GPRA lack the sensitivity for discerning the contribution of GPRA to disease development. There are ample examples in the literature that have demonstrated the reliance on a particular immunization protocol or on a particular mouse strain for the ability to distinguish the role of a particular cell type or molecule in allergic lung inflammation. For example, the contribution of the mast cell to allergic lung disease is only observed in a chronic OVA inflammation model when mice are sensitized with antigen free of alum (36). Likewise, the dependence of allergic airway disease on the eosinophil (21, 13) was more apparent when C57BL/6 mice were used rather than BALB/c. Further studies with the $GPRA^{-/-}$ mice should allow us to rule out these possibilities.

A third possibility is suggested by our analysis of expression of GPRA in the lung of BALB/c, C57BL/6 and 129/SvEv mice before and after induction of airway disease, as well as our analysis of expression of the GPRA ligand NPS in select tissues. In all cases, quantitative PCR failed to detect expression of GPRA: the signal obtained from the tissue was observed only after 35-36 cycles and is thus, outside of the range that we believe provides reliable detection of expression. Consistent with these data, northern blot analysis of RNA prepared from either naïve lung or lung tissue obtained from mice with allergic airway disease failed to detect expression of GPRA (data not shown), although expression in RNA prepared from the brain was easily observed. Our findings are similar to those of Xu *et al.,* who observed high levels of GPRA/NPSR1 expression in the brain but very low expression in the naïve lungs (37). A possible explanation for the differences in our results

and those published by Laitinen *et al*. is the method used in the analysis of the quantitative PCR, specifically the choice of the housekeeping genes used to normalize the results. The importance of the choice of housekeeping gene with which to normalize expression in tissue with an active and ongoing inflammatory response has been discussed previously (3, 6, 8). Consistent with this, we show that the threshold cycle at which the expression of a variety of common housekeeping genes, including *β-actin* and *GAPDH*, are detected varies significantly between OVA and saline challenged lung samples. Changes in levels of housekeeping genes in this model are consistent with previous reports demonstrating that β-actin, GAPDH, and elongation factor-1-α (EF-1α) are inappropriate for normalizing mRNA levels in diseased airways and can lead to erroneous results regarding gene expression in the lung (6, 8). Of the housekeeping genes included in our study, 18s rRNA was the only normalizer appropriate for assessing mRNA expression levels in OVA treated lungs. In fact, upon normalizing our data sets to β-actin, we found enhanced *GPRA* expression in the OVA treated lungs similar to that previously reported by Laitinen *et al*. While it is possible that GPRA is expressed at low levels in the lung epithelia and/or airway smooth muscle, our studies do not support the expression at the levels previously reported, nor do they indicate that these levels change dramatically in the inflamed lung. This raises the possibility that the failure to observe a change in the development of allergic lung disease in the $GPRA^{-/-}$ mice reflects a differential expression pattern of this gene in mouse and human. However, our further studies of expression of GPRA in human tissues do not support this interpretation.

The excitement over this latest asthma candidate gene was based, not only on the strong genetic evidence derived from two independent founder populations, but also on the expression of the gene in airway epithelial and smooth muscle cells and, importantly, the

changes in expression patterns of two of the isoforms in the airways of asthmatics. However, contrary to the previously published report, we could find no evidence for substantial expression of *GPRA* in normal lung samples or in tissue biopsies from the asthmatic lung by quantitative PCR. The earlier observations were based largely on the expression of GPRA detected by antibodies specific for the two isoforms of GPRA. We cannot rule out the possibility that the differences between our findings reflect an extreme disconnect between mRNA and protein levels. However, inconsistent with this interpretation, Laitinen *et al*. present northern analysis of lung tissue demonstrating detection of two, albeit faint, bands corresponding to the GPRA isoforms with a GPRA specific probe. We cannot explain these discrepancies. However, consistent with our studies of the allergic mouse airways, extensive analysis of tissues and cell lines fail to support a model in which substantial levels of GPRA are expressed by either human epithelium or airway smooth muscle cells.

While genetic studies identified GPRA as a potential risk factor for asthma, studies by Xu and colleagues simultaneously identified GPRA as the neruopeptide S receptor (NPSR). These studies demonstrated that NPSR1/GPRA is highly expressed in the brain, with the highest levels detected in the hypothalamus. They further demonstrated that central administration of NPS results in increased locomotor activity, altered sleep states, and increased anxiolytic-like effects in mice, thus suggesting that NPSR1/GPRA can play a role in arousal and anxiety (37). This raises the interesting possibility that NPSR1/GPRA may affect airway function as a result of its role in the nervous system. A number of reports suggest that the pathogenesis of many chronic inflammatory diseases including atopic dermatitis (AD), rheumatoid arthritis (RA), and asthma can be modulated by stress and emotion. For example, studies have reported that some asthmatics demonstrate a reduction

in pulmonary function in response to increased anxiety levels evoked by exposure to emotionally charged films (27), listening to stressful interactions (17), and participating in a sustained stressful life event (final academic examinations)(22). Increasing evidence suggests that the biological basis for these observations involves alterations of the stress response, which can contribute to dysfunctional interactions between the neuroendocrine and immune systems. These interactions are likely mediated by the hypothalamo-pituitary-adrenal axis (HPA axis) via regulation of circulating concentrations of corticosteroid hormones, such as corticosterone (reviewed by (10)). These hormones are potent modulators of both immune and neuronal mechanisms. Interestingly, studies in rats have demonstrated that intracerebroventricular (ICV) and paraventricular nucleus (PVN) administration of NPS significantly increases plasma levels of adrenocorticotropic hormone (ACTH) and corticosterone (30). A recent study of mice lacking corticotropin-releasing hormone (CRH) also demonstrated the ability of this pathway to modulate inflammation in a mouse model of allergic lung disease (29). This raises the possibility that polymorphisms in the *NPSR1/GPRA* gene could alter the activity of the HPA axis and in this manner impact the risk for the development of asthma, although increased activity would be predicted to inhibit, rather than enhance, inflammatory disorders.

The high expression of NPSR1/GPRA in the nervous system suggests a second possible mechanism by which altered function of this receptor might influence the pathogenesis of asthma. The human airway is highly innervated, and expression of GPRA, either on sensory or cholinergic neurons, could influence the tone of the airway smooth muscle or the response to stimuli. Although not specifically addressed, it is possible that various neuronal populations in the lung express NPSR1/GPRA. This expression would be

difficult to detect by analysis of total RNA, but could dramatically impact the pathogenesis of asthma and particularly the development of AHR. In this regard, it was of interest that the only difference discerned between the wild type and GPRA$^{-/-}$ mice was an attenuation in airway resistance in response to the thromboxane A_2 analog U46619. Analysis of a large cohort of 129/SvEv mice and co-isogenic NPSR1/GPRA$^{-/-}$ animals demonstrated a small but significant decrease in the change in airway resistance. The difference appears to be confined to the central airways, as no significant difference was observed in the G and H parameters, which are sensitive to changes in the distal lung. Previous studies have demonstrated that U46619 facilitates airway smooth muscle constriction through an M3 muscarinic acetylcholine receptor (M3 mAChR) dependent mechanism (2). It has been suggested that this mechanism likely involves afferent and efferent neural signaling (1, 2, 15). This leaves open the possibility that polymorphisms in NPSR1/GPRA could alter neurally mediated mechanisms affecting smooth muscle constriction and airway function and in this way increase the risk for asthma.

References

1. Aizawa H, Takata S, Shigyo M, Matsumoto K, Koto H, Inoue H, and Hara N. Effect of BAY u3405, a thromboxane A2 receptor antagonist, on neuro- effector transmission in canine tracheal tissue. Prostaglandins LeukotEssentFatty Acids 53: 213-217, 1995.

2. Allen IC, Hartney JM, Coffman TM, Penn RB, Wess J, and Koller BH. Thromboxane A2 induces airway constriction through an M3 muscarinic acetylcholine receptor-dependent mechanism. Am J Physiol Lung Cell Mol Physiol 290: L526-533, 2006.

3. Barber RD, Harmer DW, Coleman RA, and Clark BJ. GAPDH as a housekeeping gene: analysis of GAPDH mRNA expression in a panel of 72 human tissues. Physiol Genomics 21: 389-395, 2005.

4. Bernier V, Stocco, R, Bogusky, MJ, Joyce, JG, Parachoniak, C, Grenier, K, Arget, M, Mathieu, MC, O'Neill, GP, Slipetz, D, Crackower, MA, Tan, CM, Therien, AG. Structure/Function Relationships In The Neuropeptide S Receptor: Molecular Consequences Of The Asthma-Associated Mutation N107I. J. Biol. Chem., published online June 20, 2006, doi: 10.1074/jbc.M603691200

5. Cressman VL, Hicks EM, Funkhouser WK, Backlund DC, and Koller BH. The relationship of chronic mucin secretion to airway disease in normal and CFTR-deficient mice. Am J Respir Cell Mol Biol 19: 853-866, 1998.

6. Dheda K, Huggett JF, Bustin SA, Johnson MA, Rook G, and Zumla A. Validation of housekeeping genes for normalizing RNA expression in real-time PCR. Biotechniques 37: 112-114, 116, 118-119, 2004.

7. Feng Y, Hong X, Wang L, Jiang S, Chen C, Wang B, Yang J, Fang Z, Zang T, and Xu X. G protein-coupled receptor 154 gene polymorphism is associated with airway hyperresponsiveness to methacholine in a Chinese population. J Allergy Clin Immunol 117: 612-617, 2006.

8. Glare EM, Divjak M, Bailey MJ, and Walters EH. beta-Actin and GAPDH housekeeping gene expression in asthmatic airways is variable and not suitable for normalising mRNA levels. Thorax 57: 765-770, 2002.

9. Gupte J, Cutler G, Chen JL, and Tian H. Elucidation of signaling properties of vasopressin receptor-related receptor 1 by using the chimeric receptor approach. Proc Natl Acad Sci U S A 101: 1508-1513, 2004.

10. Haddad JJ, Saade NE, and Safieh-Garabedian B. Cytokines and neuro-immune-endocrine interactions: a role for the hypothalamic-pituitary-adrenal revolving axis. J Neuroimmunol 133: 1-19, 2002.

11. Hamelmann E, Schwarze J, Takeda K, Oshiba A, Larsen GL, Irvin CG, and Gelfand EW. Noninvasive measurement of airway responsiveness in allergic mice using barometric plethysmography. Am J Respir Crit Care Med 156: 766-775, 1997.

12. Hantos Z, Adamicza A, Govaerts E, and Daroczy B. Mechanical impedances of lungs and chest wall in the cat. J Appl Physiol 73: 427-433, 1992.

13. Humbles AA, Lloyd CM, McMillan SJ, Friend DS, Xanthou G, McKenna EE, Ghiran S, Gerard NP, Yu C, Orkin SH, and Gerard C. A critical role for eosinophils in allergic airways remodeling. Science 305: 1776-1779, 2004.

14. Immervoll T, Loesgen S, Dutsch G, Gohlke H, Herbon N, Klugbauer S, Dempfle A, Bickeboller H, Becker-Follmann J, Ruschendorf F, Saar K, Reis A, Wichmann HE, and Wjst M. Fine mapping and single nucleotide polymorphism association results of candidate genes for asthma and related phenotypes. Hum Mutat 18: 327-336, 2001.

15. Karla W, Shams H, Orr JA, and Scheid P. Effects of the Thromboxane-A2 Mimetic, U46,619, on Pulmonary Vagal Afferents in the Cat. Resp Physiol 87: 383-396, 1992.

16. Keen TJ, Inglehearn CF, Green ED, Cunningham AF, Patel RJ, Peacock RE, Gerken S, White R, Weissenbach J, and Bhattacharya SS. A YAC contig spanning the dominant retinitis pigmentosa locus (RP9) on chromosome 7p. Genomics 28: 383-388, 1995.

17. Kolbe J, Garrett J, Vamos M, and Rea HH. Influences on trends in asthma morbidity and mortality: the New Zealand experience. Chest 106: 211S-215S, 1994.

18. Kormann MS, Carr D, Klopp N, Illig T, Leupold W, Fritzsch C, Weiland SK, von Mutius E, and Kabesch M. G-Protein-coupled receptor polymorphisms are associated with asthma in a large German population. Am J Respir Crit Care Med 171: 1358-1362, 2005.

19. Laitinen T, Daly MJ, Rioux JD, Kauppi P, Laprise C, Petays T, Green T, Cargill M, Haahtela T, Lander ES, Laitinen LA, Hudson TJ, and Kere J. A susceptibility locus for asthma-related traits on chromosome 7 revealed by genome-wide scan in a founder population. Nat Genet 28: 87-91, 2001.

20. Laitinen T, Polvi A, Rydman P, Vendelin J, Pulkkinen V, Salmikangas P, Makela S, Rehn M, Pirskanen A, Rautanen A, Zucchelli M, Gullsten H, Leino M, Alenius H, Petays T, Haahtela T, Laitinen A, Laprise C, Hudson TJ, Laitinen LA, and Kere J. Characterization of a common susceptibility locus for asthma-related traits. Science 304: 300-304, 2004.

21. Lee JJ, Dimina D, Macias MP, Ochkur SI, McGarry MP, O'Neill KR, Protheroe C, Pero R, Nguyen T, Cormier SA, Lenkiewicz E, Colbert D, Rinaldi L, Ackerman SJ, Irvin CG, and Lee NA. Defining a link with asthma in mice congenitally deficient in eosinophils. Science 305: 1773-1776, 2004.

22. Liu LY, Coe CL, Swenson CA, Kelly EA, Kita H, and Busse WW. School examinations enhance airway inflammation to antigen challenge. Am J Respir Crit Care Med 165: 1062-1067, 2002.

23. Melen E, Bruce S, Doekes G, Kabesch M, Laitinen T, Lauener R, Lindgren CM, Riedler J, Scheynius A, van Hage-Hamsten M, Kere J, Pershagen G, Wickman M, and Nyberg F. Haplotypes of G protein-coupled receptor 154 are associated with childhood allergy and asthma. Am J Respir Crit Care Med 171: 1089-1095, 2005.

24. Mohn A and Koller BH. In: DNA Cloning 4, edited by Glover DM and Hames BD. New York: Oxford University Press, 1995, p. 143-184.

25. Paquette JS, Tremblay P, Bernier V, Auger FA, Laviolette M, Germain L, Boutet M, Boulet LP, and Goulet F. Production of tissue-engineered three-dimensional human bronchial models. In Vitro Cell Dev Biol Anim 39: 213-220, 2003.

26. Reinscheid RK, Xu YL, Okamura N, Zeng J, Chung S, Pai R, Wang Z, and Civelli O. Pharmacological characterization of human and murine neuropeptide s receptor variants. J Pharmacol Exp Ther 315: 1338-1345, 2005.

27. Ritz T, Steptoe A, DeWilde S, and Costa M. Emotions and stress increase respiratory resistance in asthma. Psychosom Med 62: 401-412, 2000.

28. Shin HD, Park KS, and Park CS. Lack of association of GPRA (G protein-coupled receptor for asthma susceptibility) haplotypes with high serum IgE or asthma in a Korean population. J Allergy Clin Immunol 114: 1226-1227, 2004.

29. Silverman ES, Breault DT, Vallone J, Subramanian S, Yilmaz AD, Mathew S, Subramaniam V, Tantisira K, Pacak K, Weiss ST, and Majzoub JA. Corticotropin-releasing hormone deficiency increases allergen-induced airway inflammation in a mouse model of asthma. J Allergy Clin Immunol 114: 747-754, 2004.

30. Smith KL, Patterson M, Dhillo WS, Patel SR, Semjonous NM, Gardiner JV, Ghatei MA, and Bloom SR. Neuropeptide S stimulates the hypothalamo-pituitary-adrenal axis and inhibits food intake. Endocrinology, 2006.

31. Soderhall C, Marenholz I, Nickel R, Gruber C, Kehrt R, Rohde K, Griffioen RW, Meglio P, Tarani L, Gustafsson D, Hoffmann U, Gerstner B, Muller S, Wahn U, and Lee YA. Lack of association of the G protein-coupled receptor for asthma susceptibility gene with atopic dermatitis. *J Allergy Clin Immunol* 116: 220-221, 2005.

32. Speyer CL, Rancilio NJ, McClintock SD, Crawford JD, Gao H, Sarma JV, and Ward PA. Regulatory effects of estrogen on acute lung inflammation in mice. Am J Physiol Cell Physiol 288: C881-890, 2005.

33. Tomioka S, Bates JH, and Irvin CG. Airway and tissue mechanics in a murine model of asthma: alveolar capsule vs. forced oscillations. J Appl Physiol 93: 263-270, 2002.

34. Veal CD, Reynolds NJ, Meggitt SJ, Allen MH, Lindgren CM, Kere J, Trembath RC, and Barker JN. Absence of association between asthma and high serum immunoglobulin E associated GPRA haplotypes and adult atopic dermatitis. *J Invest Dermatol* 125: 399-401, 2005.

35. Vendelin J, Pulkkinen V, Rehn M, Pirskanen A, Raisanen-Sokolowski A, Laitinen A, Laitinen LA, Kere J, and Laitinen T. Characterization of GPRA, a novel G protein-coupled receptor related to asthma. Am J Respir Cell Mol Biol 33: 262-270, 2005.

36. Williams CM and Galli SJ. Mast cells can amplify airway reactivity and features of chronic inflammation in an asthma model in mice. J Exp Med 192: 455-462, 2000.

37. Xu YL, Reinscheid RK, Huitron-Resendiz S, Clark SD, Wang Z, Lin SH, Brucher FA, Zeng J, Ly NK, Henriksen SJ, de Lecea L, and Civelli O. Neuropeptide S: a neuropeptide promoting arousal and anxiolytic-like effects. Neuron 43: 487-497, 2004.